Bioactive metabolites from Piperaceae

DISSERTATION

zur Erlangung des Doktorgrades der Naturwissenschaften
(Dr. rer. nat.)

der

Naturwissenschaftlichen Fakultät II
Chemie, Physik und Mathematik

der Martin-Luther-Universität
Halle-Wittenberg

vorgelegt von

Herr Ismail Bin Ware
geb. am 01.01.1983 in Sabah, Malaysia

This dissertation has been developed under the supervision of Prof. Dr. Ludger Wessjohann and mentorship of Dr. Katrin Franke at the Leibniz Institute of Plant Biochemistry (IPB) in cooperation with the Martin Luther University Halle-Wittenberg. Both supported the thesis by editing.

1st Reviewer: Prof. Dr. Ludger Wessjohann

2nd Reviewer: Prof. Dr. Peter Proksch

Date of public defense: 04th April 2023

HERBARIUM INSTITUT BIOSAINS, UPM

FLORA OF PENINSULAR MALAYSIA

FAMILY   : Piperaceae
SPESIES   : *Piper sarmentosum* Roxb.
LOCAL NAME   : Kaduk

LOCALITY   : Seri Menanti, Negeri Sembilan
HABITAT   : Terrestrial (Secondary Forest)
G.P.S   : -
ALT   : -

NOTE   - *Piper sarmentosum* is a sprawling herbaceous creeper, with erect stems at intervals, growing close to the ground and forming mounds of up to 60 cm in height. The stems are slightly hairy. The leaves are alternate, stalked, heart-shaped and glossy dark green. The plant is monoecious, where male and female flowers are produced on different spikes on the same plant. Leaves boiled in water and taken to treat coughs, flu and malarial fever.

COLLECTOR   : Ismail Ware
DET   : Dr. Firdaus Ismail
REFERENCE NO.   : MFI 0039/19
DATE   : February, 2019

iii

iv

Bioactive metabolites from Piperaceae

Table of contents

List of abbreviations

[α]	Specific rotation	**m**	Multiplet
BSL-1	Biosafety level 1	**_m/z_**	Mass-to-charge-ratio
calcd	calculated	**min**	Minute(s)
CC	Column chromatography	**MS**	Mass spectrometry
CD₃OD	Deuterated methanol	**MS²**	Double mass spectrometry
CE	Collision potential	**MTT**	3-(4,5-Dimethylthiazol-2-yl)-2,5-diphenyl¬tetrazolium bromide
CH₂Cl₂	Dichloromethane	**MVA**	Multivariate data analysis
CH₃OH	Methanol	**_n_-BuOH**	_n_-Butanol
CH₃CN	Acetonitrile	**NMR**	Nuclear magnetic resonance
CID	Collisioin induced dissociation	**NOESY**	Nuclear Overhauser effect spectroscopy
COSY	Correlated spectroscopy	**OD**	Optical density
CV	Crystal violet	**PC**	Principal component
d	Doublet	**PCA**	Principal component analysis
dd	Doublet of doublets	**P**	Peak number
ddd	Doublet of doublets of doublets	**QC**	Quality control sample
Da	Dalton	**QToF**	Quadrupole time-of-flight
DEPT	Distortionless enhancement by polarization transfer	**r.t.**	Room temperature
DESI	Desorption electrospray ionization	**rel. int.**	Relative intensity
DMSO	Dimethylsulfoxide	**_R_f**	Retention factor
ESI	Electrospray ionization	**ROESY**	Rotational frame Overhauser effect
EtOAc	Ethyl acetate	**RP**	Reversed phase
H₂O	Water	**s**	Singlet
HCA	Hierarchial cluster analysis	**SPE**	Solid-phase extraction
HMBC	Heteronuclear multiple bond correlation	**SWATH**	sequential window acquisition of all theoretical mass spectra
HMG	3-hydroxy-3-methylglutaroyl	**t**	Triplet
HPLC	High-performance liquid chromatography	**TIC**	Total ion chromatogram
HR	High-resolution	**TLC**	Thin-layer chromatography
HSQC	Heteronuclear single quantum correlation	**TMS**	Tetramethylsilane
IC₅₀	50% inhibitory concentration	**TOCSY**	Total correlation spectroscopy
IR (ATR)	Infrared (Attenuated total reflection)	**TOF**	Time-of-flight
IS	Internal standards	**t_R**	Retention time
_J_	Coupling constant	**UHPLC**	ultra-high performance liquid chromatography
LC₅₀	Lethal concentration 50	**UV/Vis**	Ultraviolet/visible
LC-MS	Liquid chromatography/ mass spectrometry	**XICs**	Extracted ion chromatograms

Summary

Piperaceae are well-known for their traditional medicinal and culinary uses. It is estimated to have 3700 species, which are widely distributed in tropical regions. Due to the vast number of species, there is still an enormous potential to find new bioactive drugs from chemically and biologically unexplored Piperaceae species. This work, therefore, describes the characterization and isolation of constituents from two Piperaceae species, namely *Piper sarmentosum* Roxb. and *Peperomia obtusifolia* L.. Selected biological activities of the plant extracts and isolated compounds were also assessed.

Chemical investigation of *P. sarmentosum* leaves collected in Malaysia afforded 34 natural products, including three that have not been described (**2.1**–**2.3**) (Chapter 2). Interestingly, 21 known compounds were isolated for the first time from this species. The structures of the isolated compounds were elucidated by detailed spectroscopic techniques such as MS and NMR analyses. The anthelmintic, antifungal, antibacterial, cytotoxic, and neuroprotective activities of extracts and isolated compounds were evaluated. As an example, the previously undescribed kadukoside (**2.2**) exhibited significant antifungal activity against *Septoria tritici* whereas the known *trans*-asarone (**2.15**) is the most promising constituent for anthelmintic, antifungal (against *Botrytis cinerea*) and neuroprotective activity.

Furthermore, metabolite profiles of *P. sarmentosum* organs (leaves, stems, roots, and fruits) were established by LC-HRMS/MS (Chapter 3). Detailed MS/MS fragmentation pattern analysis revealed the presence of 154 metabolites which were tentatively identified and classified as mostly alkaloids and flavonoids. Multivariate-type data analysis (LC-MS-based PCA) displayed a clear separation of *P. sarmentosum* organs, especially leaves and stems. The metabolites responsible for these separations are magnoflorines, piperolactam A and B, andamanicin, *trans*-asarone, pellitorine, brachyamide B, guineensine, nigrinodine and sarmentine, which are also unique metabolites for organ identification.

Phytochemical investigation of *P. obtusifolia* collected from an ornamental plant in Germany (Chapter 4) revealed two undescribed compounds, named peperomic ester (**4.1**) and peperoside (**4.2**) along with five known compounds. The known peperobtusin A (**4.5**), is an example that exhibits significant antiproliferative and antibacterial effects.

The overall thesis suggests that the Piperaceae family represent a valuable source of new bioactive compounds where metabolite profiling combined with multivariate data analysis has the potential to improve the efficiency of natural product prioritization and to accelerate the targeted isolation of key natural products.

Zusammenfassung

Die Piperaceae (Pfeffergewächse) sind für ihre traditionelle medizinische und kulinarische Verwendung bekannt. Es gibt schätzungsweise 3700 Arten, die in tropischen Regionen weit verbreitet sind. Aufgrund der großen Artenvielfalt besteht immer noch ein enormes Potenzial, neue bioaktive Arzneimittel aus chemisch und biologisch unerforschten Piperaceae-Arten zu finden. Diese Arbeit beschreibt daher die Charakterisierung und Isolierung von Inhaltsstoffen aus zwei Vertretern der Piperaceae, *Piper sarmentosum* Roxb. und *Peperomia obtusifolia* L.. Ausgewählte biologische Aktivitäten der Pflanzenextrakte und isolierten Verbindungen wurden ebenfalls bewertet.

Die chemische Untersuchung der Blätter von *P. sarmentosum* aus Malaysia ergab 34 Naturstoffe, darunter drei, die in der Natur nie zuvor beschrieben wurden (**2.1**-**2.3**) (Kapitel 2). Interessanterweise wurden 21 bekannte Verbindungen zum ersten Mal aus dieser Art isoliert. Die Strukturen der isolierten Verbindungen wurden durch detaillierte spektroskopische Techniken wie MS- und NMR-Analysen aufgeklärt. Die anthelmintischen, antimykotischen, antibakteriellen, zytotoxischen und neuroprotektiven Aktivitäten der Extrakte und isolierten Verbindungen wurden bewertet. Das bisher unbekannte Kadukosid (**2.2**) zeigte zum Beispiel eine signifikante antifungale Wirkung gegen *Septoria tritici*, während das bekannte *trans*-Asaron (**2.15**) die vielversprechendste anthelmintische, antifungale (gegen *Botrytis cinerea*) und neuroprotektive Aktivität aufwies.

Weiterhin wurden Metabolitenprofile von *P. sarmentosum*-Organen (Blätter, Stängel, Wurzeln und Früchte) mittels LC-HRMS/MS erstellt (Kapitel 3). Eine detaillierte Analyse der MS/MS-Fragmentierungsmuster ergab das Vorhandensein von 154 Metaboliten, die vorläufig identifiziert und hauptsächlich als Alkaloide und Flavonoide klassifiziert wurden. Die multivariate Datenanalyse (LC-MS-basierte PCA) zeigte eine klare Trennung der Organe von *P. sarmentosum,* insbesondere der Blätter und Stängel. Die Metaboliten, die für diese Trennung verantwortlich sind, wurden als Magnoflorinen, Piperolactam A und B, Andamanicin, *trans*-Asaron, Pellitorin, Brachyamid B, Guineensin, Nigrinodin und Sarmentin annotiert.

Die phytochemische Untersuchung von *P. obtusifolia* (Kapitel 4) führte zur Isolierung von zwei unbeschriebenen Verbindungen, die als Peperomic Ester (**4.1**) und Peperoside (**4.2**) bezeichnet werden, sowie fünf bekannten Verbindungen. Das bekannte Peperobtusin A (**4.5**) wies eine signifikante antiproliferative und antibakterielle Wirkung auf.

Zusammenfassend legt die Dissertationsarbeit nahe, dass die Familie der Piperaceae eine vielversprechende Quelle für neue bioaktive Verbindungen darstellen dürfte, wobei die Aufnahme von Metabolitenprofilen in Verbindung mit multivariater Datenanalyse das Potenzial hat, die Relevanz von Inhaltsstoffen besser zu beurteilen und so die gezielte Isolierung wichtiger Naturprodukte zu beschleunigen.

1. INTRODUCTION

Plants are widely recognized as an essential part of the world's biodiversity and a crucial resource for the earth. They play a pivotal role as an attractive source of new therapeutic agents due to the high structural diversity found in hundreds of thousands of species, including flowering plants, conifers, bryophytes and fern. Current estimates of the total diversity of land plants in the region of 400,000 identified species include 369,434 flowering plants. The richest terrestrial ecosystem on the earth is found in the tropical rainforest. This region has been known as the home of many fascinating medicinal plant species [1].

Since ancient times humans have used natural products, such as plants, animals, and microorganisms, as sources of medicine and foods. Medicinal plant applications were recorded as early human history based on sophisticated traditional systems from great civilizations, such as Mesopotamia, Egypt, China, India, Greeks and Romans [2]. During these periods until the end of the 17th century, medicinal plants were only applied on an empirical basis, without mechanistic knowledge on their pharmacological activities of bioactive constituents. It was only in the 18th century that Anton von Störck, an Austrian physician who investigated poisonous plants such as *Aconite* and *Colchicum*, and William Withering, an English physician who studied foxglove for the treatment of edema, laid the basis for the rational clinical investigation of medicinal plant [3].

Plants, in particular, become a valuable source of health promotion and treatment for a broad spectrum of diseases across various human communities. More than 80% of people in developing countries continue to rely on plants for their primary health care, including plant extracts, most of the time. To a certain extent, some medicinal plants have demonstrated the efficacy of herbal medicine with minimal harmful or unfavourable effects and excellent cost-effectiveness compared to synthetic drugs [4-6].

For instance, commercial drugs such as antibiotics for treating coughs are not affordable in rural regions of developing countries. However, they can be substituted by chewing the rootlets of *Piper sarmentosum* Roxb. with betel nut and swallowing the juice. In Southeast Asia, *P. sarmentosum* is easy to find and has been utilized to relieve coughs, asthma, muscle pain, and many other ailments for a long time [7].

1.1 The role of plant-derived natural plants in drug discovery

Ethnobotany studies have played a key role in drug discovery, especially for cancer, infectious diseases and other therapeutic areas, including cardiovascular diseases. Approximately 10% of plant biodiversity has been assessed regarding its bioactive potential, emphasizing the need for higher quantities of plant extracts to be researched. Thus, a

considerable number of plant species remain available to further investigation [8]. Therefore, in the past few decades, interest in traditional medicine has increased considerably among scientists due to the diverse multidimensionality of secondary metabolites ranging from simple structures to highly complex molecules with novel modes of action. These make them an attractive platform for pharmaceutical industry to discover new molecular entries with particular therapeutic applications [9,10].

Consequently, the discovery of m0odern drugs increased recently. Approximately 49% of the total molecules approved from 1981 to September 2019 are natural products or derived from these. Impressively, 67% (809 of 1205) of the new chemical entities (NCEs) registered were either natural, or products based on natural products [11]. This statistic will continue to rise as numerous natural products are presently being studied in various developmental stages of clinical investigation (phases I-III). This trend indicates that natural products significantly influence the process and development of drug discovery. Therefore, tremendous global attention has been drawn to bioactive natural products [12,13].

1.2 Medicinal plants as source of bioactive natural products

Plants have been the main source of many pharmaceutical agents and cosmetic products throughout history. Often novel drug entities are developed from traditional medicinal plants, followed by synthetic modifications to improve bioavailability and minimize the side effects [8]. For example, the isolation of the well-known anticancer drug paclitaxel (**1,** Taxol) from the bark of the Pacific yew tree *Taxus brevifolia* (Taxaceae) was reported in the 1960s. Paclitaxel containing a tricyclic diterpenoid moiety is the most well-known example of an important natural product that has impacted medicine [14]. Quinine (**2**) is the oldest antimalarial agent derived from the bark of *Cinchona officinalis.* It exhibits specific toxicity against *Plasmodium* and has fever-reducing activity [15]. In the decades following their discoveries, another antimalarial drug was found from the plant *Artemisia annua*, artemisinin (**3**). Artemisinin possesses rapid action to swiftly reduce the amount of *Plasmodium* parasites in blood patients with malaria [16].

There are many other significant drugs developed from traditional medicinal plants, a few mentioned here: Atropine (**4**) is an artefact of the tropane alkaloid (−)-hyoscyamine, which racemizes from its original plant, *Atropa belladonna,* during the extraction process [17]. Atropine is used as a mydriatic agent in ophthalmology and has other medicinal uses as an antispasmodic and intravenous drug during anaesthesia [18]. Other drugs used in clinical medicine are morphine (**5**) and galantamine (**6**). Morphine is one of the oldest medications naturally derived from the poppy plant, *Papaver somniferum*, used to treat acute and chronic

severe pain and is considered the gold standard of analgesics [19]. At the same time galantamine was discovered in *Galanthus* and the *Amaryllidaceae* family used to treat patients with Alzheimer's diseases [20] (Figure 1.1).
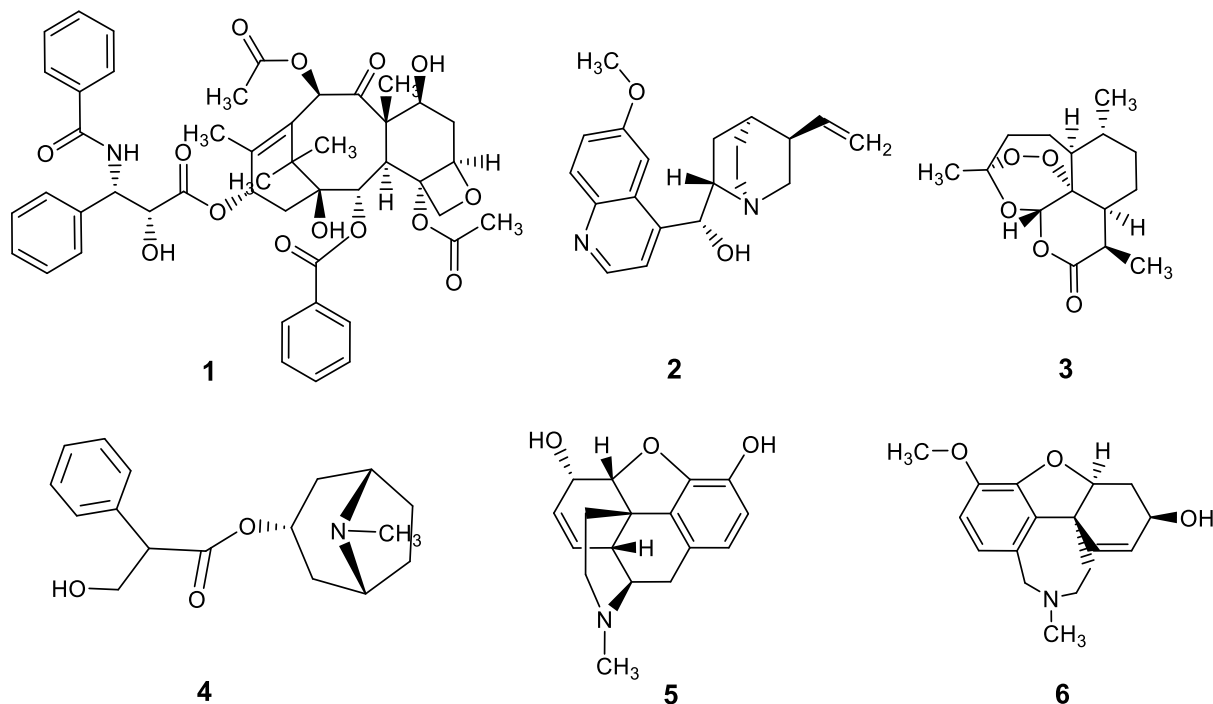
Figure 1.1: Several plant-derived natural products for therapeutics use: taxol (**1**), quinine (**2**), artemisinin (**3**), atropine (**4**), morphine (**5**) and galantamine (**6**).

The recent success of medicinal plant-derived drugs inspires and motivates many researchers with different backgrounds to collaborate effectively to guarantee future therapeutic entities that can add substantial value to the cure of a variety of human diseases. Additionally, the scientific developments and technologies in recent years, including improved analytical tools, genome mining and engineering strategies and microbial culturing advances, are all vital to the success of natural products based drug discovery [9].

1.3 Analytical research in drug discovery

The plant kingdom includes many species, which produce a diversity of bioactive compounds with different chemical scaffolds [9]. The discovery and characterization of these compounds have sparked the development of numerous products and medicines, motivating groups of scientists to focus their efforts on obtaining molecules from plants, bacteria, fungi, and other natural sources. The classical approach to the discovery of bioactive natural products typically begins with the biological screening of crude extracts, followed by fractionation procedures until the bioactive compound(s) is isolated and identified [9,21,22].

In the last decades, five strategies for identifying bioactive compounds from plant extracts were developed: bioactivity-guided fractionation, metabolite profiling approach, direct phytochemical isolation, synergy-directed fractionation and metabolism-directed approach [23]. The complete characteristics of the isolated compounds were obtained in detail using a combination of advanced analytical techniques such as high-resolution mass spectrometry (HRMS), nuclear magnetic resonance spectroscopy (NMR), and chiroptical techniques (e.g. circular dichroism) [24]. Although successful, the classical tools that have led to the discovery of chemical entities are time-consuming and often inefficient for the finding of new compounds in drug development. To address these shortcomings, very efficient hyphenation techniques between separation and spectroscopic instruments, such as metabolomics approaches, now enable the identification of highly complex molecular structures even within complex mixtures of compounds [11].

1.3.1   Metabolic profiling and multivariate data analysis

Metabolomics (alternatively referred to as metabolic profiling or metabonomics) has emerged in the late 1990s in response to the development of proteomics [25,26]. It is a relatively new subfield of "omics" that is primarily concerned with the identification and quantification of the small molecules (< 1500 Da) in a variety of biological systems and fields of research [27,28].

Metabolomic analysis can be classified into two approaches, targeted and untargeted metabolomics. The metabolites quantified in targeted metabolomics are known and represent specific pathways or classes of molecules. By contrast, untargeted metabolomics is used to identify and quantify as many metabolites as possible [29,30]. The term "targeted metabolomics" refers to absolute quantification, more precisely using an internal standard and semi-quantitative or quantitative analysis to detect known compounds associated with predefined pathways based on the study's hypotheses [29-31]. Untargeted metabolomics is the process of quantifying all metabolites present in a sample without prior knowledge of these metabolites. In addition, these untargeted approaches employ relative quantification (fold change) and sample comparison [29,30,32]. The challenges of untargeted metabolomics are achieving completeness as much as possible, metabolite identification, characterization of unknown small molecules, and the time required to process the generated data [30,32].

Metabolomics has evolved significantly over the last two decades and is now primarily defined as the study of metabolites using advanced high throughput analytical approaches and informatics [33-35]. This technology can also be used to determine the types and contents of metabolites at various developmental stages or in different tissue or organs [36-38]. Nowadays,

metabolomics is primarily performed through two techniques, nuclear magnetic resonance (NMR) spectroscopy and mass spectrometry (MS). The NMR technique specially focused on high-performance analytical studies by being a more cost-effective and less time-consuming technology than MS. Additionally, it is highly reproducible and quantitative NMR remains the only suitable technique for the quantification or structural identification of unknown compounds [39]. In contrast, available databases for analysis of NMR spectra cover only a subset of the relevant compounds. In addition, the technique's low sensitivity makes the detection and identification of minor compounds more challenging. Nevertheless, technology capable of partially solving this deficiency is being implemented by employing higher magnetic fields to enhance sensitivity with even higher potential [40,41].

Conversely, MS-based metabolomics features a higher sensitivity and resolution, owing to its speed and wide dynamic range. However, as with any technique, it has drawbacks that limit its application, such as difficulty detecting metabolites at trace levels or unequal ionization. In contrast, the constant improvement of sample processing methods, the coupling of chromatographic technology (e.g., liquid and gas chromatographies), and high sensitivity favour the acquisition of massive amounts of information, which impedes their subsequent processing. Later, identifying the metabolites is another challenge again due to the large amount of data obtained after peak alignment and the database limitation. Despite these drawbacks, MS is considered an ideal technique with promising potential in metabolomics research. The continuous improvement in the technology used is expected to resolve these deficiencies gradually [40,42]. Although different technologies MS, NMR or other methods, all approaches of metabolite profiling produce a huge amount of data. Owing to the complex nature of the data, the combination of metabolomics and multivariate data analysis (MVA) approaches, such as principal component analysis (PCA) including loading plots and, have proven to be effective tools for predicting bioactive constituents in natural products research [43-45].

Principal Component Analysis (PCA) is the most frequently used and fundamental technique for multivariate data analysis. PCA is a highly effective tool for unsupervised data analysis without previous knowledge of the samples. In addition, it enables the visualization of information contained in a large data set into a few principal components while retaining as much variability as possible within that set [46]. This technique was used to reduce the dimension of the spectral data to a manageable number of components, thereby simplifying subsequent analysis. Like all statistical techniques, PCA has some limitations and can be misused. Scaling variables can result in significantly different PCA results, and it is very important that the scaling is not adjusted to match prior knowledge of the data [47].

1.4   Piperaceae family

Piperaceae is commonly known as the pepper family. The name Piperaceae is derived from the Sanskrit word 'pipali', meaning berry. It also gave rise to the Greek 'peperi', the Latin 'piper' and the English 'pepper'. Originally this referred to the Indian long pepper, *Piper longum* L. [48]. Among the pepper species, *Piper nigrum* L. (black pepper) dominated and became the world's most important spice. This pepper is characterized as the "King of Spices" and has been incredibly popular since ancient times. It was one of the most traded spices worldwide, often referred to as "black gold" because it was used as currency along the commercial routes connecting Asia and Europe [49,50].

Phylogenetic analyses confirm that the Piperaceae family is part of the Piperales order and is the most archaic of pantropical flowering plants [51]. Around 4300 species of Piperales have been identified in this basal angiosperms' major order including the Piperaceae family. The Piperaceae family alone is estimated to have 3700 species, which are widely distributed in tropical regions [52], having its center of origin in Peninsular Malaysia and a broad dispersion in the American tropics [53]. Such a large number of species among the basal species is astounding compared to the size of the other Magnolidae families, which have a few hundred or fewer. The Piperaceae family is represented by five genera, *Verhuellia, Zippelia, Manekia, Piper* and *Peperomia* (Fig. 1.2), with all genera widely distributed in tropical and sub-tropical regions [54]. Previously *Zippelia* and *Manekia* were considered sisters to all other genera of Piperaceae, but a recent revision replaced them by *Verhuelia* as the most basal [55]. *Peperomia* and *Piper* are the richest genera in this family, with approximately 1700 and 2000 species, respectively (Fig. 1.2) [54].
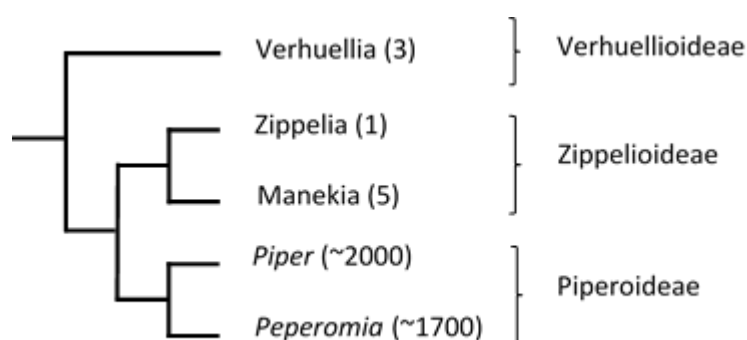
Figure 1.2: Phylogenetic relationship among genera, number of species and sub-families of Piperaceae [54].

1.4.1   *Piper sarmentosum* Roxb.

The genus *Piper includs* important medicinal plants used in various medicine systems [56]. They are distributed pantropically; however, their exact distribution is not easy to ascertain, mainly due to the high number of taxa [57]. Nevertheless, the crucial contributions

of medicinal plants in traditional healing systems have primarily been recorded in the literature. Therefore, it is not surprising that many people from developing countries have remained to depend on medicinal plants for principal health care and home medication. The well-known species *Piper nigrum* L. (black pepper*), Piper betle* L. (betel), *Piper longum* L. (long pepper), *Piper methysticum* G. Forst. (kava) and *Piper cubeba* Bojer (cubeb) had been brought up to the highest level of use into a variety of fields and industries, including pharmaceutical botany, traditional medicine, aromatic industries, foods, and landscaping [58].

Figure 1.3: Photos of *Piper sarmentosum* Roxb. (**A**) *P. sarmentosum* plant and (**B**) fruits (Photos taken from greenhouse Gondwanaland area in Leipzig Zoological Garden)

Piper sarmentosum Roxb. (Piperaceae) is a creeping plant whose vernacular name varies from country to country (Figure 1.3). It is known as *Kaduk* and *Pokok Kadok* in Malaysia, *Chaplu* in Thailand, *Sirih duduk, Akar buguor* or *Mengkadak* in Indonesia, *Bolalot* in Vietnam and *Jiaju, Gelou, Jialou* and *Shanlou* in China [59-61]. This plant species is widely distributed in Northeast India, Southeast Asia, and parts of China and has been commonly used in traditional medicine and food flavouring agents [62,63]. In Malaysia, the plant is also eaten raw as vegetable*,* and the leaves are boiled in water and taken to relieve fever in malaria and treat coughs, flu, and rheumatism [64]. Furthermore, the whole plant, roots, leaves and fruits of *P. sarmentosum* has been used to treat colds, gastritis, rheumatoid joint pain, abdominal pain, toothache, diabetes mellitus and other diseases for many decades [65].

Modern pharmacological studies have shown that crude extracts of *P. sarmentosum* possess a wide range of biological activities such as antibacterial and anti-fungal [66,67], anti-osteoporosis [68,69], anti-depression and neuroprotective [70,71], anti-inflammatory [72,73], anti-cancer [74], hypoglycemic [75], insecticidal [76,77], and antihypertensive activities [78,79]. Furthermore, various of its chemical constituents, including essential oils, alkaloids, flavonoids, lignans and steroids, have been isolated mostly from the leaves and aerial parts of *P. sarmentosum* [65]. Thus, knowledge of the structural diversity of *P. sarmentosum* gave an impetus reason for finding new exciting compounds and activities, which was conducted in this study.

1.4.2   *Peperomia obtusifolia* (L.) A.Dietr.

The *Peperomia* species are found mainly in humid or mountainous forests in South and Central America, Asia, Africa, and Oceania [51]. The plants are valuable as ornamental plants, and several medicinal uses were described, but phytochemical constituents are poorly investigated compared to Piper species [54]. The most chemically studied is *Peperomia pellucida* (L.) Kunth due to its worldwide distribution and various applications in traditional medicine [80-82]. However, in our present study, we focused on another species, *Peperomia obtusifolia* (L.) A.Dietr (Figure 1.4).

Peperomia obtusifolia is well-known as an ornamental plant due to beautiful succulent leaves, which vary in shape and variegation present in many of its diverse varieties [83,84]. It is characterized by oblong, glossy green foliage and has short, somewhat brittle stems.

The plant is mainly distributed from Mexico to the northern part of South America and largely cultivated elsewhere. It prevalently is known as baby rubber or paragua plant. Despite its dominating decorative use, some communities in Central America use this plant to treat insect and snake bites and as a skin cleanser [85]. Previous studies on *P. obtusifolia* resulted in the isolation of chromanes, flavonoids, lignans and other secondary metabolites [86-90]. In addition, a few biological activities were described for compounds isolated from this species, such as trypanocidal [87], anti-inflammatory [91], and antibacterial activities [90]. The fruit stems have a strong lovage smell (Liebstöckel, "Maggi").

Figure 1.4: Photo of *Peperomia obtusifolia* (L.) A.Dietr. (Taken from IPB's ornamental plant)

1.5   Significance of research

Piperaceae is the most archaic family of pantropical flowering plants, with nearly 4000 species. Many of these species have economic and social significance with valuable culinary spices and traditional medicine. Even though a few species have been highly investigated, as discussed above (**1.4.1** and **1.4.2**), the vast majority of Piperaceae species have not yet been explored chemically. Among the species that have not been investigated intensively are *Piper sarmentosum* Roxb. and *Peperomia obtusifolia* (L.) A.Dietr.

A comprehensive review study on *P. sarmentosum* has been reported only recently (in parallel to this work) and demonstrated that more than 140 phytochemicals had been isolated and identified [65]. Most of the isolated phytochemicals of this plant were collected from different geographical regions such as Vietnam, Thailand and China. Regarding bioactivities, most of the literature data only provide the biological screening of extracts or fractions, i.e. as a complex mixture of secondary metabolites, which does not allow the identification of the active compounds. In the context of *P. obtusifolia*, only a few studies have been reported for its phytochemicals and biological activities.

Despite the fact that *P. sarmentosum* is widely distributed in Malaysia, only a few publications relating to its isolation by Malaysian researchers have been reported. Thus, as a country endowed with vast biodiversity resources and designated as one of the biodiversity hotspots, high-value herbal products have been identified as one of the key areas of Malaysia's emerging bio-economy. As initiative areas, Malaysia has listed several potential plants, including *P. sarmentosum*, to emphasize the herbal's scientific content toward nutraceutical claims and high-value botanical drugs [92].

Based on the above reports, there is an urgent need to explore the phytochemicals of the selected Piperaceae species', *Piper sarmentosum* and *Peperomia obtusifolia,* using modern techniques in isolation of novel compounds from these species. In addition, the comparative analysis of organ-specific metabolite profiles, especially *P. sarmentosum,* is necessary in order to compare their metabolite variations. The biological activities of the phytoconstituents of *P. sarmentosum* and *P. obtusifolia* are similarly important to be investigated for developing pharmaceutical and herbal formulation documentation.

1.6 Aims and scope of the study

The general objective of the present thesis was to isolate and characterize the bioactive phytochemicals from two species of Piperaceae medicinal plants and further in-depth investigation of the secondary metabolites profiles using LC-ESI-HRMS as advanced analytical technique.

In particular, the following aspects were covered within these investigations:

- Isolation, characterization and structural elucidation of secondary metabolites from selected members of the Piperaceae family, namely *Piper sarmentosum* and *Peperomia obtusifolia.*
- Bioactivity screening of extracts and isolated compounds for the evaluation as potential sources of new bioactive natural products.
- Characterization and comparison of secondary metabolites from different organs of *Piper sarmentosum.*
- The interpretation of fragmentation pathways obtained from high-resolution mass spectrometry experiments for metabolite annotation.

1.7 References

1. Brummitt, N.; Araújo, A.C.; Harris, T., Areas of plant diversity—What do we know? *Plants, People, Planet*. **2021**, 3, 33-44.
2. Cragg, G.M.; Newman, D.J., Natural products: a continuing source of novel drug leads. *Biochim. Biophys. Acta*. **2013**, 1830, 3670-95.
3. Sneader, W., Herbals. In: Sneader W, editor. *Drug Discovery: A history* **2005**.
4. Parham, S.; Kharazi, A.Z.; Bakhsheshi-Rad, H.R.; Nur, H.; Ismail, A.F.; Sharif, S.; *et* al., Antioxidant, antimicrobial and antiviral properties of herbal materials. *Antioxidants* **2020**, 9, 1309.
5. Bisi-Johnson, M.A.; Obi, C.L.; Samuel, B.B.; Eloff, J.N.; Okoh, A.I., Antibacterial activity of crude extracts of some South African medicinal plants against multidrug resistant etiological agents of diarrhoea. *BMC Complement. Alternative. Med*. **2017**, 17, 321.
6. Ribeiro, V.P.; Arruda, C.; Abd El-Salam, M.; Bastos, J.K., Brazilian medicinal plants with corroborated anti-inflammatory activities: a review. *Pharm. Biol*. **2018**, 56, 253-68.
7. Seyyedan, A.; Yahya, F.; Kamarolzaman Mohammad Fauzi, F.; Suhaili, Z.; Desa Mohd Nasir, M.; Khairi Hussain, M.; *et* al., Review on the ethnomedicinal, phytochemical and pharmacological properties of *Piper sarmentosum*: scientific justification of its traditional use. *CellMed*. **2013**, 3, 19.1-.32.
8. Majolo, F.; de Oliveira Becker Delwing, L.K.; Marmitt, D.J.; Bustamante-Filho, I.C.M.; Goettert, M.I., Medicinal plants and bioactive natural compounds for cancer treatment: Important advances for drug discovery. *Phytochem. Lett*. **2019**, 31, 196-207.
9. Atanasov, A. G.; Zotchev, S. B.; Dirsch, V. M.; Orhan, I. E.; Banach, M.; Rollinger, J. M.; Barreca, D.; Weckwerth, W.; Bauer, R.; Bayer, E. A.; Majeed, M.; Bishayee, A.; Bochkov, V.; Bonn, G. K.; Braidy, N.; Bucar, F.; Cifuentes, A.; D'Onofrio, G.; Bodkin, M.; Diederich, M.; Dinkova-Kostova, A. T.; Efferth, T.; El Bairi, K.; Arkells, N.; Fan, T.-P.; Fiebich, B. L.; Freissmuth, M.; Georgiev, M. I.; Gibbons, S.; Godfrey, K. M.; Gruber, C. W.; Heer, J.; Huber, L. A.; Ibanez, E.; Kijjoa, A.; Kiss, A. K.; Lu, A.; Macias, F. A.; Miller, M. J. S.; Mocan, A.; Müller, R.; Nicoletti, F.; Perry, G.; Pittalà, V.; Rastrelli, L.; Ristow, M.; Russo, G. L.; Silva, A. S.; Schuster, D.; Sheridan, H.; Skalicka-Woźniak, K.; Skaltsounis, L.; Sobarzo-Sánchez, E.; Bredt, D. S.; Stuppner, H.; Sureda, A.; Tzvetkov, N. T.; Vacca, R. A.; Aggarwal, B. B.; Battino, M.; Giampieri, F.; Wink, M.; Wolfender, J.-L.; Xiao, J.; Yeung, A. W. K.; Lizard, G.; Popp, M. A.; Heinrich, M.; Berindan-Neagoe, I.; Stadler, M.; Daglia, M.; Verpoorte, R.; Supuran, C. T.; the International Natural Product Sciences, T., Natural products in drug discovery: Advances and opportunities. *Nat. Rev. Drug Discov*. **2021,** 20, 200-216.10. Salmeron-Manzano, E.; Garrido-Cardenas, J.A.; Manzano-Agugliaro, F., Worldwide research trends on medicinal plants. *Int. J. Environ. Res. Public Health* **2020**, 17, 3376
11. Newman, D.J.; Cragg, G.M., Natural products as sources of new drugs over the nearly four decades from 01/1981 to 09/2019. *J. Nat. Prod*. **2020**, 83, 770-803.
12. Nile, S.H.; Kai, G.Y., Recent clinical trials on natural products and traditional Chinese medicine combating the COVID-19. *Indian J. Microbiol*. **2021**, 61, 10-15.
13. Ghareeb, M.A.; Tammam, M.A.; El-Demerdash, A.; Atanasov, A.G., Insights about clinically approved and preclinically investigated marine natural products. *Curr. Res. Biotechnol*. **2020**, 2, 88-102.
14. Sadeghi-aliabadi, H.; Yegdaneh, A., Taxol and related compounds. In: Ramawat, K.G.; Mérillon, J.M.; editors. Natural products: Phytochemistry, botany and metabolism of alkaloids, phenolics and terpenes. Berlin, Heidelberg: *Springer* Berlin Heidelberg; **2013**. p. 3159-3171.
15. Achan, J.; Talisuna, A.O.; Erhart, A.; Yeka, A.; Tibenderana, J.K.; Baliraine, F.N.; *et* al., Quinine, an old anti-malarial drug in a modern world: role in the treatment of malaria. *Malar. J*. **2011**, 10, 144.
16. Van Voorhis, W.C.; Hooft van Huijsduijnen, R.; Wells, T.N.C., Profile of William C. Campbell, Satoshi Ōmura, and Youyou Tu, 2015 Nobel Laureates in physiology or medicine. *Proc. Natl. Acad. Sci. U S A*. **2015**, 112, 15773-6.
17. Śramska, P.; Maciejka, A.; Topolewska, A.; Stepnowski, P.; Haliński, Ł.P., Isolation of atropine and scopolamine from plant material using liquid-liquid extraction and EXtrelut® columns. *J. Chromatogr. B Analyt. Technol. Biomed. Life Sci*. **2017**, 1043, 202-208.

18. Kwakye, G.F.; Jiménez, J.; Jiménez, J.A.; Aschner, M., *Atropa belladonna* neurotoxicity: Implications to neurological disorders. Food Chem *Toxicol*. **2018**, 116, 346-353.
19. Pathan, H.; Williams, J., Basic opioid pharmacology: an update. *Br. J. Pain*. **2012**, 6, 11-16.
20. Heinrich, M., Galanthamine from *Galanthus* and other Amaryllidaceae-chemistry and biology based on traditional use. *Alkaloids Chem. Biol*. **2010**, 68, 157-165.
21. Demarque, D.P.; Dusi, R.G.; de Sousa, F.D.M.; Grossi, S.M.; Silverio, M.R.S.; Lopes, N.P.; *et* al., Mass spectrometry-based metabolomics approach in the isolation of bioactive natural products. *Sci. Rep*. **2020**, 10, 1051.
22. Espindola, L.S.; Dusi, R.G.; Demarque, D.P.; Braz, R.; Yan, P.C.; Bokesch, H.R.; *et* al., Cytotoxic triterpenes from *Salacia crassifolia* and metabolite profiling of Celastraceae species. *Molecules* **2018**, 23, 1494.
23. Atanasov, A.G.; Waltenberger, B.; Pferschy-Wenzig, E.M.; Linder, T.; Wawrosch, C.; Uhrin, P.; *et* al., Discovery and resupply of pharmacologically active plant-derived natural products: A review. *Biotechnol. adv*. **2015**, 33, 1582-1614.
24. Hostettmann, K.; Wolfender, J.L.; Terreaux, C., Modern screening techniques for plant extracts. *Pharm. Biol*. **2001**, 39, 18-32.
25. Castelli, F.A.; Rosati, G.; Moguet, C.; Fuentes, C.; Marrugo-Ramírez, J.; Lefebvre, T.; *et* al., Metabolomics for personalized medicine: the input of analytical chemistry from biomarker discovery to point-of-care tests. *Anal. Bioanal. Chem*. **2022**, 414, 759-789.
26. Oliver, S.G.; Winson, M.K.; Kell, D.B.; Baganz, F., Systematic functional analysis of the yeast genome. *Trends Biotechnol*. **1998**, 16, 373-378.
27. Guillotin, S.; Delcourt, N., Marine neurotoxins' effects on environmental and human health: An OMICS overview. *Mar. Drugs*. **2021**, 20.18.
28. Deborde, C.; Moing, A.; Roch, L.; Jacob, D.; Rolin, D.; Giraudeau, P., Plant metabolism as studied by NMR spectroscopy. *Prog. Nucl. Magn. Reson. Spectrosc*. **2017**, 102-103, 61-97.
29. Cambiaghi, A.; Ferrario, M.; Masseroli, M., Analysis of metabolomic data: tools, current strategies and future challenges for omics data integration. *Brief Bioinform*. **2017**, 18, 498-510.
30. Braga, C.P.; Adamec J., Metabolome analysis. *Encycl. Bioinform. Comput. Biol. ABC Bioinforma*. **2018**. p. 463-475.
31. Roberts, L.D.; Souza, A.L.; Gerszten, R.E.; Clish, C.B., Targeted metabolomics. Curr Protoc *Mol. Biol.* **2012**, 30, 2.1-24.
32. Anderson, B.G.; Raskind, A.; Habra, H.; Kennedy, R.T.; Evans, C.R., Modifying chromatography conditions for improved unknown feature identification in untargeted metabolomics. *Anal. Chem*. **2021**, 93, 15840-9.
33. Beger, R.D.; Dunn, W.B.; Bandukwala, A.; Bethan, B., Broadhurst, D.; Clish, C.B.; *et* al., Towards quality assurance and quality control in untargeted metabolomics studies. *Metabolomics* **2019**, 15, 4.
34. Pinu, F.R.; Goldansaz, S.A.; Jaine, J., Translational metabolomics: Current challenges and future opportunities. *Metabolites* **2019**, 9, 108
35. Szeremeta, M.; Pietrowska, K.; Niemcunowicz-Janica, A.; Kretowski, A.; Ciborowski, M., Applications of metabolomics in forensic toxicology and forensic medicine. *Int. J. Mol. Sci.* **2021**, 22, 3010.
36. Cao, H.; Ji, Y.; Li, S.C.; Lu, L.; Tian, M.; Yang, W.; *et* al., Extensive metabolic profiles of leaves and stems from the medicinal plant *Dendrobium officinale* Kimura et Migo. *Metabolites* **2019**, 9, 215.
37. Dossou, S.S.K.; Xu, F.T.; Cui, X.H.; Sheng, C.; Zhou, R.; You, J.; *et* al., Comparative metabolomics analysis of different sesame (*Sesamum indicum* L.) tissues reveals a tissue-specific accumulation of metabolites. *BMC Plant Biol*. **2021**, 21, 352.
38. Olas, J.J.; Apelt, F.; Watanabe, M.; Hoefgen, R.; Wahl, V., Developmental stage-specific metabolite signatures in *Arabidopsis thaliana* under optimal and mild nitrogen limitation. *Plant Sci*. **2021**, 303, 110746.
39. Miggiels, P.; Wouters, B.; Van Westen, G.J.P.; Dubbelman, A.C.; Hankemeier, T., Novel technologies for metabolomics: More for less. *TrAC Trend Anal. Chem.* **2019**, 120, 115323.
40. Agregan, R.; Echegaray, N.; Nawaz, A.; Hano, C.; Gohari, G.; Pateiro, M.; *et* al., Foodomic-based approach for the control and quality improvement of dairy products. *Metabolites* **2021**, 11, 818.

41. Markley, J.L.; Bruschweiler, R.; Edison, A.S.; Eghbalnia, H.R.; Powers, R.; Raftery, D.; *et* al., The future of NMR-based metabolomics. *Curr. Opin. Biotech*. **2017**, 43, 34-40.

42. Ren, J.L.; Zhang, A.H.; Kong, L.; Wang, X.J., Advances in mass spectrometry-based metabolomics for investigation of metabolites. *RSC Adv*. **2018**, 8, 22335-50.

43. Saesong, T.; Allard, P.M.; Ferreira Queiroz, E.; Marcourt, L.; Nuengchamnong, N.; Temkitthawon, P.; *et* al., Discovery of lipid peroxidation inhibitors from *Bacopa* Species prioritized through multivariate data analysis and multi-informative molecular networking. *Molecules* **2019**, 24, 2989.

44. Brigante, F.I.; Podio, N.S.; Wunderlin, D.A.; Baroni, M.V., Comparative metabolite fingerprinting of chia, flax and sesame seeds using LC-MS untargeted metabolomics. *Food Chem*. **2022**, 371, 131355.

45. Wu, C.; Wang, H.; Liu, Z.; Xu, B.; Li, Z.; Song, P.; *et* al., Untargeted metabolomics coupled with chemometrics for leaves and stem barks of dioecious *Morus alba* L. *Metabolites* **2022**, 12, 106.

46. Elhawary, E.A.; Mostafa, N.M.; Labib, R.M.; Singab, A.N., Metabolomic profiles of essential oils from selected rosa varieties and their antimicrobial activities. *Plants* **2021**, 10, 1721.

47. Lever, J.; Krzywinski, M.; Altman, N., Principal component analysis. *Nat Methods*. 2017, 14, 641-642.

48. Oyemitan, I.A., African medicinal spices of genus *Piper*. In: Kuete V, editor. Medicinal spices and vegetables from Africa: *Academic Press*; **2017**. p. 581-597.

49. Reed, K.; Leleković, T., First evidence of rice (*Oryza cf. sativa* L.) and black pepper (*Piper nigrum*) in Roman Mursa, Croatia. *Archaeol. Anthropol. Sci*. **2019**, 11, 271-278.

50. Takooree, H.; Aumeeruddy, M.Z.; Rengasamy, K.R.R.; Venugopala, K.N.; Jeewon, R.; Zengin, G.; *et* al., A systematic review on black pepper (*Piper nigrum* L.): from folk uses to pharmacological applications. *Crit. Rev. Food Sci*. **2019**, 59, S210-S243.

51. Wanke, S.; Samain, M.S.; Vanderschaeve, L.; Mathieu, G.; Goetghebeur, P.; Neinhuis, C., Phylogeny of the genus *Peperomia* (Piperaceae) inferred from the trnK/matK Region (cpDNA). *Plant Biol*. **2006**, 8, 93-102.

52. Simmonds, S.E.; Smith, J.F.; Davidson, C.; Buerki, S., Phylogenetics and comparative plastome genomics of two of the largest genera of angiosperms, *Piper* and *Peperomia* (Piperaceae). *Mol. Phylogenet. Evol*. **2021**, 163, 107229.

53. Suwanphakdee, C.; Chantaranothai, P., A new species and three taxonomic changes in *Piper* (Piperaceae) from Thailand. *Blumea.* **2011**, 56, 235-239.

54. Gutierrez, Y.V.; Yamaguchi, L.F.; de Moraes, M.M.; Jeffrey, C.S.; Kato, M.J., Natural products from *Peperomia*: occurrence, biogenesis and bioactivity. *Phytochem. Rev*. **2016**, 15, 1009-1033.

55. Wanke, S.; Jaramillo, M.A.; Borsch, T.; Samain, M.S.; Quandt, D.; Neinhuis, C., Evolution of Piperales—matK gene and trnK intron sequence data reveal lineage specific resolution contrast. *Mol. Phylogenet. Evol*. **2007**, 42, 477-497.

56. Kumar, S.; Kamboj, J.; Suman Sharma, S., Overview for various aspects of the health benefits of *Piper longum* Linn. Fruit. *J. Acupunct. Meridian Stud*. **2011**, 4, 134-140.

57. Palchetti, E.; Biricolti, S.; Gori, M.; Rota Nodari, G.; Gandolfi, N., Papini, A., Two new Malagasy species of genus *Piper* L. (Piperaceae), *Piper malgassicum* and *Piper tsarasotrae* , and their phylogenetic position. *Turk. J. Bot*. **2018**, 42, 610-622.

58. Salehi, B.; Zakaria, Z.A.; Gyawali, R.; Ibrahim, S.A.; Rajkovic, J.; Shinwari, Z.K.; *et* al., *Piper* species: A comprehensive review on their phytochemistry, biological activities and applications. *Molecules* **2019**, 24, 1364.

59. Rukachaisirikul, T.; Siriwattanakit, P.; Sukcharoenphol, K.; Wongvein, C.; Ruttanaweang, P.; Wongwattanavuch, P.; *et* al., Chemical constituents and bioactivity of *Piper sarmentosum*. *J. Ethnopharmacol*. **2004**, 93, 173-176.

60. Ismail, S.M.; Sundar, U.M.; Hui, C.K.; Aminuddin, A.; Ugusman, A., *Piper sarmentosum* attenuates TNF-alpha-induced VCAM-1 and ICAM-1 expression in human umbilical vein endothelial cells. *J. Taibah. Univ. Med. Sci*. **2018**, 13, 225-231.

61. Atiax, E.; Ahmad, F.; Sirat, H.; Arbain, D., Antibacterial activity and cytotoxicity screening of sumatran Kaduk (*Piper sarmentosum* Roxb.). *Iran. J. Pharmacol. Ther*. **2011**, 10, 1-5.

62. Sim, K.M.; Mak, C.N.; Ho, L.P., A new amide alkaloid from the leaves of *Piper sarmentosum*. *J. Asian Nat. Prod. Res*. **2009**, 11, 757-760.

63. Burkill, I.H.; Birtwistle, W.; Foxworthy, F.W.; Scrivenor, J.B.; Watson, J.G., A dictionary of the economic products of the Malay Peninsula: governments of Malaysia and Singapore by the Ministry of Agriculture and cooperatives; **1966**.

64. Ab Rahman, M.R.; Abdul Razak, F.; Mohd Bakri, M., Evaluation of wound closure activity of *Nigella sativa, Melastoma malabathricum, Pluchea indica*, and *Piper sarmentosum* extracts on scratched monolayer of human gingival fibroblasts. *Evid. Based Complement. Alternat. Med.* **2014**, 2014, 190342.

65. Sun, X.; Chen, W.; Dai, W.; Xin, H.; Rahmand, K.; Wang, Y., *et al.*, *Piper sarmentosum* Roxb.: A review on its botany, traditional uses, phytochemistry, and pharmacological activities. *J. Ethnopharmacol.* **2020**, 263, 112897.

66. Rahman, S.F.S.A.; Omar, D., Development of bio-formulations of *Piper sarmentosum* extracts against bacterial rice diseases. *Curr. Biotechnol.* **2018**, 8, 453-463.

67. Chaimanee, V.; Thongtue, U.; Sornmai, N.; Songsri, S.; Pettis, J.S., Antimicrobial activity of plant extracts against the honeybee pathogens, *Paenibacillus larvae* and *Ascosphaera apis* and their topical toxicity to *Apis mellifera* adults. *J. Appl. Microbiol.* **2017**, 123, 1160-1167.

68. Estai, M.A.; Soelaiman, I.N.; Shuid, A.N.; Das, S.; Ali, A.M.; Suhaimi, F.H., Histological changes in the fracture callus following the administration of water extract of *Piper sarmentosum* (daun kadok) in estrogen-deficient rats. *Iran. J. Med. Sci.* **2011**, 36, 281-288.

69. Ramli, E.S.M.; Soelaiman, I.N.; Othman, F.; Ahmad, F.; Shuib, A.N.; Mohamed, N.; *et al.*, The effects of *Piper sarmentosum* water extract on the expression and activity of 11beta-hydroxysteroid dehydrogenase type 1 in the bones with excessive glucocorticoids. *Iran. J. Med. Sci.* **2012**, 37, 39-46.

70. Khan, M.; Elhussein, S.A.A.; Khan, M.M.; Khan, N., Anti-acetylcholinesterase activity of *Piper sarmentosum* by a continuous immobilized-enzyme assay. *APCBEE Procedia.* **2012**, 2, 199-204.

71. Li, Q.; Qu, F.L.; Gao, Y.; Jiang, Y.P.; Rahman, K.; Lee, K.H.; *et al.*, *Piper sarmentosum* Roxb. produces antidepressant-like effects in rodents, associated with activation of the CREB-BDNF-ERK signaling pathway and reversal of HPA axis hyperactivity. *J. Ethnopharmacol.* **2017**, 199, 9-19.

72. Yeo, E.T.Y.; Wong, K.W.L.; See, M.L.; Wong, K.Y.; Gan, S.Y.; Chan, E.W.L., *Piper sarmentosum* Roxb. confers neuroprotection on beta-amyloid (Abeta)-induced microglia-mediated neuroinflammation and attenuates tau hyperphosphorylation in SH-SY5Y cells. *J. Ethnopharmacol.* **2018**, 217, 187-194.

73. Azlina, M.F.N.; Qodriyah, H.M.S.; Akmal, M.N.; Ibrahim, I.A.A.; Kamisah, Y., In vivo effect of *Piper sarmentosum* methanolic extract on stress-induced gastric ulcers in rats. *Arch. Med. Sci.* **2019**, 15, 223-231.

74. Ariffin, S.H.Z.; Wan Omar, W.H.; Ariffin, Z.Z.; Safian, M.F.; Senafi, S.; Abdul Wahab, R.M., Intrinsic anticarcinogenic effects of *Piper sarmentosum* ethanolic extract on a human hepatoma cell line. *Cancer Cell Int.* **2009**, 9, 6.

75. Krisanapun, C.; Wongkrajang, Y.; Temsiririrkkul, R.; Phornchirasilp, S.; Peungvicha, P., In vitro evaluation of anti-diabetic potential of *Piper sarmentosum* Roxb. extract. *FASEB J.* **2012**, 26, 686.7-7.

76. Hematpoor, A.; Paydar, M.; Liew, S.Y.; Sivasothy, Y.; Mohebali, N.; Looi, C.Y.; *et al.*, Phenylpropanoids isolated from *Piper sarmentosum* Roxb. induce apoptosis in breast cancer cells through reactive oxygen species and mitochondrial-dependent pathways. *Chem. Biol. Interact.* **2018**, 279, 210-218.

77. Baba, M.S.; Hassan, Z.A.A., *Piper Sarmentosum* leaf as a promising non-toxic antiparasitic agent against trypanosoma evansi-induced mice. *Malays. J. Microsc.* **2019**, 15, 46-60.

78. Mohd Zainudin, M.; Zakaria, Z.; Megat Mohd Nordin, N.A., The use of *Piper sarmentosum* leaves aqueous extract (Kadukmy™) as antihypertensive agent in spontaneous hypertensive rats. *BMC Complement. Altern. Med.* **2015**, 15, 54.

79. Fauzy, F.H.; Mohd Zainudin, M.; Ismawi, H.R.; Elshami, T.F.T., *Piper sarmentosum* leaves aqueous extract attenuates vascular endothelial dysfunction in spontaneously hypertensive rats. *Evid. Based Complement. Alternat. Med.* **2019**, 2019, 7198592.

80. Ng, Z.X.; Than, M.J.Y.; Yong, P.H., *Peperomia pellucida* (L.) Kunth herbal tea: Effect of fermentation and drying methods on the consumer acceptance, antioxidant and anti-inflammatory activities. *Food Chem.* **2021**, 344, 128738.

81.   de Moraes, M.M.; Kato, M.J., Biosynthesis of Pellucidin A in *Peperomia pellucida* (L.) HBK. *Front. Plant Sci*. **2021**, 12, 641717.

82.   Alves, N.S.F.; Setzer, W.N.; da Silva, J.K.R., The chemistry and biological activities of *Peperomia pellucida* (Piperaceae): A critical review. *J. Ethnopharmacol*. **2019**, 232, 90-102.

83.   Ilyas, S.; Naz, S.; Aslam, F.; Parveen, Z.; Ali, A., Chemical composition of essential oil from in vitro grown *Peperomia Obtusifolia* through GC-MS. *Pak. J. Bot*. **2014**, 46, 667-672.

84.   Shen, G.W.; Seeley, J.G., The effect of shading and nutrient supply on variegation and vutrient content of variegated cultivars of *Peperomia obtusifolia*. *J. Am. Soc. Hortic. Sci*. **1983**, 108, 429-433.

85.   Batista, A.N.L.; Santos-Pinto, J.; Batista, J.M. Jr.; Souza-Moreira, T.M.; Santoni, M.M.; Zanelli, C.F.; *et* al., The combined use of proteomics and transcriptomics reveals a complex secondary metabolite network in *Peperomia obtusifolia*. *J. Nat. Prod*. **2017**, 80, 1275-1286.

86.   Tanaka, T.; Asai, F.; Iinuma, M., Phenolic compounds from *Peperomia obtusifolia. Phytochemistry* **1998**, 49, 229-32.

87.   da Silva Mota, J.; Leite, A.C.; Batista Junior, J.M.; Noeli Lopez, S.; Luz Ambrosio, D.; Duo Passerini, G.; *et* al., In vitro trypanocidal activity of phenolic derivatives from *Peperomia obtusifolia. Planta Med*. **2009**, 75, 620-623.

88.   Mota, J.S.; Leite, A.C.; Kato, M.J.; Young, M.C.; Bolzani Vda, S.; Furlan, M., Isoswertisin flavones and other constituents from *Peperomia obtusifolia. Nat. Prod. Res*. **2011**, 25, 1-7.

89.   Batista, J.M.; Batista, A.N.L.; Kato, M.J.; Bolzani, V.S.; Lopez, S.N.; Nafie, L.A.; *et* al., Further monoterpene chromane esters from *Peperomia obtusifolia*: VCD determination of the absolute configuration of a new diastereomeric mixture. *Tetrahedron Lett*. **2012**, 53, 6051-6054.

90.   Ruiz Mostacero, N.; Castelli, M.V.; Cutro, A.C.; Hollmann, A.; Batista, J.M. Jr.; Furlan, M.; *et* al., Antibacterial activity of prenylated benzopyrans from *Peperomia obtusifolia* (Piperaceae). *Nat. Prod. Res*. **2019**, 1-5.

91.   Tamayose, C.I.; Romoff, P.; Toyama, D.O.; Gaeta, H.H.; Costa, C.R.C.; Belchor, M.N.; *et* al., Non-clinical studies for evaluation of 8-C-rhamnosyl apigenin purified from *Peperomia obtusifolia* against acute edema. *Int. J. Mol. Sci*. **2017**, 18, 1972

92.   Tan, T.Y.C.; Lee, J.C.; Yusof, N.A.M.; The, B.P.; Mohamed, A.F.S., Malaysian herbal monograph development and challenges. *J. Herb. Med*. **2020**, 23, 100380.

Chapter 2

-

Characterization and bioactive potential of secondary metabolites isolated from *Piper sarmentosum* Roxb.

Abstract*

Piper sarmentosum Roxb. (Piperaceae) is a traditional medicinal plant in South East Asian countries. The chemical investigation on this species resulted in the isolation of three previously not described compounds, namely 4"-(3-hydroxy-3-methylglutaroyl)-2"-β-D-glucopyranosyl vitexin (**2.1**), kadukoside (**2.2**), and 6-O-*trans-p*-coumaroyl-D-glucono-1,4-lactone (**2.3**), together with 31 known compounds. Of these known compounds, 21 compounds were isolated for the first time from *P. sarmentosum*. The structures of the compounds were established by 1D and 2D NMR techniques and HREIMS analyses. The compounds were evaluated for their anthelmintic (against *Caenorhabditis elegans*), antifungal (against *Botrytis cinerea*, *Septoria tritici* and *Phytophthora infestans*), cytotoxic (against PC-3 and HT-29 human cancer cells lines), antibacterial (against *Aliivibrio fischeri*) and neuroprotective (against Aβ-deposition in an astrocyte cell assay) activities. Based on our biological screening, three of these isolated compounds namely, methyl 3-(4-methoxyphenyl)propionate (**2.8**), isoasarone (**2.12**), and *trans*-asarone (**2.15**) have demonstrated anthelmintic activity against *Caenorhabditis elegans* with IC_{50} values ranging from 0.9 to 2.04 mM. Furthermore, kadukoside (**2.2**) was most active against *S. tritici* with IC_{50} at 5.0 ± 0.02 µM. Kadukoside (**2.2**) also induced 94% inhibition of pathogen growth of *P. infestans* by treating it at a concentration of 125 µM. Moreover, *trans*-asarone (**2.15**), piperolactam A (**2.23**), and dehydroformouregine (**2.24**) displayed a dose-dependent effect against the fungus *B. cinerea* from 1.5 to 125 µM, with more than 80% inhibition at a concentration of 125 µM. Additionally, five compounds, aristolactam B II (**2.22**), dehydroformouregine (**2.24**), magnosalicin (**2.30**), andamanicin (**2.31**), and magnosalin (**2.32**) exhibited cytotoxic effects against HT-29 and three compounds, cepharadione A (**2.21**), aristolactam B II (**2.22**) and piperolactam A (**2.23**) displayed cytotoxic activity against PC-3 cell lines at 10 µM. Moreover, paprazine (**2.19**), cepharadione A (**2.21**) and piperolactam A (**2.23**) inhibited bacterial growth of the gram negative *A. fischerii* by more than 85% at concentration of 100 µM and isoasarone (**2.12**), *trans*-asarone (**2.15**) and aristolactam BII (**2.22**) showed some neuroprotective potential.

16

2.1 Introduction

The Piperaceae family comprises numerous medicinal plants widely used in tropical and subtropical regions around the world. It consists of five genera namely *Verhuellia, Zippelia, Manekia, Piper and Peperomia* [1]. The most described being the *Piper* and *Peperomia* genera [1,2]. The *Piper* genus contains about 1000 - 2000 species with dominant species in their native habitat [3]. Many species of *Piper* have been used as traditional medicine, which have been applied to treat toothache, fever, chest, pain, cough, asthma, etc. [2]. Previous phytochemicals studies of the *Piper* genus resulted in the isolation of amide alkaloids, lignans, neolignans and phenylpropanoids as major phytochemical constituents [2,4]. These isolated compounds displayed a wide range of biological activities including antifungal, antitumor, anti-inflammatory and antioxidant activities [2,5-7].

Piper sarmentosum Roxb. (Piperaceae) is a creeping plant whose vernacular name varies from country to country. It is known as *Kaduk* and *Pokok Kadok* in Malaysia, *Chaplu* in Thailand, *Sirih duduk, Akar buguor* or *Mengkadak* in Indonesia, *Bolalot* in Vietnam and *Jiaju, Gelou, Jialou* and *Shanlou* in China [8-10]. This species is widely distributed in tropical countries in Northeast India, Southeast Asia and parts of China and has been commonly used in traditional medicine and also as food flavoring agents [11,12]. In Malaysia, the plant is also eaten raw as vegetable and the leaves are boiled in water and taken to relieve fever in malaria and treat coughs, flu, and rheumatism [13]. Furthermore, the whole plant, roots, leaves and fruits of *P. sarmentosum* has been used for the treatment of colds, gastritis, rheumatoid joint pain, abdominal pain, toothache, diabetes mellitus, worm infections and other diseases for many decades [14,15].

Modern pharmacological studies have shown that crude extracts of *P. sarmentosum* possess a wide range of biological activities such as antibacterial [16], anti-fungal [17], anti-osteoporosis [18,19], anti-depression and neuroprotective [20,21], anti-inflammatory [22,23], anti-cancer [24], hypoglycemic [25], insecticidal [26,27], and antihypertensive activities [28, 29]. A variety of chemical constituents, including essential oils, alkaloids, flavonoids, lignans and steroids, have been isolated mostly from the leaves and aerial parts of *P. sarmentosum* [14]. However, although a large number of chemical components have been isolated and identified from this species, only a few pure compounds have been studied with respect to their biological activity.

In the present study, we report the isolation, structure elucidation and biological effects of the previously undescribed compounds **2.1-2.3** along with 31 known compounds from the methanolic leaf extract of *P. sarmentosum*.

2.2 Results and discussion

The dried leaves of *P. sarmentosum* were extracted with 80% of methanol. The crude extract was suspended in H₂O and successively devided by liquid-liquid partition between water and *n*-hexane, ethyl acetate and *n*-butanol. The constituents were purified by semi-preparative HPLC and repeated column chromatography on silica gel, Sephadex LH20, RP and Diaion HP20; which yielded three hitherto undescribed compounds (**2.1-2.3**) together with 31 known compounds (Figure 2.1). The known compounds include eight alkaloids, three lignans, two flavonoids, two amides, twelve phenolics, two terpenes, and a mixture of sterols which were identified by spectroscopic analysis and comparison of the data obtained with literature values.
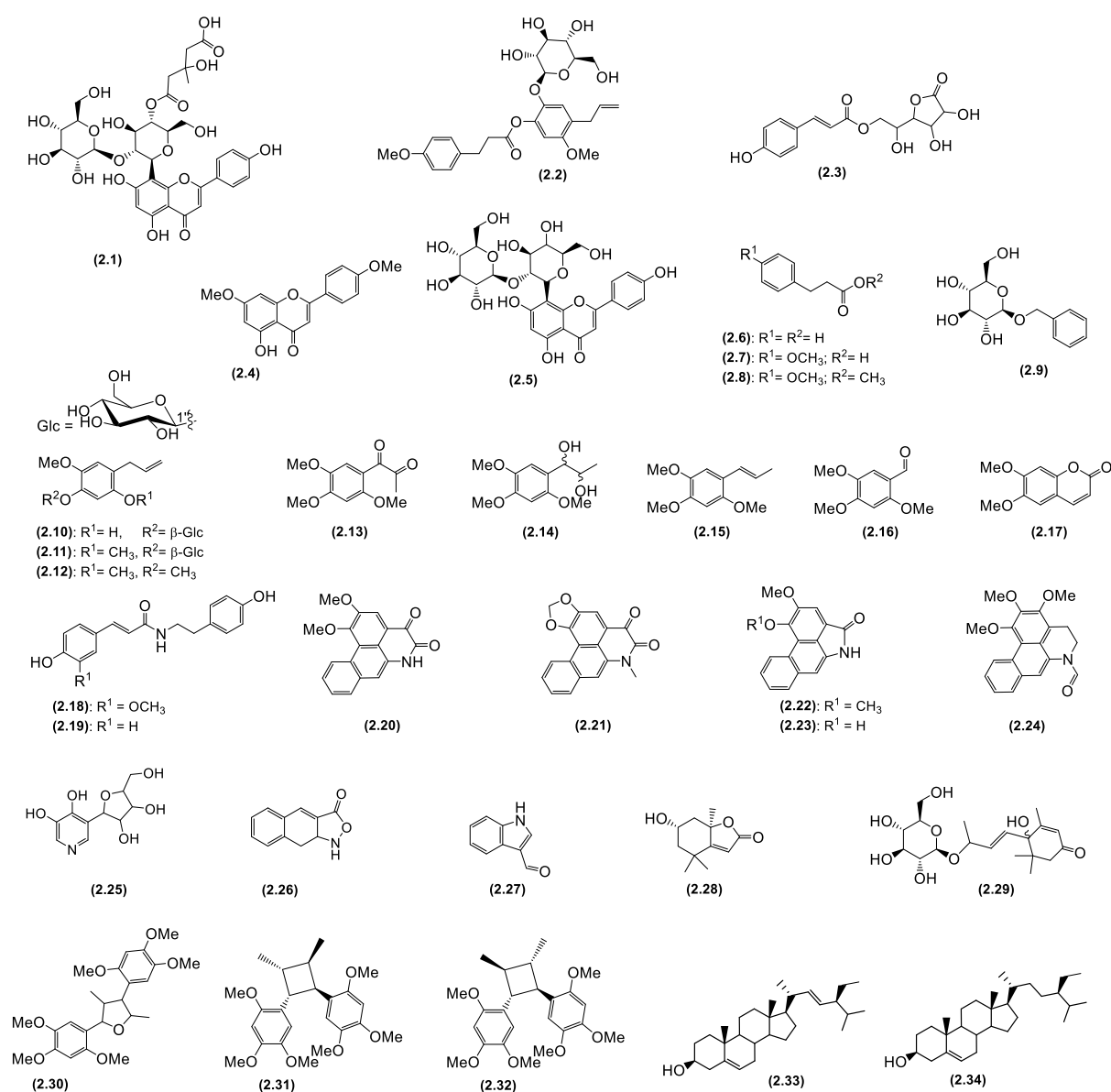
Figure 2.1: Chemical structures of isolated compounds from *P. sarmentosum*

Compound **2.1** was isolated as brownish liquid and has a molecular formula of $C_{33}H_{36}O_{19}$, which was deduced from the (-) HRESIMS [M-H]$^-$ ion at *m/z* 737.1937, calcd. for $C_{33}H_{37}O_{19}$ 737.1935. The ^{1}H-NMR and ^{13}C-NMR data (Table 2.1) indicate an olefinic signal at δ_H 6.62/ δ_C 103.6 which was typical of a H-3 flavone signal, an aromatic signal at δ_H 6.24/δ_C 99.4 that confirms the pentasubstituted status of ring A, two doublets at δ_H 8.04 (2H, d, *J* = 8.7 Hz, H-2′/6′) and δ_H 7.03 (2H, d, *J* = 8.7 Hz, H-3′/5′), typical of a A_2B_2 spin system on the ring B. Altogether, these data determined the aglycone component of **2.1** as apigenin structure [30]. The NMR data revealed a C-8 (or C-6)- substituted flavone comprising two anomeric sites resonating at (δ_H 5.09 / δ_C 73.8) and at (δ_H 4.26 / δ_C 105.3) that were diagnostic of their *C*-glycosylated and *O*-glycosylated status, respectively. The other signals between δ_H 2.76 and 5.26 can be assumed as caused by the protons of sugars. In addition, high field signals at δ_H 2.72, 2.73, 2.83 and 1.46 indicated the presence of some other substitute groups.

^{1}H and ^{13}C signals of **2.1** were further assigned by extensive analysis of HSQC, ^{1}H-^{1}H COSY and HMBC spectra (Figure 2.2). HMBC experiments show correlation between the anomeric proton δ_H 5.09 (H-1″) and apigenin C-7/9 confirming that the disaccharide is bound by a *C*-glycosidic linkage at C-8. A further HMBC correlation from the anomeric proton δ_H 4.26 (H-1‴) to C-2″ (δ_C 80.7) revealed the interglycosidic linkage (1→2). The large coupling constant of the anomeric protons ($J_{H-1″-H-2″}$ = 10.1 Hz and $J_{H-1‴-H-2‴}$ = 7.7 Hz) determined the *β*–configuration of both sugar moieties. The spectral data of **2.1** show similarity to those of 2″-glucosylvitexin (**2.5**) [31], with some differences at C-4″ of the gly-1 unit. The downfield chemicals shift of the gly-1 methin proton (Table 2.1) suggested acylation of the gly-1 unit at C-4. This proton signal was correlated in the HMBC spectrum with a carboxylic carbon at δ_C 172.2. The HSQC and HMBC spectra show this carboxyl to belong to an aliphatic acyl moiety, which is successively linked to a methylene group [δ_C 46.2; δ_H 2.73; 2.83], a central quaternary carbon (δ_C 70.9), another methylene group [δ_C 46.4; δ_H 2.72; 2.83], and a terminal carboxyl (δ_C 174.8). Additionally, the central quaternary carbon (C-3‴) shows a HMBC correlation with a methyl group at δ_H 1.46 (3H, s) and δ_C 27.7. Consequently, the aliphatic acyl moiety was identified as a 3-hydroxy-3-methylglutaroyl (HMG) substituent. The compound showed negative optical rotation of $[\alpha]_D^{24}$ -10.93 (*c* 0.15, CH_3OH). An isomeric flavone derivative with a similar structure to **2.1** was reported from flowers of *Trollius chinensis* (Ranunculaceae), however, with the HMG position located at C-6 of a gly-2 galactosyl unit [32]. On the basic of all these data, **2.1** was identified as 4″-(3-hydroxy-3-methylglutaroyl)-2″-*β*-D-glucopyranosyl vitexin.
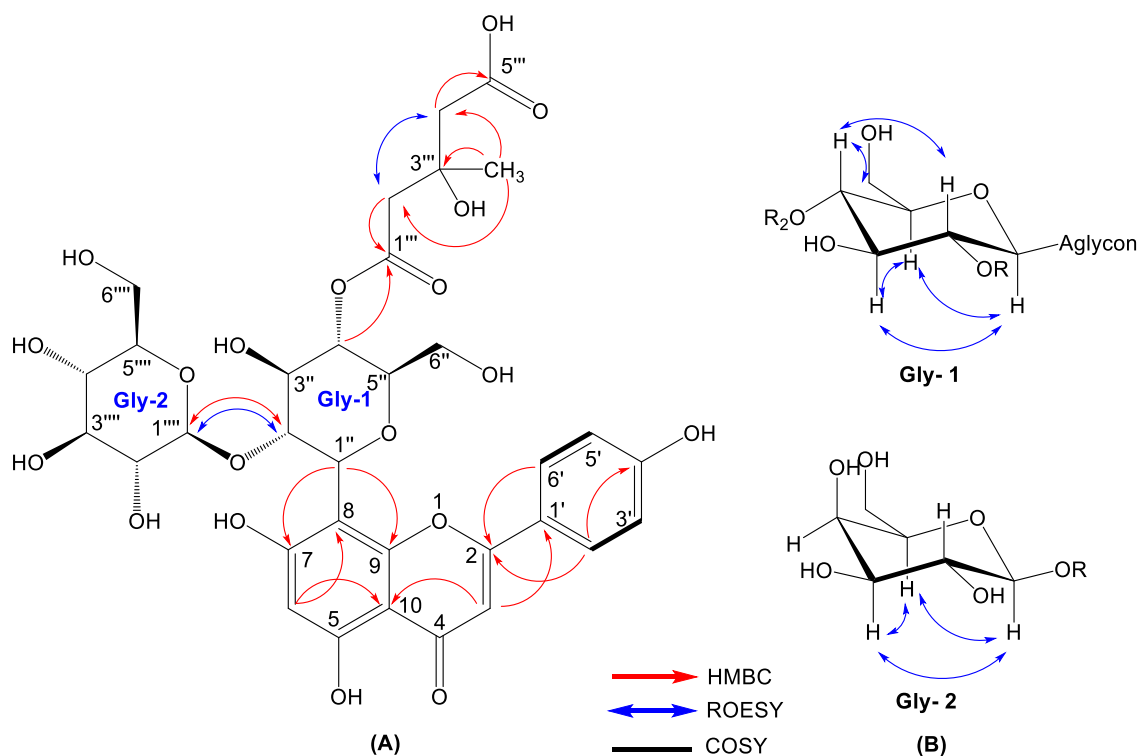
Figure 2.2: Detail of NMR characteristics of compound **2.1**. (**A**) Full structure; (**B**) Detail of ROESY correlation of glucose moieties.

Table 2.1. ^{1}H- and ^{13}C-NMR data of **2.1** (in CD$_3$OD; δ in ppm, *J* in Hz)

Pos.	δ$_H$[a], Mult. *J* (Hz)	δ$_C$[b]	Pos.	δ$_H$[a], Mult. *J* (Hz)	δ$_C$[b]
2		166.5	5″	3.66 m	80.7
3	6.62 s	103.6	6″A	3.77	62.7
4		184.2	6″B	3.67	62.7
5		162.7	1‴		172.2
6	6.24 s	99.4	2‴A	2.83	46.2
7		164.5	2‴B	2.73	46.2
8		104.9	3‴		70.9
9		158.2	4‴A	2.83	46.4
10		105.7	4‴B	2.72	46.4
1′		123.5	5‴		174.8
2′	8.04 d 8.7	130.1	3‴-CH$_3$	1.46 s	27.7
3′	7.03 d 8.7	117.2	1⁗	4.26 d 7.7	105.3
4′		162.9	2⁗	2.97 t 8.0	75.7
5′	7.03 d 8.7	117.2	3⁗	3.15 m	77.6
6′	8.04 d 8.7	130.1	4⁗	3.11 m	71.3
1″	5.09 d 10.1	73.8	5⁗	2.76 m	77.0
2″	4.42 t 9.4	80.7	6⁗A	3.41	62.4
3″	3.96 m	77.7	6⁗B	3.31	64.4
4″	5.26 t 9.6	72.7			

[a]) Recorded 400 MHz. [b]) Recorded at 100 MHz.

Compound **2.2** was obtained as a brownish liquid from the ethyl acetate fraction. The molecular formula was deduced to be C$_{26}$H$_{32}$O$_{10}$ based on the molecular ion peak at *m/z* 505.2036 ([M+H]$^+$, calcd. 505.2068) in the positive ion HR-ESI-MS. The NMR data of

compound **2.1** (Table 2.2) show the presence of an 3-(4-methoxyphenyl) propanoic acid moiety [33]. The structure of this part is the same as compound **2.7**. Furthermore, NMR spectroscopic data also revealed similarities to those of 4-allyl-2,5-dimethoxyphenol-1-*β*-D-glucopyranoside, **(2.11)** [34] indicating that both compounds possess a similar structural unit except for the position of the glycosyl moiety.

The HMBC long-range correlation (Fig. 2.3) gave cross-peak from the anomeric proton signal of the glycosyl moiety at $\delta = 4.58$ (H-1″) to C-2 (δ_C 140.1), from the aromatic protons singlet at $\delta = 6.98$ (H-3) to C-1 (δ_C 147.9) and C-5 (δ_C 155.3), from $\delta = 6.47$ (H-6) to C-2 (δ_C 140.1), and C-4 (δ_C 120.7) and from the aliphatic proton at $\delta = 3.22$ (H-7) to C-5 (δ_C 155.3) and C-3 (δ_C 121.8). This indicated that the glycosyl moiety is bound to C-2 and not at C-1 as found in **2.11.** This conclusion is supported by the NOESY correlation of H-1″ (δ_H 4.58) to H-3 (δ_H 6.98) and H-6 (δ_H 6.47) to 5-OMe (δ_H 3.73). Based on the HR-ESI-MS and 1D- and 2D-NMR information, compound **2.2** was determined as 4-allyl-5-methoxy-2-(*β*-D-glucopyranosyloxy-3-(4-methoxyphenyl) propanoate, given the trival name kadukoside, based on the Malaysian species name kaduk.
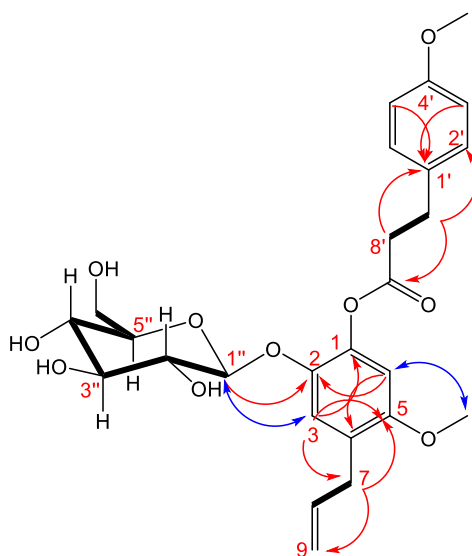
^{1}H-^{1}H COSY (▬▬), HMBC (➝) and NOESY (◄──►)

Figure 2.3: Key ^{1}H-^{1}H COSY, HMBC and NOESY correlation of compound **2.2** (kadukoside)

Table 2.2. ^{1}H- and ^{13}C-NMR data of **2.2** (in CD$_3$OD; δ in ppm, *J* in Hz)

Pos.	δ$_H$^{a}, Mult. *J* (Hz)	δ$_C$^{b}	Pos.	δ$_H$^{a}, Mult. *J* (Hz)	δ$_C$^{b}
1	-	147.9	3′/5′	6.81 d 8.6	114.9
2	-	140.1	4′	-	159.6
3	6.98 s	121.8	7′	2.84 t 7.7	31.3
4	-	120.7	8′	2.54 t 7.7	37.2
5	-	155.3	9′	-	176.9
6	6.47 s	100.9	4′-OMe′	3.75	55.2
7	3.22 d 6.4	34.6	1″	4.58 d 7.2	106.0
8	5.91 ddt 16.7, 9.7, 6.4	138.7	2″	3.44 m	75.0
9A	5.00 dd 16.7, 1.9	115.2	3″	3.42	77.7
9B	4.94 dd 9.7, 1.9	115.2	4″	3.30 m	71.2
5-OMe	3.73	56.2	5″	3.34	78.2
1′	-	134.2	6A″	3.71	62.3
2′/6′	7.12 d 8.6	130.3	6B″	3.87	62.3

^{a}) Recorded 400 MHz. ^{b}) Recorded at 100 MHz.

Compound **2.3** was obtained as colorless liquid from the *n*-butanol fraction. The molecular formula was determined to be C$_{15}$H$_{16}$O$_8$, based on HR-ESI-MS of the deprotonated ion at *m/z* 323.0769 (M-H)$^-$, calcd. 323.0772. The ^{1}H NMR data showed the presence of *para*-substituted benzene ring proton signals [δ 7.47 (2H, d, *J* = 8.7 Hz, H-2′, 6′), 6.81 (2H, d, *J* = 8.7 Hz, H-3′, 5′)] and olefinic double bond proton signals [δ 7.67 (1H, d, *J* = 16 Hz, H-7′), [δ 6.38 (1H, d, *J* = 16 Hz, H-8′). In particular, the coupling constant value (*J* = 16 Hz) of the olefinic double bond proton signals reveals that the double bond is *trans*. These NMR data supported the partial structure of **2.3** as a *trans p*-coumaroyl group. An extensive analysis of 1D and 2D NMR experiments allowed the complete assignments of the protons and carbons of the sugar part. These assignments were further confirmed by COSY and 1D TOCSY correlation of sugar H-2 (δ$_H$ 4.32), H-3 (δ$_H$ 4.39), H-4 (δ$_H$ 4.59), H-5 (δ$_H$ 4.24) and H-6 (δ$_H$ 4.35 and 4.44). The NMR spectra indicate a sugar moiety which was identified as D-glucono-1,4-lactone by coupling constants [35]. HMBC correlation observed from proton δ$_H$ 4.35/4.44 (H-6A/6B) to *trans p*-coumaroyl group at C-9′ indicated the connectivity of both moieties. Based on these analyses, the planar structure of **2.3** was determined as shown in Figure 2.4.

The relative stereochemistry of **2.3** was deduced from the NOESY correlation. This correlation of H-3 to H-4; H-4 to H-5; H-6B to H-5 suggested that H-3, H-4, H-5, and H-6B are positioned on the same side. Furthermore, the compound showed positive optical rotation $[\alpha]_D^{23}$ +4.04 (*c* 0.25, CH$_3$OH). By comparison to the data reported by Tanaka and co-workers (Table 2.3), who described a L-galactono-1,4-lactone derivative which was isolated from hops (*Humulus lupulus* L.), compound **2.3** is suggested to be 6-O-*trans*-*p*-coumaroyl-D-glucono-1,4-lactone.
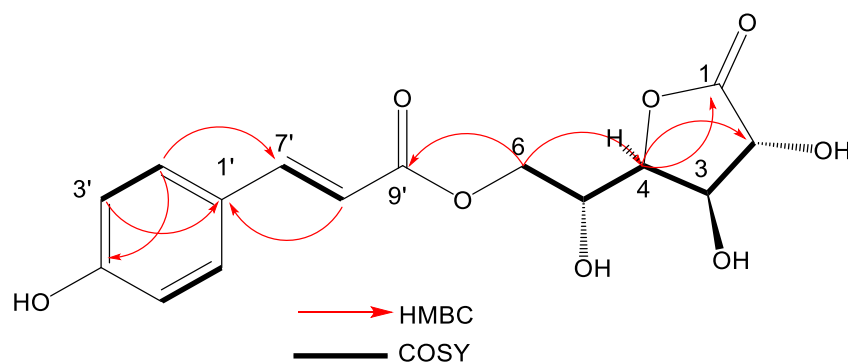
Figure 2.4: Key ^{1}H-^{1}H COSY and HMBC correlations of compound **2.3**

Table 2.3: ^{1}H and ^{13}C NMR comparison data of compound **2.3** and similar structure. (CD$_3$OD)

Pos.	Compound **2.3**		Tanaka et al. **[36]**	
	δ_H Mult. J (Hz) (400 MHz)	δ_C (100 MHz)	δ_H Mult. J (Hz) (600 MHz)	δ_C (150MHz)
1		177.1		176.0
2	4.32 d 4.7	74.8	4.38 d 8.7	75.6
3	4.39 dd 5.4, 4.7	74.9	4.33 t 8.7	74.4
4	4.59 dd 6.3, 5.4	81.3	4.19 dd 8.7, 2.4	81.4
5	4.24 ddd 6.63, 6.3, 3.3	69.3	4.07 m	67.8
6A	4.35 dd 11.7, 3.3	66.9	4.29 dd 11.1, 6.0	65.9
6B	4.44 dd 11.7, 6.3	66.9	4.33 dd 11.1, 6.9	65.9
1'		127.2		127.1
2'	7.47 d 8.7	131.2	7.47 d 9.0	131.2
3'	6.81 d 8.7	116.8	6.81 d 9.0	116.8
4'		161.3		161.4
5'	6.81 d 8.7	116.8	6.81 d 9.0	116.8
6'	7.47 d 8.7	131.2	7.47 d 9.0	131.2
7'	7.67 d 16.0	146.9	7.67 d 15.9	147.0
8'	6.38 d 16.0	114.9	6.37 d 15.9	114.8
9'		169.1		168.9

In addition, ten of the known compounds, namely hydrocinnamic acid (**2.6**) [37], 3-(4-methoxyphenyl) propanoic acid (**2.7**) [33], methyl 3-(4-methoxyphenyl)propionate (**2.8**) [38], isoasarone (**2.12**) [39], *trans*-asarone (**2.15**) [39], cepharadione A (**2.21**) [40], piperolactam A (**2.23**) [41], loliolide (**2.28**) [42] and mix of stigmasterol (**2.33**) [43] and *β*-sitosterol (**2.34**) [43] were identified by comparison with literature data. These known compounds have already been isolated from *P. sarmentosum* [14,44,45].

Furthermore, twelve compounds, 5-hydroxy-7,4'-dimethoxyflavone (**2.4**) [46], benzyl-*β*-D-glucopyranoside (**2.9**) [47], 1-(2,4,5-trimethoxyphenyl)-1,2-propanedione (**2.13**) [48], 1 ′,2 ′-dihydroxyasarone (**2.14**) [49], asaraldehyde (**2.16**) [50], *trans-N*-feruloyltyramine (**2.18**) [51], paprazine (**2.19**) [51], norcepharadione B (**2.20**) [52], aristolactam B II (**2.22**) [53], reseoside (**2.29**) [54], andamanicin (**2.31**) [55], and magnosalin (**2.32**) [55] were previously isolated from

other *Piper* species such as *P. capense* L.f. [56], *P. crocatum* Ruiz & Pav. [57], *P. cubeba* L. [58, 59], *P. sumatranum* (Miq.) C. DC. [49], *P. puberulum* (Benth.) Maxim. [60], *P. ribesioides* Wall. [61], *P. clusii* (Miq.) C.DC. [49,62]*,* and *P. aduncum* L. [63]. This indicated a close relationship among the *Piper* species.

Moreover, another nine compounds a herein reported for the Piperaceae family for the first time. These compounds comprise the flavonoid-C-glycoside 2″-*O*-*β*-L-galactopyranosyl-vitexin (**2.5**) [64] that was previously isolated from *Trollius ledebouri* (Ranunculaceae). Three phenolic compounds, citrusin C (**2.10**) [65], 4-allyl-2,5-dimethoxyphenol-1-*β*-D-gluco-pyranoside (**2.11**) [34] and scoparone (**2.17**) [66] were reported from *Morina nepalensis* (Caprifoliaceae) [65], *Pelargonium sidoides* (Geraniaceae) [34] and *Jatropha multifidi* (Euphorbiaceae) [66], respectively. Furthermore, the four alkaloids dehydroformouregine (**2.24**) [67], 3-[2,3-dihydroxy-4-(hydroxymethyl) tetrahydrofuran-1-yl] pyridine-4,5-diol (**2.25**) [68], naphthisoxazol A (**2.26**) [69] and indole-3-carboxaldehyde (**2.27**) [70] were previously isolated from *Guatteria ouregou* (Annonaceae) [67]*, Tenebrio molitor* [68], *Glehnia littoralis* (Umbelliferae) [69], and *Isatis ingigotica* (Brassicaceae) [70], respectively. Lastly, a lignan, magnosalicin (**2.30**) [71] was found in *Magnolia* species (Magnoliaceae) [72]. The structures of these known compounds were identified by spectroscopic analyses and by comparison with data reported in the literature.

Earlier review studies of *P. sarmentosum* have reported diverse pharmacological activities, either as an extract or for some pure compounds [14]. Therefore, the compounds isolated from this species were tested for their anthelmintic, antifungal, cytotoxic, antibacterial and neuroprotective properties. These biological examinations were conducted by using established non-pathogenic model organisms and human cancer cell lines (Biosafety level-1) which were used for rapid screening assays.

The anthelmintic activity was evaluated against *Caenorhabditis elegans*. This biological screening demonstrated that three phenylpropanoids, methyl 3-(4-methoxyphenyl)propionate (**2.8**)*,* isoasarone (**2.12**), and *trans*-asarone (**2.15**), show promising anthelmintic activity against *C. elegans* with $100.0 \pm 0.0\%$, $73.0 \pm 1.7\%$, and $97.4 \pm 0.9\%$ percentage mortality, respectively, at a tested concentration of 500 ppm (Figure S2.27: Supplementary data). These promising compounds **2.8, 2.12**, and **2.15** were re-tested against *C. elegans* with different concentrations ranging from 500 ppm to 100 ppm in order to determine the concentration that kills 50% (LC_{50}) of the nematodes. As expressed in Figure 2.5, the LC_{50} values calculated by in-house macro program in Microsoft Excel 2013 were estimated to be 174.6 ppm corresponding to 0.9 mM, 425.4 ppm/ 2.0 mM, and 341.9 ppm/ 1.6 mM, for compounds **2.8, 2.12**, and **2.15** respectively.
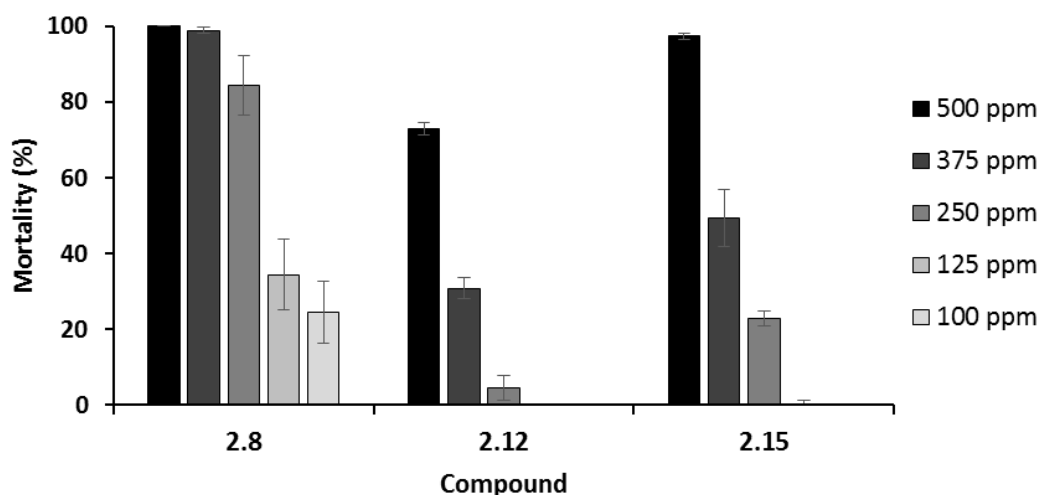
Figure 2.5: Anthelmintic activity against *C. elegans* of methyl 3-(4-methoxyphenyl)propionate **(2.8)**, isoasarone **(2.12)**, and *trans*-asarone **(2.15)**. Positive control ivermectin 10 µg/mL killed 100% of the nematodes (data not shown). Mortality % based on three replicates.

The activity of *trans*-asarone (**2.15**) is in accordance with data published by McGaw et al. [73] on the anthelmintic activity against *C. elegans* of its isomer *β*-asarone isolated from *Acorus* species (Acoraceae). To the best of our knowledge, there are no reports on the anthelmintic activity of isoasarone (**2.12**) and methyl-3-(4-methoxyphenyl)propionate (**2.8**). However, isoasarone (**2.12**) has been reported to be toxic against the mosquitos *Aedes aegypti, Aedes albopictus* and *Culex quinquefasciatus* [39], while compound **2.8** exhibited strong antifeedant activity [74]. The obtained results provides scientific evidence of the anthelmintic activity of *P. sarmentosum* leaves, which are traditionally used to treat worm infections [15].

An earlier study indicated that *P. sarmentosun* extracts have antifungal properties [17]. However, there is lack of information on compounds responsible for that activity. Therefore, all isolated compounds were tested for their antifungal effects against three phytopathogenic ascomycetes *Botrytis cinerea* Pars, and *Septoria triciti* Desm. and the oomycete *Phytophthora infestans* (Mont.). Briefly, the isolated compounds were tested at a highest concentration of 125 µM, while the commercially available fungicides epoxiconazole and terbinafine at the same concentration as tested samples served as positive controls (Table S2.3: Supplementary data). As shown in Table S2.3, seven compounds including the four phenylpropanoids derivatives, kadukoside (**2.2**), methyl 3-(4-methoxyphenyl)propionate (**2.8**), isoasarone (**2.12**) and *trans*-asarone (**2.15**), the two alkaloids piperolactam A (**2.23**) and dehydroformouregine (**2.24**), and the flavonoid 5-hydroxy-7,4'-dimethoxyflavone (**2.4**) exhibited activity against the fungi *B. cinerea, S. tritici* or *P. infestans* with inhibition rates of about 40% at a concentration of 125 µM after seven days after inoculation.

Based on the first hits determined at 125 µM concentration in the initial rapid-screening and sample availability, five compounds were subjected to dose-dependency studies against the fungi *S. tritici, B. cinerea* and *P. infestans*. The pathogens were treated with compound concentrations ranging from 1.5 to 125 µM, followed by assay read-out and data analyses. As displayed in Figure 2.6A, compound **2.2** was most the active one against *S. tritici* with inhibition rates of more than 75% at the concentrations of 14 µM and higher, and 48% inhibition at 5 µM. Thus, the IC_{50} of **2.2** calculated by SigmaPlot software was 5.0 ± 0.02 µM. Kadukoside (**2.2**) displayed the highest inhibition activity against the oomycete *P. infestans* when treated at a concentration of 125 µM (Figure 2.6C). As depicted in Figure 2.6B, the remaining three compounds (**2.15, 2.23**, and **2.24**) exhibited significant activity against *B. cinerea*, with the exception of **2.2** and **2.12**, which showed low/moderate activity. All three compounds had a dose-dependent effect on the fungi *B. cinerea* from 1.5 to 125 µM. Most importantly, more than 80% inhibition was observed against the fungi *B. cinerea* at the highest concentration tested.

The results of compounds **2.23** and **2.24** suggest that the alkaloid scaffold is responsible for the antifungal activity. Similar antifungal activity was reported for piperolactam D and stigmalactam isolated from the aerial parts of *Piper parviflorum* C. DC. [75]. The substituents and their positions were suggested to be relevant for the distinct antifungal bioactivity [76]. Moreover, isoasarone (**2.12**) and *trans*-asarone (**2.15**) have been previously found in *P. sarmentosun* and other species such as *Boesenbergia pulcherrima* (Zingiberaceae) [77] and *Acorus species* (Acoraceae) [78]. Both of these compounds have been reported to possess antifungal activity against *Candida albicans* [79]. Surprisingly, an earlier study showed that *trans*-asarone has no *in-vivo* growth inhibition against *B. cinerea* at a concentration of 125 and even 1000 ppm [80].
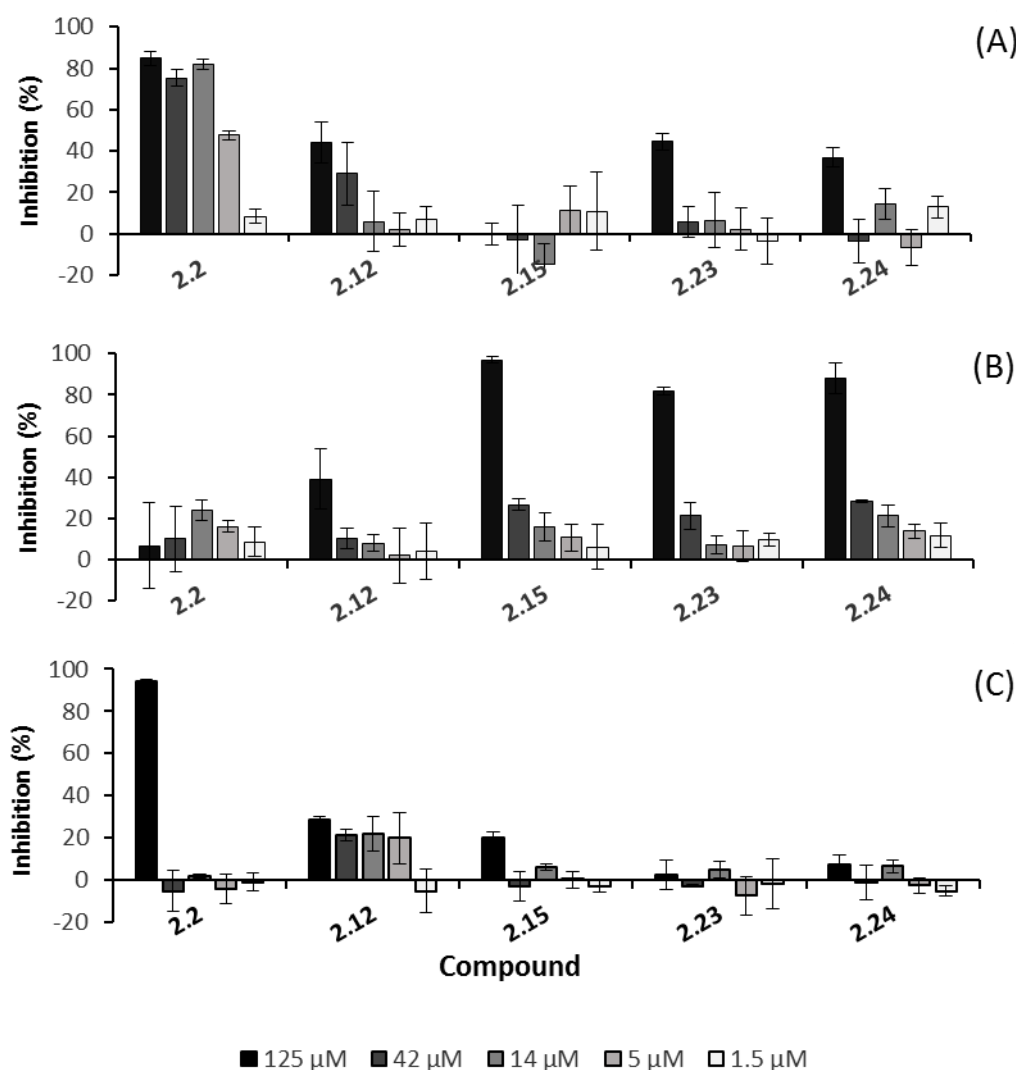
Figure 2.6: Antifungal activity of compounds **2.2**, **2.12**, **2.15**, **2.23**, and **2.24** against the phytopathogenic ascomycetes (A) *Septoria triciti* Desm, (B) *Botrytis cinerea* Pars and (C) *Phytophthora infestans* (Mont.). Epoxiconazole in five different concentrations was used as a positive control for *S. triciti* and *B. cinerea* causing 100% inhibition, whereas terbinafine (125 µM) served as positive control for *P. infestans* inducing 100% inhibition after the inoculation period (data not shown).

The cytotoxicity and impact of most isolated compounds on the metabolic cell viability of HT-29 (human colorectal adenocarcinoma) and PC-3 (human prostate adenocarcinoma) cancer cell lines was evaluated at 10 nM and 10 µM. The compounds' effect on the cancer cell viability was determined by conducting an MTT assay, and general cytotoxic effects were determined by using a CV assay, both after 48 h treatment with the compounds under investigation. A very potent permeabilizer of cell membranes, digitonin (125 µM), was used as a positive control compromising the cells to the point of 0% of cell viability after 48 h.

As demonstrated in Figure 2.7, most of the compounds tested displayed cell viability over 80% at the highest concentration of 10 µM. This indicates that compounds are weakly or inactive against the specific cell lines. Meanwhile, compounds with cell viability below 80% at

a concentration of 10 µM could be considered potentially cytotoxic and need further investigation. Briefly, five compounds including two alkaloids, aristolactam BII (**2.22**) and dehydroformouregine (**2.24**); and three neolignans, magnosalicin (**2.30**), andamanicin (**2.31**), and magnosalin (**2.32**) displayed cell viability below 80% against HT-29 cell line either in MTT or CV assay at 10 µM. The observed HT-29 cell viabilities in the MTT assay were $68.4 \pm 1.5\%$, $76.4 \pm 3.5\%$ and $62.5 \pm 4.2\%$ for compounds **2.22**, **2.31** and **2.32**, respectively. While in the CV assay the cell viability was $52.9 \pm 2.2\%$, $80.9 \pm 5.9\%$, $71.7 \pm 3.3\%$, $67.8 \pm 2.2\%$ and $61.7 \pm 3.4\%$ for compounds **2.22**, **2.24**, **2.30**, **2.31** and **2.32**, respectively. Interestingly, there were no significant variances in cytotoxicity between compounds **2.31** and **2.32,** which possess stereochemical differences in the position of methyl groups at C-1 and C-2. In addition, three alkaloid compounds, cepharadione A (**2.21**), aristolactam BII (**2.22**), and piperolactam A (**2.23**) reduced cell viability of the PC-3 cell line below 80% at the highest concentration of 10 µM. The IC_{50} values of all compounds could be estimated to be above 10 µM.

Out of these seven isolated compounds, only compounds **2.21**, **2.22** and **2.23** were previously tested against HT-29 cell lines. Compound **2.22** previously demonstrated cytotoxic effects with an IC_{50} value of 26 µg/ml [81], whereas for compounds **2.21** and **2.23** no activity was reported against HT-29 cell lines [82]. Furthermore, no data on **2.21**, **2.22** and **2.23** against the human prostate (PC-3) cancer cell line has been published.

Although cytotoxicity against HT-29 and PC-3 cell lines has not been reported for these three neolignans (**2.30** – **2.32**), magnosalicin (**2.30**) was recently reported to exhibit significant anti-$A\beta_{42}$ aggregation activity with an inhibitory rate of 61% at 100 µM, in contrast to 69% for the positive control EGCG [83]. Compounds **2.31** and **2.32** were previously isolated from the leaves of *Perilla frutescens* (Labiatae) and displayed inhibition of nitric oxide syntheses (IC_{50} 53.5 µM and 5.9 µM, respectively) and tumor necrosis factor-α in lipopolysaccharide-activated RAW 264.7 cells [55].
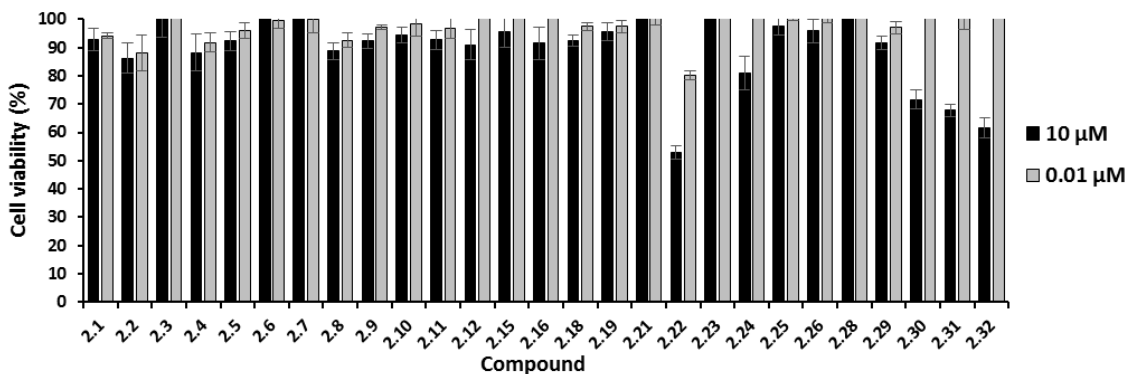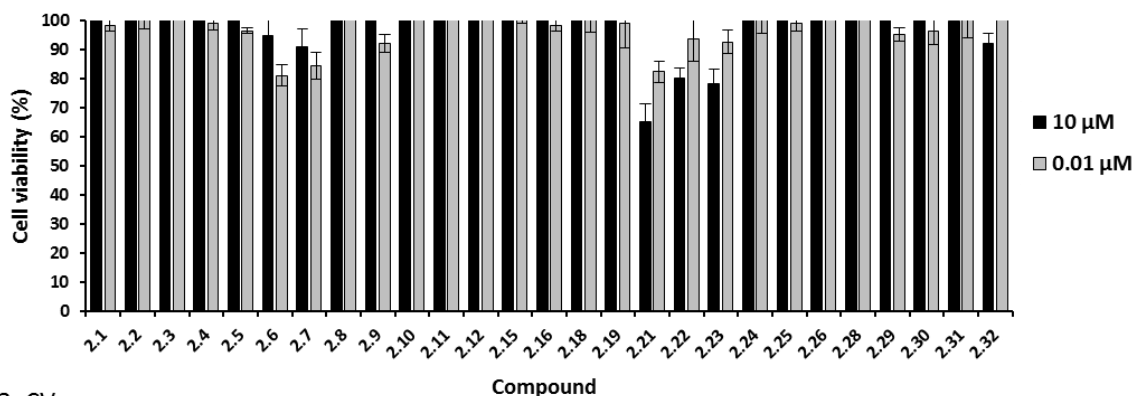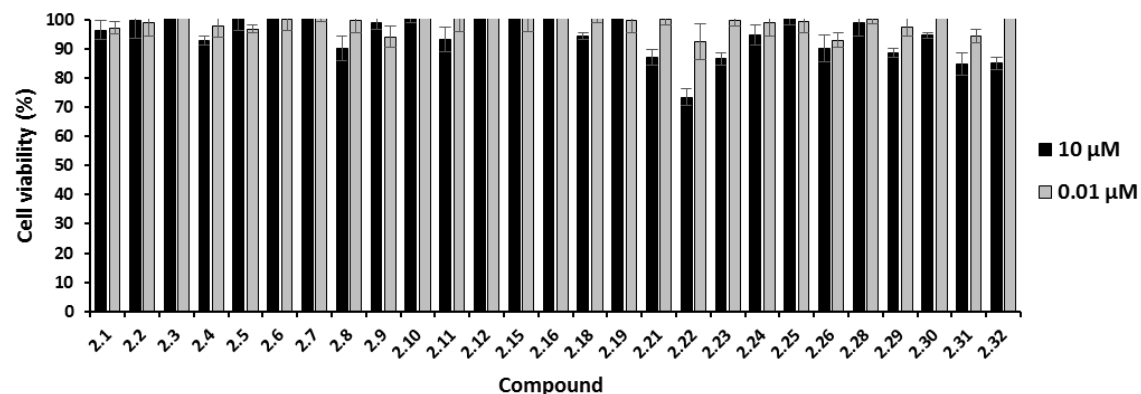
Figure 2.7: Antiproliferative and cytotoxic activities (MTT and CV) of most isolated compounds from *P. sarmentosum* against human colorectal (HT-29) and prostate (PC-3) cancer cell lines. Digitonin (125 μM) was used as positive control compromising the cells to the point of 0% of cell viability after 48 h (data not shown).
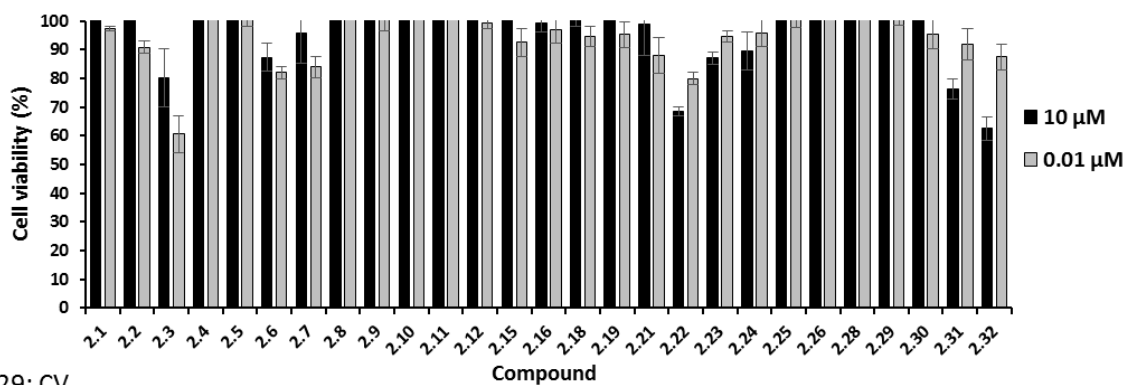
Furthermore, all compounds **2.1 - 2.34** were screened for their antibacterial activity against the gram-negative bacterium *Aliivibrio fischerii* at 1, 10 and 100 μM. As indicated in Figure 2.8, five alkaloid compounds namely, *trans*-*N*-feruloyltyramine (**2.18**), paprazine (**2.19**), cepharadione A (**2.21**), piperolactam A (**2.23**) and dehydroformouregine (**2.24**), induced over 40% inhibition of bacterial growth at the highest concentration of 100 μM. Lower concentrations showed no inhibition or even promoted the bacterial growth. In general, alkaloids are nitrogen-containing organic compounds with often significant biological activities. They exist widely in the plant world [4].

The antibacterial activity of compound **2.19** with 85.4% inhibition at a concentration of 100 μM was about a two-fold better than that of the structurally related compound **2.18** (40.7% inhibition). The observed differences in inhibition between the two compounds may have been due to the presence of different functional groups at C-3 of the *p*-coumaroyl moiety. Our results of these two compounds were similar to those reported by Mata *et* al., which indicated that an extra methoxy group in the *p*-coumaroyl unit lowered the antibacterial activity [84]. Furthermore, compound **2.19** which was isolated previously from *Cannabis sativa* (Cannabaceae) roots has been reported to possess antibacterial activity against a different gram-negative bacterium, *Escherichia coli* with an IC_{50} value of 0.8 μg/mL [85].

Moreover, two alkaloid compounds **2.21** and **2.23** exhibited nearly 100% inhibition of the gram-negative bacterium *A. fischerii* at the highest concentration of 100 μM. Contrary to our results, compound **2.21** which was isolated recently from the aerial parts of *Piper wallichii* (Miq.) Hand.-Mazz. showed a different trend in antibacterial activity. This compound was only active against the gram-positive bacteria *Bacillus cereus*, *Bacillus subtilis* and *Staphylococcus aureus*; however, it was inactive against the three tested pathogenic gram-negative bacteria *E. coli*, *Pseudomonas aeruginosa* and *Shigella sonnei* [86]. This could be because the compound may exhibit selective antibacterial activity against different gram-positive and gram-negative bacteria. With regards to compound **2.23**, similar antibacterial properties have been described. For example, in an antimycobacterial bioassay-guided chromatographic study on *Piper sanctum* (Miq.) Schl. leaves performed by Mata et al. [84], compound **2.23** displayed good growth inhibition against *Mycobacterium tuberculosis* with an MIC value of 8 μg/mL. Compound **2.24** (dehydroformouregine) showed moderate antibacterial activity with 41.1% inhibition against the gram-negative bacterium *A. fischerii* at 100 μM. Despite this compound having been previously isolated from *Guatteria ouregou* [67], there is no pharmacological activity reported, specifically no antibacterial activity; thus to the best of our knowledge, this is the first report of the antibacterial activity of compound **2.24**.
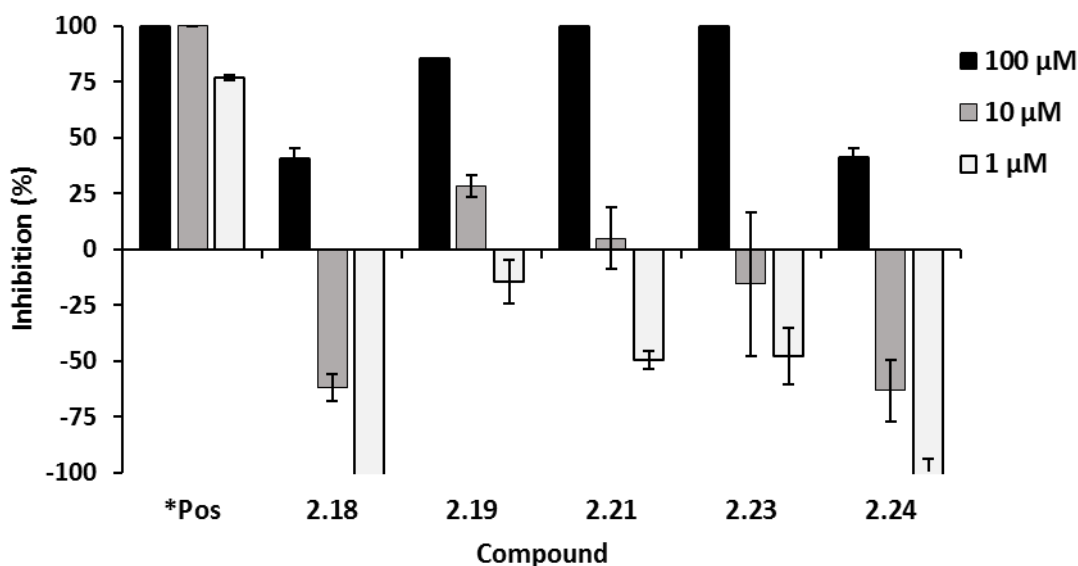
Figure 2.8: Antibacterial assay of compounds **2.18**, **2.19**, **2.21**, **2.23** and **2.24** against gram-negative *Aliivibrio fischerii*. Results were compared to chloramphenicol which was the positive control labelled as ***Pos**.

Some of the constituents with different structural features as isoasarone (**2.12**), *trans*-asarone (**2.15**), norcepharadione B (**2.20**), aristolactam BII (**2.22**), magnosalicin (**2.30**), andamanicin (**2.31**), and magnosalin (**2.32**) were submitted to the Leibniz Institute of Neurobiology in Magdeburg to evaluate their neuroprotective potential in an astrocyte cell assay. Three compounds **2.12**, **2.15** and **2.22** significantly inhibited the uptake and deposition of toxic Aβ-peptides in these cells (results not shown). These three potential compounds have been investigated previously for neuroprotective activity. The significant activity of *trans*-asarone (**2.15**) is consistent with the data published by Lee et al., [87], on the activity of **2.15** in protecting PC12 cells (rat pheochromocytoma cells) from Aβ aggregate-induced toxicity. It also reduced LPS-induced NO production by BV2 microglial cells significantly [87]. Similar to aristolactam BII (**2.22**), which has been shown to have substantial neuroprotective effects on glutamate-injured primary cultures of rat cortical cells by directly inhibiting nitric oxide production [88]. However, isoasarone (**2.12**) results contradict those of Kim et al.,[89], who found no significant inhibition of nitric oxide (NO) and prostaglandin E2 (PGE2) production in LPS-activated microglia cells, which correlated with anti-neuroinflammatory activity.

In summary, it is remarkable to note that the cell toxicity of the constituents is absent or low. Some isolated compounds from *P. sarmentosum* possess mild anthelmintic, antifungal, cytotoxic, antibacterial and neuroprotective activities. For those with a stronger effect ($IC_{50} < 10$ μM), a detailed mode for the specific biological activity should be addressed in future investigations.

2.3   **Materials and methods**

2.3.1   General methods

The following instruments were used for obtaining physical and spectroscopic data: Column chromatography was performed on silica gel (400 - 630 mesh, Merck, Germany), Sephadex LH-20 (Fluka, Steinheim, Germany) and Diaion HP20 (Supelco, Bellefonte, PA, USA). Fractions and substances were monitored by TLC. TLC was conducted on precoated Kieselgel 60 F 254 plates (Merck, Darmstadt, Germany) and the spots were detected either by examining the plates under an UV lamp at 254 and 366 nm or by treating the plates with vanillin or natural product reagents. The UV spectra were recorded on a Jasco V-770 UV-Vis/NIR spectrophotometer (Jasco, Pfungstadt, Germany), meanwhile specific rotation was measured with a Jasco P-2000 digital polarimeter (Jasco, Pfungstadt, Germany).

NMR spectra were obtained with an Agilent DD2 400 system at +25 °C (Varian, Palo Alto, CA, USA) using a 5-mm inverse detection cryoprobe. The compounds were dissolved in CD_3OD (99.8% D) or $CDCl_3$ (99.8% D), and the spectra were recorded at 399.915 MHz (^1H) and 100.569 MHz (^{13}C). 1D (^1H , ^{13}C, and TOCSY) and 2D ($^1H,^{13}C$ HSQC, $^1H,^{13}C$ HMBC, ^1H-^1H COSY, $^1H,^1H$ ROESY and $^1H,^1H$ NOESY) spectra were measured using standard CHEMPACK 8.1 pulse sequences implemented in the Varian VNMRJ 4.2 spectrometer software (Varian, Palo Al-to, CA, USA). ^1H chemical shifts are referenced to internal TMS (^1H $\delta = 0$ ppm), while ^{13}C chemical shifts are referenced to CD_3OD (^{13}C $\delta = 49$ ppm) or $CDCl_3$ (^{13}C $\delta = 77.0$ ppm).

The semi-preparative HPLC was performed on a Shimadzu prominence system (Kyoto, Japan) equipped with LabSolutions software, LC-20AT pump, SPD-M20A diode array detector, SIL-20A auto sampler and FRC-10A fraction collector unit. Chromatographic separation was carried out using a YMC Pack C18 column (5 µm, 120 Å, 150 mm x 10 mm I.D, YMC, USA) using H_2O (A) and CH_3CN (B) as eluents at a flow rate of 2.2 mL/min.

The high-resolution mass spectra in both positive and negative ion modes were acquired using either an Orbitrap Elite Mass spectrometer or API 3200 Triple Quadrupole System. The Orbitrap Elite Mass spectrometer (Thermofisher Scientific, Bremen, Germany) was equipped with an HRESI electrospray ion source (spray voltage 4.0 kV, capillary temperature 275 °C, source heater temperature 80 °C, FTMS resolution 100.000), whereas API 3200 Triple Quadrupole System (Sciex, Framingham, MA, USA) was equipped with a turbo ion spray source, which performs ionization with an ion spray voltage on 70 eV. During the measurement, the mass/charge range from 50 to 2000 was scanned.

2.3.2   Plant material

The dried powdered leaves of *P. sarmentosum* were supplied by the Institute of Bioproduct Development, Universiti Teknologi Malaysia. The plant material was collected in January 2019 from Negeri Sembilan, Malaysia. A voucher was authenticated (Number: MFI 0039/19) by Dr. Mohd Firdaus Ismail, a botanist at the Institute of Biosciences, Universiti Putra Malaysia. A duplicate of the Herbarium specimen is kept at the Bioorganic Chemistry Department of the Leibniz Institute of Plant Biochemistry, Germany.

2.3.3   Extraction and isolation

The dried leaf powder (400 g) was extracted five times (1.2 L/each) with 80% aqueous MeOH at room temperature. The combined extracts were concentrated under reduced pressure to obtain a MeOH extract (107 g). The extract was suspended in distilled water (250 ml) and partitioned with *n*-hexane, EtOAc and *n*-BuOH, yielding 18, 9 and 17 g of residue, respectively. Further fractionation of the remained aqueous fraction was not extended due to unpromising biological activity. The EtOAc-soluble fraction (9 g) was subjected to a silica gel column (Lengh, L = 40 cm; diameter, d = 5.5 cm) and eluted with a stepwise gradient of CH_2Cl_2:EtOAc:MeOH (1:0:0 to 0:0:1) to yield ten fractions (E1-E10). Fraction E3 (436 mg) underwent column chromatography (CC) over Sephadex LH-20 (L = 77 cm; d = 2.7 cm) eluted with MeOH to afford eight subfractions (E3a – E3h). Compound **2.27** (2.8 mg, R_f = 0.49, MeOH:CH_2Cl_2 /1:9) was obtained from fraction E3e (2.8 mg). Fraction E3c (32.2 mg) was further purified by silica gel CC (L = 35 cm; d = 1.2 cm) eluting with *n*-Hex, DCM and MeOH in gradient elution to give compound **2.28** (2.3 mg, R_f= 0.51, MeOH:CH_2Cl_2 /1:9). Compound **2.22** (1.9 mg, R_f = 0.67, MeOH:CH_2Cl_2 /1:9) was isolated from fraction E3d (128.3 mg) via repeated silica gel CC (L = 60 cm; d = 1.0 cm) using a step gradient of *n*-Hex-DCM-MeOH (1:0:0 to 0:0:1).

Fraction E5 (164 mg) was separated by a Sephadex LH-20 column (L = 72 cm; d = 1.5 cm) eluted with MeOH to produce seven subfractions (E5a – E5g). Compound **2.14** (17.5 mg, R_f = 0.54, MeOH:CH_2Cl_2 /1:9) was afforded from fraction E5b (100.5 mg) over repeated silica CC (L = 35 cm; d = 1.2 cm) eluted with *n*-Hex:DCM:MeOH (2:8:0 to 0:9:1). Compound **2.23** (3.0 mg, R_f = 0.62, MeOH:CH_2Cl_2 /1:9) was obtained from fraction E5f (3.0 mg). Further purification of fraction E5c (34.1 mg) using a silica gel column (L = 47 cm; d = 2.0 cm) in step gradient of *n*-Hex:DCM:MeOH (3:7:0 to 0:9:1) afforded compounds **2.18** (7.9 mg, R_f = 0.48, MeOH:CH_2Cl_2 /1:9) and **2.19** (16.3 mg, R_f= 0.38, MeOH:CH_2Cl_2 /1:9).

Fraction E6 (701 mg) was fractionated over a Sephadex LH-20 column (L = 77 cm; d = 2.7 cm) eluted with DCM/MeOH (1:1) yielding six subfractions (E6a – E6f). Fraction E6c

(128 mg) was further purified using silica CC (L = 90 cm; d = 1.3 cm) in gradient elution of *n*-Hex:DCM:MeOH (1:0:0 to 0:7:3) to give 17 subfractions (E6c1 – E6c17) including **2.21** (2.2 mg, R_f = 0.8, MeOH:CH$_2$Cl$_2$ /1:9) and **2.7** (0.8 mg, R_f = 0.38, MeOH:CH$_2$Cl$_2$ /1:9). Purification of fraction E6c15 (16.8 mg) on semipreparative RP-HPLC in a gradient system [H$_2$O (A), MeCN (B); 0 min – 10% B > 0-14 min 52% B > 14-16 min 52-100% B, flow rate 3.0 mL/min] afforded compounds **2.10** (1.9 mg, t_R = 10.7 min) and **2.11** (6.4 mg, t_R = 14.4 min). Compound **2.20** (0.6 mg, R_f = 0.66, MeOH:CH$_2$Cl$_2$ /1:9) was obtained from fraction E6c8 (2.7 mg) by SPE cartridges (Chromabond@ C-18, 1ml / 100 mg) eluted in step gradient of H$_2$O: MeOH (1:0 to 0:1). Fraction E6d (205 mg) and E6e (32 mg) were combined together and further fractionated via silica gel (L = 47 cm; d = 2.0 cm) in step gradient of *n*-Hex:DCM:MeOH (3:7:0 to 0:9:1) affording nine subfractions (E6de1 – E6de9). Compound **2.6** (2.4 mg R_f = 0.64, MeOH:CH$_2$Cl$_2$ /1:9) was obtained from fraction E6de1 (4.9 mg) through SPE cartridges (Chromabond@ C-18, 1ml / 100 mg) eluted with MeOH:H$_2$O (1:9). Similarly, compound **2.2** (4.8 mg, R_f = 0.12, MeOH:CH$_2$Cl$_2$ /1:9) was purified from E6de8 (19.2 mg) over a SPE cartridge (Chromabond@ C-18, 1ml / 100 mg) eluted with MeOH:H$_2$O (1:9).

The *n*-hexane-soluble fraction (17 g) was subjected to silica gel CC (L = 40 cm; d = 5.5 cm) and eluted with a stepwise gradient of *n*-Hex:CH$_2$Cl$_2$:MeOH (1:0:0 to 0:7:3) to yield ten fractions (H1-H10). Compounds **2.8** (33.7 mg, R_f = 0.53, EtOAc:*n*-hex /2.5:7.5), **2.12** (1453 mg, R_f = 0.49, EtOAc:*n*-hex /2.5:7.5), **2.15** (1543 mg, R_f = 0.46, EtOAc:*n*-hex /2.5:7.5), **2.16** (34.4 mg, R_f = 0.1, *n*-Hex:CH$_2$Cl$_2$/ 1:9) and **2.30** (7.0 mg, R_f = 0.17, EtOAc:*n*-hex /3:7) were obtained from fraction H3 (4843 mg) via repeated column chromatographic separation using Sephadex LH-20 (L = 75 cm; d = 2.0 cm) eluted with DCM/MeOH (1:1) followed by silica gel (L = 75 cm; d = 2.0 cm) in step gradient of *n*-Hex: EtOAc (9:1 to 4:6). Further separation of fraction H4 (965 mg) over Sephadex LH-20 (L = 40 cm; d = 5.5 cm) (DCM/MeOH, 1:1) afforded two subfractions (H4a – H4b). Mixture of compounds **2.33** and **2.34** (187 mg, R_f = 0.4, MeOH:CH$_2$Cl$_2$ /5:9.5) were produced from fraction H4b by gradient elution of a silica column (L = 76 cm; d = 2.0 cm) using *n*-Hex:DCM:MeOH (1:0:0 to 0:9:1). Fraction H5 (704 mg) was subjected to Sephadex LH-20 CC (L = 76 cm; d = 3.3 cm) eluted with DCM/MeOH (1:1) to give four subfractions (H5a – H5d). Compounds **2.31** (46.2 mg, R_f = 0.16, EtOAc:*n*-hex/ 3:7) and **2.32** (31.0 mg, R_f = 0.16, EtOAc:*n*-hex/ 3:7) were afforded from fraction H5b (298 mg) via silica gel (L = 44 cm; d = 1.5 cm) eluted with *n*-hex and EtOAc in a stepwise gradient (8:2 to 3:7). Fraction H5c (132 mg) was further purified over silica gel (L = 44 cm; d = 1.5 cm) eluted with *n*-hex and EtOAc (8:2 to 0:1) to provide four subfractions (H5c1 – H5c4). Compounds **2.17** (0.80 mg, t_R = 7.0 min) and **2.13** (0.85 mg, t_R = 8.8 min) were isolated from fraction H5c1 (5.4 mg) by semipreparative RP-HPLC using water (A) and MeCN (B) as eluent, and the

gradient program was 0-12.5 min (25-50%B), 12.5-20 min (50-100%B), and 20-22 min (100%B). Further chromatography of fraction H5c3 (24.7 mg) via silica CC (L = 32 cm; d = 1.0 cm) eluted with *n*-hex and EtOAc (1:1) yielded compound **2.24** (5.4 mg, R_f = 2.8, EtOAc:*n*-hex/ 3:7). Compound **2.4** (13.2 mg, R_f = 0.52, EtOAc:*n*-hex/ 1:1) was afforded from fraction H5c4 (13.2 mg).

The *n*-BuOH-soluble fraction was subjected to a Diaion-HP20 column (L = 60 cm; d = 2.8 cm) and eluted with an increasing solvent ratio of water and methanol to give five fractions (B1-B5). Fraction B2 (1490 mg) was further purified over Sephadex LH-20 (L = 68 cm; d = 2.5 cm) eluted with MeOH to produce three subfractions (B2a – B2c). Compound **2.25** (13.3 mg, R_f = 0.34, MeOH:EtOAc/ 2:8) was yielded from fraction B2a (30.3 mg) by silica CC (L = 40 cm; d = 1.5 cm) (EtOAc: MeOH, 8:2 to 7.5:2.5). Fraction B2b (952 mg) was chromatographed via RP-18 CC (L = 55 cm; d = 2.1 cm) using water and MeOH as eluent, and the gradient elution was 10 to 50% of MeOH to afford six subfractions (B2b1 – B2b6). Compound **2.26** (28.7 mg, R_f = 0.45, MeOH:EtOAc/ 7:3) was afforded from fraction B2b5 (411 mg) by silica gel CC eluted (L = 43 cm; d = 2.5 cm) with EtOAc:MeOH (1:1 to 0.5:9.5). Separation of fraction B3 (4749 mg) via Sephadex LH-20 CC (L = 68 cm; d = 2.5 cm) eluted with MeOH gave four subfractions (B3a – B3d). Further purification of fraction B3a (1366 mg) using silica CC (L = 65 cm; d = 2.0 cm) eluted with a stepwise gradient of EtOAc:MeOH (9:1 to 4.5:5.5) produced 12 subfractions (B3a1 – B3a12). Compound **2.29** (38.2 mg, R_f = 0.69, MeOH:EtOAc/ 3:7) was afforded from fraction B3a1 (38.2 mg). Fraction B3a9 (81 mg) was further separated over semipreparative RP-HPLC and eluted with a mixture of water (A) and MeCN (B), and the gradient elution was 0-12.5 min (10-48% B) and 12.5-13.5 min (48% B) to give sub-fraction 9a (13.6 mg, t_R = 6.2 min). Further purification was performed on sub-fraction 9a by semipreparative RP-HPLC with water and 0.1% of TFA in MeOH as mobile phase. Detail gradient program used was 0-23 min (22-50% B) and 23-24 min (50-100% B) to afford compound **2.1** (2.0 mg, t_R = 19.9 min). Fraction B3b was subjected to silica CC (L = 73 cm; d = 2.3 cm) eluted with EtOAc:MeOH (4:1 to 1:1) to obtain eight subfractions (B3b1 – B3b8). Fraction B3b2 (95 mg) was purified via semipreparative RP-HPLC using water (A) and MeCN (B) as eluents. The gradient program was 0-15 min (10-29%B), 15-17 min (29-100%B) and 17-20 min (100%B) to yield eight subfractions B3b2a – B3b2h including compound **2.3** (10.3 mg, t_R = 12.8 min) from B3b2g (10.3 mg). Compound **2.9** (3.7 mg, t_R = 11 min) was purified from fraction B3b2a (16.0 mg) over modified RP-HPLC method via water and MeCN as eluent (92:8, isocratic elution, 3 ml/min). Compound **2.5** (226 mg, R_f = 0.26, MeOH:EtOAc/ 4:6) was isolated from fraction B3b5 (226 mg).

Compound **2.1**: 4"-(3-Hydroxy-3-methylglutaroyl)-2"-*β*-D-glucopyranosyl vitexin. Brownish liquid; $[\alpha]_D^{24}$ -10.93 (*c* 0.15, CH₃OH); UV λ_max, (MeOH) (log e) 202 (5.0), 271 (5.1), 335 (5.2); ¹H-NMR (400 MHz, CD₃OD): Table 2.1; ¹³C-NMR (100 MHz, CD₃OD): Table 2.1; negative ion HRESIMS [M-H]⁻ at *m/z* 737.1937, (calcd. for C₃₃H₃₇O₁₉: 737.1935)

Compound **2.2**: 4-Allyl-3-methoxyphenol-6-β-D-glucopyranoside-3-(4-methoxyphenyl) propanoic acid. Brownish liquid; UV λ_max, (MeOH) (log e) 202 (4.75), 223 (4.80), 384 (5.03); ¹H-NMR (400 MHz, CD₃OD): Table 2.2; ¹³C-NMR (100 MHz, CD₃OD): Table 2.2; positive ion HRESIMS [M+H]⁺ peak at *m/z* 505.2036, (calcd. for C₂₆H₃₂O₁₀: 505.2068)

Compound **2.3**: 6-O-*trans*-*p*-Coumaroyl-D-glucono-1,4-lactone. Colorless liquid; $[\alpha]_D^{23}$ +4.04 (*c* 0.25, CH₃OH); UV λ_max, (MeOH) (log e) 210 (4.4), 226 (4.5), 312 (4.6); ¹H-NMR (400 MHz, CD₃OD): Table 2.3; ¹³C-NMR (100 MHz, CD₃OD): Table 2.3; negative ion HRESIMS [M-H]⁻ *m/z* 323.0769, (calcd. for C₁₅H₁₆O₈: 323.0772).

2.3.4 Biological activities

2.3.4.1 Anthelmintic assay

The anthelmintic bioassay was conducted using the Bristol N2 wild type strain of the model organism *Caenorhabditis elegans*, which was previously demonstrated to correlate with anthelmintic activity against parasitic trematodes [90]. The nematodes were cultured on NGM (Nematode Growth Media) petri plates using the uracil auxotroph *E. coli* strain OP50 as food source according to the methods described by Stiernagle [91]. The anthelmintic bioassay was performed according to method developed by Thomsen et al. [90]. The solvent DMSO (2%) and the standard anthelmintic drug ivermectin (10 μg/mL) were used as negative and positive controls in all the assays, respectively. All assays were performed in triplicate.

2.3.4.2 Antifungal assay

The antifungal activity was performed against phytopathogenic ascomycetes *Botrytis cinerea* Pars, and *Septoria triciti* Desm. and the oomycete *Phytophthora infestans* (Mont.) de Bary in 96-well microtiter plate assays with minor modification as described by Otto et al. [92]. In brief, the isolated compounds were tested at a highest concentration of 125 μM, while solvent DMSO was serving as negative control (max. concentration 2.5%), and the commercially available fungicides epoxiconazole and terbinafine (Sigma-Aldrich, Damstadt, Germany) served as reference compounds. The pathogen growth was assessed seven days after inoculation by the optical density (OD) at ʎ 405 nm measurement with a TecanGENios Pro microplate

reader (five measurements per well using multiple reads in 3 x 3 square). Each experiment was performed in triplicates.

2.3.4.3 Cytotoxicity assay

The cytotoxicity and impact on the metabolic cell viability of isolated compounds at 10 nM and 10 μM was evaluated against PC-3 (human prostate adenocarcinoma) and HT-29 (human colorectal adenocarcinoma) cancer cell lines. Both cell lines were purchased from ATCC (Manassas, USA). The cell culture medium RPMI 1640, the supplements FCS and L-glutamine, as well as PBS and trypsin/EDTA were purchased from Capricorn Scientific GmbH (Ebsdorfergrund, Germany). Culture flasks, multi-well plates and further cell culture plastics were from Greiner Bio-One GmbH (Frickenhausen, Germany) and TPP (Trasadingen, Switzerland), respectively. Resazurin used for the cell viability assays was purchased from Sigma-Aldrich GmbH (Taufkirchen, Germany). PC-3 and HT-29 cells were cultured in RPMI 1640 medium supplemented with 10% heat-inactivated FCS, 2 mM L-glutamine and 1% penicillin/streptomycin, and in a humidified atmosphere with 5% CO_2 at 37°C. Routinely, cells were cultured in T-75 flasks until reaching subconfluency (~ 80%), subsequently cells were harvested by washing with PBS and detaching by using trypsin/EDTA (0.05% in PBS) prior to cell passaging and seeding for sub-culturing and assays in 96-well plates, respectively [93].

The cell handling and assay techniques were in accordance to the method with minor modification as described by Khan et al. [93]. In brief, anti-proliferative and cytotoxic effects of the compounds were investigated by performing colorimetric MTT (3-(4,5-dimethylthiazol-2-yl)-2,5-diphenyltetrazolium bromide) and CV (crystal violet)-based cell viability assays (Sigma-Aldrich, Taufkirchen, Germany), respectively. For this purpose, cells were seeded in low densities in 96-well plates using the aforementioned cell culture medium. The cells were allowed to adhere for 24 h, followed by the 48 h compound treatment. Based on 20 mM DMSO stock solutions, the compounds were diluted in standard growth media to reach final concentrations of 10 nM and 10 μM for cell treatment. For control measures, cells were treated in parallel with 125 μM digitonin (positive control, for data normalization set to 0% cell viability). Each data point was determined in technical quadruplicates and two independent biological replicates. As soon as the 48 h incubation was finished, cell viability was measured.

For the MTT assay, cells were washed once with PBS, followed by incubation with MTT working solution (0.5 mg/mL MTT in culture medium) for 1 h under standard growth conditions. After discarding the MTT solution, DMSO was added in order to dissolve the formed formazan, followed by measuring formazan absorbance at 570 nm, and additionally at

the reference/background wavelength of 670 nm, by using a SpectraMax M5 multi-well plate reader (Molecular Devices, San Jose, CA, USA).

For the CV assay, cells were washed once with PBS and fixed with 4% paraformaldehyde (PFA) for 20 min at room temperature (RT). After discarding the PFA solution, the cells were left to dry for 10 min and then stained with 1% crystal violet solution for 15 min at RT. The cells were washed with water and were dried overnight at RT. Afterwards, acetic acid (33% in ultrapure water) was added to the stained cells and absorbance was measured at 570 nm and 670 nm (reference wavelength) using a SpectraMax M5 multi-well plate reader (Molecular Devices, San Jose, CA, USA). For data analyses, GraphPad Prism version 8.0.2, SigmaPlot 14.0 and Microsoft Excel 2013 were used. The results are shown as a percentage of the control values obtained from untreated cultures, i.e. cell viability in percent.

2.3.4.4 Antibacterial assay against Aliivibrio fischerii

The isolated compounds were tested at concentrations of 1 and 100 µM against the Gram-negative *Aliivibrio fischerii* test strain DSM507 (batch no. 1209), with chloramphenicol (100 µM) serving as a positive control as previously reported [94,95].

In brief, 25 ml BOSS medium containing fresh glycerol was incubated at 100 rpm and 23 ° C for 16 to 18 hours before being diluted with fresh BOSS medium to an appropriate cell number (luminescence value between 30,000 and 50,000 RLU). The assay was carried out in 96 well black flat bottomed plates (Brand cell GradeTM premium, STERILE R) with a final volume of 200 µl of BOSS medium containing 1% DMSO per well (100 µl of diluted bacterial solution and 100 µl of test solution). The plates were incubated in the dark for 24 hours without a lid and without shaking at a temperature of 23 °C and a humidity of 100 percent. The bioluminescence (measured in relative luminescence units, RLU) is proportional to cell density and was calculated after 24 hours using the TecanGeniosPro microplate reader. As a result, the entire 1000 ms wavelength range was detected without any preliminary shaking to avoid secondary oxygen effects. The results (mean standard deviation value, n = 6) are given as relative values (percent inhibition) to the negative control (bacterial growth, 1 % DMSO without test compound). Negative values indicate that bacterial growth is accelerating or that luminescence is increasing.

2.4   Conclusion

Investigation of *P. sarmentosum* extract yielded three new compounds (**1**-**3**) and 31 known ones. The structures of these compounds were confirmed by several spectroscopic techniques, i.e ^{1}H-NMR, ^{13}C-NMR, 2D NMR, and HRMS. The isolated compounds were

evaluated for their anthelmintic, antifungal, cytotoxic, antibacterial and neuroprotective activities. It is remarkable to note that only very few compounds showed cytotoxic effects, and only at high concentration. Some isolated compounds showed anthelmintic, antifungal, antibacterial and neuroprotective potential. Our finding suggests that *P. sarmentosum* likely is not very toxic and is an important source of mild health-promoting effects.

2.5   References

1.   Gutierrez, Y.V.; Yamaguchi, L.F.; de Moraes, M.M.; Jeffrey, C.S.; Kato, M.J., Natural products from *Peperomia*: occurrence, biogenesis and bioactivity. *Phytochem. Rev.* **2016**, 15, 1009-1033.
2.   Salehi, B.; Zakaria, Z.A.; Gyawali, R.; Ibrahim, S.A.; Rajkovic, J.; Shinwari, Z.K.; Khan, T.; Sharifi-Rad, J.; Ozleyen, A.; Turkdonmez, E.; Valussi, M.; Tumer, T.B.; Monzote Fidalgo, L.; Martorell, M.; Setzer, W.N., *Piper* species: A comprehensive review on their phytochemistry, biological activities and applications. *Molecules* **2019**, 24, 1364.
3.   Islam, M.T.; Hasan, J.; Snigdha, H.; Ali, E.S.; Sharifi-Rad, J.; Martorell, M.; Mubarak, M.S., Chemical profile, traditional uses, and biological activities of *Piper chaba* Hunter: A review. *J. Ethnopharmacol.* **2020**, 257, 112853.
4.   Gutierrez, R.M.; Gonzalez, A.M.; Hoyo-Vadillo, C., Alkaloids from *Piper*: a review of its phytochemistry and pharmacology. *Mini Rev. Med. Chem.* **2013**, 13, 163-193.
5.   Da Silva, J.K.R.; Pinto, L.C.; Burbano, R.M.R.; Montenegro, R.C.; Guimaraes, E.F.; Andrade, E.H.A.; Maia, J.G.S., Essential oils of Amazon *Piper* species and their cytotoxic, antifungal, antioxidant and anti-cholinesterase activities. *Ind. Crop Prod.* **2014**, 58, 55-60.
6.   Mgbeahuruike, E.E.; Yrjonen, T.; Vuorela, H.; Holm, Y., Bioactive compounds from medicinal plants: Focus on *Piper* species. *S. Afr. J. Bot.* **2017**, 112, 54-69.
7.   Branquinho, L.S.; Santos, J.A.; Cardoso, C.A.L.; Mota, J.D.S.; Junior, U.L.; Kassuya, C.A.L.; Arena, A.C., Anti-inflammatory and toxicological evaluation of essential oil from *Piper glabratum* leaves. *J. Ethnopharmacol.* **2017**, 198, 372-378.
8.   Rukachaisirikul, T.; Siriwattanakit, P.; Sukcharoenphol, K.; Wongvein, C.; Ruttanaweang, P.; Wongwattanavuch, P.; Suksamrarn, A., Chemical constituents and bioactivity of *Piper sarmentosum*. *J. Ethnopharmacol.* **2004**, 93, 173-176.
9.   Atiax, E.; Ahmad, F.; Sirat, H.; Arbain, D., Antibacterial activity and cytotoxicity screening of Sumatran Kaduk (*Piper sarmentosum* Roxb.). *Iran. J. Pharmacol. Ther.* **2011**, 10, 1-5.
10.   Ismail, S.M.; Sundar, U.M.; Hui, C.K.; Aminuddin, A.; Ugusman, A., *Piper sarmentosum* attenuates TNF-alpha-induced VCAM-1 and ICAM-1 expression in human umbilical vein endothelial cells. *J. Taibah Univ. Med. Sci.* **2018**, 13, 225-231.
11.   Burkill, I.H.; Birtwistle, W.; Foxworthy, F.W.; Scrivenor, J.B.; Watson, J.G., *A dictionary of the economic products of the Malay Peninsula*. governments of Malaysia and Singapore by the Ministry of Agriculture and cooperatives: **1966**.
12.   Sim, K.M.; Mak, C.N.; Ho, L.P., A new amide alkaloid from the leaves of *Piper sarmentosum*. *J. Asian Nat. Prod. Res.* **2009**,11, 757-760.
13.   Ab-Rahman, M.R.; Abdul Razak, F.; Mohd Bakri, M., Evaluation of wound closure activity of *Nigella sativa*, *Melastoma malabathricum, Pluchea indica, and Piper sarmentosum* extracts on scratched monolayer of human gingival fibroblasts. *Evid. Based Complement. Alternat. Med.* **2014**, 2014, 190342.
14.   Sun, X.; Chen, W.; Dai, W.; Xin, H.; Rahmand, K.; Wang, Y.; Zhang, J.; Zhang, S.; Xu, L.; Han, T., *Piper sarmentosum* Roxb.: A review on its botany, traditional uses, phytochemistry, and pharmacological activities. *J. Ethnopharmacol.* **2020**, 263, 112897.
15.   Devanthran, K.; Unyah, Z.; Majid, R.A.; Abdullah, W.O., In vitro activity of *Piper sarmentosum* ethanol leaf extract against *Toxoplasma gondii* tachyzoites. *Trop. J. Pharm. Res.* **2017**, 16, 2667-2673.

16. Sanusi, A.; Umar, R.A.; Zahary, M.N.; Rohin, M.A.K.; Pauzi, M.; Ismail, S., Chemical compositions and antimicrobial properties of *Piper sarmentosum* - A Review. *IOSR J. Dent. Med. Sci.* **2017**, 16, 62-65.

17. Chaimanee, V.; Thongtue, U.; Sornmai, N.; Songsri, S.; Pettis, J.S., Antimicrobial activity of plant extracts against the honeybee pathogens, *Paenibacillus larvae* and *Ascosphaera apis* and their topical toxicity to *Apis mellifera* adults. *J. App. Microbiol.* **2017**, 123, 1160-1167.

18. Estai, M.A.; Soelaiman, I.N.; Shuid, A.N.; Das, S.; Ali, A.M.; Suhaimi, F.H., Histological changes in the fracture callus following the administration of water extract of *Piper sarmentosum* (*daun kadok*) in estrogen-deficient rats. *Iran. J. Med. Sci.* **2011**, 36, 281-288.

19. Ramli, E.S.M.; Soelaiman, I.N.; Othman, F.; Ahmad, F.; Shuib, A.N.; Mohamed, N.; Muhammad, N.; Suhaimi, F., The effects of *Piper sarmentosum* water extract on the expression and activity of 11β-hydroxysteroid dehydrogenase type 1 in the bones with excessive glucocorticoids. *Iran. J. Med. Sci.* **2012**, 37, 39-46.

20. Khan, M.; Elhussein, S.A.A.; Khan, M.M.; Khan, N., Anti-acetylcholinesterase activity of *Piper sarmentosum* by a continuous immobilized-enzyme Assay. *APCBEE Procedia.* **2012**, 2, 199-204.

21. Li, Q.; Qu, F.L.; Gao, Y.; Jiang, Y.P.; Rahman, K.; Lee, K.H.; Han, T.; Qin, L.P., *Piper sarmentosum* Roxb. produces antidepressant-like effects in rodents, associated with activation of the CREB-BDNF-ERK signaling pathway and reversal of HPA axis hyperactivity. *J. Ethnopharmacol.* **2017**, 199, 9-19.

22. Yeo, E.T.Y.; Wong, K.W.L.; See, M.L.; Wong, K.Y.; Gan, S.Y.; Chan, E.W.L., *Piper sarmentosum* Roxb. confers neuroprotection on beta-amyloid (Aβ)-induced microglia-mediated neuroinflammation and attenuates tau hyperphosphorylation in SH-SY5Y cells. *J. Ethnopharmacol.* **2018**, 217, 187-194.

23. Azlina, M.F.N.; Qodriyah, H.M.S.; Akmal, M.N.; Ibrahim, I.A.A.; Kamisah, Y., In vivo effect of *Piper sarmentosum* methanolic extract on stress-induced gastric ulcers in rats. *Arch. Med. Sci.* **2019**, 15, 223-231.

24. Ariffin, S.H.Z.; Wan Omar, W.H.; Ariffin, Z.Z.; Safian, M.F.; Senafi, S.; Abdul Wahab, R.M., Intrinsic anticarcinogenic effects of *Piper sarmentosum* ethanolic extract on a human hepatoma cell line. *Cancer Cell Int.* **2009**, 9, 6.

25. Krisanapun, C.; Wongkrajang, Y.; Temsiririrkkul, R.; Phornchirasilp, S.; Peungvicha, P., In vitro evaluation of anti-diabetic potential of *Piper sarmentosum* Roxb. extract. *FASEB J.* **2012**, 26, 686.7-686.7.

26. Hematpoor, A.; Paydar, M.; Liew, S.Y.; Sivasothy, Y.; Mohebali, N.; Looi, C.Y.; Wong, W. F.; Azirun, M.S.; Awang, K., Phenylpropanoids isolated from *Piper sarmentosum* Roxb. induce apoptosis in breast cancer cells through reactive oxygen species and mitochondrial-dependent pathways. *Chem. Biol. Interact.* **2018**, 279, 210-218.

27. Baba, M.S.; Hassan, Z.A.A., *Piper Sarmentosum* leaf as a promising non-toxic antiparasitic agent against trypanosoma evansi-induced mice. *Malays. J. Microsc.* **2019**, 15, 46-60.

28. Mohd Zainudin, M.; Zakaria, Z.; Megat Mohd Nordin, N.A., The use of *Piper sarmentosum* leaves aqueous extract (Kadukmy™) as antihypertensive agent in spontaneous hypertensive rats. *BMC Complement. Altern. Med.* **2015**, 15, 54.

29. Fauzy, F.H.; Mohd Zainudin, M.; Ismawi, H.R.; Elshami, T.F.T., *Piper sarmentosum* leaves aqueous extract attenuates vascular endothelial dysfunction in spontaneously hypertensive rats. *Evid. Based Complement. Alternat. Med.* **2019**, 2019, 7198592.

30. Bjoroy, O.; Rayyan, S.; Fossen, T.; Kalberg, K.; Andersen, O.M., C-glycosylanthocyanidins synthesized from C-glycosylflavones. *Phytochemistry* **2009**, 70, 278-287.

31. Isayenkova, J.; Wray, V.; Nimtz, M.; Strack, D.; Vogt, T., Cloning and functional characterisation of two regioselective flavonoid glucosyltransferases from *Beta vulgaris*. *Phytochemistry* **2006**, 67, 1598-1612.

32. Liu, J.Y.; Li, S.Y.; Feng, J.Y.; Sun, Y.; Cai, J N.; Sun, X.F.; Yang, S.L., Flavone C-glycosides from the flowers of *Trollius chinensis* and their anti-complementary activity. *J. Asian Nat. Prod. Res.* **2013**, 15, 325-331.

33. Esaki, H.; Aoki, F.; Umemura, M.; Kato, M.; Maegawa, T.; Monguchi, Y.; Sajiki, H., Efficient h/d exchange reactions of alkyl-substituted benzene derivatives by means of the Pd/C-H(2)-D(2)O system. *Chemistry* **2007**, 13, 4052-4063.

34. Godecke, T.; Kaloga, M.; Kolodziej, H., A phenol glucoside, uncommon coumarins and flavonoids from *Pelargonium sidoides* DC. *Z. Naturforsch. B.* **2005**, 60, 677-682.

35. Ayer, W.A.; Racok, J.S., The metabolites of Talaromycesflavus: Part 1. Metabolites of the organic extracts. *Can. J. Chem.* **1990**, 68, 2085-2094.

36. Tanaka, Y.; Yanagida, A.; Komeya, S.; Kawana, M.; Honma, D.; Tagashira, M.; Kanda, T.; Shibusawa, Y., Comprehensive separation and structural analyses of polyphenols and related compounds from bracts of hops (*Humulus lupulus* L.). *J. Agric. Food Chem.* **2014**, 62, 2198-2206.

37. Pascual Teresa, J.D.; Urones, J.G.; Marcos, I.S.; Núñez, L.; Basabe, P., Diterpenoids and flavonoids from *Cistus palinhae*. *Phytochemistry* **1983**, 22, 2805-2808.

38. Yang, D.; Wong, M.K.; Yan, Z., Regioselective intramolecular oxidation of phenols and anisoles by dioxiranes generated in situ. *J. Org. Chem.* **2000**, 65, 4179-4184.

39. Hematpoor, A.; Liew, S.Y.; Chong, W.L.; Azirun, M.S.; Lee, V.S.; Awang, K., Inhibition and larvicidal activity of phenylpropanoids from *Piper sarmentosum* on acetylcholinesterase against mosquito vectors andt Their binding mode of interaction. *PLoS One* **2016**, 11, e0155265.

40. Elban, M.A.; Chapuis, J.C.; Li, M.; Hecht, S.M., Synthesis and biological evaluation of cepharadiones A and B and related dioxoaporphines. *Bioorg. Med. Chem.* **2007**, 15, 6119-6125.

41. Lin, C.F.; Hwang, T.L.; Chien, C.C.; Tu, H.Y.; Lay, H.L., A New Hydroxychavicol dimer from the roots of *Piper betle*. *Molecules* **2013**, 18, 2563-2570.

42. Yan, Z.H.; Han, Z.Z.; Hu, X.Q.; Liu, Q.X.; Zhang, W.D.; Liu, R.H.; Li, H.L., Chemical constituents of *Euonymus alatus*. *Chem. Nat. Compd.* **2013**, 49, 340-342.

43. Azman, N.A.N.; Alhawarri, M.B.; Rawa, M.S.A.; Dianita, R.; Gazzali, A.M.; Nogawa, T.; Wahab, H.A., Potential anti-acetylcholinesterase activity of *Cassia timorensis* DC. *Molecules* **2020**, 25, 4545.

44. Li, C.Y.; Tsai, W.J.; Damu, A.G.; Lee, E.J.; Wu, T.S.; Dung, N.X.; Thang, T.D.; Thanh, L., Isolation and identification of antiplatelet aggregatory principles from the leaves of *Piper lolot*. *J. Agric. Food Chem.* **2007**, 55, 9436-9442.

45. Piyatida, P.; Suenaga, K.; Ohno, O.; Kato-Noguchi, H., Isolation of allelopathic substance from *Piper sarmentosum* Roxb. *Allelopathy J.* **2012**, 30, 93-102.

46. Akramov, D.K.; Bacher, M.; Zengin, G.; Bohmdorfer, S.; Rosenau, T.; Azimova, S.S.; Mamadalieva, N.Z., Chemical composition and anticholinesterase activity of *Lagochilus inebrians*. *Chem. Nat. Compd.* **2019**, 55, 575-577.

47. Seigler, D.S.; Pauli, G.F.; Nahrstedt, A.; Leen, R., Cyanogenic allosides and glucosides from *Passiflora edulis* and *Carica papaya*. *Phytochemistry* **2002**, 60, 873-882.

48. Tsuruga, T.; Ebizuka, Y.; Nakajima, J.; Chun, Y.T.; Noguchi, H.; Iitaka, Y.; Sankawa, U., Biologically active constituents of *Magnolia salicifolia*: Inhibitors of induced histamine release from rat mast cells. *Chem. Pharm. Bull.* **1991**, 39, 3265-3271.

49. Koul, S.K.; Taneja, S.C.; Malhotra, S.; Dhar, K.L., Phenylpropanoids and (−)-ledol from two *Piper* species. *Phytochemistry* **1993**, 32, 478-480.

50. Devari, S.; Rizvi, M.A.; Shah, B.A., Visible light mediated chemo-selective oxidation of benzylic alcohols. *Tetrahedron Lett.* **2016**, 57, 3294-3297.

51. Xie, L.W.; Atanasov, A.G.; Guo, D.A.; Malainer, C.; Zhang, J.X.; Zehl, M.; Guan, S.H.; Heiss, E.H.; Urban, E.; Dirsch, V.M.; Kopp, B., Activity-guided isolation of NF-κB inhibitors and PPARγ agonists from the root bark of *Lycium chinense* Miller. *J. Ethnopharmacol.* **2014**, 152, 470-477.

52. Lo, W.L.; Chang, F.R.; Wu, Y.C., Alkaloids from the leaves of *Fissistigma glaucescens*. *J. Chin. Chem. Soc.* **2000**, 47, 1251-1256.

53. Yang, X.N.; Jin, Y.S.; Zhu, P.; Chen, H.S., Amides from *Uvaria microcarpa*. *Chem. Nat. Compd.* **2010**, 46, 324-326.

54. Otsuka, H.; Yao, M.; Kamada, K.; Takeda, Y., Alangionosides G-M: glycosides of megastigmane derivatives from the leaves of *Alangium premnifolium*. *Chem. Pharm. Bull.* **1995**, 43, 754-759.

55. Ryu, J.H.; Son, H.J.; Lee, S.H.; Sohn, D.H., Two neolignans from *Perilla frutescens* and their inhibition of nitric oxide synthase and tumor necrosis factor-alpha expression in murine macrophage cell line RAW 264.7. *Bioorg. Med. Chem. Lett.* **2002**, 12, 649-651.

56. Mbaveng, A.T.; Wamba, B.E.N.; Bitchagno, G.T.M.; Tankeo, S.B.; Celik, I.; Atontsa, B.C.K.; Lonfouo, A.H.N.; Kuete, V.; Efferth, T., Bioactivity of fractions and constituents of *Piper capense* fruits towards a broad panel of cancer cells. *J. Ethnopharmacol.* **2021**, 271, 113884.

57. Gong, Y.; Li, H.X.; Guo, R.H.; Widowati, W.; Kim, Y.H.; Yang, S.Y.; Kim, Y.R., Anti-allergic inflammatory components from the leaves of *Piper crocatum* Ruiz & Pav. *Biol. Pharm. Bull.* **2021**, 44, 245-250.

58. Usia, T.; Watabe, T.; Kadota, S.; Tezuka, Y., Potent CYP3A4 inhibitory constituents of *Piper cubeba*. *J. Nat. Prod.* **2005**, 68, 64-68.

59. Alqadeeri, F.; Rukayadi, Y.; Abbas, F.; Shaari, K., Antibacterial and antispore activities of isolated compounds from *Piper cubeba* L. *Molecules* **2019**, 24,3095.

60. Zheng, Y.K.; Su, B.J.; Wang, Y.Q.; Wang, H.S.; Liao, H.B.; Liang, D., New tyramine- and aporphine-type alkamides with NO release inhibitory activities from *Piper puberulum*. *J. Nat. Prod.* **2021**, 84, 1316-1325.

61. Salleh, W.M.N.H.W.; Hashim, N.A.; Khamis, S., Chemical constituents of *Piper ribesioides*. *Chem. Nat. Compd.* **2021**, 57, 795-797.

62. Mahindru, R.N.; Taneja, S.C.; Dhar, K.L.; Brown, R.T., Reassignment of structures of the neolignans, magnosalin and andamanicin. *Phytochemistry* **1993**, 32, 1073-1075.

63. Luyen, B.T.T.; Thao, N.P.; Widowati, W.; Fauziah, N.; Maesaroh, M.; Herlina, T.; Kim, Y.H., Chemical constituents of *Piper aduncum* and their inhibitory effects on soluble epoxide hydrolase and tyrosinase. *Med. Chem. Res.* **2017**, 26, 220-226.

64. Zou, J.H.; Yang, J.S.; Dong, Y.S.; Zhou, L.; Lin, G., Flavone C-glycosides from flowers of *Trollius ledebouri*. *Phytochemistry* **2005**, 66, 1121-1125.

65. Teng, R.W.; Wang, D.Z.; Wu, Y.S.; Lu, Y.; Zheng, Q.T.; Yang, C.R., NMR assignments and single-crystal X-ray diffraction analysis of deoxyloganic acid. *Magn. Reson. Chem.* **2005**, 43, 92-96.

66. Woo, S.Y.; Wong, C.P.; Win, N.N.; Lae, K.Z.W.; Woo, B.; Elsabbagh, S.A.; Liu, Q.Q.; Ngwe, H.; Morita, H., Anti-melanin deposition activity and active constituents of *Jatropha multifida* stems. *J. Nat. Med.* **2019**, 73, 805-813.

67. Cortes, D.; Hocquemiller, R.; Leboeuf, M.; Cave, A.; Moretti, C., Alkaloids of Annonaceae . Part 68. Alkaloids from the leaves of *Guatteria ouregou*. *J. Nat. Prod.* **1986**, 49, 878-884.

68. Yun, E.Y.; Hwang, J.S.; Kim, M.A.; Baek, M.H.; Jun, M.R.; Youn, K.J.; Lee, S.A., A novel compound isolated from *Tenebrio molitor* larvae and separation method thereof. Patent: WO2017175915A1 (12.10. **2017**).

69. Li, G.Q.; Zhang, Y.B.; Guan, H.S., A new isoxazol from *Glehnia littoralis*. *Fitoterapia* **2008**, 79, 238-239.

70. Sun, D.D.; Dong, W.W.; Li, X.; Zhang, H.Q., Indole alkaloids from the roots of *Isatis ingigotica* and their antiherpes simplex virus type 2 (HSV-2) activity in vitro. *Chem. Nat. Compd.* **2010**, 46, 763-766.

71. Muraoka, A.; Sawada, T.; Morimoto, E.; Tanabe, G., Chalcones as synthetic intermediates. A facile route to (±)-magnosalicin, an antiallergy neolignan. *Chem. Pharm. Bull.* **1993**, 41, 772-774.

72. Tsuruga, T.; Ebizuka, Y.; Nakajima, J.; Chun, Y.T.; Noguchi, H.; Iitaka, Y.; Sankawa, U., Isolation of a new neolignan, magnosalicin, from *Magnolia salicifolia*. *Tetrahedron Lett.* **1984**, 25, 4129-4132.

73. McGaw, L.J.; Jager, A.K.; van Staden, J., Isolation of β-asarone, an antibacterial and anthelmintic compound, from *Acorus calamus* in South Africa. *S. Afr. J. Bot.* **2002**, 68, 31-35.

74. Unelius, C.R.; Bohman, B.; Nordlander, G., Comparison of phenylacetates with benzoates and phenylpropanoates as antifeedants for the pine weevil, *Hylobius abietis*. *J. Agric. Food Chem.* **2018**, 66, 11797-11805.

75. Shi, Y.N.; Liu, F.F.; Jacob, M.R.; Li, X.C.; Zhu, H.T.; Wang, D.; Cheng, R.R.; Yang, C.R.; Xu, M.; Zhang, Y.J., Antifungal amide alkaloids from the aerial parts of *Piper flaviflorum* and *Piper sarmentosum*. *Planta Med.* **2017**, 83, 143-150.

76. Tabopda, T.K.; Ngoupayo, J.; Liu, J.; Mitaine-Offer, A.C.; Tanoli, S.A.K.; Khan, S.N.; Ali, M. S.; Ngadjui, B.T.; Tsamo, E.; Lacaille-Dubois, M.A.; Luu, B., Bioactive aristolactams from *Piper umbellatum*. *Phytochemistry* **2008**, 69, 1726-1731.

77.	Park, C.J.; Kim, H.S.; Lee, D.W.; Kim, J.; Choi, Y.H., Identification of antifungal constituents of essential oils extracted from *Boesenbergia pulcherrima* against Fusarium wilt (*Fusarium oxysporum*). *App. Biol. Chem.* **2020**, 63, 34.

78.	Bai, Y.; Sun, Y.; Xie, J.; Li, B.; Bai, Y.; Zhang, D.; Liang, J.; Xiao, C.; Zhong, A.; Cao, Y.; Zheng, X., The asarone-derived phenylpropanoids from the rhizome of *Acorus calamus* var. *angustatus* Besser. *Phytochemistry* **2020**, 170, 112212.

79.	Wang, Z.J.; Zhu, Y.Y.; Yi, X.; Zhou, Z.S.; He, Y.J.; Zhou, Y.; Qi, Z.H.; Jin, D.N.; Zhao, L.X.; Luo, X.D., Bioguided isolation, identification and activity evaluation of antifungal compounds from *Acorus tatarinowii* Schott. *J. Ethnopharmacol.* **2020**, 261, 113119.

80.	Lee, H.S., Fungicidal property of active component derived from *Acorus gramineus* rhizome against phytopathogenic fungi. *Bioresource Technol.* **2007**, 98, 1324-1328.

81.	Tsai, I.L.; Lee, F.P.; Wu, C.C.; Duh, C.Y.; Ishikawa, T.; Chen, J.J.; Chen, Y.C.; Seki, H.; Chen, I.S., New cytotoxic cyclobutanoid amides, a new furanoid lignan and anti-platelet aggregation constituents from *Piper arborescens*. *Planta Med.* **2005**, 71, 535-542.

82.	Wu, T.S.; Leu, Y.L.; Chan, Y.Y., Constituents from the stem and root of *Aristolochia kaempferi*. *Biol. Pharm. Bull.* **2000**, 23, 1216-1219.

83.	Zou, J.; Zhang, S.; Zhao, H.; Wang, Y.H.; Zhou, Z.Q.; Chen, G.D.; Hu, D.; Li, N.; Yao, X.S.; Gao, H., Biotransformation of α-asarone by *Alternaria longipes* CGMCC 3.2875. *Chin. J. Nat. Med.* **2021**, 19, 700-705.

84.	Mata, R.; Morales, I.; Perez, O.; Rivero-Cruz, I.; Acevedo, L.; Enriquez-Mendoza, I.; Bye, R.; Franzblau, S.; Timmermann, B., Antimycobacterial compounds from *Piper sanctum*. *J. Nat. Prod.* **2004**, 67, 1961-1968.

85.	Elhendawy, M.A.; Wanas, A.S.; Radwan, M.M.; Azzaz, N.A.; Toson, E.S.; ElSohly, M.A., Chemical and biological studies of *Cannabis sativa* roots. *Med. Cannabis Cannabinoids.* **2019**, 1, 104-111.

86.	Nongmai, C.; Kanokmedhakul, K.; Promgool, T.; Paluka, J.; Suwanphakdee, C.; Kanokmedhakul, S., Chemical constituents and antibacterial activity from the stems and leaves of *Piper wallichii*. *J. Asian Nat. Prod. Res.* **2022**, 24, 344-352.

87.	Lee, J.E.; Kim, N.; Yeo, J.Y.; Seo, D.G.; Kim, S.; Lee, J.S.; Hwang, K.W.; Park, S.Y., Anti-amyloidogenic effects of asarone derivatives from *Perilla frutescens* leaves against beta-amyloid aggregation and nitric oxide production. *Molecules* **2019**, 24, 4297.

88.	Kim, S.R.; Sung, S.H.; Kang, S.Y.; Koo, K.A.; Kim, S.H.; Ma, C.J.; Lee, H.S.; Park, M.J.; Kim, Y.C., Aristolactam BII of *Saururus chinensis* attenuates glutamate-induced neurotoxicity in rat cortical cultures probably by inhibiting nitric oxide production. *Planta Med.* **2004**, 70, 391-396.

89.	Kim, K.H.; Choi, J.W.; Choi, S.U.; Ha, S.K.; Kim, S.Y.; Park, H.J.; Lee, K.R., The chemical constituents of *Piper kadsura* and their cytotoxic and anti-neuroinflammtaory activities. *J. Enzym Inhib. Med. Chem.* **2011**, 26, 254-260.

90.	Thomsen, H.; Reider, K.; Franke, K.; Wessjohann, L.A.; Keiser, J.; Dagne, E.; Arnold, N., Characterization of constituents and anthelmintic properties of *Hagenia abyssinica*. *Sci. Pharm.* **2012**, 80, 433-446.

91.	Stiernagle, T., Maintenance of *C. elegans*. *WormBook : the online review of C. elegans biology.* **2006**, 1-11.

92.	Otto, A.; Laub, A.; Porzel, A.; Schmidt, J.; Wessjohann, L.; Westermann, B.; Arnold, N., Isolation and total synthesis of albupeptins A-D: 11-residue peptaibols from the fungus *Gliocladium album*. *Eur. J. Org. Chem.* **2015**, 2015, 7449-7459.

93.	Khan, M.F.; Nasr, F.A.; Noman, O.M.; Alyhya, N.A.; Ali, I.; Saoud, M.; Rennert, R.; Dube, M.; Hussain, W.; Green, I.R.; Basudan, O.A.M.; Ullah, R.; Anazi, S. H.; Hussain, H., Cichorins D-F: Three new compounds from *Cichorium intybus* and their biological effects. *Molecules* **2020**, 25, 4160.

94.	Stark, S. Utilization of the Ugi four-component reaction for the synthesis of lipophilic peptidomimetics as potential antimicrobials. Dissertation MLU Halle-Wittenberg, **2016**.

95.	Ware, I.; Franke, K.; Hussain, H.; Morgan, I.; Rennert, R.; Wessjohann, L.A. Bioactive Phenolic Compounds from *Peperomia obtusifolia*. *Molecules* 2022, 27, 4363.

Chapter 3

-

Organ-specific metabolite variations in *Piper sarmentosum* Roxb. approached by LC-MS-based metabolic profiling

Abstract*

Piper sarmentosum Roxb. (Piperaceae) is a traditional medicinal plant widely distributed in the tropical and subtropical regions of Asia, offering both health and culinary benefits. In this study the secondary metabolites in different organs of *P. sarmentosum* were identified and quantitatively described. The metabolic profiles of leaves, roots, stems and fruits were determined using liquid chromatography high-resolution mass spectrometry (LC-HRMS/MS) combined with multivariate data analysis. Detailed MS/MS fragmentation pattern analysis revealed the presence of 154 metabolites which were tentatively identified and classified, mostly alkaloids and flavonoids. The correlations between the organs and the relative abundance of these compounds were presented using multivariate analysis which consist of principle component analyses and hierarchical clustering. Both multivariate-type analyses displayed a clear diversity of *P. sarmentosum* organs with magnoflorines, piperolactam A and B, andamanicin, *trans*-asarone, pellitorine, brachyamide B, guineensine, nigrinodine and sarmentine as organ specific metabolites, and thus potential markers for organ identification. Overall, this study provides extensive data on the metabolic profiles of *P. sarmentosum*, supplying useful information for bioactive compounds discovery and their preferential formation in specific organs. This can be used to optimize production and harvesting as well as to maximize the plant's economic value as herbal medicine or in food applications.

Keywords: Piperaceae; LC-MS; metabolomics; plant organ biomarkers (chemical); medicinal plant; food plant

---

3.1   Introduction

The genus *Piper* is the largest genus of the Piperaceae, comprising about 2000 species widely distributed in tropical and subtropical regions [1]. About 600 species are reported from Asia, most of them are distributed in the Malesia region [2]. Many of these *Piper* species have long been used in traditional medicine of for food purpose. Only few of them have been pharmacologically proven activities [3].

Piper sarmentosum Roxb. is common in several Asian countries. The whole plant, leaves, fruits, stems and roots have been used as medicine for many decades and have significant medicinal and nutritional value [4]. The tender leaves of *P. sarmentosum* are consumed as vegetables and traditionally used in Malaysia and Indonesia to treat malaria, cough and rheumatic pain [5,6]. People in southern Thailand commonly employ the whole plant to treat muscle pain and hyperglycemia [7,8]. In Chinese folk medicine, the whole plant, dry aerial parts, leaves, roots or fruits are used to treat a variety of diseases such as uterine bleeding, rheumatic bone pain, traumatic injuries, insect and snake bites, toothache, fever, and stomach pain. In addition, some communities in the southern part of China often use roots, fruits and leaves as traditional edible vegetables [9,10].

Several studies have been reported on *P. sarmentosum,* mainly focusing on the constituents and pharmacological activities of the leaves [3,10,11]; (see also chapter 2). In addition, a number of pharmacological studies have recently been conducted in Malaysia, which showed that the extract of *P. sarmentosum* leaves has vascular protective, neuroprotective, anti-obesity, and anti-hyperlipidemia activity [12-14]. However, little is known about the metabolite composition and medicinal value of other organs. Moreover, the metabolite profiles and chemical differences of different organs of *P. sarmentosum* have not been systematically elucidated by metabolite profiling before.

LC-MS-based metabolite profiling is the method of choice to address the complex patterns of biologically active natural products in herbal plants [15]. In its state-of-the-art implementation, this technique relies on the ultra-high performance liquid chromatography (UHPLC) coupled on-line to electrospray ionisation-quadrupole time-of-flight mass spectrometry (ESI-QqTOF-MS). Currently, UHPLC is the best method of liquid chromatography in terms of resolution, sensitivity, and throughput, while QqTOF-MS is one of the most sensitive, accurate, fast and processive detector, which is ideal for identification and quantification of a wide range of natural products in the most complex and challenging samples. Due to its powerful strategic combination of high resolution and sensitivity, the coupling of UHPLC to ESI-QqTOF-MS has been successfully used to analyze complex samples [16]. The

high throughput of this platform gave access to discriminating different plant varieties [16-18], plant organs [19], plant developmental stages [20,21], the geographical origin of plants [22-24], and determining the quality of traditional medicinal plants and processed products [25-28].
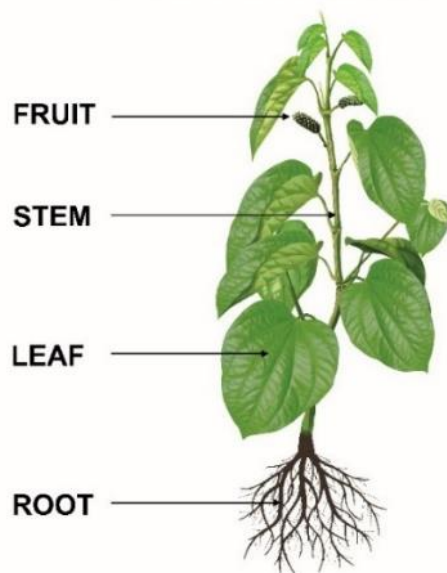
Figure 3.1: Schematic diagram of the whole *Piper sarmentosum* plant showing fruit, stem, leaf and root used in this study.

Therefore, in the present study, the metabolic profiles of four different organs of *P. sarmentosum,* namely the leaf, stem, root and fruit (Figure 3.1), were comprehensively characterized by UHPLC coupled on-line to ESI-QqTOF-MS. The variability of metabolite contents was estimated, and potential biomarkers of each organ could be assessed by multivariate analysis, i.e. principal component analysis (PCA) and hierarchical clustering. These statistical methods provide a comprehensive and intuitive description of the chemical constituents in the four organs of *P. sarmentosum* which can serve as valuable resources for further functional studies on the species.

3.2 Results and discussion

3.2.1 LC-MS fingerprints

The present study employed the high-resolution RP-UHPLC-ESI-QqTOF-MS to determine the intra-organ variation and relative abundances of metabolites extracted from leaf, stem, root and fruit of *P. sarmentosum*. The aim was to achieve high chromatographic resolution to detect as many individual chemical species in a single batch analysis, as possible. First, to determine the appropriate ion detection mode, the SWATH experiments were performed in both positive and negative ionization modes. According to the results of these experiments, LC-MS analysis in positive ion mode revealed essentially more peaks, better

sensitivity and more rich and explicit structural information. This can be explained by the presence of numerous metabolites in the test samples, as e.g. alkaloids, that are more likely to be ionized in the positive ion mode than in negative one. Therefore, only the positive ionization mode was used for all further series of MS analyses.

In order to monitor the reproducibility of sample preparation and instrument performance, aliquots of a quality control (QC) sample (i.e. an extract prepared from the mixed plant powder of all organs) were systematically measured between sample sequences. The stability of retention times and UHPLC performance were also examined by the presence of orcinol ($C_7H_8O_2$) and kinetin ($C_{10}H_9N_5O$) as internal standards (IS). Both of these cost efficient and routinely used ISs eluted at specific retention times, (4.9 min for orcinol and 5.3 min for kinetin), showed good ionization properties and not appearing in any organs of *P. sarmentosum in vivo*.

3.2.2   Analysis and comparison of LC-MS fingerprints

The representative total ion chromatograms (TICs) acquired with the extracts, isolated from the different organs, are shown in Figure 3.2. The efficient RP-UHPLC separation of *P. sarmentosum* metabolites was successfully achieved in 23 minutes. Most of the major peaks exhibited clearly different intensities in the TICs acquired with the extracts prepared from different organs. For example, the TIC of fruit extract showed lower intensity of peaks eluting between 5 and 10 minutes compared to the extracts prepared from other organs (Figure 3.2). On the other hand, the peaks eluting between 11 and 17 minutes demonstrated clearly higher intensity in this extract. Under the conditions employed in the current study, the fruit extracts contained less polar/semi-polar compounds, although these extracts were enriched in non-polar compounds. In contrast, the leaf extracts were featured with the opposite pattern of relative metabolite abundances. Thus, our results clearly demonstrated that the patterns of characteristic *P. sarmentosum* metabolites depend on the plant organ.

In this study, these patterns were analyzed by electrospray (ESI) high-resolution-mass spectrometry (HR-MS) to enable the determination of the elemental composition. Based on this data, complemented with mass spectral fragmentation patterns obtained in MS/MS experiments, databases and co-elution experiments with authentic standard reference compounds (see 3.2.3 for details) the most prominent peaks found in the t_R range of 11 – 17 min (Figure 3.2) could be assigned to the groups of piperamides and phenylpropanoids. For example, peaks **P93**, **P95**, **P112**, **P114** and **P136** were putatively identified as nigrinodine, *trans*-asarone, sarmentine, brachyamide B and guineensine, respectively.
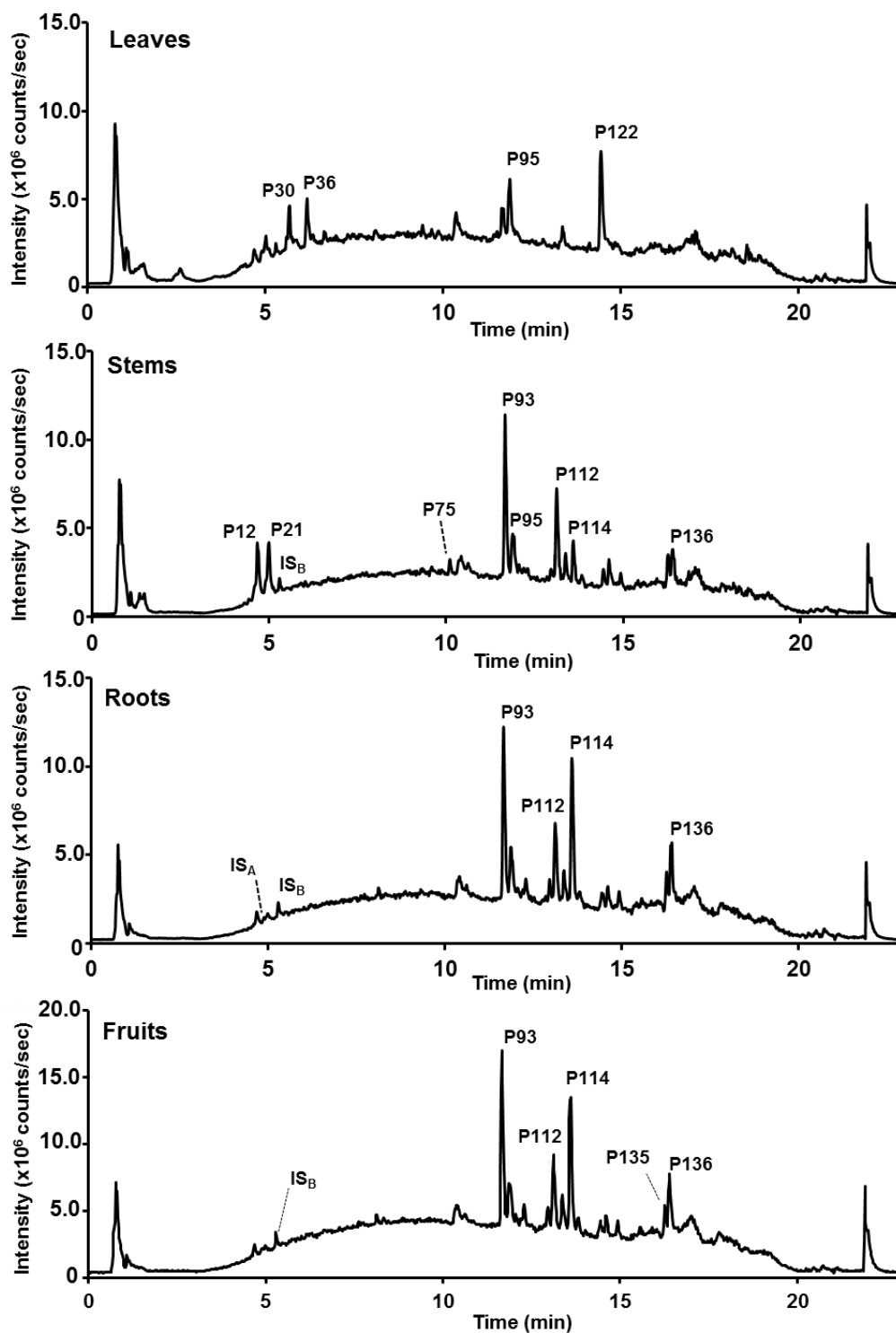
Figure 3.2: Comparison of total ion chromatogram (TIC) in positive ion mode of *P. sarmentosum* organs: leaves, stems, roots and fruits. IS_A = internal standard orcinol, IS_B = internal standard kinetin, and P = peak number.

3.2.3 Tentative identification of constituents of *P. sarmentosum*

The untargeted metabolomics analysis, which was used to characterize the metabolite composition of *P. sarmentosum* MeOH extracts, revealed the differences between the plant

organs. For annotation or identification of contributing compound species detected in the untargeted analysis, their MS1 accurate monoisotopic ions were used to determine the possible elemental composition. As the mass accuracy of 5 ppm corresponded to the specification of the mass spectrometer used, this value was considered in the MS1 analysis. Moreover, a comparison of the fragmentation patterns with those reported in the literature and databases such as Reaxys, MetFrag and PeakView were performed to assign the compounds. The mass accuracy of fragment ions of 15 ppm was considered during the annotation process. This annotation strategy is well-established and is widely used [29-31]. In addition, isolated and fully elucidated compounds obtained from our previous work (Chapter 2) were applied as reference compounds for identification of individual metabolites by comparison of their *m/z* values, retention times and fragmentation patterns. Since structurally different compounds require different suitable collision voltages to obtain fragment information [32-34], a range of collision voltages between 15 and 60 V was used in the MS/MS analysis to identify metabolites as described in section 3.3.3.

As a result, a total of 154 compounds were unambiguously identified in the extracts of four *P. sarmentosum* organs by co-elution with authentic standards verified by NMR spectroscopy data or tentatively identified by *m/z* values and MS/MS fragmentation patterns.. The identified species were numbered according to the order of their elution time (Figure 3.2, and Table 3.1). According to the obtained LC-MS data, alkaloids appeared to be the predominant metabolites, with 111 compounds annotated. In addition, 15 flavonoids and 28 other compounds were identified. The detailed list of individual compounds annotated by both MS and the MS/MS including their fragment ions are shown in Table 3.1.

Table 3.1: RP-UHPLC-QqTOF-MS/MS of metabolites annotated in four organs of *P. sarmentosum* in positive ionization mode.

Peak no.	t_R (min)	Molecular formula	Precursor ion	[M+H]⁺, [m/z]	Diff. (ppm)	ᵃMS², [m/z] m/z (key ions, rel. intensity [%])	CID, eV	Tentative identification	Type of alkaloids
Alkaloids									
P1	1.71	C₁₅H₂₂NO₇	M+H	328.1386	-1.52	310.1295 (**100**), 292.1201 (28), 282.1356 (3), 264.1231 (10), 246.1109 (2), 178.0861 (10), 166.0857 (10), 132.00808 (3), 120.0811 (7).	20	Fructosyl-phenylalanine	
P2	2.59	C₁₁H₁₀NO₂	M+H	188.0706	0.00	146.0603 (**100**), 144.0808 (18), 118.0657 (28)	20	ᵇNaphthisoxazol A	
P3	2.60	C₁₁H₁₃N₂O₂	M+NH₄	205.0971	-0.49	188.0708 (**100**), 170.0585 (1), 159.0905 (4), 146.0592 (16), 144.0805 (5), 132.0791 (2), 130.0640 (1), 118.0636 (4)	15	3-Indoleacrylic acid	
P5	4.09	C₁₉H₂₄NO₃	M+H	314.1751	0.00	299.1215 (21), 298.1066 (15), 271.1321 (19), 269.1173 (39), 237.0909 (19), 209.0942 (18), 175.0750 (**m**, 32), 145.0620 (8), 137.0590 (15), 107.0482 (**k**, 46), 58.0651 (88)	30	Armepavine (isomer)	Benzylisoquinolines
P6	4.19	C₁₈H₂₂NO₅	M+H	332.1484	-2.41	315.1242 (4), 181.0864 (10), 164.0709 (**l**, **100**), 146.0595 (13), 118.0645 (6)	20	Dimetolquinol	Benzylisoquinolines
P7	4.29	C₂₃H₃₀NO₈	M+H	448.1966	0.00	286 (**100**), 269 (93), 237 (17), 209 (11), 178 (18), 175 (13), 145.0640 (13), 143.0489 (19), 137.0583 (21), 107.0489 (**k**, 95)	40	Isococlaurine 6-O-glucoside (isomer)	Benzylisoquinolines
P9	4.44	C₁₇H₂₀NO₃	M+H	286.1436	-0.70	269.1179 (82), 237.0882 (5), 209.0960 (13), 175.0744 (**m**, 11), 145.0630 (4), 143.0473 (6), 137.0579 (3), 137.0579 (7), 107.0489 (**k**, 24)	20	Coclaurine	Benzylisoquinolines
P10	4.56	C₂₃H₃₀NO₈	M+H	448.1957	-2.01	430.1871 (**100**), 412.1718 (5), 286.1447 (14), 269.1162 (12), 251.0889 (4), 177.0545 (4), 107.0490 (**k**, 4)	30	Isococlaurine 6-O-glucoside	Benzylisoquinolines
P11	4.58	C₁₂H₁₄NO₃	M+H	220.0970	0.91	218.0827 (54), 137.0589 (32), 119.0484 (10), 91.0529 (17)	30	Oleracein E	Aporphines
P12	4.66	C₂₀H₂₄NO₄	M+H	342.1702	0.58	299.1289 (12), 297.1128 (**100**), 282.0888 (20), 265.0869 (75), 237.0904 (11), 58.0654 (38)	30	Magnoflorine	Aporphines
P15	4.72	C₂₁H₂₆NO₄	M+H	356.1853	-0.84	311.1277 (20), 296.1066 (15), 285.1119 (15), 280.1076 (19), 279.1014 (11), 257.1159 (7), 72.0800 (22), 58.0646 (68)	30	Xanthoplanine	Aporphines
P16	4.88	C₁₉H₂₄NO₄	M+H	330.1711	3.33	299.1288 (11), 267.1026 (8), 192.1020 (**l**, **100**), 175.0756 (**m**, 27), 143.0488 (10), 137.0596 (**k**, 28)	30	Reticuline	Benzylisoquinolines
P17	4.96	C₂₀H₂₂NO₄	M+H	340.1547	1.18	325.1294 (6), 308.1287 (8), 309.1377 (14), 295.0970 (65), 263.0708 (17)	20	Dehydrolirioferine (isomer)	Benzylisoquinolines
P21	5.00	C₂₀H₂₄NO₄	M+H	342.1705	1.46	297.1134 (**100**), 282.0895 (2), 265.0867 (78), 237.0907 (2), 58.0651 (3)	25	Magnoflorine (isomer)	Aporphines
P22	5.02	C₁₉H₂₄NO₃	M+H	314.1756	1.59	269.1168 (10), 209.0951 (15), 175.0741 (**m**, 7), 145.0646 (10), 143.0481 (18), 121.0645 (16), 107.0487 (**k**, **100**), 58.0658 (30)	40	Armepavine	Benzylisoquinolines
P24	5.23	C₁₉H₂₂NO₃	M+H	312.1587	-2.24	294.1510 (**100**), 249.0911 (32), 217.0652 (50), 58.0654 (47)	25	Pulchine	Aporphines
P25	5.25	C₂₀H₂₂NO₄	M+H	340.1550	2.06	325.1317 (34), 308.1284 (48), 295.0972 (**100**), 269.0900 (9), 263.0708 (80)	25	Dehydrolirioferine	Aporphines

Table 3.1: Continued

Peak no.	t_R (min)	Molecular formula	Precursor ion	$[M+H]^+$ [m/z]	Diff. (ppm)	[a]MS^2, [m/z] m/z (key ions, rel. intensity [%])	CID, eV	Tentative identification	Type of alkaloids
P26	5.35	$C_{17}H_{20}NO_3$	M+H	286.1435	-1.05	269.1184 (78), 237.0905 (24), 209.0946 (10), 178.0852 (**l**, 10), 175.0729 (**m**, 27), 145.0634 (8), 143.0475 (13), 137.0900 (22), 107.0483 (**k, 100**)	25	Coclaurine (isomer)	Benzylisoquinolines
P27	5.37	$C_{20}H_{20}NO_5$	M+H	356.1501	2.53	311.0914 (**100**), 296.0687 (7), 279.0663 (7), 251.0701 (3), 58.0656 (2)	25	Leucoxine	Aporphines
P41	6.59	$C_{20}H_{24}NO_2$	M+H	310.1798	-1.29	265.1238 (**100**), 250.0996 (58), 234.1042 (26), 58.0651 (20)	30	Atherospermine	
P42	6.67	C_9H_8NO	M+H	146.0597	-2.05	118.0652 (**100**), 91.0541 (19)	20	[b]Indole-3-carboxaldehyde	
P44	6.69	$C_{15}H_{16}NO_5$	M+H	290.1015	-2.76	272.0918 (11), 154.0871 (**a**, 38), 152.0709 (6), 137.0595 (**i**, 12), 137.0238 (**b**, 34)	15	N-[2-(3,4-dihydroxyphenyl)ethyl]-3,4-dihydroxybenzamide	Phenolic amides B
P46	6.85	$C_{13}H_{18}NO_2$	M+H	220.1326	-2.73	202.1198 (3), 131.0483 (**b**, 5), 105.0688 (**d**, 17), 91.0544 (5), 88.0756 (**a**, 67), 70.0650 (9)	20	1-(2-Hydroxypyrrolidin-yl)-3-phenylpropaal	Phenolic amides A
P50	7.44	$C_{17}H_{18}NO_3$	M+H	284.1279	-0.70	147.0453 (**b, 100**), 121.0650 (**i**, 46), 119.0497 (3)	25	[b]Paprazine	Phenolic amides B
P52	7.50	$C_{15}H_{16}NO_4$	M+H	274.1069	-1.82	154.0481 (**j**, 9), 138.0908 (**a**, 69), 137.0231 (**b**, 78), 121.0657 (**i, 100**)	20	Houttuynamide A	Phenolic amides B
P55	7.63	$C_{18}H_{20}NO_4$	M+H	314.1382	-1.59	177.0552 (**b, 100**), 147.0444 (32), 121.0658 (**i**, 14)	20	[b]trans-N-feruloyltyramine	Phenolic amides B
P57	8.16	$C_{15}H_{20}NO_3$	M+H	262.1434	-1.53	191.0719 (**b, 100**), 176.0458 (3), 163.0761 (**d**, 13), 160.0513 (3), 148.0522 (5), 133.0555 (1), 123.0793 (1), 119.0473 (1), 105.0693 (3), 98.0602 (**c**, 5), 72.0809 (**a**, 1), 55.0537 (3)	30	4'-Demethoxy-piperlotine C	Phenolic amides A
P58	8.34	$C_{38}H_{41}N_2O_{10}$	M+H	685.2736	-2.92	548.1947 (**b₂,100**), 520.1975 (**d₂**, 58), 394.1298 (37), 383.1143 (80), 357.1354 (11), 351.0883 (27), 231.0650 (21)	35	Lignanamides A	Lignanamides
P59	8.40	$C_{16}H_{18}NO_3$	M+H	272.1271	-3.67	255.1043 (10), 151.0758 (**l**, 26), 105.0339 (**k, 100**), 91.0538 (3)	20	Norcoclaurine	Benzylisoquinolines
P60	8.46	$C_{37}H_{39}N_2O_9$	M+H	655.2631	-2.90	518.1823 (**b₂, 100**), 490.1889 (**d₂**, 64), 394.1306 (11), 353.1031 (22), 327.1207 (11), 321.0761 (10), 231.0645 (14)	30	8-Methoxy-cannabisin D	Lignanamides
P61	8.52	$C_{16}H_{22}NO_4$	M+H	292.1538	-1.71	221.0925 (**b, 100**), 206.0588 (44), 193.0968 (**d**, 1), 191.0340 (7), 181.0961 (1), 178.0633 (3), 167.0694 (1), 163.0390 (1), 150.0678 (0.5), 135.0429 (0.5), 107.0490 (0.5), 98.0602 (**c**, 8), 70.0647 (**a**, 0.5)	30	Piperlotine C	Phenolic amides A
P62	8.56	$C_{15}H_{20}NO_3$	M+H	262.1431	-2.67	1910707 (**b, 100**), 176.0461 (6), 163.0752 (**d**, 45), 160.0511 (7), 148.0519 (14), 132.0563 (5), 120.0565 (3), 119.0477 (5), 98.05594 (**c**, 5), 72.0810 (**a**, 1), 55.0540 (3)	35	4'-Demethoxy-piperlotine C (isomer-A)	Phenolic amides A
P63	8.73	$C_{15}H_{10}NO_3$	M+H	252.0662	2.78	234.0534 (7), 224.0693 (14), 197.0579 (7), 196.0763 (13), 178.0670 (7)	30	Hippacine	
P64	8.75	$C_{16}H_{16}NO_4$	M+H	286.1063	-3.84	268.0948 (**100**), 254.0903 (19), 238.0844 (44), 237.0766 (5), 198.0529 (5)	20	Ganoapplanatumine B	

Table 3.1: Continued

Peak no.	t_R (min)	Molecular formula	Precursor ion	$[M+H]^+$ [m/z]	Diff. (ppm)	^{a}MS² [m/z] m/z (key ions, rel. intensity [%])	CID, eV	Tentative identification	Type of alkaloids
P65	8.91	$C_{16}H_{22}NO_4$	M+H	292.1534	-3.08	221.0831 (**b, 100**), 206.0591 (25), 193.0874 (**d**, 7), 191.0352 (3), 190.0638 (7), 189.0562 (1), 178.0634 (3), 175.0392 (1), 162.0689 (2), 161.0611 (2), 149.0599 (1), 135.0453 (1), 133.0660 (1), 98.0604 (**c**, 4), 72.0805 (2), 70.0654 (**a**, 1), 55.0548 (2)	30	Piperlotine C (isomer)	Phenolic amides A
P66	8.97	$C_{18}H_{20}NO_3$	M+H	298.1429	-3.02	177.0555 (**b, 100**), 149.0605 (4), 145.0299 (41), 117.0333 (10), 105.0697 (**i**, 19)	25	Feruloylphenethylamine	Phenolic amides B
P68	9.54	$C_{37}H_{39}N_2O_9$	M+H	655.2634	-2.44	518.1819 (**b$_2$**, 23), 492.2034 (**d$_2$**, 22), 381.0976 (14), 355.1181 (23)	25	8-Methoxy-cannabisin D (isomer)	Lignanamides
P69	9.58	$C_{14}H_{18}NO_2$	M+H	232.1323	-3.88	161.0602 (**b, 100**), 133.0647 (**d**, 26), 118.0413 (12), 98.0591 (**c**, 3), 90.0454 (3), 72.0801 (**a**, 5), 55.0548 (3)	30	Piperlotine A	Phenolic amides A
P70	9.60	$C_{16}H_{12}NO_3$	M+H	266.0813	0.38	251.0580 (**100**), 223.0612 (9), 195.0679 (37), 168.0556 (7), 167.0728 (37)	40	^{b}Piperolactam A	Aporphines
P71	9.76	$C_{18}H_{14}NO_4$	M+H	308.0905	-3.89	293.0714 (77), 265.0774 (**100**), 237.0797 (4), 209.0855 (74), 208.0770 (4), 181.0893 (7)	40	^{b}Norcephardione B	Aporphines
P72	9.85	$C_{14}H_{16}NO_2$	M+H	230.1170	-2.61	161.0597 (**b, 100**), 133.0639 (**d**, 36), 118.0397 (5), 105.0684 (5), 96.0432 (**c**, 18), 78.0332 (7), 68.0501 (**a**, 9)	30	3-(4-Methoxyphenyl)-1-(pyrrol-1-yl)propan-1-one	Phenolic amides A
P73	9.91	$C_{15}H_{20}NO_3$	M+H	262.1436	-0.76	191.0714 (**b, 100**), 176.0464 (5), 163.0758 (**d**, 31), 148.0519 (41), 120.0564 (1), 119.0488 (4), 98.0597 (**c**, 5), 91.0543 (5), 72.0805 (**a**, 5), 55.0543 (4)	35	4'-Demethoxy-piperlotine C (isomer-B)	Phenolic amides A
P74	9.91	$C_{34}H_{29}N_2O_8$	M+H	593.1903	-2.53	456.1101 (**b$_2$, 100**), 430.1305 (18), 428.1130 (**d$_2$**, 15), 344.1492 (13), 330.1345 (6), 250.0510 (6), 236.0711 (13), 207.0654 (6), 121.0642 (25)	30	Lignanamides B	Lignanamides
P75	10.11	$C_{17}H_{14}NO_4$	M+H	296.0922	1.69	281.0697 (44), 280.0514 (4), 266.0462 (6), 264.0670 (12), 263.0592 (74), 236.0707 (4), 235.0642 (**100**)	30	Piperolactam B	Aporphines
P76	10.15	$C_{18}H_{14}NO_4$	M+H	308.0914	-0.97	292.0623 (80), 290.0827 (**100**), 264.0672 (96), 247.0642 (74)	35	Piperadione/Aristolodione	Aporphines
P77	10.27	$C_{18}H_{14}NO_5$	M+H	324.0864	-0.62	309.0645 (52), 308.0563 (84), 291.0534 (63), 263.0573 (15)	30	Cepharanone D	Aporphines
P78	10.33	$C_{16}H_{20}NO_3$	M+H	274.1439	0.36	161.0601 (**g**, 5), 139.0996 (**f**, 14), 137.0577 (5), 135.0438 (**e, 100**), 124.0745 (24), 123.0817 (5), 117.0684 (8), 113.0588 (8), 99.0444 (5), 98.0594 (**c**, 5), 95.0854 (8), 72.0902 (**a**, 14)	30	Piperamide-C5:1 (2E)	Piperamides E
P79	10.35	$C_{14}H_{16}NO_3$	M+H	246.1120	-2.03	214.0875 (**100**), 196.0761 (33), 186.0917 (29), 133.0648 (30), 114.0550 (**c**, 62), 105.0697 (9), 82.0286 (**a**, 30)	15	Piperlotine G	Phenolic amides A
P80	10.44	$C_{16}H_{18}NO_3$	M+H	272.1277	-1.47	201.0568 (**b, 100**), 173.0599 (**d**, 6), 171.0446 (11), 159.0438 (**g**, 3), 143.0491 (11), 135.0445 (**e**, 38), 115.0543 (11), 98.05893 (**c**, 6), 72.0905 (**a**, 1), 55.0541 (2)	30	Piperyline	Piperamides E
P81	10.60	$C_{18}H_{12}NO_4$	M+H	306.0750	-3.59	278.0815 (**100**), 263.0567 (24), 248.0701 (43), 220.0750 (49)	40	^{b}Cepharadione A	Aporphines
P82	10.64	$C_{16}H_{18}NO_3$	M+H	272.1279	-0.73	201.0561 (**b, 100**), 173.0603 (**d**, 7), 171.0446 (12), 159.0443 (**g**, 3), 143.0493 (15), 135.0445 (**e**, 41), 115.0544 (16), 98.0600 (**c**, 5), 70.0653 (**a**, 1), 55.0544 (2)	30	Piperyline (isomer-A)	Piperamides E

Table 3.1: Continued

Peak no.	t_R (min)	Molecular formula	Precursor ion	[M+H]$^+$, [m/z]	Diff. (ppm)	^{a}MS^2, [m/z] m/z (key ions, rel. intensity [%])	CID, eV	Tentative identification	Type of alkaloids
P83	10.64	$C_{18}H_{14}NO_5$	M+H	324.0857	-2.78	309.0670 (39), 308.0573 (**100**), 292.0615 (19), 291.0548 (53), 290.0472 (35), 263.0595 (51), 235.0623 (19)	35	Cepharanone D (isomer)	Aporphines
P84	10.88	$C_{16}H_{18}NO_3$	M+H	272.1276	-1.84	201.0550 (**b, 100**), 173.0592 (**d**, 6), 171.0439 (15), 159.0435 (**g**, 5), 143.0487 (11), 137.0835 (**f**, 3), 135.0439 (**e**, 35), 115.0538 (15), 98.0598 (**c**, 5), 55.0540 (2)	30	Piperyline (isomer-B)	Piperamides E
P87	11.09	$C_{17}H_{14}NO_3$	M+H	280.0959	-3.21	265.0739 (22), 264.0647 (39), 149.0247 (24)	25	^{b}Aristolactam BII	Aporphines
P88	11.15	$C_{19}H_{20}NO_3$	M+H	310.1433	-1.61	278.1193 (44), 265.1238 (24), 250.1244 (44), 233.0977 (**100**)	15	N-formylnornuciferin	Aporphines
P91	11.61	$C_{17}H_{20}NO_3$	M+H	286.1430	-2.80	201.0553 (**b, 100**), 173.0609 (**d**, 6), 171.0443 (24), 159.0441 (**g**, 7), 151.0934 (4), 143.0486 (31), 135.0438 (**e**, 32), 117.0695 (1), 115.0539 (32), 112.0745 (**c**, 6), 86.0954 (**a**, 1), 84.0938 (3), 69.0696 (4)	35	Piperine	Piperamides A
P92	11.66	$C_{18}H_{20}NO_3$	M+H	298.1430	-2.68	227.0715 (**b, 100**), 199.0759 (**d**, 20), 197.0600 (19), 169.0657 (47), 161.0604 (**g**, 7), 159.0439 (3), 150.0910 (5), 141.0702 (19), 135.0429 (**e**, 1), 131.0490 (7), 98.0602 (**c**, 36), 72.0810 (**a**, 3), 70.0645 (1)	25	Piperettyline-like compound	Piperamides E
P93	11.66	$C_{18}H_{22}NO_3$	M+H	300.1590	-1.33	229.0956 (**b**, 4), 201.0904 (**d**, 10), 187.0747 (5), 171.0901 (1), 161.0596 (**g**, 73), 139.0982 (**h**, 7), 135.0433 (**e**, 8), 131.0488 (**100**), 124.0750 (7), 103.0537 (18), 98.0595 (**c**, 23), 84.0912 (1), 72.0806 (**a**, 8)	25	Nigrinodine	Piperamides E
P97	11.90	$C_{18}H_{16}NO_4$	M+H	310.1064	-3.22	295.0855 (44), 294.0742 (7), 280.0618 (67), 279.0901 (13), 277.0753 (71), 276.0658 (13), 262.,513 (16), 252.0649 (10), 250.0873 (18), 249.0800 (26), 221.0836 (9)	30	Aristolactam BIII	Aporphines
P98	11.92	$C_{18}H_{20}NO_3$	M+H	298.1437	-0.34	227.0728 (**b, 100**), 199.0767 (**d**, 25), 197.0612 (25), 171.0934 (1), 169.0661 (53), 161.0633 (**g**, 8), 159.0444 (3), 150.0913 (8), 141.0705 (23), 135.0444 (**e**, 1), 131.0493 (10), 124.0760 (3), 115.0537 (3), 103.0542 (3), 98.0608 (**c**, 56), 72.0903 (**a**, 3), 70.0854 (1), 55.0547 (5)	25	Piperettyline-like compound (isomer-A)	Piperamides E
P99	11.98	$C_{20}H_{22}NO_4$	M+H	340.1540	-0.88	308.1302 (**100**), 295.1349 (81), 293.1057 (30), 280.1355 (16), 263.1076 (26), 249.1150 (18)	20	Dehydronorglaucine	Aporphines
P100	12.00	$C_{19}H_{18}NO_3$	M+H	308.1274	-2.27	293.1072 (42), 280.1316 (25), 277.1123 (19), 249.1163 (31)	20	N-demethyl-N-formyl-dehydronuciferine	Aporphines
P101	12.08	$C_{18}H_{24}NO_3$	M+H	302.1744	-2.32	272.1650 (1), 231.1029 (**b**, 10), 213.0917 (**d**, 13), 201.0915 (4), 187.0756 (4), 180.1393 (17), 154.1227 (5), 140.1068 (1), 135.0453 (**e, 100**), 98.0601 (**c**, 16), 84.0808 (1), 72.0814 (**a**, 39), 70.0654 (3), 55.0538 (1)	25	Piperamide-C7:1 (6E)	Piperamides E
P102	12.21	$C_{18}H_{20}NO_3$	M+H	298.1440	0.67	227.0714 (**b, 100**), 199.0764 (**d**, 25), 197.0600 (28), 169.0651 (45), 161.0597 (**g**, 9), 150.0913 (6), 141.0899 (23), 139.0937 (1), 131.0493 (10), 124.0763 (1), 115.0538 (3), 103.0543 (3), 98.0600 (**c**, 41), 72.0808 (**a**, 4), 70.0643 (1), 55.0543 (3)	25	Piperettyline-like compound (isomer-B)	Piperamides E
P103	12.27	$C_{19}H_{18}NO_3$	M+H	308.1274	-2.27	293.1077 (10), 280.1362 (22), 277.1117 (11), 249.1198 (5)	20	N-demethyl-N-formyl-dehydronuciferine (isomer)	Aporphines

Table 3.1: Continued

Peak no.	t_R (min)	Molecular formula	Precursor ion	$[M+H]^+$, [m/z]	Diff. (ppm)	[a]MS[2], [m/z] m/z (key ions, rel. intensity [%])	CID, eV	Tentative identification	Type of alkaloids
P104	12.29	$C_{18}H_{26}NO_2$	M+H	288.1951	-2.43	194.1546 (1), 168.1384 (4), 151.1120 (66), 133.1010 (12), 121.0845 (22), 109.0641 (3), 105.691 (2), 95.0493 (13), 93.0694 (4), 91.0541 (2), 81.0326 (3), 69.0692 (3), 67.0544 (1)	20	Ottonoidenamide	Piperamides B
P105	12.31	$C_{18}H_{24}NO_3$	M+H	302.1745	-1.99	229.0869 (b, 6), 203.1082 (d, 17), 201.0920 (22), 187.0754 (3), 180.1388 (5), 173.0965 (5), 161.0510 (g, 100), 135.0442 (e, 19), 131.0498 (53), 107.0493 (1), 103.0541 (8), 100.0759 (c, 1), 81.0701 (13), 79.0542 (1), 74.0966 (a, 4), 57.0702 (4)	20	Chingchengenamide A	Piperamides B
P106	12.41	$C_{14}H_{22}NO$	M+H	220.1694	-0.91	149.0949 (b, 5), 137.0828 (24), 136.0745 (5), 121.1009 (d, 5), 107.0490 (100), 98.0593 (c, 37), 93.0587 (5), 91.0634 (10), 79.0531 (15), 77.0376 (9), 72.0801 (a, 5), 70.0651 (10), 55.0544 (47)	30	N-Isobutyl-2,4,6,8-decatetraenamide	Piperamides C
P107	12.53	$C_{18}H_{22}NO_3$	M+H	300.1594	0.00	227.0705 (b, 100), 201.0892 (d, 39), 199.0751 (43), 197.0598 (53), 171.0789 (13), 169.0644 (60), 161.0583 (g, 18), 141.0693 (27), 131.0487 (40), 103.0535 (13), 79.0526 (6), 57.0694 (i, 19)	25	3,4-Dehydrofutoamide	Piperamides B
P108	12.75	$C_{19}H_{24}NO_3$	M+H	314.1747	-1.27	229.0834 (b, 1), 201.0925 (d, 4), 192.1385 (1), 187.0757 (1), 171.0310 (1), 166.1243 (1), 161.0609 (g, 39), 153.1152 (h, 3), 140.1070 (1), 138.0920 (9), 131.0502 (100), 112.0765 (c, 11), 103.0548 (15), 86.0971 (a, 5), 84.0806 (1), 69.0703 (3)	30	Piperdardine	Piperamides A
P109	12.80	$C_{19}H_{22}NO_3$	M+H	312.1603	2.88	227.0716 (b, 100), 199.0758 (d, 15), 197.0631 (15), 169.0660 (50), 161.0612 (g, 7), 141.0695 (15), 131.0487 (7), 112.0750 (c, 31), 86.0970 (a, 6), 69.0704 (8)	25	Piperettine	Piperamides A
P110	12.98	$C_{20}H_{24}NO_3$	M+H	326.1752	0.31	255.1031 (b, 4), 227.1069 (d, 5), 187.0754 (9), 165.1152 (h, 100), 161.0594 (g, 32), 150.0905 (5), 135.0439 (e, 4), 131.0488 (29), 103.0538 (4), 98.0599 (c, 58), 72.0804 (a, 3), 70.0643 (1)	25	6,7-Dehydro-brachyamide B	Piperamides E
P111	13.06	$C_{19}H_{22}NO_3$	M+H	312.1582	-3.84	227.0720 (b, 100), 199.0759 (d, 22), 197.0603 (30), 169.0650 (42), 161.0582 (g, 10), 141.0692 (14), 138.0894 (4), 131.0489 (8), 115.0530 (6), 112.0753 (c, 58), 86.0963 (a, 4), 69.0701 (14)	25	Piperettine (isomer)	Piperamides A
P112	13.14	$C_{14}H_{24}NO$	M+H	222.1852	0.00	194.1906 (2), 168.1744 (1), 150.0918 (h, 15), 124.0761 (27), 110.0963 (15), 98.0604 (c, 71), 95.0492 (15), 91.0539 (3), 81.0342 (100), 72.0810 (a, 13), 70.0654 (14), 69.0698 (10), 67.0545 (29), 53.0390 (92), 55.0540 (38)	40	Sarmentine	Pyrrolamides
P113	13.32	$C_{20}H_{26}NO_4$	M+H	338.1384	-0.89	323.1179 (21), 310.1471 (18), 307.1236 (100), 279.1285 (46)	30	[b]Dehydroformouregine	Aporphines
P114	13.39	$C_{20}H_{26}NO_3$	M+H	328.1898	-2.74	229.1236 (d, 22), 199.1124 (7), 161.0600 (g, 11), 135.0449 (e, 100), 131.0494 (7), 98.0602 (c, 22), 84.0804 (5), 72.0812 (a, 12)	30	Brachyamide B	Piperamides E
P116	13.59	$C_{14}H_{26}NO$	M+H	224.2006	-1.34	168.1390 (j, 39), 151.1121 (b, 13), 123.1168 (d, 18), 112.0760 (13), 109.1010 (33), 98.0901 (46), 95.0496 (42), 93.0696 (12), 83.0855 (21), 81.0344 (61), 79.0538 (16), 74.0966 (a, 1), 69.0701 (54), 67.0544 (43), 57.0704 (i, 100)	30	Pellitorine	Piperamides C
P117	13.83	$C_{20}H_{28}NO_3$	M+H	330.2056	-2.42	229.1217 (d, 1), 208.1695 (2), 161.0590 (g, 1), 135.0440 (e, 100), 131.0479 (1), 98.0597 (c, 9), 84.0604 (1), 72.0807 (a, 11), 70.0650 (1)	30	Tricholein	Piperamides E

Table 3.1: Continued

Peak no.	t_R (min)	Molecular formula	Precursor ion	[M+H]$^+$, [m/z]	Diff. (ppm)	^{a}MS^2, [m/z] m/z (key ions, rel. intensity [%])	CID, eV	Tentative identification	Type of alkaloids
P118	14.02	$C_{22}H_{26}NO_3$	M+H	352.1896	-3.12	253.1194 (**d**, 1), 239.1052 (1), 223.1125 (1), 213.0901 (1), 187.0754 (**100**), 165.1149 (34), 157.0649 (44), 150.0913 (4), 135.0423 (**e**, 3), 129.0696 (22), 128.0618 (5), 98.0595 (**c**, 31), 70.0647 (**a**, 1), 55.0541 (2)	30	1-(Pyrrolidinyl-11-(3',4'-methylenedioxyphenyl)-2,4,8,10-undecatetraen-1-one	Piperamides E
P119	14.14	$C_{18}H_{14}NO_4$	M+H	308.0906	-0.32	293.0707 (**100**), 292.0618 (21), 276.0666 (9), 275.0581 (14), 265.0754 (12), 262.0868 (9), 247.0646 (9)	30	1,2:9,10-Bismethylenedioxy-5,6-dihydro-4H-dibenzo[de,g]quinoline	Aporphines
P120	14.24	$C_{21}H_{28}NO_3$	M+H	342.2052	-3.51	255.1015 (**b**, 2), 229.1224 (**d**, 2), 227.1053 (5), 197.0943 (1), 187.0773 (4), 181.1454 (**h**, 21), 166.1228 (4), 161.0598 (**g**, 44), 135.0426 (6), 131.0487 (**100**), 103.0533 (**e**, 16), 86.0951 (**a**, 1), 79.0528 (1), 71.0843 (5)	30	Pipernonaline (isomer)	Piperamides A
P121	14.42	$C_{22}H_{28}NO_3$	M+H	354.2060	-1.13	255.1388 (**d**, 7), 241.1222 (6), 187.0757 (**100**), 161.0594 (**g**, 6), 157.0692 (49), 135.0438 (**e**, 16), 129.0699 (30), 128.0801 (6), 98.0569 (**c**, 15), 72.0815 (**a**, 7)	30	1-(Pyrrolidinyl-11-(3',4'-methylenedioxyphenyl)-2,4,10-undecatrien-1-one	Piperamides E
P123	14.48	$C_{21}H_{28}NO_3$	M+H	342.2054	-2.92	257.1174 (**b**, 3), 229.1223 (**d**, 37), 199.1114 (12), 187.0744 (6), 171.0790 (5), 161.0594 (**g**, 18), 135.0441 (**e**, **100**), 131.0480 (12), 112.0754 (**c**, 31), 98.0955 (8), 86.0983 (**a**, 52), 84.0803 (8), 69.0702 (14)	30	Pipernonaline/Pipernonatine	Piperamides A
P124	14.50	$C_{15}H_{28}NO$	M+H	238.2162	-1.26	168.1390 (**j**, **100**), 151.1126 (**b**, 32), 123.1172 (**d**, 36), 112.0754 (23), 109.1014 (48), 100.1121 (23), 98.0903 (47), 95.0494 (56), 83.0956 (21), 81.0638 (43), 71.0859 (43), 69.0706 (**i**, 81), 67.0550 (45), 55.0550 (45)	30	Homopellitorine / N-2'-methylbutyl-2E,4E-decadienamide	
P125	14.61	$C_{22}H_{28}NO_3$	M+H	354.2063	-0.28	255.1390 (**d**, 4), 215.1071 (3), 187.0760 (3), 173.0601 (2), 161.0600 (**g**, 3), 135.0447 (**e**, **100**), 131.0490 (6), 98.0602 (**c**, 39), 91.0540 (3), 84.0805 (4), 72.0811 (**a**, 12), 55.0543 (3)	30	1-(Pyrrolidinyl-11-(3',4'-methylenedioxyphenyl)-2,4,10-undecatrien-1-one (isomer)	Piperamides E
P128	14.93	$C_{22}H_{30}NO_3$	M+H	356.2220	0.00	283.1337 (**b**, 1), 255.1399 (**d**, 2), 215.1071 (1), 187.0769 (1), 175.0758 (2), 161.0605 (**g**, 4), 135.0450 (**e**, **100**), 131.0498 (7), 107.0857 (2), 103.0545 (2), 93.0697 (2), 91.0543 (3), 86.0969 (3), 79.0538 (2), 74.0963 (**a**, 1), 67.0548 (1), 57.0702 (6)	30	Retrofractamide B	Piperamides B
P129	15.13	$C_{22}H_{30}NO_3$	M+H	356.2211	-2.53	285.1486 (**b**, 3), 255.1393 (**d**, 3), 234.1884 (5), 187.0760 (5), 161.0605 (**g**, 6), 135.0444 (**e**, **100**), 131.0495 (7), 98.0594 (**c**, 11), 84.0808 (13), 74.0956 (**a**, 1), 72.0810 (10)	30	Piperstachine	Piperamides B
P131	15.22	$C_{18}H_{28}NO$	M+H	274.2159	-2.19	165.1153 (**100**), 164.1070 (15), 150.0913 (**h**, 15), 136.1123 (4), 109.1004 (3), 98.0603 (**c**, 95), 95.0484 (3), 72.0817 (**a**, 3), 70.0549 (3), 67.0542 (2), 55.0542 (**i**, 3)	25	1-(Pyrrolidinyl-14-2,4,7,9-tetradecatetraen-1-one	Pyrrolamides
P132	15.34	$C_{16}H_{28}NO$	M+H	250.2164	-0.40	232.2049 (3), 196.2059 (9), 182.1901 (3), 179.1417 (**b**, 4), 152.1079 (9), 150.0920 (**h**, 14), 138.0917 (8), 124.1117 (8), 109.1009 (8), 98.0602 (**c**, 97), 97.1006 (17), 95.0493 (27), 83.0488 (8), 81.0691 (18), 72.0810 (**a**, 26), 70.0652 (18), 55.0543 (**i**, 63), 53.0386 (58)	35	2,4-Dodecadienoic acid pyrrolidide	Pyrrolamides

Table 3.1: Continued

Peak no.	t_R (min)	Molecular formula	Precursor ion	[M+H]+ [m/z]	Diff. (ppm)	^{a}MS^2 [m/z] m/z (key ions, rel. intensity [%])	CID, eV	Tentative identification	Type of alkaloids
P133	15.58	$C_{16}H_{30}NO$	M+H	252.2320	-0.79	198.1711 (**j**, 53), 179.1434 (**b**, 10), 154.1229 (**d**, 13), 126.0915 (13), 109.1012 (14), 98.0601 (**c**, 29), 97.1016 (24), 95.0853 (49), 93.0705 (8), 84.0403 (8), 83.0959 (18), 81.0339 (41), 79.0539 (14), 74.0954 (**c**, 3), 69.0702 (29), 67.0545 (18), 57.0545 (**i**, 18), 55.0548 (37)	30	Kalecide	Piperamides C
P134	15.80	$C_{24}H_{32}NO_3$	M+H	382.2362	-3.92	309.1495 (**b**, 7), 281.1557 (**d**, 14), 260.1999 (24), 241.1218 (17), 227.1081 (7), 215.1090 (8), 201.0916 (6), 187.0750 (10), 161.0800 (**g**, 43), 135.0438 (**e**, **100**), 131.0508 (22), 98.0591 (**c**, 17), 74.0961 (**a**, 7), 72.0804 (17), 57.0684 (7)	25	Dehydroguineesine	Piperamides B
P135	16.29	$C_{24}H_{32}NO_3$	M+H	382.2363	-3.66	311.1674 (**b**, 1), 283.1719 (**d**, 1), 213.0928 (1), 201.0920 (1), 187.0766 (4), 175.0760 (2), 161.0808 (**g**, 9), 135.0451 (**e**, **100**), 131.0500 (15), 103.0545 (3), 98.0606 (**c**, 26), 84.0812 (22), 81.0334 (2), 72.0812 (**a**, 5), 55.0545 (3)	35	Brachyamide A	Piperamides E
P136	16.40	$C_{24}H_{34}NO_3$	M+H	384.2525	-2.08	311.1664 (**b**, 4), 283.1715 (**d**, 8), 187.0762 (4), 175.0758 (4), 161.0602 (**g**, 9), 135.0446 (**e**, **100**), 131.0491 (5), 123.0439 (4), 109.1010 (5), 95.0851 (2), 86.0965 (18), 81.0994 (2), 74.0961 (**a**, 1), 57.0999 (3)	30	Guineensine	Piperamides B
P137	16.83	$C_{24}H_{36}NO_3$	M+H	386.2677	-3.37	313.1826 (**b**, 36), 285.1875 (**d**, 1), 264.2325 (6), 175.0766 (7), 161.0600 (**g**, 17), 135.0446 (**e**, **100**), 131.0497 (4), 109.1011 (3), 95.0855 (4), 86.0967 (19), 81.0703 (3), 74.0968 (**a**, 4), 57.0999 (4)	30	Piperflaviflorine A	Piperamides B
P138	16.84	$C_{24}H_{34}NO_3$	M+H	384.2524	-2.34	313.1819 (**b**, 6), 262.2164 (4), 175.0755 (4), 161.0603 (**g**, 9), 135.0441 (**e**, **100**), 131.0437 (7), 98.0588 (**c**, 15), 84.0806 (15), 72.0803 (**a**, 7)	35	Dihydrobrachyamide A	Piperamides E
P139	17.01	$C_{25}H_{36}NO_3$	M+H	398.2680	-2.51	311.1662 (**b**, 6), 283.1703 (**d**, 15), 187.0749 (2), 161.0593 (**g**, 3), 135.0442 (**e**, 24), 131.0437 (1), 107.0491 (1), 100.1118 (10), 95.08046 (1), 88.1112 (1), 81.0688 (1)	25	(2E,12E)-Pipertridecadienamide	Piperamides A
P140	17.25	$C_{22}H_{34}NO$	M+H	328.2629	-1.83	178.1221 (7), 164.1064 (**h**, 12), 126.0906 (20), 119.0844 (11), 107.0847 (11), 105.0689 (11), 98.0597 (**100**), 91.0540 (17), 81.0693 (16), 79.0539 (12), 72.0800 (17), 67.0534 (**i**, 11), 55.0541 (20)	30	1-(Piperidinyl)-2,4,7,9,11-heptadecapentaen-1-one	Piperamides D
P141	17.43	$C_{18}H_{32}NO$	M+H	278.2471	-2.52	250.2538 (17), 224.2375 (11), 164.1062 (6), 152.1066 (**h**, 11), 136.0749 (13), 124.0753 (64), 110.0954 (26), 98.0595 (**c**, **100**), 95.0489 (25), 81.0696 (25), 79.0533 (29), 72.0809 (**a**, 47), 70.0645 (17), 69.0699 (25), 67.0539 (29), 55.0543 (**i**, 64), 53.0388 (60)	40	Achilleaamide	Pyrrolamides
P142	17.78	$C_{22}H_{36}NO$	M+H	330.2782	-2.72	259.2068 (**b**, 6), 236.2014 (9), 222.1353 (13), 208.1706 (8), 152.1077 (**h**, 16), 139.0996 (12), 124.0758 (14), 121.1013 (18), 119.0859 (14), 107.0862 (26), 98.0604 (**c**, **100**), 95.0859 (32), 93.0703 (43), 91.0541 (14), 81.0705 (34), 79.0545 (13), 72.0816 (**a**, 56), 67.0546 (42), 55.0541 (**i**, 16)	30	1-(Pyrrolidinyl)-18-2,4,11,13-octadecatetraen-1-one	Pyrrolamides
P143	17.79	$C_{26}H_{38}NO_3$	M+H	412.2834	-2.91	339.1982 (**b**, 53), 311.2033 (**d**, 13), 290.2498 (9), 161.0605 (**g**, 17), 135.0455 (**e**, **100**), 86.0972 (30), 81.0696 (3), 57.0704 (2)	30	Brachystamide B	Piperamides B
P144	17.86	$C_{26}H_{36}NO_3$	M+H	410.2674	-3.90	339.1998 (**b**, 5), 288.2342 (4), 187.0780 (3), 161.0603 (**g**, 13), 135.0453 (**e**, **100**), 98.0606 (**c**, 25), 84.0811 (18), 81.0340 (5), 72.0815 (**a**, 6), 55.0547 (3)	40	1-(Pyrrolidinyl)-15-(3',4'-methylenedioxyphenyl)-2,4,14-pentadecatrien-1-one	Piperamides E

Table 3.1: Continued

Peak no.	t_R (min)	Molecular formula	Precursor ion	[M+H]+, [m/z]	Diff. (ppm)	[a]MS2, [m/z] m/z (key ions, rel. intensity [%])	CID, eV	Tentative identification	Type of alkaloids
P145	18.25	$C_{22}H_{38}NO$	M+H	332.2935	-3.91	276.2377 (**j**, 7), 233.2235 (**d**, 7), 208.1695 (21), 185.1174 (29), 166.1219 (21), 147.0799 (30), 135.1171 (37), 133.1023 (26), 128.1058 (26), 121.1015 (90), 109.1009 (49), 107.0954 (60), 95.0951 (84), 93.0699 (**100**), 91.0536 (36), 83.0850 (20), 81.0332 (8), 79.0542 (47), 69.0700 (27), 67.0540 (27), 57.0698 (**i**, 56)	30	N-isobutyl- 2,4,10,12-octadecacatetraenmide	Piperamides C
P146	18.39	$C_{26}H_{38}NO_3$	M+H	412.2830	-3.88	341.2134 (**b**, 5), 313.2174 (**d**, 1), 290.2510 (8), 161.0603 (**g**, 12), 135.0452 (**e**, **100**), 131.0491 (6), 98.0609 (**c**, 11), 84.0813 (18), 72.0812 (**a**, 17)	40	1-(Pyrrolidinyl)-15-(3',4'-methylenedioxyphenyl)-12,14-pentadecadien-1-one	Piperamides D
P147	18.47	$C_{22}H_{38}NO$	M+H	332.2940	-2.41	278.2501 (**j**, 3), 259.2063 (**b**, 4), 250.2184 (5), 231.2102 (**d**, 4), 222.1853 (5), 166.1231 (15), 135.1172 (19), 133.1011 (11), 128.1069 (5), 121.1012 (32), 109.1012 (23), 107.0953 (26), 95.0857 (38), 93.0701 (30), 91.0540 (16), 83.0855 (6), 81.0702 (35), 79.0543 (15), 74.0965 (**a**, 5), 69.0706 (11), 67.0545 (31), 57.0702 (**i**, 32)	30	N-isobutyl- 2,4,10,12-octadecacatetraenmide (isomer)	Piperamides C
P148	18.63	$C_{22}H_{36}NO$	M+H	330.2786	-1.51	234.1869 (2), 178.1232 (9), 164.1072 (9), 150.0919 (**h**, 8), 137.0826 (8), 124.0753 (20), 121.1021 (7), 119.0855 (9), 107.0850 (14), 98.0601 (**c**, **100**), 95.0853 (30), 93.0698 (23), 91.0539 (18), 81.0895 (21), 79.0544 (23), 72.0809 (**a**, 22), 67.0544 (56), 55.0543 (**i**, 53)	40	1-(Pyrrolidinyl)-2,4,10,12-octadecacatetraenmide	Pyrrolamides
P149	18.88	$C_{22}H_{38}NO$	M+H	332.2941	-2.11	166.1228 (**h**, 4), 152.1079 (23), 139.0992 (13), 126.0916 (17), 124.0762 (72), 98.0604 (**100**), 95.0855 (25), 93.0698 (17), 91.0536 (6), 81.0699 (32), 79.0543 (13), 72.0813 (38), 67.0545 (**i**, 19), 55.0548 (45)	40	1-(Piperidinyl)-2,4,11-heptadecatrien-1-one	Piperamides D
P150	19.04	$C_{22}H_{42}NO$	M+H	336.3251	-2.97	226.2172 (18), 198.1843 (32), 170.1539 (25), 156.1369 (20), 142.1211 (28), 123.0798 (42), 109.1009 (24), 97.0644 (49), 95.0844 (30), 81.0688 (20), 74.0961 (**a**, 68), 69.0696 (42), 57.0691 (**i**, **100**), 55.0535 (21)	30	Pipericine	Piperamides C
P151	19.22	$C_{22}H_{38}NO$	M+H	332.2937	-3.31	250.2169 (3), 236.2025 (4), 222.1859 (4), 166.1219 (**h**, 4), 152.1073 (36), 139.0982 (11), 126.0913 (9), 124.0761 (60), 98.0602 (**100**), 95.0856 (28), 93.0690 (16), 91.0538 (5), 81.0697 (28), 79.0541 (15), 72.0811 (40), 67.0543 (**i**, 38), 55.0545 (39)	40	1-(Piperidinyl)-2,4,11-heptadecatrien-1-one	Piperamides D
P152	19.26	$C_{20}H_{36}NO$	M+H	306.2786	-1.63	278.2849 (5), 252.2592 (4), 235.2056 (**b**, 1), 180.1382 (1), 152.1071 (**h**, 5), 150.0909 (2), 138.0903 (3), 124.0756 (8), 109.1006 (4), 98.0599 (**c**, 42), 95.343 (7), 83.0436 (4), 81.0335 (20), 72.0909 (**a**, 13), 70.0650 (5), 67.0544 (5), 55.0545 (**i**, 12), 53.0395 (6)	35	1-(Pyrrolidinyl)-2,4-hexadecadienmide	Pyrrolamides
P153	19.39	$C_{22}H_{40}NO$	M+H	334.3093	-3.29	261.2221 (**b**, 1), 233.2268 (2), 180.1372 (1), 137.1329 (3), 135.1164 (4), 128.1072 (4), 123.1173 (5), 109.1009 (7), 107.0852 (4), 97.1011 (4), 95.0351 (8), 83.0953 (3), 81.0700 (5), 74.0964 (**a**, 1), 67.0536 (1), 57.0703 (**i**, 8)	25	N-isobutyl-2,4,12-octadecatrienamide	Piperamides C
P154	19.67	$C_{22}H_{38}NO$	M+H	332.2944	-1.20	304.3026 (2), 278.2837 (3), 152.1073 (**h**, 11), 150.0922 (23), 138.0922 (7), 126.0911 (9), 124.0763 (60), 98.0601 (**c**, **100**), 95.0856 (30), 93.0699 (18), 91.0538 (17), 81.0694 (26), 79.0542 (34), 72.0808 (**a**, 26), 70.0657 (23), 55.0545 (**i**, 94)	50	1-(Pyrrolidyl)-2,4,12-octadecatrienamide	Pyrrolamides

Table 3.1: Continued

Flavonoids

Peak no.	t_R (min)	Molecular formula	Precursor ion	$[M+H]^+$ [m/z]	Diff. (ppm)	$^aMS^2$ [m/z] m/z (rel. intensity [%])	CID, eV	Tentative identification
P29	5.41	$C_{26}H_{29}O_{14}$	M+H	565.1539	-2.30	547.15 (85), 529.1394 (62), 511.1286 (86), 499.1243 (68), 457.1161 (34), 445.1148 (39), 427.1081 (72), 409.0944 (37), 295.0675 (14)	25	Isoschaftoside
P30	5.69	$C_{27}H_{31}O_{15}$	M+H	595.1657	0.00	475.1249 (3), 433.1178 (89), 415.1050 (60), 397.0942 (37), 367.0829 (11), 337.0727 (20), 313.0748 (**100**), 283.0616 (12), 271.0617 (28)	40	[b]Vitexin 2''-*O*-galactoside
P31	5.82	$C_{27}H_{31}O_{14}$	M+H	579.1709	0.17	433.1141 (**100**), 415.1033 (41), 397.0905 (17), 379.0803 (3), 367.0804 (6), 337.0731 (5), 313.0714 (23), 295.0602 (3), 283.0605 (5), 271.0620 (3)	35	Vitexin-2''-*O*-rhamnoside
P32	5.84	$C_{26}H_{29}O_{14}$	M+H	565.1536	-2.83	433.1161 (**100**), 415.1050 (38), 397.0932 (30), 367.0901 (14), 337.0750 (19), 313.0734 (44)	35	Vitexin 2''-*O*-pentoside
P34	5.94	$C_{21}H_{21}O_{10}$	M+H	433.1120	-2.08	415.1032 (79), 397.0931 (62), 379.0816 (19), 367.0822 (22), 337.0719 (19), 313.0716 (**100**), 295.0615 (6), 283.0611 (17)	30	Vitexin
P36	6.18	$C_{33}H_{39}O_{19}$	M+H	739.2074	-0.81	577.1591 (51), 559.1480 (29), 475.1263 (57), 313.0730 (34), 271.0623 (9)	30	[b]Vitexin 4''-(3-hydroxy-3-methylglutaroyl)-2''-*O*-β-D-galactopyranoside
P37	6.29	$C_{26}H_{29}O_{14}$	M+H	565.1536	-2.83	403.1050 (**100**), 385.0926 (11), 367.0937 (9), 313.0715 (18), 283.0614 (7), 271.0622 (30)	25	Vitexin 2''-*O*-arabinopyranoside
P38	6.33	$C_{33}H_{39}O_{18}$	M+H	723.2119	-1.66	577.1553 (**100**), 559.1439 (60), 459.1289 (40), 313.0713 (99), 271.0607 (13)	35	Vitexin 4''-(3-hydroxy-3-methylglutaroyl)-2''-*O*-pentoside
P39	6.45	$C_{27}H_{29}O_{14}$	M+H	577.1535	-2.95	559.1465 (16), 433.1160 (3), 415.1065 (4), 313.0731 (25), 295.0613 (4), 271.0606 (4)	20	Vitexin 4''-(3'''-hydroxy-3'''-methyl-glutarate)
P43	6.67	$C_{39}H_{49}O_{24}$	M+H	901.2358	-0.44	739.2129 (13), 637.1618 (17), 577.1625 (31), 559.1639 (9), 325.0961 (**100**), 307.0845 (17), 271.0628 (9), 163.0398 (21)	30	Acetylated flavonoid glycosides- A
P47	6.94	$C_{44}H_{49}O_{23}$	M+H	945.2641	-1.90	681.1854 (11), 577.1555 (27), 559.1455 (17), 369.1207 (**100**), 351.1087 (41), 313.0715 (28), 271.0605 (10), 225.0740 (9), 207.0651 (58)	40	Acetylated flavonoid glycosides- B
P48	6.98	$C_{43}H_{47}O_{22}$	M+H	915.2543	-1.09	651.1671 (10), 577.1547 (22), 559.1430 (19), 339.1071 (**100**), 271.0605 (9), 177.0544 (87)	40	Acetylated flavonoid glycosides- C
P54	7.57	$C_{43}H_{47}O_{22}$	M+H	915.2535	-1.97	651.1821 (21), 577.1538 (51), 559.1480 (30), 339.1105 (19), 271.0581 (30), 177.0524 (**100**)	40	Acetylated flavonoid glycosides- D
P86	10.98	$C_{16}H_{13}O_5$	M+H	285.0754	-1.05	285.0764 (14), 270.0519 (31), 242.0573 (**100**), 153.0183 (9)	50	Acacetin
P115	13.53	$C_{17}H_{15}O_5$	M+H	299.0908	-2.01	284.0695 (8), 256.0746 (**100**), 241.0511 (5), 227.0714 (3), 213.0551 (5), 197.0608 (3), 167.0344 (14), 124.0154 (8)	50	[b]Apigenin dimethylether

Table 3.1: Continued

Other metabolites

Peak no.	t_R (min)	Molecular formula	Precursor ion	[M+H]⁺, [m/z]	Diff. (ppm)	ᵃMS², [m/z] m/z (rel. intensity [%])	CID, eV	Tentative identification
P4	3.75	$C_{14}H_{28}NO_{10}$	M+NH₄	370.1703	-1.35	353.1434 (24), 335.1338 (50), 307.1032 (**100**), 289.0941 (56), 271.0798 (10), 163.0503 (42), 145.0500 (29), 127.0375 (13), 103.0375 (7), 85.0293 (4)	15	3,7-Anhydro-1,2-dideoxy-D-glycero-D-gulo-oct-1-enitol-6-yl-β-D-galactopyranoside
P8	4.37	$C_{13}H_{19}O_6$	M+H	271.1177	0.37	197.0677 (9), 179.0677 (9), 151.0370 (7), 147.0649 (6), 125.0586 (19)	15	ᵇBenzyl-β-D-glucoside
P13	4.68	$C_{17}H_{13}O_3$	M+H	265.0860	0.38	250.0603 (27), 237.0907 (34), 222.0672 (21), 219.0905 (39), 209.0977 (47), 191.0835 (21)	25	Quinone derivatives
P14	4.68	$C_{18}H_{17}O_4$	M+H	297.1119	-0.67	282.0888 (68), 265.0854 (46), 237.0904 (63), 219.0828 (25), 209.0980 (31), 207.0800 (31), 191.0864 (25), 165.0696 (20)	30	Tanshinol B
P18	4.98	$C_9H_7O_2$	M+H	147.0440	-0.68	119.0497 (**100**), 91.0550 (86), 65.0393 (5)	20	Coumarin
P19	4.99	$C_{17}H_{13}O_3$	M+H	265.0858	-0.38	250.0969 (**100**), 237.0905 (37), 233.0597 (30), 222.0691 (9), 205.0655 (22)	25	Quinone derivatives
P20	4.99	$C_{18}H_{17}O_4$	M+H	297.1119	-0.67	282.0875 (48), 267.0670 (14), 265.0962 (**100**), 254.0936 (17), 250.0629 (18), 247.0746 (14), 239.0725 (14), 237.0926 (54), 233.0617 (48), 222.0697 (17), 209.0952 (10), 205.0653 (61)	30	Tanshinol B (isomer)
P23	5.11	$C_{19}H_{31}O_8$	M+H	387.2008	-1.29	225.1479 (30), 207.1387 (**100**), 189.1274 (6), 149.0944 (6), 113.0607 (7)	15	ᵇRoseoside
P28	5.39	$C_{16}H_{32}NO_{10}$	M+NH₄	398.2014	-1.76	381.1735 (4), 363.1659 (47), 307.1029 (**100**), 289.0922 (14), 271.0802 (4), 187.0610 (3), 163.0605 (47), 145.0482 (19), 127.0386 (7), 103.0393 (4)	15	Dimethylallyl 6-O-α-arabinopyranosyl-β-D-glucopyranoside
P33	5.89	$C_{22}H_{36}NO_{13}$	M+NH₄	522.2167	-2.68	505.1856 (1), 360.1673 (4), 343.1417 (33), 325.1153 (65), 289.0922 (6), 181.0874 (**100**), 163.0593 (24), 145.0493 (13), 140.0464 (4), 127.0393 (3), 85.0279 (1)	15	Coniferinoside
P35	6.02	$C_{28}H_{44}NO_{13}$	M+NH₄	602.2806	-0.17	585.2547 (1), 423.2019 (**100**), 405.1911 (27), 387.1793 (4), 355.1529 (2), 251.1277 (1), 193.0843 (1), 167.0697 (1)	15	8,8'-Bisdihydrosiringenin glucoside
P40	6.53	$C_{11}H_{17}O_3$	M+H	197.1168	-2.03	179.1072 (29), 161.0957 (4), 135.1168 (11), 133.1006 (3), 107.0856 (3)	15	ᵇLoliolide
P45	6.77	$C_{20}H_{32}NO_{10}$	M+NH₄	446.2014	-1.57	429.1784 (7), 411.1678 (22), 307.1042 (**100**), 289.0933 (13), 271.0824 (3), 163.0604 (22), 145.0494 (10), 127.0390 (6)	15	Rosavin
P49	7.33	$C_{11}H_{11}O_4$	M+H	207.0645	-3.38	192.0414 (31), 191.0337 (61), 179.0699 (9), 163.0395 (66), 151.0747 (**100**), 136.0513 (24), 121.0645 (14), 107.0493 (17), 91.0529 (11)	30	ᵇScoparone
P51	7.46	$C_{12}H_{15}O_3$	M+H	207.1012	-1.93	192.0775 (7), 177.0906 (7), 176.0837 (**100**), 161.0591 (15)	20	3,4-Dimethoxybenzalacetone
P53	7.50	$C_{22}H_{37}O_{11}$	M+H	477.2318	-2.51	459.2245 (7), 441.2163 (3), 395.1535 (3), 339.1859 (3), 307.1057 (20), 289.0906 (5), 171.1391 (**100**), 163.0600 (12), 153.1259 (5), 145.0518 (4), 135.1135 (3), 107.0837 (3), 95.0873 (3), 93.0694 (4)	15	Limonen-di-glucopyranosides

Table 3.1: Continued

Peak no.	t_R (min)	Molecular formula	Precursor ion	$[M+H]^+$, [m/z]	Diff. (ppm)	$^aMS^2$, [m/z] m/z (rel.intensity [%])	CID, eV	Tentative identification
P56	7.72	$C_{10}H_{13}O_4$	M+H	197.0809	0.51	182.0578 (13), 169.0865 (15), 154.0622 (60), 139.0390 (19), 138.0675 (**100**), 123.0441 (15)	25	[b]Asarylaldehyde
P67	9.53	$C_{11}H_{11}O_4$	M+H	207.0648	-1.93	179.0635 (35), 177.0544 (48), 175.0399 (17), 164.0455 (35), 151.0387 (81), 149.0602 (**100**), 147.0458 (38), 134.0346 (17), 121.0259 (14), 119.0488 (57), 91.0536 (30)	25	3-(7-methoxy-1,3-benzodioxol-5-yl)prop-2-enal
P85	10.96	$C_{11}H_{13}O_4$	M+H	209.0804	-1.91	193.0509 (9), 179.0359 (**100**), 149.0903 (7), 135.0443 (7), 134.0379 (3), 121.0654 (11), 107.0496 (5), 106.0417 (9), 105.0345 (4), 91.0554 (21), 79.0550 (7), 77.0394 (8)	35	Methyl kakuol
P89	11.45	$C_{12}H_{17}O_3$	M+H	209.1166	-2.87	194.0961 (**100**), 181.0886 (54), 179.0717 (83), 178.1007 (53), 177.0925 (20), 168.0794 (8), 163.0769 (20), 151.0765 (51), 149.0605 (12), 121.0666 (30), 91.0550 (7)	25	Asarone (isomer-A)
P90	11.49	$C_{22}H_{27}O_6$	M+H	387.1796	-1.55	327.1805 (79), 225.1117 (73), 219.1020 (6), 163.0746 (58), 121.0647 (**100**)	15	Eudesmin
P94	11.68	$C_{12}H_{17}O_3$	M+H	209.1168	-1.91	194.0946 (15), 181.0864 (7), 178.0996 (15), 177.0909 (3), 168.0802 (**100**), 162.0679 (3), 153.0552 (22), 151.0760 (1), 125.0594 (1)	20	[b]Isoasarone
P95	11.87	$C_{12}H_{17}O_3$	M+H	209.1171	-0.48	194.0950 (46), 181.0869 (24), 179.0726 (**100**), 178.0997 (26), 177.0914 (6), 163.0757 (18), 162.0678 (8), 151.0763 (73), 147.0790 (8), 136.0520 (17), 123.0447 (15), 121.0648 (20), 107.0495 (7), 91.0543 (15)	30	[b]Trans-asarone
P96	11.88	$C_{24}H_{33}O_7$	M+H	433.2209	-2.77	265.1448 (92), 247.1337 (98), 237.1491 (19), 225.1104 (14), 216.1150 (36), 209.1184 (69), 197.0803 (27), 181.0868 (**100**)	25	Grandisin
P122	14.45	$C_{24}H_{33}O_6$	M+H	417.2267	-1.20	385.1992 (5), 249.1497 (**100**), 217.1229 (39), 209.1178 (29), 181.0860 (17)	15	[b]Andamanicin
P126	14.72	$C_{24}H_{33}O_6$	M+H	417.2276	0.96	385.2042 (8), 249.1508 (**100**), 209.1176 (14), 181.0846 (6)	15	Heterotropan
P127	14.83	$C_{24}H_{33}O_6$	M+H	417.2267	-1.20	249.1500 (**100**), 181.0851 (3)	15	[b]Magnosalin
P130	15.13	$C_{12}H_{17}O_3$	M+H	209.1169	-1.43	194.0951 (**100**), 181.0968 (82), 179.0710 (79), 178.1000 (11), 177.0935 (12), 168.0794 (7), 177.0997 (46), 163.0767 (13), 162.0670 (12), 151.0756 (60), 147.0813 (10), 136.0515 (12), 135.0903 (12), 123.0436 (12), 121.0661 (12), 91.0531 (9)	25	Asarone (isomer-B)

[a] Relative intensity of parent ion is 100% if none of fragment ions stated
[b] Confirmed by co-elution with authentic standards (isolated compounds with the structure confirmed by NMR spectroscopy).

3.2.3.1 Alkaloids

Piper is a rich source of alkaloids, for which numerous biological activities have been reported [35,36]. Furthermore, the quality of *Piper* species is usually assessed by their metabolite content [37]. In this study, a variety of alkaloids, mostly amides, were putatively identified from *P. sarmentosum.* According to their structure, these alkaloids can be classified into types A-E piperamides, as defined according to previous studies [16,26,38-40]. In addition to these groups, other alkaloids such as phenolic amides A-B, lignanamides, aporphines, and isoquinolines were also annotated. As shown in Figure 3.3, the piperamides were classified according to their chemical structure and the general characteristics of fragmentation ions were determined. Structurally, types A, B and E have the same benzodioxole group at the terminal part of the fatty acid with different piperidine, isobutylamine or pyrrolidine moieties at the other terminal. In contrast, types C, D and pyrrolamide have the same fatty acid chain on the left side with isobutylamine, piperidine or pyrrolidines on the other side.

The structures can be assumed according to the characteristic fragments of the different alkaloid types, mainly types A-E. All piperamides show a typical cleavage of the N-CO bond resulting in the formation of an (aryl) acylium cation (**b**) and the corresponding protonated amine part (**a**). This is often followed by further cleavage of CO leading to fragment **d**. Thereby, especially the specific neutral losses of the amine part give valuable structural information. Thus, the loss of piperidine ($C_5H_{11}N$, 85.0891 Da) and/or formylpiperidine ($C_6H_{11}NO$, 113.0841 Da) indicate the presence of type A or type D piperamides. The unique loss of isobutylamine ($C_4H_{11}N$, 73.0891 Da) or formylisobutylamine ($C_5H_{11}NO$, 101.0841 Da) refers to the presence of type B and type C piperamides, respectively. Similarly, the presence of a pyrrolidine unit is connected to the unique neutral losses of the amine moiety (C_4H_9N, 71.0735 Da) or formylpyrrolidine (C_5H_9NO, 99.0684 Da) (Figure 3.3). The typical fragment ions, **g** at m/z 161 $[C_{10}H_9O_2 + H]^+$, ion **e** at m/z 135 $[C_8H_7O_2 + H]^+$, and m/z 131 (**g**-CH_2O), indicated the existence of a benzodioxole group. These features proved the structure of the terminal part of type A, B and E piperamides.
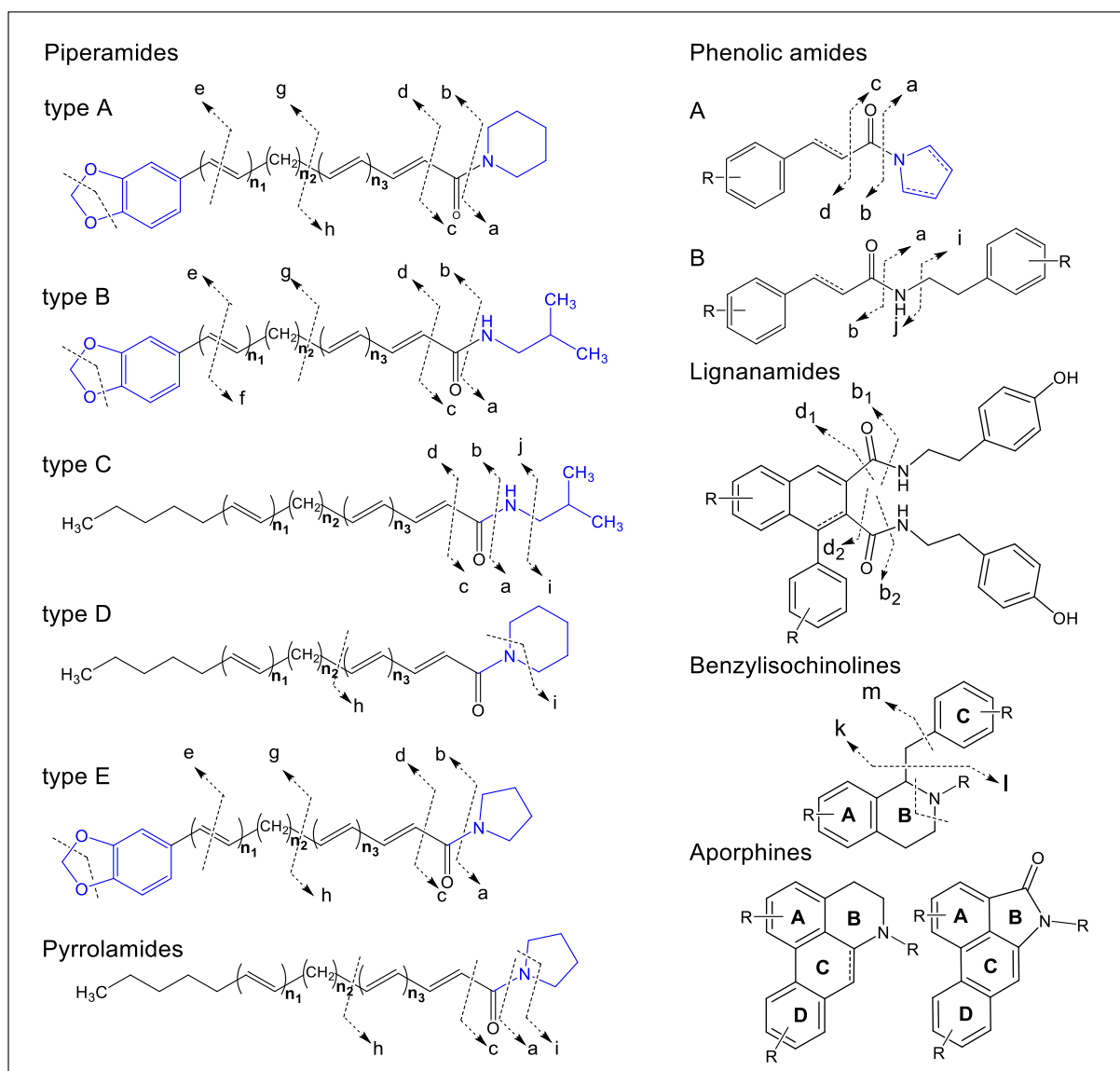
Figure 3.3: Classification of major alkaloid types found in *P. sarmentosum* and their characteristic fragmentation ions.

For instance, the mass spectroscopic cleavage pathways for type A, B and E piperamides with molecular ions [M+H]$^+$ at *m/z* 314.1747 (**P108**), 302.1745 (**P105**) and 300.1590 (**P93**), respectively, were determined based on MS/MS data as shown in Figure 3.4. The MS/MS data of these molecular ions show the same fragment ions at the *m/z* values of **b** (229), **d** (201), 187, **g** (161), **e** (135), **g** - CH$_2$O (131) and 103 (**g** - CH$_2$O - CO) in positive ion mode indicative for the aryl acyl part containing a benzodioxole group. The neutral losses are in accordance with the presence of a piperadine (**P108**), isobutylamine (**P105**) and pyrrolidine (**P93**) moiety. By matching the MS/MS spectra with those reported in the literature and databases, these compounds could be putatively identified as piperdardine (**P108**), chingchengenamide A (**P105**) and nigrinodine (**P93**), respectively [16,41,42]. The number of double bonds in the other

compounds could be calculated by the degree of unsaturation and their positions were estimated by the fragmentation losses and the literature data.
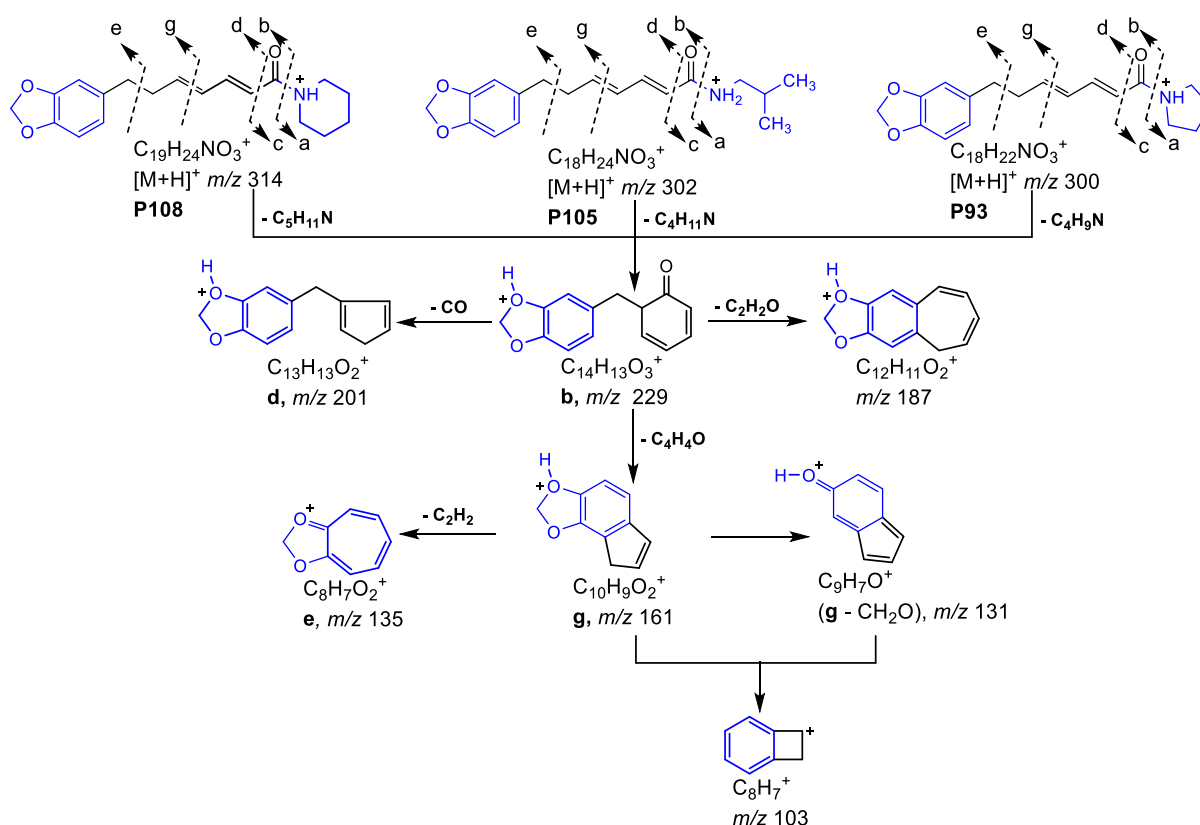
Figure 3.4: The general fragmentation patterns of selected piperamides **P108** (*m/z* 314), **P105** (*m/z* 302), and **P93** (*m/z* 300).

Moreover, several alkaloid groups were detected and identified like aporphines. The aporphine group possesses a common isoquinoline skeleton in a highly conjugated tetracyclic structure and multiple methoxy, methylenedioxy, or hydroxyl substituents attached to this aromatic system conferring on the class a great structural diversity [43]. The most of the MS/MS fragmentation patterns of aporphines-type compounds contain characteristic neutral losses of the substituents on A and D rings and N vicinal moieties through B ring cleavage. Peak **P12** with a molecular parent ion of *m/z* 342 [M+H]$^+$ exhibited a major fragment ion at *m/z* 297 ($C_{18}H_{17}O_4^+$) which was attributed to the elimination of $(CH_3)_2NH$, representing a key characteristic of the aporphines fragmentation pathway (Figure 3.5). Subsequently, the fragment ions at *m/z* 282 ($C_{17}H_{14}O_4^{\bullet+}$) and *m/z* 265 ($C_{17}H_{13}O_3^+$) were produced by the consecutive losses of $^{\bullet}CH_3$ and CH_3OH, respectively, from the fragment ion at *m/z* 297. The subsequent removal of CO from the fragment ion at *m/z* 265 to *m/z* 237 ($C_{16}H_{13}O_2^+$) is described as the preferred fragment pathway of metabolites with methoxy and hydroxyl groups in A ring [44-46]. Thus, peak **P12** with the molecular ion [M+H]$^+$ *m/z* 342 was deduced as magnoflorine comparing with the reported data [46].
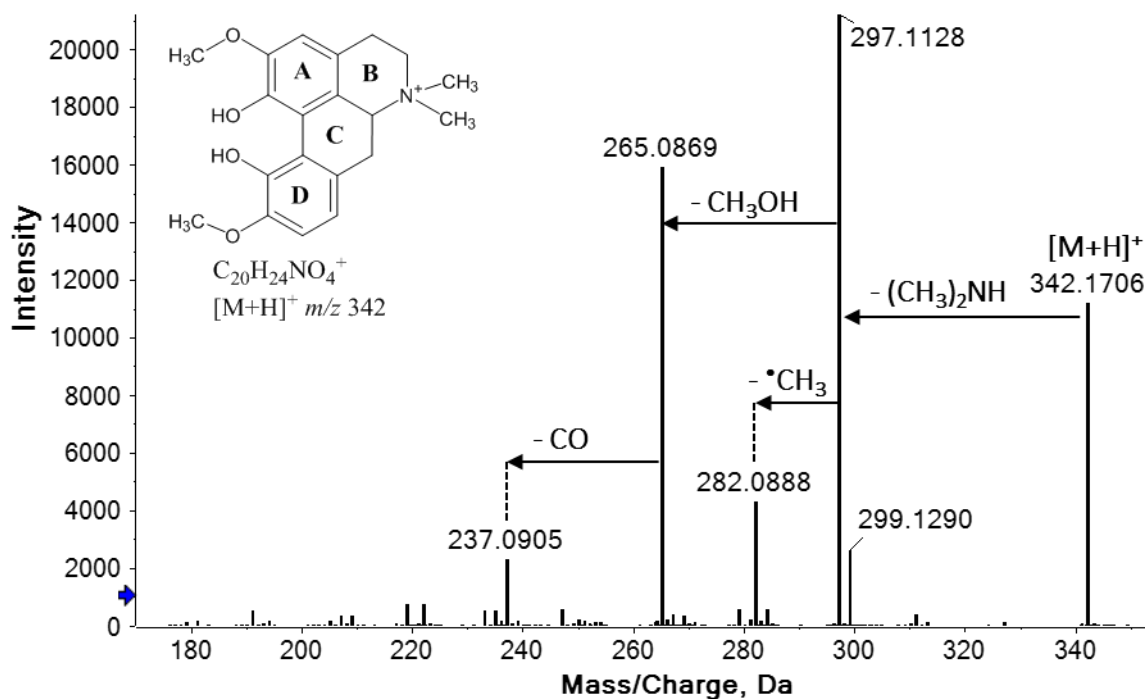
Figure 3.5: MS/MS spectrum of magnoflorine (**P12**).

A large group of alkaloids present possess the benzylisoquinoline-type skeleton. Figure 3.3 and 3.6 depict the MS fragmentation patterns of this group, which strongly indicate the presence of key ions (**k, l, m**) and the loss of the NH group. The **k**-type ion represents the benzyl group and is generated on the MS/MS secondary to the formation of ion **l**. The **l** ion is produced on the MS^2 after an "even electron"- type McLafferty rearrangement, involving the nitrogen proton and the aromatic ring of the benzyl conjugate [47]. The **m** ion occurs as a rearrangement after the elimination of the benzyl groups and amine moiety [45]. The *m/z* values of these key ions indicate the substituents present in the benzyl (ring C) and the isoquinoline part (ring A).

For example, the fragmentation of peak **P16** (*m/z* 330) among the compounds listed in the group of benzylisoquinolines is shown in Figure 3.6. It was identified as a tertiary amine by the loss of 31 Da, $[M+H-CH_3NH_2]^+$ in the MS/MS spectrum, resulting in an ion with *m/z* 299. The ion **l** with *m/z* 192 indicates the vicinal OCH$_3$ and OH group present at ring A. Furthermore, ion **k** with *m/z* 137 suggests the existence of OCH$_3$ and OH on the benzyl moiety. This data was supported by the **m** ion of this compound, with *m/z* 175. Therefore, peak **P16** was postulated as the well-known alkaloid reticuline by comparison with literature data [45].
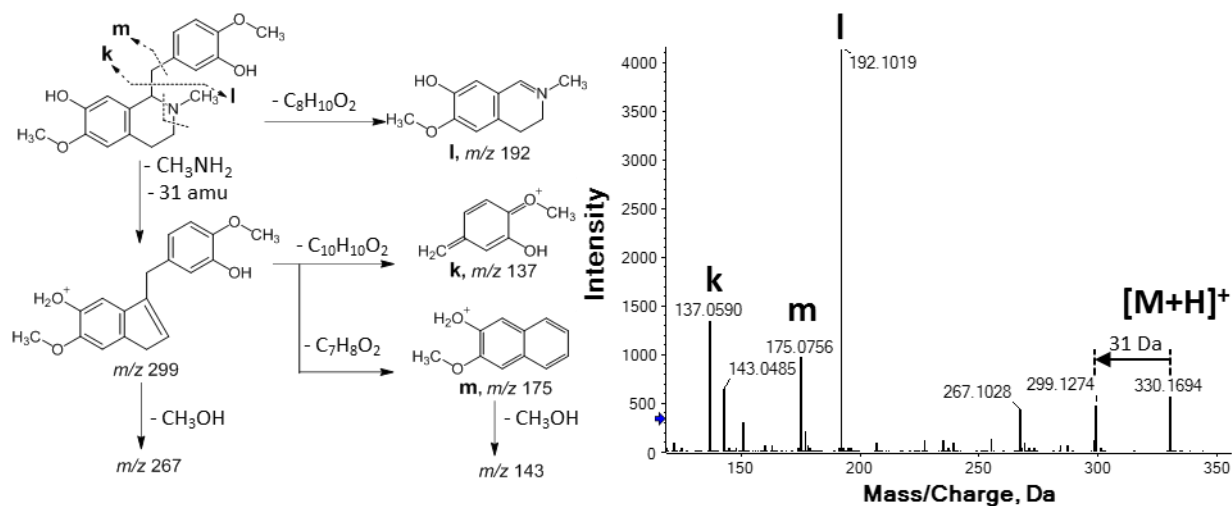
Figure 3.6: Proposed fragmentation pathway and MS^2 spectra of reticuline (**P16**)

The detected phenolic amides, which included coumaroyl or feruloyl groups as well as various amino groups, generated fragment ions at *m/z* 147 and 177, respectively. Many of them contained a tyramine moiety (137 Da), which lost a NH$_3$ to form a vinylphenol ion **i** at *m/z* 121 [48]. Compound **P50** displaying a [M + H]$^+$ at *m/z* 284.1290 (C$_{17}$H$_{18}$O$_3$N, cal. 284.1281) in the MS^2 spectrum was identified to be paprazine which produced fragment ions **b** at *m/z* 147 and ion **i** at *m/z* 121 (Figure 3.7). The **b** ion at *m/z* 147 was yielded by the neutral loss of a tyramine unit. Whereas peak **P55** displaying a [M + H]$^+$ at *m/z* 314.1403 (C$_{18}$H$_{20}$O$_4$N, cal. 314.1387) was identified as *trans-N*-feruloyltyramine; the characteristics product ions at *m/z* 177 represent ion **b** and *m/z* 121 as ion **i** indicate the existence of feruloyl and tyramine moieties (Figure 3.7). The substances behind both peaks **P50** and **P55** were confirmed by isolated compounds.
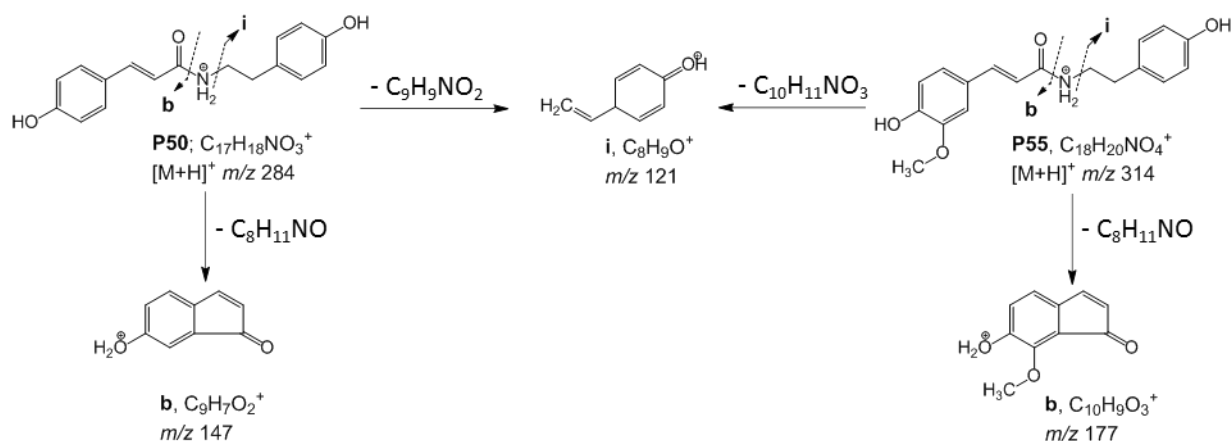
Figure 3.7: Key characteristics product ions **b** and **i** of paprazine (**P50**), and *trans-N*-feruloyltyramine (**P55**).

65

3.2.3.2 Flavonoids

Flavonoids consist of a large group of compounds, most antioxidants, that possess various biochemical properties, such as antibacterial, anti-inflammatory and anti-cancer activities, and play a pivotal role as colouring components of flowering plants [49]. MS/MS analysis can provide structural information about flavonoids including the structure of aglycones, glycosylation patterns and the presence of other substituents such as 3-hydroxy-3-methylglutaryl and acetyl residues [50]. According to previous studies of *P. sarmentosum*, the flavonoid aglycone identified was mainly apigenin (aglycon *m/z* 271). Several types of flavonoid substitutions have also been reported, such as *C*-glycosyl and *O*-glycosyl flavones as mono- and di- glycosides.

In the present study, a total of 15 compounds were chemically assigned as flavone derivatives, which were variously *O*- or *C*-glycosylated and modified as 3-hydroxy-3-methylglutaryl and acylatyl esters, by comparing their accurate monoisotopic ions and unique fragments with databases, literature and isolated compounds. All compounds were assigned to possess an apigenin aglycone in our study based on the corresponding fragment peaks appearing at *m/z* 313 ($C_{17}H_{13}O_6^+$) and *m/z* 271 ($C_{15}H_{11}O_5^+$). The identification of flavonoids is summarized in Table 3.1.

3.2.3.2.1 (3-Hydroxy-3-methylglutaryl) glycosides and derivatives

The fragmentation behavior of a 3-hydroxy-3-methylglutaryl residue (HMG) attached to a sugar moiety is mainly characterized by diagnostic ions of $[M + H - 264]^+$, $[M + H - 162]^+$, and/or $[M + H - 102]^+$ [51, 52]. Peaks **P36**, **P38** and **P39** were consistent with the presence of an HMG substituent on the saccharide residue. For example, the MS/MS spectra for peak **P36** (*m/z* 739.2130, $C_{33}H_{39}O_{19}^+$) show fragment ions at *m/z* 577, 559, 475, 313 and 271 as explained in Figure 3.8. The fragment ions are resulting from neutral losses of 264, 162 and 102 Da indicating the simultaneous loss of HMG and glucose residues. The abundant ion at *m/z* 475 ($[M+H-264]^+$) is further decomposed by the loss of a second $C_6H_{10}O_5$ leading to ions at *m/z* 313 and *m/z* 271. The ion at *m/z* 313 is indicative for flavonoid *C*-glycosides. The identity of peak **P36** was confirmed by comparison with the retention time and fragment ions of the isolated compound.
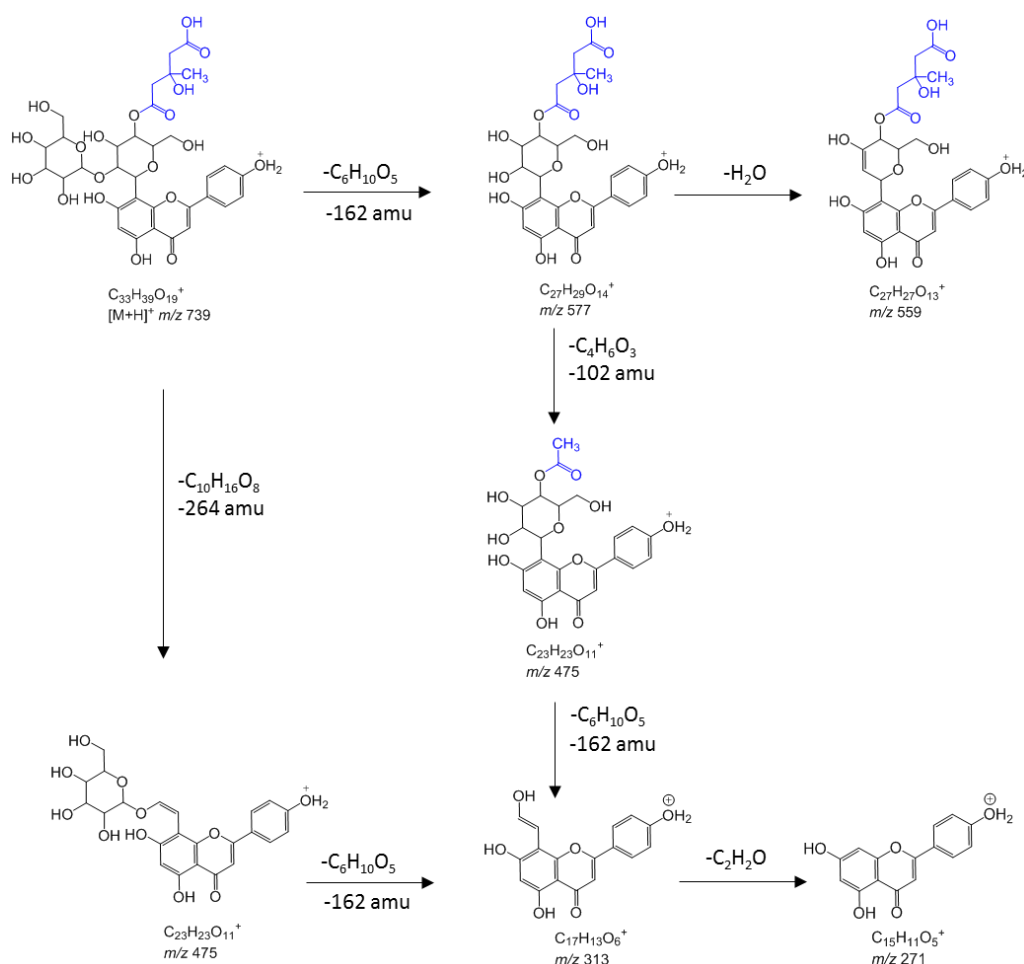
Figure 3.8: Proposed mass spectral fragmentation of the $[M+H]^+$ ion of the peak **P36**

3.2.3.2.2 Acylated *O*-glycoside flavones

The most common acyl groups generally found as substituents of flavonoids are hydroxycinnamic acids such as caffeic, ferulic, and sinapic acid. The characteristic product ions of the most commonly encountered acyl groups were previously reported [52-54]. Based on the characteristic ion fragments and neutral losses observed for this type of flavonoid, four acyl containing compounds linked to glycosides, **P43**, **P47**, **P48** and **P54** were identified. Peak **P48** and **P54** (Figure 3.9), for example, are isomers, that both have a molecular weight of 914 Da. The characteristic ions at *m/z* 339 ($C_{16}H_{19}O_8^+$) and 177 ($C_{10}H_9O_3^+$) and the neutral losses of 264 and 162 suggest that both compounds contain feruloyl and HMG substituents. However, the relative intensity of the ion *m/z* 339 was higher for peak **P48** (100%) than **P54** (19%), indicating that the feruloyl-glycoside was linked to hydroxyl in another glucose substituent (-*O*) for peak **P48**. In contrast, feruloyl-glycoside of **P54** occurred on the *C*-6 of flavone due to the lower relative intensity of *m/z* 339. These *C*-6 isomers often elute later than the 8-*C*-glycoside isomers. To the best of our knowledge, acylated *O*-glycosyl flavones with two groups are previously undescribed in the genus *Piper*.
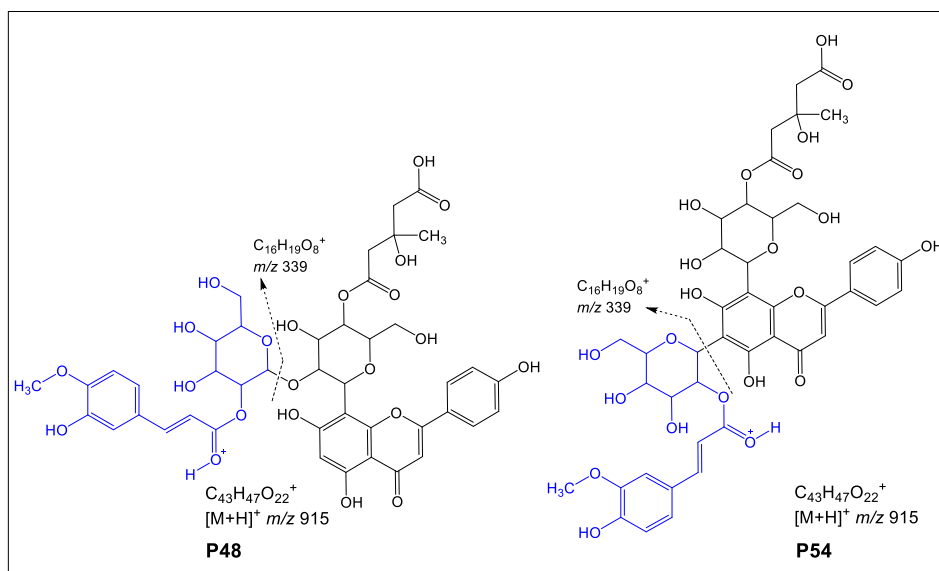
Figure 3.9: Proposed structures of peaks **P48** and **P54** with characteristic fragment ion at *m/z* 339

3.2.3.3 Other metabolites

Aside from those listed above, another 28 compounds were classified as asarone, coumarin, lignan and glucoside-derivatives. As a typical representative, the MS/MS fragmentation of peak **P95** was investigated as shown in Figure 3.10. Its protonated molecular ion was *m/z* 209.1182 in positive ion mode, and its main fragment appeared at *m/z* 179.0726 [M+H-30]$^+$ corresponding to the loss of C_2H_6. The radical fragment *m/z* 194.0950 [M+H-15]$^{\cdot+}$ was yielded through demethylation. The fragment ion *m/z* 151.0763 [M+H-28]$^+$ was produced by decarboxylation of fragment *m/z* 179. Peak **P95** represented the most abundant peak in *P. sarmentosum* which could be detected in all organs. The retention time and fragmentation
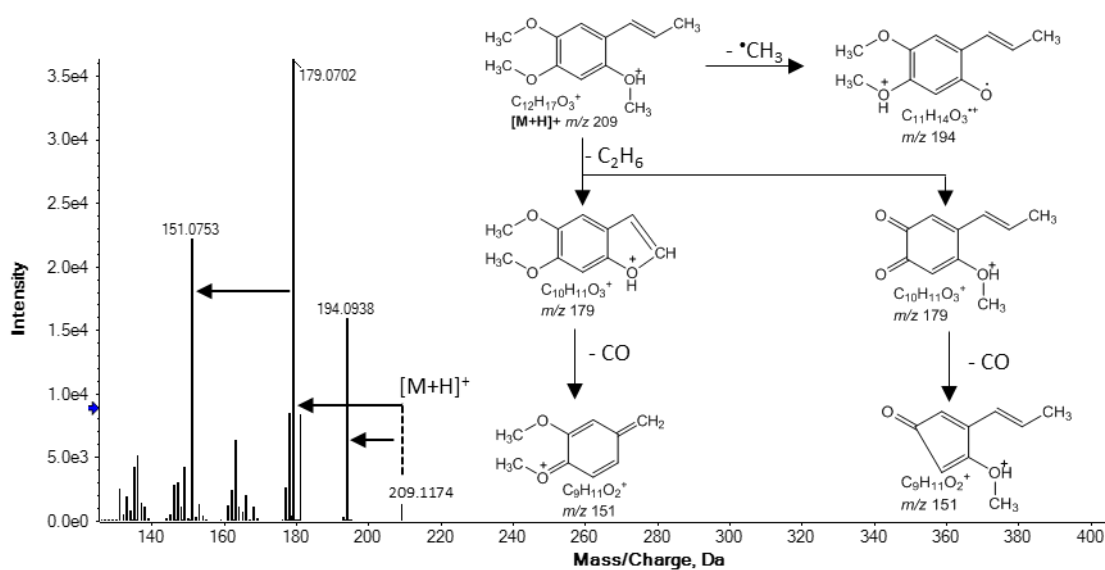
Figure 3.10: MS/MS spectral fragmentation of the [M+H]$^+$ ion of *trans*-asarone (**P95**).

pattern of **P95** at *m/z* 209.1182 [M+H]$^+$ were consistent with the isolated compound *trans*-asarone.

3.2.4 Untargeted comparison of metabolite profiles of different organs

Due to its high mass accuracy, sensitivity and resolution, the HR-QqTOF-MS is the most efficient analytical platform for online structural elucidation of multiple components in plants [55]. The inter-sample alignment of the individual TICs corresponding to all features in the dataset resulted in a consensus peak table (data matrix comprising individual features as defined pairs of t_R-*m/z* values) containing 1272 entries. These matched features comprised protonated molecular ions and other adducts, as well as in-source fragmentation products associated with characteristic neutral losses (Matrix data not shown). The data matrix was subjected to multivariate statistics analysis with MetaboAnalyst software.

Principal component analysis (PCA) is the method of multivariate statistics, which is recognized to be an efficient tool for reducing complex data sets and providing important insight into the variation within and between experimental groups. The results of the PCA analysis accomplished with our dataset (score and loadings plots) are shown in Figure 3.11. As can be seen from the score plot, approximately 86% of total variance was accounted by the first two identified principle components. The first component (PC1) was responsible for 65% of the total variance, whereas the second component (PC2) explained 21% of the total variance. Thus, the maximal possible variance observed between the different organs was explained by PC1. The leaves were separated from the other organs in PC1, whereas PC2 indicates that stems appeared to be significantly different from other organs in terms of their metabolite patterns. The loadings plot gives access to the features contributing to the separation of organs, which is primarily due to differences in their abundance within the various test samples and specific *p* value (Figure 3.11B).

The presence of highly intense chromatographic signals corresponding to the neolignane andamanicin (**P122**), flavonoids (**P30**, **P36**) and the phenyl propanoid *trans*-asarone (**P95**) led to the positioning of leaves in a single group in PCA. Interestingly, as indicated by the PCA loading plots, **P122** was represented by two different features, namely its protonated molecular ion [M+H]$^+$ (feature m765, t_R 14.5 min, *m/z* 417.2256) and the corresponding ammonium adduct [M+NH$_4$]$^+$ (feature m793, t_R 14.5 min, *m/z* 434.2530). Additionally, existence of the unique aporphine-type compounds in stems, like magnoflorines (**P12**, **P21**), piperolactam B (**P75**) and peperolactam A (**P70**), had a powerful discriminating effect for their separation from the other groups in the score plots. Finally, as can be seen from the TICs in Figure 3.2, the metabolite profiles of fruits and roots are quite similar. Therefore, the corresponding individual

Figure 3.11: Principle component analysis (PCA) with scores (A) and loadings (B) plots accomplished with 1272 features annotated in the RP-UHPLC-QqTOF-MS data of leaf, stem, root and fruit extracts from *Piper sarmentosum*.

samples are located in the same part of the PCA score plot. This fact can be explained by higher contents (manifested in the LC-MS dataset by higher relative intensities of corresponding molecular ionic species) of the piperamides, specifically - pellitorine (**P116**), brachyamide B (**P114**) and guineensine (**P136**), resulting, therefore, in the clustering of fruit and root samples together (Figure 3.11). Interestingly, peaks **P93** (nigrinodine) and **P112** (sarmentine), which are both derived from piperamide-type compounds, represent strong negative loadings located in the left side of PC1 compared to other common features (Figure 3.11B). With the exception of the leaves, this indicates the relative high content of both P93 and P112 in all organs. The relative abundances of individual metabolites, corresponding to the most significant loadings (i.e. the most significant ones for the separation between the plant organs) are illustrated by boxplots as displayed in Figure 3.12.

Our results clearly indicate that production and accumulation of secondary metabolites are organ-specific [19,56]. Additionally, as demonstrated by the differential responses of plant organs to environmental stressors, the stress adaptation responses are organ-specific [57]. This results in the existence of well-defined organ-specific patterns of metabolite accumulation, which facilitates interaction with the environment and to establish defense mechanisms [58, 59]. Obviously, this factor affects the nutritional and medicinal value of the plant organs.

Figure 3.12: Boxplots showing the significantly different metabolites identified in the four organs of *P. sarmentosum*. Vertical bars represent the normalized relative concentration of metabolites, and x-axis depicts the different plant organs, A = fruits (red), B = leaves (green), C = roots (blue), D = stems (cyan).

3.2.5   Hierarchical cluster analysis of identified metabolites

Hierarchical clustering with heat map representation proved to be an excellent tool to address the distribution and relative abundances of the individual identified phytochemicals in different organs of *P. sarmentosum*.

The heatmap was constructed using a hierarchical clustering algorithm based on the inter-sample similarities in the relative abundances of all annotated metabolites (Figure 3.13). Altogether, the hierarchical clustering was performed based on 154 annotated compounds with assigned structure from different organs belonging to the two major groups, **A**-alkaloids and **B**-flavonoids including other metabolites. The individual replicates obtained from the same organ cluster nicely together indicating good reproducibility of results. The heatmap clearly showed the organ-specific accumulation of individual metabolites in leaves, stems, roots and fruits, indicating essential metabolic difference between the *P. sarmentosum* organs. Based on this dataset, seven clusters could be assigned including Cluster I-IV for alkaloids and Cluster V-VII for flavonoids and other metabolites (Figure 3.13).

Cluster I was primarily composed of lignanamides (**P58**, **P60**, **P68**, **P74**) and specific piperamides such as piperettyline-like compounds (**P92**, **P98**, **P102**) and piperettines (**P109**, **P111**). The accumulation of these compounds was found in the roots. Several plants including *Piper* species have been reported to contain lignanamides such *P. puberulum* and *P. flaviflorum* [60,61]. However, no comparative analysis of lignanamides among the organ has been reported. The general biosynthesis pathway of lignanamides in another plant species, *Cannabis sativa* L., has been discussed in the past, however, detailed mechanisms and molecular events throughout the biosynthesis of lignanamides remain inconclusive [62]. Lignanamides are naturally occurring plant compounds that results from an oxidative coupling mechanism with hydroxycinnamic acid amides (HCAAs) as intermediates [63]. The formation of HCAAs is catalyzed by hydroxycinnamoyl-CoA:tyramine N-(hydroxycinnamoyl) transferase (THT), an enzyme that accumulates in several plants, including potato and tobacco [64]. The function of HCAAs in strengthening plant defense, as a response to fungal and pathogen challenge, has been described in potato tubers, onion roots and tomatoes [65].

Aporphines and benzylisoquinolines belong to the large group of isoquinoline alkaloids were mainly present in Cluster II. Isoquinoline alkaloids such as magnoflorine (**P12, P21**), cepharadione A (**P81**), aristolactam BIII (**P97**), coclaurines (**P9, P26**), and reticuline (**P16**) are among the metabolites responsible for the formation of this cluster. These compounds had elevated levels in stems. Several studies found that most of these phytochemicals are abundant in specialized cell sites [66,67]. For example, the analysis of isoquinoline alkaloids in the stems

of *Sinomenium acutum* showed a differential distribution of alkaloids, especially within the outer cortical regions, phloem and xylem [66]. In opium poppy (*Papaver somniferum*), sieve elements and specialized laticifers of the phloem produce and accumulate isoquinolines alkaloids, respectively [68]. The colocalization to vascular tissue might explain the predominant occurrence in stems. Basically, these compounds are biosynthetically produced *via* the phenylpropanoid pathway, and the primary pathway of biosynthesis is common to all these plants i.e., from norcoclaurine to reticuline. However, occasionally some mixed pathways may also occur to provide structural divergence. In general, isoquinoline alkaloids play a role in defense against pathogens, and their ecological functions also appear to include plant-interactions [69-71].

The hierarchical clustering mostly revealed a high number of phenolic amides for Cluster III. These distinct type of metabolites accumulated predominantly in leaves and fruits. Specific components such as **P50** (paprazine) and **P72** were present in greater abundance in leaves. Paprazine represents as tyramine derivative that contribute to active plant defense responses in infected leaf material. Biosynthesis of paprazine in tomato leaves was induced in response to wounding [72], and it was found to be associated with the resistance reactions of pepper leaves infected with *Xanthomonas campestris* [73]. According to Newman et al. [73], the richness of phenolic amides such as paprazine was preceded by an increase in the extractable activity of tyrosine decarboxylase as well as increases in the transcription of genes encoding phenylalanine ammonia-lyase and tyramine hydroxycinnamoyl transferase. This gene-gene type interaction is accompanied by cell death, producing a necrotizing reaction or hypersensitive response of the plant. A previous study discovered that large amounts of hydroxycinnamic acid amides such as paprazine and *trans-N*-feruloyltyramine on tomato leaves were detected after bacterial infection. This suggested that phenolic amides play a key in plant resistance to pathogens [74].

The most promising group of phytochemicals in *Piper* species are piperamides, including piperine (**P91**), pellitorine (**P116**), retrofractamide B (**P128**) and guineensine (**P136**), which were classified in Cluster IV. The majority of these metabolites was detected in fruits and not in the other organs. Similar occurrences of these constituents were also reported in fruits of other *Piper* species such as *P. nigrum* L. and *P. longum* L. [16,41]. The observations of these chemical compounds in *Piper* fruits were supported by Schnabel and collaborator's study of piperine synthase from *P. nigrum*. They suggested that the accumulation of piperine and
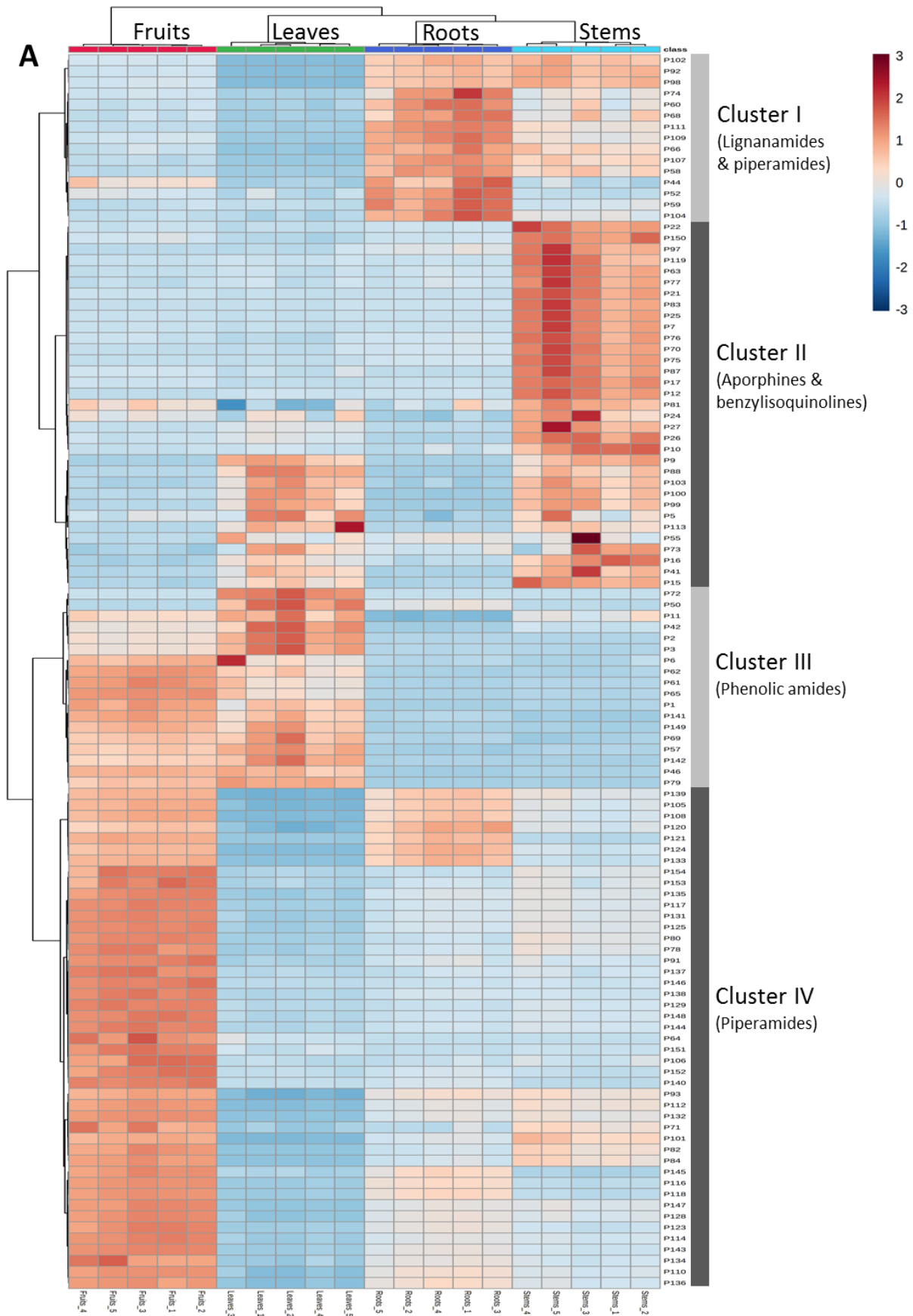
Figure 3.13: Continued
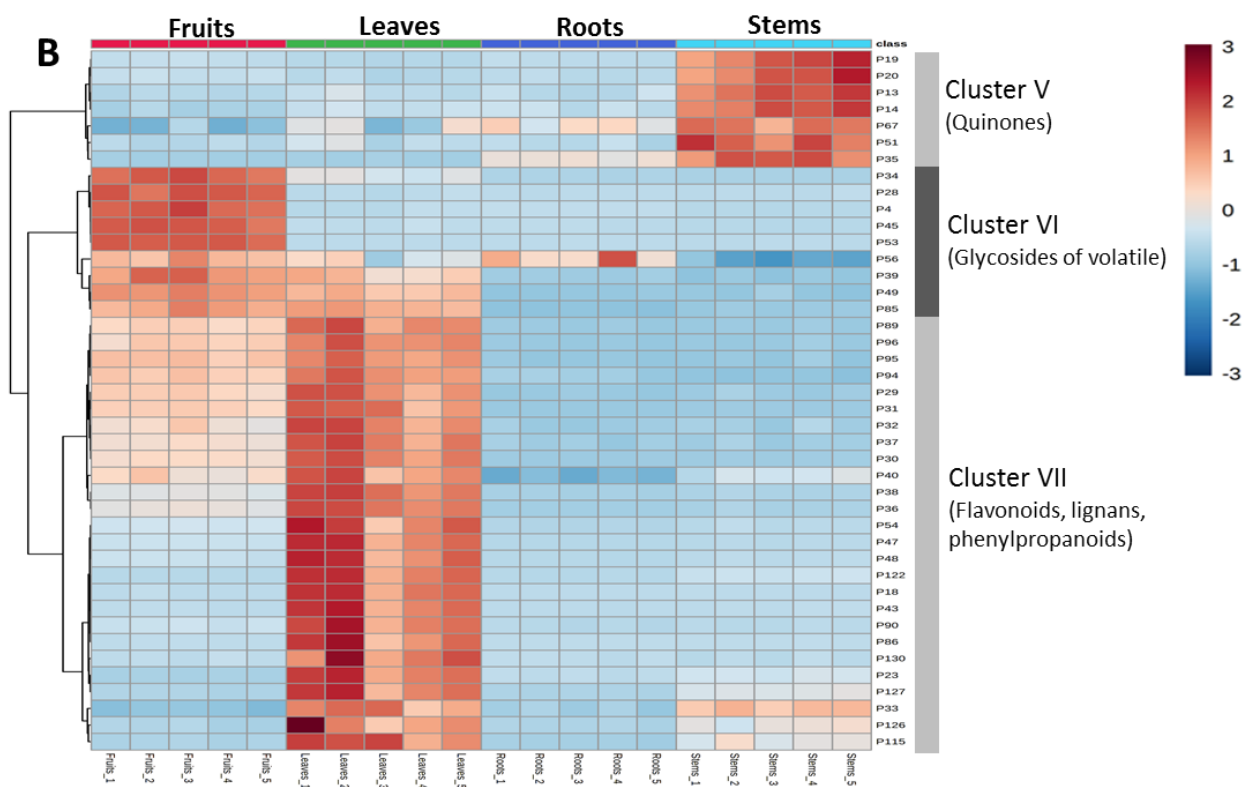
Figure 3.13: Heatmap analysis of relative distributions of alkaloids (**A**) and flavonoids and other metabolites (**B**), identified in different organs. The heatmap was established using a hierarchical clustering algorithm based on similarities among annotated metabolites. The red and blue colour in the heatmap represent an increase and a decrease of metabolite level compared to the average, respectively.

piperamides are related to piperine synthase (piperoyl-CoA: piperidine piperoyl transferase) and other BAHD-type enzymes that are preferentially expressed in fruits organ [75]. These secondary metabolites have a significant ecological impact on fruit-frugivore interactions and plant reproductive success [76].

Moreover, piperamides have numerous advantages for human health, food industrial use, and potential agricultural prospects. For example, the major metabolite in this organ, pellitorine, was reported to possess insecticidal, anticancer, and antiplatelet aggregation properties [77]. In addition, piperine, a well-known compound derived from this species, has a wide range of biological activities and a distinct sharp flavor [78,79]. This could explain why the fruits from *Piper* are predominantly used as food complementary especially in spices. Thus, these results provide insights into the possibility that *P. sarmentosum* fruits might be utilized as an alternative to other *Piper* fruits.

Cluster VI is composed of glycosides of volatile compounds such as **P4, P28, P45**, and **P53**, which are primarily found in fruits. *Piper* fruits are particularly appreciated for their characteristic flavors and aromas that develop as fruits ripen [80]. A significant proportion of

potential flavor contributors have been reported to exist as volatile compounds. Volatile aroma compounds are typically discovered in plants in two forms: "free" and "bound" to a sugar unit. These compounds are not odoriferous when bound; however, upon (enzymetic or abiotic) glycoside hydrolysis, these metabolites are liberated [81]. Moreover, the hydrolysis of glycosides may occur during the ripening process and subsequent release of additional volatile compounds may enhance the fruit flavor. Previous studies, e.g. on the model plant *Arabidopsis thaliana,* indicate that glycosides are produced by glycosyltranferase enzymes, which add an activated sugar unit to the aglycone in the cytosol of the plant cell [82-84]. Recently, the analysis of the 7-deoxyloganetin glucosyltransferase-like (GGT) gene during fruit development of various *Piper nigrum* L. varieties revealed that increased GGT expression in *Piper* fruits correlates with increased volatile and nonvolatile metabolite content [85].

Finally, Cluster VII mainly contained flavonoids, including flavone-*C*-glycosides, and other metabolites such as phenylpropanoids. In addition, specific lignans are present in this cluster and were found in relatively high amount in leaves. The nature of the flavonoid accumulation in plants indicates their important biological role. Flavones exercise a diverse range of functions, including developmental roles, pathogen attack protection, and resistance to unfavorable environmental conditions like high-level UV radiation and water stress [86].

In general, flavonoids are synthesized starting from the phenylpropanoid pathway to the last step of flavonoids biosynthesis. The end of the biosynthesis involves various chemical modifications on the flavonoid aglycons, such as hydroxylations, *C*- and *O*-methylations, glycosylations, prenylations and acylations, which increase their diversity and contribute to chemical properties [87]. There are many enzymes involved in the flavonoid pathway including phenylalanine ammonia-lyase (PAL), chalcone synthase (CHS), and flavanone 3′-hydroxylase (F3′H) [88-90]. The majority of flavonoid metabolism enzymes are recovered in leaf mesophyll [91,92]. This explains the greater content of flavonoids in the leaves compared to other organs. Leaves are the plant parts from *P. sarmentosum* which are preferentially consumed in Malaysia and which were shown to possess vascular protective, neuroprotective, anti-obesity, and anti-hyperlipidemia activity [12-14]. These activities might be connected to the content of flavonoids and lignans which possess a high antioxidative potential [93]. Previous research has found that the total flavonoids content (TFC) of *P. sarmentosum* leaves can reach 120.5 mg/kg of dry weight, including apigenin [94]. According to Ugusman et al. [95], there is a positive correlation between the presence of flavonoids in *P. sarmentosum* leaves and its protective effects against oxidative stress. Another literature reported that plant leaf extracts exhibited anti-inflammatory, antibacterial and insecticidal properties [5,96,97]. In our previous study, we discovered that simple phenylpropionate compounds, such as *trans*-asarone (**P95**), which was

isolated from leaves, have promising antifungal and anthelmintic properties (see Chapter 2). Another study revealed that asarone and its derivatives have an inhibitory effect on mosquitoes and other insects, particularly larvae, and could reduce the hatching rates of eggs [98,99].

Based on these data, the conclusion about the predominant occurrence of specific metabolite classes in different organs of *P. sarmentosum* is summarized in Figure 3.14.
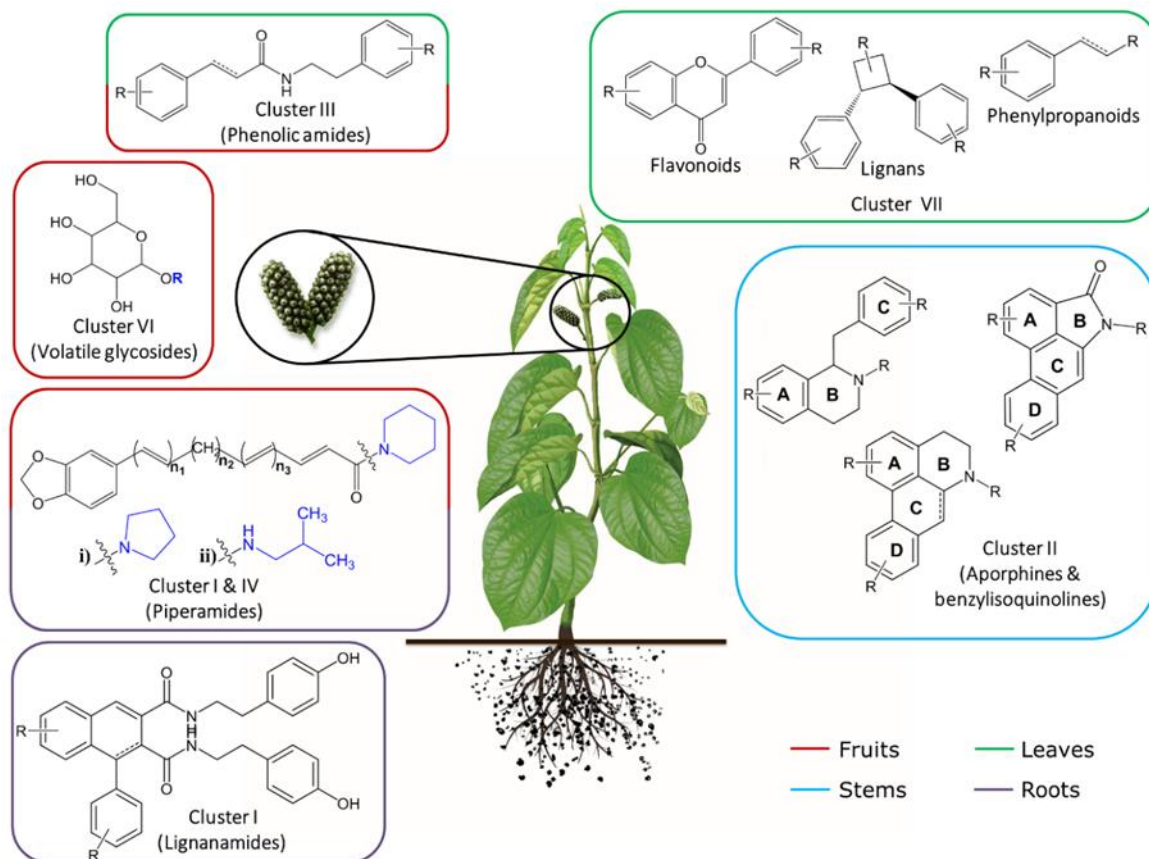
Figure 3.14: Predominant occurrence of compound classes in organs of *P. sarmentosum.*

In summary, UHPLC-QTOF-MS/MS was used to characterize the metabolic profiles of various organs from *P. sarmentosum*. These are clearly separated in distinct cluster by principle component analysis and hierarchical clustering. Diverse alkaloid structures were identified and characterized along with flavonoids and other metabolites as dominant compound classes in these profiles. Similar to other *Piper* species, *P. sarmentosum* has economic, medicinal, and nutritional value. The current study, however, reveals that roots and fruits share a large number of common phytochemicals, as evidenced by TICs, PCA score and loadings plot, and hierarchical clustering analysis. This finding may support the culinary uses of roots by some communities in southern China. Furthermore, despite the presence of similar chemical diversity in different organs, *P. sarmentosum*'s leaves, stems, roots, and fruits also contain specific

compounds, qualitatively and quantitatively. These can be used for the discrimination among organs and exploited for selective harvesting.

3.3   Materials and methods

3.3.1   Chemicals

All chemical standards, LCMS grade methanol, acetonitrile and ammonium formate were obtained from Merck (Darmstadt, Germany). Water was purified in-house on the water conditioning and purification system Millipore Milli-Q Gradient A10 (resistance 18 mΩ/cm, Merck Millipore, Darmstadt, Germany).

3.3.2   Plant materials and extraction

Piper sarmentosum Roxb. was collected in January 2019 from Negeri Sembilan, Malaysia. A voucher was authenticated (Number: MFI 0039/19) by Dr. Mohd Firdaus Ismail, botanist at the Institute of Biosciences, Universiti Putra Malaysia. A duplicate of the Herbarium specimen is kept at the Bioorganic Chemistry Department collection of Leibniz Institute of Plant Biochemistry, Germany. In particular, various plant organs such as leaves, stems, roots and fruits were collected from different plants. After the organs were sorted, samples were pooled, cleaned, and dried in the oven at 50°C for 92 hours. The dried samples were ground in a Mixer Mill MM 400 ball mill with a 20 mm stainless steel ball (Retsch, Haan, Germany) at a vibration frequency of 30 Hz for 60 seconds. Briefly, for sample preparation 4 mg dried plant organs were weighed into a 2 mL centrifuge tube. Then 1 mL of methanol containing 2 pmol/µL of kinetin and 50 pmol/µL orcinol as internal standard were added, vortexed vigorously for 20 seconds, and extraction was performed by an ultrasound bath (40°C) for 20 minutes. The extracted samples were centrifuged for 15 minutes at 14,000x g and a clear supernatant per extract was transferred to an LCMS vial for analysis. All four organs were blended equivalently as a quality control (QC) sample to evaluate instrument stability. The QC sample was inserted in every six injections during the RP-UHPLC- QTOF MS analysis.

3.3.3   LC-MS and MS/MS

Analysis of the extracts relied on reversed phase-ultra high performance liquid chromatography (with 3 mmol/L aq. ammonium formate and acetonitrile as eluents A and B, respectively) coupled on-line to electrospray ionization quadrupole-time-of-flight mass spectrometry (RP-UHPLC-QqTOF-MS). For this, 5 µL of individual extracts were injected in Waters ACQUITY I-Class UPLC System (Waters GmbH, Eschborn, Germany). After a two-min wash at 5% eluent B, the samples were separated at the flow rate of 400 µL/min on a EC

150/2 NUCLEOSHELL RP C18 column (150 x 2 mm, particle size 2.7 µm) thermostated at 40 °C in a linear gradient to 95% eluent B in 17 min. After a 2 min isocratic step at 95% eluent B, the column was re-equilibrated at 5% eluent B during 9 min. The column effluents were infused via a Turbo V™ ion source in a hybrid QqTOF mass spectrometer Sciex TripleTOF 6600 LC-MS System (AB Sciex, Darmstadt, Germany), operated in positive sequential window acquisition of all theoretical mass spectra (SWATH) mode and controlled by Analyst™ TF Software 1.8 software. The source was hold at 450 °C with nebulizer (GS1), drying (GS2) and curtain (CUR) gases set to 60, 70 and 55 psig, respectively, whereas the ion spray voltage was 5.5 kV in positive. The SWATH experiments were acquired with 1.11 s period time in the TOF-MS scan and product ion scan *m/z* range of 65 – 1250. The data were acquired at the pulser frequency of 19.1 Hz and the accumulation times of 100 and 20 ms for TOF-MS and product ion scans, respectively. The MS/MS data were acquired in 48 SWATH windows of 25 *m/z* each with collision potential (CE), collision energy spread (CES) and declustering potential (DP) set to 45, 35 and 35V in positive mode. The targeted MS/MS data were acquired in positive ion mode at CEs of 15, 20, 30, 40, 50 and 60 V with CES set to 0 V and DP set to 35 V (total cycle time 0.9 s, 16 scans per cycle, scan accumulation time 50 ms).

3.3.4 Metabolite profiles and MS data analysis

The acquired chromatograms and spectra were examined in PeakView TM software (version 2.2) to accesses data quality and to adjust the settings for further processing. Deconvolution of the mass spectra, peak peaking, retention time-based alignment, feature filtering and quantitation of individual signals in extracted ion chromatograms (XICs), i.e. integration of peak areas, were accomplished in MSDial software (version 4.12) after conversion of the raw data in ABF (analysis base file) format. The optimized peak detection parameters for processing in MSDial were set as follows: MS1 tolerance - 0.015 *m/z*, MS2 tolerance - 0.025 *m/z*, minimum peak width – 5 s, minimum peak height – 2000 counts, for alignment: retention time tolerance - 0.15 min, MS1 tolerance - 0.015 *m/z*.

Relative quantitation relied on integrated peak areas as intensity values of corresponding analytes. For this, the integrated peak areas of the metabolites annotated in each sample were organized as a digital matrix which was subjected to processing and statistical interpretation by means of the MetaboAnalyst 5.0 online platform (free available at www.metaboanalyst.ca). Prior to the statistical analysis, the data were filtered to remove the features which were detected in less than 20% of samples. Imputation of zero values relied on the MetImp algorithm (https://metabolomics.cc.hawaii.edu/software/MetImp/) and the random forest method for analytes detected at least in 80% of samples. Variables of the data sets were pareto-scaled and

median normalized before multivariate analysis. Principal component analysis (PCA) was used to address intra- and inter-group variability and to assess the underlying group separation in the data.

3.3.5 Metabolite annotation

Metabolites were annotated or identified and characteristics based on their corresponding accurate high-resolution *m/z*, chromatographic retention time and fragmentation patterns with those reported in the literature, databases such as Peakview, MetFrag, and reference standards, respectively. Briefly, a compound was deemed identified if the following criteria were met: the retention time (RT) was ± 0.1 min of reference standard and the mass error of MS1 was below or equal to 5 ppm. Then, the fragmentation patterns of MS/MS spectra were analyzed to identify the metabolites. Of course, this allows only a most likely on a annotation and not save identification when no reference compounds are available.

3.4 Conclusion

In this study, RP-UHPLC-QqTOF-MS and MS/MS were used to characterize the metabolic profiles of leafs, stems, fruits and roots from *P. sarmentosum.* As a result, altogether 154 secondary metabolites were annotated. The identified compounds were dominated by diverse alkaloids together with flavonoids and lignans. In addition, the relative abundances of these metabolites in various organs were assessed. Roots and fruits shared a large number of common phytochemicals, especially piperamides types A-E, as evidenced by TICs, PCA score and loadings plots, and hierarchical clustering analysis. On one hand, this finding indicates the similarity to other *Piper* fruits and the potential economic, medicinal, and nutritional value of *P. sarmentosum.* On the other hand, it may support the culinary application of roots by some communities in southern China. Stems generally contained the most significant amounts of aporphine alkaloids compared with other organs. In contrast, the leaves contained relatively high amounts of flavonoids. Moreover, several compounds were successfully identified, screened and quantified as biomarker metabolites for the discrimination of the *P. sarmentosum* organs. The results obtained in this study provide valuable insight into the distribution of bioactive compounds in different *P. sarmentosum* organs and can help to maximize the plant's economic value as herbal medicine or in food applications.

3.5   References

1.   Quijano-Abril, M. A.; Callejas-Posada, R.; Miranda-Esquivel, D. R., Areas of endemism and distribution patterns for Neotropical *Piper* species (Piperaceae). *J. Biogeogr.* **2006,** 33, 1266-1278.
2.   Asmarayani, R., Phylogenetic relationships in Malesian–Pacific *Piper* (Piperaceae) and their implications for systematics. *TAXON* **2018,** 693-724.
3.   Salehi, B.; Zakaria, Z. A.; Gyawali, R.; Ibrahim, S. A.; Rajkovic, J.; Shinwari, Z. K.; Khan, T.; Sharifi-Rad, J.; Ozleyen, A.; Turkdonmez, E.; Valussi, M.; Tumer, T. B.; Monzote Fidalgo, L.; Martorell, M.; Setzer, W. N., *Piper* species: A comprehensive review on their phytochemistry, biological activities and applications. *Molecules* **2019,** 24, 1364.
4.   Burkill, I. H.; Birtwistle, W.; Foxworthy, F. W.; Scrivenor, J. B.; Watson, J. G., *A dictionary of the economic products of the Malay Peninsula.* governments of Malaysia and Singapore by the Ministry of Agriculture and cooperatives: 1966.
5.   Zakaria, Z. A.; Patahuddin, H.; Mohamad, A. S.; Israf, D. A.; Sulaiman, M. R., In vivo anti-nociceptive and anti-inflammatory activities of the aqueous extract of the leaves of *Piper sarmentosum*. *J. Ethnopharmacol.* **2010,** 128, 42-8.
6.   Hussain, K.; Hashmi, F. K.; Latif, A.; Ismail, Z.; Sadikun, A., A review of the literature and latest advances in research of *Piper sarmentosum. Pharm. Biol.* **2012,** 50, 1045-52.
7.   Ridtitid, W.; Rattanaprom, W.; Thaina, P.; Chittrakarn, S.; Sunbhanich, M., Neuromuscular blocking activity of methanolic extract of *Piper sarmentosum* leaves in the rat phrenic nerve-hemidiaphragm preparation. *J. Ethnopharmacol.* **1998,** 61, 135-42.
8.   Chanwitheesuk, A.; Teerawutgulrag, A.; Rakariyatham, N., Screening of antioxidant activity and antioxidant compounds of some edible plants of Thailand. *Food Chem* **2005,** 92, 491-497.
9.   Chaveerach, A.; Mokkamul, P.; Sudmoon, R.; Tanee, T., Ethnobotany of the Genus *Piper* (Piperaceae) in Thailand. *Ethnobot. Res. Appl.* **2006,** 4, 223-231.
10.   Sun, X.; Chen, W.; Dai, W.; Xin, H.; Rahmand, K.; Wang, Y.; Zhang, J.; Zhang, S.; Xu, L.; Han, T., *Piper sarmentosum* Roxb.: A review on its botany, traditional uses, phytochemistry, and pharmacological activities. *J. Ethnopharmacol.* **2020,** 263, 112897.
11.   Li, C. Y.; Tsai, W. J.; Damu, A. G.; Lee, E. J.; Wu, T. S.; Dung, N. X.; Thang, T. D.; Thanh, L., Isolation and identification of antiplatelet aggregatory principles from the Leaves of *Piper lolot. J. Agric. Food Chem.* **2007,** 55, 9436-9442.
12.   Md. Salleh, M. F. R. R.; Aminuddin, A.; Hamid, A. A.; Salamt, N.; Japar Sidik, F. Z.; Ugusman, A., *Piper sarmentosum* Roxb. attenuates vascular endothelial dysfunction in nicotine-induced Rats. *Front. Pharmacol.* **2021,** 12, 1495.
13.   Chan, E. W. L.; Yeo, E. T. Y.; Wong, K. W. L.; See, M. L.; Wong, K. Y.; Yap, J. K. Y.; Gan, S. Y., *Piper sarmentosum* Roxb. attenuates beta amyloid (A β)-induced neurotoxicity via the inhibition of amyloidogenesis and tau hyperphosphorylation in SH-SY5Y cells. *Curr. Alzheimer Res.* **2021,** 18, 80-87.
14.   Kumar, S. R.; Ramli, E. S. M.; Nasir, N. A. A.; Ismail, N. M.; Fahami, N. A. M., Methanolic extract of *Piper sarmentosum* attenuates obesity and hyperlipidemia in fructose-induced metabolic syndrome rats. *Molecules* **2021,** 26.
15.   Wolfender, J.-L.; Marti, G.; Thomas, A.; Bertrand, S., Current approaches and challenges for the metabolite profiling of complex natural extracts. *J. Chromatogr. A* **2015,** 1382, 136-164.
16.   Luca, S. V.; Minceva, M.; Gertsch, J.; Skalicka-Woźniak, K., LC-HRMS/MS-based phytochemical profiling of *Piper* spices: Global association of piperamides with endocannabinoid system modulation. *Food Res. Int.* **2021,** 141, 110123.
17.   Afzan, A.; Kasim, N.; Ismail, N. H.; Azmi, N.; Ali, A. M.; Mat, N.; Wolfender, J. L., Differentiation of *Ficus deltoidea* varieties and chemical marker determination by UHPLC-TOFMS metabolomics for establishing quality control criteria of this popular Malaysian medicinal herb. *Metabolomics* **2019,** 15, 35.
18.   Farag, M. A.; Gad, H. A.; Heiss, A. G.; Wessjohann, L. A., Metabolomics driven analysis of six *Nigella* species seeds *via* UPLC-qTOF-MS and GC-MS coupled to chemometrics. *Food Chem.* **2014,** 151, 333-342.
19.   Pei, H.; Su, W.; Gui, M.; Dou, M.; Zhang, Y.; Wang, C.; Lu, D., Comparative analysis of chemical constituents in different parts of lotus by UPLC and QToF-MS. *Molecules* **2021,** 26.

20. Oh, J. H.; Ha, I. J.; Lee, M. Y.; Kim, E. O.; Park, D.; Lee, J. H.; Lee, S. G.; Kim, D. W.; Lee, T. H.; Lee, E. J.; Kim, C. K., Identification and metabolite profiling of alkaloids in aerial parts of *Papaver rhoeas* by liquid chromatography coupled with quadrupole time-of-flight tandem mass spectrometry. *J. Sep. Sci.* **2018,** 41, 2517-2527.

21. El Senousy, A. S.; Farag, M. A.; Al-Mandy, D. A.; Wessjohann, L. A., Developmental changes in leaf phenolics composition from three artichoke cvs. (*Cynara scolymus*) as determined *via* UHPLC-MS and chemometrics. *Phytochemistry* **2014,** 108, 67-76.

22. Schutz, D.; Achten, E.; Creydt, M.; Riedl, J.; Fischer, M., Non-Targeted LC-MS metabolomics approach towards an authentication of the geographical origin of grain maize (*Zea mays* L.) samples. *Foods* **2021,** 10.

23. Farag, M. A.; El-Kersh, D. M.; Ehrlich, A.; Choucry, M. A.; El-Seedi, H.; Frolov, A.; Wessjohann, L. A., Variation in *Ceratonia siliqua* pod metabolome in context of its different geographical origin, ripening stage and roasting process. *Food Chem.* **2019,** 283, 675-687.

24. Hegazi, N. M.; Khattab, A. R.; Frolov, A.; Wessjohann, L. A.; Farag, M. A., Authentication of saffron spice accessions from its common substitutes *via* a multiplex approach of UV/VIS fingerprints and UPLC/MS using molecular networking and chemometrics. *Food Chem.* **2022,** 367.

25. Lee, J. W.; Ji, S. H.; Choi, B. R.; Choi, D. J.; Lee, Y. G.; Kim, H. G.; Kim, G. S.; Kim, K.; Lee, Y. H.; Baek, N. I.; Lee, D. Y., UPLC-QTOF/MS-based metabolomics applied for the quality evaluation of four processed *Panax ginseng* products. *Molecules* **2018,** 23.

26. Li, K.; Fan, Y.; Wang, H.; Fu, Q.; Jin, Y.; Liang, X., Qualitative and quantitative analysis of an alkaloid fraction from *Piper longum* L. using ultra-high performance liquid chromatography-diode array detector-electrospray ionization mass spectrometry. *J. Pharm. Biomed. Anal.* **2015,** 109, 28-35.

27. Farag, M. A.; Porzel, A.; Mahrous, E. A.; El-Massry, M. M.; Wessjohann, L. A., Integrated comparative metabolite profiling via MS and NMR techniques for Senna drug quality control analysis. *Anal. Bioanal. Chem.* **2015,** 407, 1937-1949.

28. El-Hawary, E. A.; Zayed, A.; Laub, A.; Modolo, L. V.; Wessjohann, L.; Farag, M. A., How does LC/MS compare to UV in coffee authentication and determination of antioxidant effects? Brazilian and Middle Eastern coffee as case studies. *Antioxidants* **2022,** 11.

29. Alseekh, S.; Aharoni, A.; Brotman, Y.; Contrepois, K.; D'Auria, J.; Ewald, J.; J, C. E.; Fraser, P. D.; Giavalisco, P.; Hall, R. D.; Heinemann, M.; Link, H.; Luo, J.; Neumann, S.; Nielsen, J.; Perez de Souza, L.; Saito, K.; Sauer, U.; Schroeder, F. C.; Schuster, S.; Siuzdak, G.; Skirycz, A.; Sumner, L. W.; Snyder, M. P.; Tang, H.; Tohge, T.; Wang, Y.; Wen, W.; Wu, S.; Xu, G.; Zamboni, N.; Fernie, A. R., Mass spectrometry-based metabolomics: a guide for annotation, quantification and best reporting practices. *Nat. Methods* **2021,** 18, 747-756.

30. Li, Z.; Zhang, X.; Liao, J.; Fan, X.; Cheng, Y., An ultra-robust fingerprinting method for quality assessment of traditional Chinese medicine using multiple reaction monitoring mass spectrometry. *J. Pharm. Anal.* **2021,** 11, 88-95.

31. Wu, Z.; Wang, X.; Chen, M.; Hu, H.; Cao, J.; Chai, T.; Wang, H., A study on tissue-tpecific metabolite variations in *Polygonum cuspidatum* by high-resolution mass spectrometry-based metabolic profiling. *Molecules* **2019,** 24.

32. Szabo, D.; Schlosser, G.; Vekey, K.; Drahos, L.; Revesz, A., Collision energies on QTof and Orbitrap instruments: How to make proteomics measurements comparable? *J. Mass Spectrom.* **2021,** 56, e4693.

33. Li, C. R.; Hou, X. H.; Xu, Y. Y.; Gao, W.; Li, P.; Yang, H., Manual annotation combined with untargeted metabolomics for chemical characterization and discrimination of two major crataegus species based on liquid chromatography quadrupole time-of-flight mass spectrometry. *J. Chromatogr. A* **2020,** 1612, 460628.

34. Revesz, A.; Rokob, T. A.; Jeanne Dit Fouque, D.; Turiak, L.; Memboeuf, A.; Vekey, K.; Drahos, L., Selection of collision energies in proteomics mass spectrometry experiments for best peptide identification: Study of mascot score energy dependence reveals double optimum. *J. Proteome Res.* **2018,** 17, 1898-1906.

35. Pei, H.; Xue, L.; Tang, M.; Tang, H.; Kuang, S.; Wang, L.; Ma, X.; Cai, X.; Li, Y.; Zhao, M.; Peng, A.; Ye, H.; Chen, L., Alkaloids from black pepper (*Piper nigrum* L.) exhibit anti-inflammatory activity in murine macrophages by inhibiting activation of NF-κB pathway. *J. Agric. Food Chem.* **2020,** 68, 2406-2417.

36.   Islam, M. T.; Hasan, J.; Snigdha, H.; Ali, E. S.; Sharifi-Rad, J.; Martorell, M.; Mubarak, M. S., Chemical profile, traditional uses, and biological activities of *Piper chaba* Hunter: A review. *J. Ethnopharmacol.* **2020,** 257, 112853.

37.   Mayr, S.; Bec, K. B.; Grabska, J.; Schneckenreiter, E.; Huck, C. W., Near-infrared spectroscopy in quality control of *Piper nigrum*: A comparison of performance of benchtop and handheld spectrometers. *Talanta* **2021,** 223, 121809.

38.   Sun, C.; Pei, S.; Pan, Y.; Shen, Z., Rapid structural determination of amides in *Piper longum* by high-performance liquid chromatography combined with ion trap mass spectrometry. *Rapid Commun. Mass Spectrom.* **2007,** 21, 1497-503.

39.   Rios, M. Y.; Gomez-Calvario, V., H-1 and C-13 NMR data, occurrence, biosynthesis, and biological activity of Piper amides. *Magn. Reson. Chem.* **2019,** 57, 993-993.

40.   Luca, S. V.; Gaweł-Bęben, K.; Strzępek-Gomółka, M.; Czech, K.; Trifan, A.; Zengin, G.; Korona-Glowniak, I.; Minceva, M.; Gertsch, J.; Skalicka-Woźniak, K., Insights into the Phytochemical and Multifunctional Biological Profile of Spices from the Genus *Piper*. *Antioxidants* **2021,** 10, 1642.

41.   Yu, L.; Hu, X. L.; Xu, R. R.; Ba, Y. Y.; Chen, X. Q.; Wang, X.; Cao, B.; Wu, X., Amide alkaloids characterization and neuroprotective properties of *Piper nigrum* L.: A comparative study with fruits, pericarp, stalks and leaves. *Food Chem.* **2022,** 368.

42.   Wolff, T.; Santos, P. F. P.; Valente, L. M. M.; Magalhaes, A.; Tinoco, L. W.; Pereira, R. C. A.; Guimaraes, E. F., Piperamides from *Piper ottonoides* by NMR and GC-MS based mixture analysis. *J. Brazilian Chem. Soc.* **2015,** 26, 2321-2330.

43.   Stévigny, C.; Jiwan, J.-L. H.; Rozenberg, R.; de Hoffmann, E.; Quetin-Leclercq, J., Key fragmentation patterns of aporphine alkaloids by electrospray ionization with multistage mass spectrometry. *Rapid Commun. Mass Spectrom.* **2004,** 18, 523-528.

44.   Carnevale Neto, F.; Andréo, M. A.; Raftery, D.; Lopes, J. L. C.; Lopes, N. P.; Castro-Gamboa, I.; Lameiro de Noronha Sales Maia, B. H.; Costa, E. V.; Vessecchi, R., Characterization of aporphine alkaloids by electrospray ionization tandem mass spectrometry and density functional theory calculations. *Rapid Commun. Mass Spectrom.* **2020,** 34, e8533.

45.   Conceição, R. S.; Reis, I. M. A.; Cerqueira, A. P. M.; Perez, C. J.; Junior, M. C. d. S.; Branco, A.; Ifa, D. R.; Botura, M. B., Rapid structural characterisation of benzylisoquinoline and aporphine alkaloids from *Ocotea spixiana* acaricide extract by HPTLC-DESI-MSn. *Phytochem. Anal.* **2020,** 31, 711-721.

46.   Sim, H. J.; Yoon, S. H.; Kim, M. S.; Kim, B.; Park, H. M.; Hong, J., Identification of alkaloid constituents from *Fangchi* species using pH control liquid-liquid extraction and liquid chromatography coupled to quadrupole time-of-flight mass spectrometry. *Rapid Commun. Mass Spectrom.* **2015,** 29, 837-854.

47.   Schmidt, J.; Raith, K.; Boettcher, C.; Zenk, M. H., Analysis of benzylisoquinoline-type alkaloids by electrospray tandem mass spectrometry and atmospheric pressure photoionization. *Eur. J. Mass Spectrom.* **2005,** 11, (3), 325-33.

48.   Xiao, X.; Ren, W.; Zhang, N.; Bing, T.; Liu, X. J.; Zhao, Z. W.; Shangguan, D. H., Comparative study of the chemical constituents and bioactivities of the extracts from fruits, leaves and root barks of *Lycium barbarum*. *Molecules* **2019,** 24.

49.   Kumar, S.; Pandey, A. K., Chemistry and biological activities of flavonoids: an overview. *Sci. World J.* **2013,** 2013, 162750.

50.   Hu, L.; Liang, Z.; Wang, Y.; Wei, G.; Huang, Y. C., Identification of *C*-glycosyl flavones and *O*-glycosyl flavones in five *Dendrobium* species by high-performance liquid chromatography coupled with electrospray ionization multi-stage tandem MS. *Rapid Commun. Mass Spectrom.* **2021**, e9158.

51.   Rodríguez-Rivera, M. P.; Lugo-Cervantes, E.; Winterhalter, P.; Jerz, G., Metabolite profiling of polyphenols in peels of Citrus limetta Risso by combination of preparative high-speed countercurrent chromatography and LC–ESI–MS/MS. *Food Chem.* **2014,** 158, 139-152.

52.   Wang, Y.; Liao, X.; Zhou, C.; Hu, L.; Wei, G.; Huang, Y.; Lei, Z.; Ren, Z.; Liu, Z.; Liu, Z., Identification of C-glycosyl flavones and quality assessment in *Dendrobium nobile*. *Rapid Commun. Mass Spectrom.* **2021,** 35, e9012.

53.   Pascale, R.; Acquavia, M. A.; Cataldi, T. R. I.; Onzo, A.; Coviello, D.; Bufo, S. A.; Scrano, L.; Ciriello, R.; Guerrieri, A.; Bianco, G., Profiling of quercetin glycosides and acyl glycosides in sun-dried peperoni di Senise peppers (*Capsicum annuum* L.) by a combination of LC-ESI(-)-

MS/MS and polarity prediction in reversed-phase separations. *Anal. Bioanal. Chem.* **2020,** 412, 3005-3015.

54.   Parejo, I.; Jáuregui, O.; Viladomat, F.; Bastida, J.; Codina, C., Characterization of acylated flavonoid-O-glycosides and methoxylated flavonoids from *Tagetes maxima* by liquid chromatography coupled to electrospray ionization tandem mass spectrometry. *Rapid Commun. Mass Spectrom.* **2004,** 18, 2801-10.

55.   Han, Y. X.; Wang, P. F.; Zhao, M.; Chen, L. M.; Wang, Z. M.; Liu, X. Q.; Gao, H. M.; Gong, M. X.; Li, H.; Zhu, J. Z.; Liu, C. G., Chemical profiling of Xueshuan Xinmaining tablet by HPLC and UPLC-ESI-Q-TOF/MS. *Evid. Based Complement. Alternat. Med.* **2018,** 2018, 2781597.

56.   Wu, C.; Liu, H.; Rong, X.; Liu, J.; Ding, W.; Cheng, X.; Xing, J.; Wang, C., Phytochemical composition profile and space–time accumulation of secondary metabolites for *Dracocephalum moldavica* Linn. via UPLC–Q/TOF–MS and HPLC–DAD method. *Biomed. Chromatogr.* **2020,** 34, e4865.

57.   Trapp, S. C.; Croteau, R. B., Genomic organization of plant terpene synthases and molecular evolutionary implications. *Genetics* **2001,** 158, 811-832.

58.   Selmar, D.; Kleinwachter, M., Influencing the product quality by deliberately applying drought stress during the cultivation of medicinal plants. *Ind. Crops Prod.* **2013,** 42, 558-566.

59.   Yang, L. L.; Yang, L.; Yang, X.; Zhang, T.; Lan, Y. M.; Zhao, Y.; Han, M.; Yang, L. M., Drought stress induces biosynthesis of flavonoids in leaves and saikosaponins in roots of *Bupleurum chinense* DC. *Phytochemistry* **2020,** 177.

60.   Zheng, Y.-k.; Su, B.-j.; Wang, Y.-q.; Wang, H.-s.; Liao, H.-b.; Liang, D., New Tyramine- and Aporphine-Type Alkamides with NO Release Inhibitory Activities from *Piper puberulum. J. Nat.Prod.* **2021,** 84, 1316-1325.

61.   Wu, Y.; Zheng, C. J.; Deng, X. H.; Qin, L. P., Two New Bis-alkaloids from the Aerial Part of *Piper flaviflorum. Helv. Chim. Acta* **2013,** 96, 951-955.

62.   Leonard, W.; Zhang, P. Z.; Ying, D. Y.; Fang, Z. X., Lignanamides: sources, biosynthesis and potential health benefits - a minireview. *Crit. Rev. Food Sci. Nutr.* **2021,** 61, 1404-1414.

63.   Flores-Sanchez, I. J.; Verpoorte, R., Secondary metabolism in cannabis. *Phytochem. Rev.* **2008,** 7, 615-639.

64.   Yoshikawa, M.; Yamaguchi, S.; Murakami, T.; Matsuda, H.; Yamahara, J.; Murakami, N., Absolute stereostructures of trifoliones A, B, C, and D, new biologically active diterpenes from the tuber of *Sagittaria trifolia* L. *Chem. Pharm. Bull.* **1993,** 41, 1677-1679.

65.   Facchini, P. J.; Hagel, J.; Zulak, K. G., Hydroxycinnamic acid amide metabolism: physiology and biochemistry. *Can. J. Bot.* **2002,** 80, 577-589.

66.   Yi, L.; Liang, Z.-T.; Peng, Y.; Yao, X.; Chen, H.-B.; Zhao, Z.-Z., Tissue-specific metabolite profiling of alkaloids in Sinomenii Caulis using laser microdissection and liquid chromatography–quadrupole/time of flight-mass spectrometry. *J. Chromatogr. A* **2012,** 1248, 93-103.

67.   Gorpenchenko, T. Y.; Grigorchuk, V. P.; Bulgakov, D. V.; Tchernoded, G. K.; Bulgakov, V. P., Tempo-spatial pattern of stepharine accumulation in *Stephania glabra* morphogenic Tissues. *Int. J. Mol. Sci.* **2019,** 20, 808.

68.   Samanani, N.; Alcantara, J.; Bourgault, R.; Zulak, K. G.; Facchini, P. J., The role of phloem sieve elements and laticifers in the biosynthesis and accumulation of alkaloids in opium poppy. *Plant J.* **2006,** 47, 547-563.

69.   Morris, J. S.; Facchini, P. J., Isolation and characterization of reticuline N-methyltransferase involved in biosynthesis of the aporphine alkaloid magnoflorine in opium poppy. *J. Biol. Chem.* **2016,** 291, 23416-23427.

70.   Marques, J. V.; Dalisay, D. S.; Yang, H.; Lee, C.; Davin, L. B.; Lewis, N. G., A multi-omics strategy resolves the elusive nature of alkaloids in *Podophyllum* species. *Mol. Biosyst.* **2014,** 10, 2838-2849.

71.   Priestap, H. A.; Velandia, A. E.; Johnson, J. V.; Barbieri, M. A., Secondary metabolite uptake by the *Aristolochia*-feeding papilionoid butterfly *Battus polydamas*. *Biochem. Syst. Ecol.* **2012,** 40, 126-137.

72.   Pearce, G.; Marchand, P. A.; Griswold, J.; Lewis, N. G.; Ryan, C. A., Accumulation of feruloyltyramine and p-coumaroyltyramine in tomato leaves in response to wounding. *Phytochemistry* **1998,** 47, 659-664.

73. Newman, M. A.; von Roepenack-Lahaye, E.; Parr, A.; Daniels, M. J.; Dow, J. M., Induction of hydroxycinnamoyl-tyramine conjugates in pepper by *Xanthomonas campestris*, a plant defense response activated by hrp gene-dependent and hrp gene-independent mechanisms. *Mol. Plant-Microbe Interact.* **2001,** 14, 785-92.

74. Zacares, L.; Lopez-Gresa, M. P.; Fayos, J.; Primo, J.; Belles, J. M.; Conejero, V., Induction of *p*-coumaroyldopamine and feruloyldopamine, two novel metabolites, in tomato by the bacterial pathogen *Pseudomonas syringae*. *Mol. Plant-Microbe Interact.* **2007,** 20, 1439-48.

75. Schnabel, A.; Athmer, B.; Manke, K.; Schumacher, F.; Cotinguiba, F.; Vogt, T., Identification and characterization of piperine synthase from black pepper, *Piper nigrum* L. *Commun. Biol.* **2021,** 4, 445.

76. Whitehead, S. R.; Bowers, M. D., Chemical ecology of fruit defence: synergistic and antagonistic interactions among amides from *Piper*. *Funct. Ecol.* **2014,** 28, 1094-1106.

77. Jeon, H.-J.; Kim, K.; Kim, Y.-D.; Lee, S.-E., Naturally occurring *Piper* plant amides potential in agricultural and pharmaceutical industries: perspectives of piperine and piperlongumine. *Appl. Biol. Chem.* **2019,** 62, 63.

78. Haq, I.-U.; Imran, M.; Nadeem, M.; Tufail, T.; Gondal, T. A.; Mubarak, M. S., Piperine: A review of its biological effects. *Phytother. Res.* **2021,** 35, 680-700.

79. Quijia, C. R.; Chorilli, M., Characteristics, biological properties and analytical methods of piperine: A Review. *Crit. Rev. Anal. Chem.* **2020,** 50, 62-77.

80. Takahashi, M.; Hirose, N.; Ohno, S.; Arakaki, M.; Wada, K., Flavor characteristics and antioxidant capacities of hihatsumodoki (*Piper retrofractum* Vahl) fresh fruit at three edible maturity stages. *J. Food Sci. Technol.* **2018,** 55, 1295-1305.

81. Hjelmeland, A. K.; Ebeler, S. E., Glycosidically bound volatile aroma compounds in grapes and wine: A review. *Am. J. Enol. Vitic.* **2015,** 66, 1-11.

82. Vogt, T.; Jones, P., Glycosyltransferases in plant natural product synthesis: characterization of a supergene family. *Trends Plant Sci.* **2000,** 5, 380-386.

83. Bowles, D.; Lim, E. K.; Poppenberger, B.; Vaistij, F. E., Glycosyltransferases of lipophilic small molecules. *Annu. Rev. Plant Biol.* **2006,** 57, 567-597.

84. Jones, P.; Vogt, T., Glycosyltransferases in secondary plant metabolism: tranquilizers and stimulant controllers. *Planta* **2001,** 213, 164-174.

85. Khew, C. Y.; Harikrishna, J. A.; Wee, W. Y.; Lau, E. T.; Hwang, S. S., Transcriptional sequencing and gene expression analysis of various genes in fruit development of three different black pepper (*Piper nigrum* L.) varieties. *Int. J.f Genomics* **2020,** 2020, 1540915.

86. Hostetler, G. L.; Ralston, R. A.; Schwartz, S. J., Flavones: Food sources, bioavailability, metabolism, and bioactivity. *Adv. Nutr.* **2017,** 8, 423-435.

87. Falcone Ferreyra, M. L.; Rius, S.; Casati, P., Flavonoids: Biosynthesis, biological functions, and biotechnological applications. *Front. Plant Sci.* **2012,** 3.

88. Ferreyra, M. L. F.; Serra, P.; Casati, P., Recent advances on the roles of flavonoids as plant protective molecules after UV and high light exposure. *Physiologia Plantarum* **2021,** 173, 736-749.

89. Wessjohann, L. A.; Keim, J.; Weigel, B.; Dippe, M., Alkylating enzymes. *Curr. Opin. Chem. Biol.* **2013,** 17, 229-235.

90. Wessjohann, L.; Bauer, A.-K.; Dippe, M.; Ley, J.; Geißler, T., Biocatalytic synthesis of natural products by *O-* methyltransferases. In *Applied Biocatalysis: From Fundamental Science to Industrial Applications*, 2016; pp 121-146.

91. Böttner, L.; Grabe, V.; Gablenz, S.; Böhme, N.; Appenroth, K. J.; Gershenzon, J.; Huber, M., Differential localization of flavonoid glucosides in an aquatic plant implicates different functions under abiotic stress. *Plant Cell Environ.* **2021,** 44, 900-914.

92. Printz, B.; Lutts, S.; Hausman, J.-F.; Sergeant, K., Copper trafficking in plants and its implication on cell wall dynamics. *Front. Plant Sci.* **2016,** 7.

93. Rodriguez-Garcia, C.; Sanchez-Quesada, C.; Toledo, E.; Delgado-Rodriguez, M.; Gaforio, J. J., Naturally lignan-rich foods: A dietary tool for health promotion? *Molecules* **2019,** 24.

94. Miean, K. H.; Mohamed, S., Flavonoid (myricetin, quercetin, kaempferol, luteolin, and apigenin) content of edible tropical plants. *J. Agric. Food Chem.* **2001,** 49, 3106-12.

95. Ugusman, A.; Zakaria, Z.; Hui, C. K.; Nordin, N. A.; Mahdy, Z. A., Flavonoids of *Piper sarmentosum* and its cytoprotective effects against oxidative stress. *EXCLI J.* **2012,** 11, 705-714.

96. Lee, J. H.; Cho, S.; Paik, H. D.; Choi, C. W.; Nam, K. T.; Hwang, S. G.; Kim, S. K., Investigation on antibacterial and antioxidant activities, phenolic and flavonoid contents of some Thai edible plants as an alternative for antibiotics. *Asian-Australas. J. Anim. Sci.* **2014,** 27, 1461-1468.
97. Baba, M. S.; Hassan, Z. A. A., *Piper Sarmentosum* leaf as a promising non-toxic antiparasitic agent against trypanosoma evansi-induced mice. *Malays. J. Microsc.* **2019,** 15, 46-60.
98. Hematpoor, A.; Liew, S. Y.; Chong, W. L.; Azirun, M. S.; Lee, V. S.; Awang, K., Inhibition and larvicidal activity of phenylpropanoids from *Piper sarmentosum* on acetylcholinesterase against mosquito vectors andt Their binding mode of interaction. *PLoS One* **2016,** 11, e0155265.
99. Hematpoor, A.; Liew, S. Y.; Azirun, M. S.; Awang, K., Insecticidal activity and the mechanism of action of three phenylpropanoids isolated from the roots of *Piper sarmentosum* Roxb. *Sci. Rep.* **2017,** 7, 12576.

Chapter 4

-

Bioactive phenolic compounds from *Peperomia obtusifolia*

Abstract*

Peperomia obtusifolia (L.) A.Dietr., native to Middle America, is an ornamental plant also traditionally used due to its mild antimicrobial properties. Chemical investigation on the leaves of *P. obtusifolia* resulted in the isolation of two previously not described compounds, named peperomic ester (**4.1**) and peperoside (**4.2**), together with five known compounds, viz. *N*-[2-(3,4-dihydroxyphenyl)ethyl]-3,4-dihydroxybenzamide (**4.3**), becatamide (**4.4**), peperobtusin A (**4.5**), peperomin B (**4.6**), and arabinothalictoside (**4.7**). The structures of these compounds were elucidated by 1D and 2D NMR techniques and HREIMS analyses. Compounds **4.1-4.7** were evaluated for their anthelmintic (against *Caenorhabditis elegans*), antifungal (against *Botrytis cinerea, Septoria tritici and Phytophthora infestans*), antibacterial (against *Bacillus subtilis* and *Aliivibrio fischeri*), and antiproliferative (against PC-3 and HT-29 human cancer cell lines) activities. The known peperobtusin A (**4.5**) was the most active compound against the PC-3 cancer cell line with IC_{50} values of 25.6 µM and 36.0 µM in MTT and CV assays, respectively. This compound also induced 90% inhibition of bacterial growth of the Gram-positive *B. subtilis* by at a concentration of 100 µM. In addition, compound **4.3** showed anti-oomycotic activity against *P. infestans* with an inhibition value of 56% by using a concentration of 125 µM. However, no anthelmintic activity was observed.

Keywords: Piperaceae, *Peperomia obtusifolia*, isolation, cytotoxicity, anticancer, antibacterial

4.1 Introduction

Peperomia is one of the two major genera of the Piperaceae family with approximately 1700 species common in almost all tropical areas [1]. Plants of the genus *Peperomia* possess numerous uses as traditional medicine to treat asthma, gastric ulcers, bacterial infection, pain and inflammation [2]. *Peperomia* species produce several classes of secondary metabolites such as flavonoids, secolignans, prenylated phenolic substances, chromenes, polyketides [3], lignans, tetrahydrofurans, terpenoids, meroterpenoids, and amides [1,4,5]. Some compounds from *P. pellucida*, *P. doclouxii*, *P. dindygulensis* and *P. blanda* were reported to exhibit cytotoxic effects [2,6-8].

Peperomia obtusifolia (L.) A.Dietr. is widely distributed from Mexico to the northern part of South America. It prevalently is known as *baby rubber* or *paragua* plant. In spite of its dominating decorative use, some communities in Central America use this plant to treat insect and snake bites and also as a skin cleanser [9]. Previous studies on *P. obtusifolia* resulted in the isolation of chromanes, flavonoids, lignans and other secondary metabolites [10-14]. Several biological activities were described for compounds isolated from this species such as trypanocidal [11], anti-inflammatory [15], and antibacterial activities [14]. In the present study, we report the isolation, structure elucidation and biological effects of two previously undescribed compounds (**4.1** and 4.**2**) along with five known compounds (**4.3-4.7**) from the methanolic leaf extract of *P. obtusifolia*.

4.2 Results and discussion

The dried leaves of *P. obtusifolia* were extracted with 80% aqueous methanol. The crude extract was suspended in water and successively fractioned by liquid-liquid partition between water and *n*-hexane, and water and ethyl acetate. The constituents were purified by preparative HPLC and repeated column chromatography on silica gel, Sephadex LH20 and Diaion HP20; which yielded two so far undescribed compounds (**4.1** and **4.2**), as well as two amide derivatives (**4.3** and **4.4**), a chromane (**4.5**), a secolignan (**4.6**), and an unusual phenolic nitroalkyl diglycoside (**4.7**) (Figure 4.1). The chemical structures of **4.1** and **4.2** were elucidated by detailed spectroscopic techniques.
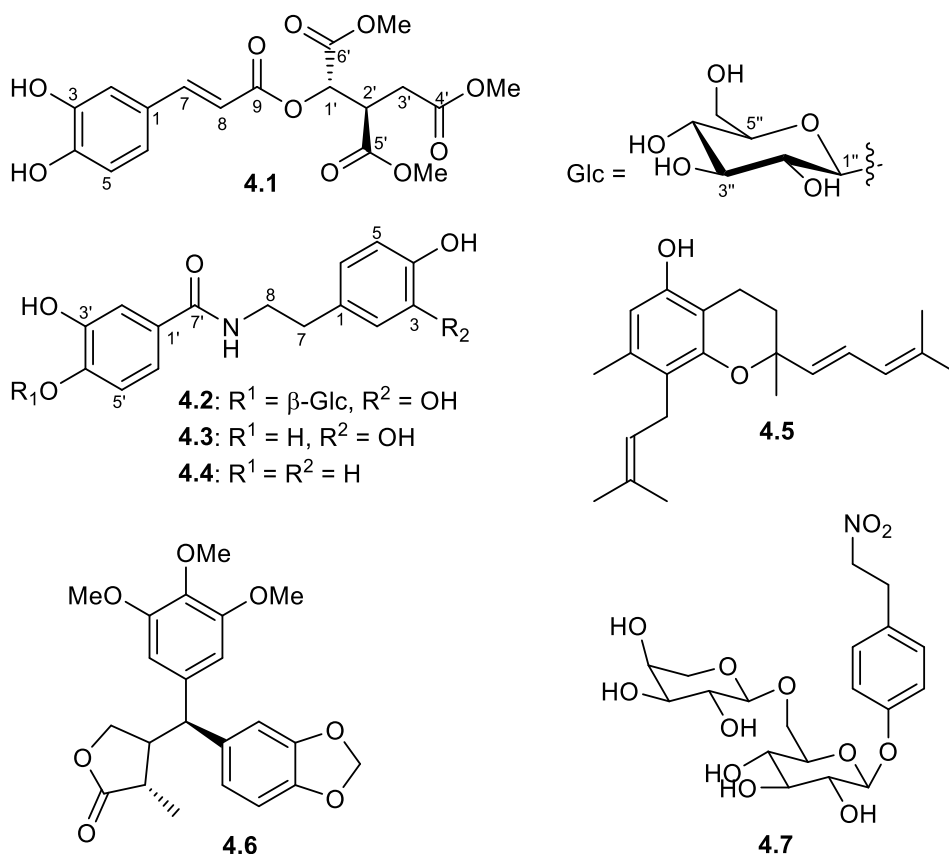
Figure 4.1: Chemical structures of compounds **4.1**-**4.7**.

Compound **4.1** was obtained as a brownish liquid from the aqueous fraction. The HR-ESI-MS measurements of the deprotonated molecular ion at *m/z* 395.0975 [M-H]$^-$ indicated the molecular formula $C_{18}H_{20}O_{10}$. The IR spectrum revealed the presence of hydroxyl (3402 cm^{-1}) and carbonyl groups (1715 cm^{-1}). Inspection of the ^{1}H NMR data (Table 4.2) exhibited characteristic signals of an ABX aromatic system at δ 7.06 (1H, d, *J* = 2.1 Hz, H-2), 6.79 (1H, d, *J* = 8.2 Hz, H-5), and 6.97 (1H, d, *J* = 8.2, 2.1 Hz, H-6) and of one *E*-configured double bond [7.59 (1H, d, *J* = 15.8 Hz, H-7), 6.29 (1H, d, *J* = 15.8 Hz, H-8)]. In addition, ^{1}H NMR data also showed the presence of two saturated methine groups [δ 5.46 (1H, d, *J* = 3.9 Hz, H-1′), 3.62 (1H, ddd, *J* = 9.0 , 5.5, 3.9 Hz, H-2′) and one methylene group [δ 2.85 (1H, dd, *J* = 17.2, 9.0 Hz, H-3′a), 2.66 (1H, d, *J* = 17.2 , 5.5 Hz, H-3′b)] along with three methoxy groups at δ 3.68, 3.73, and 3.77. The ^{13}C data (Table 4.2) exhibited one sp^2 quaternary carbon [δ$_C$ 127.4 (C-1)], two oxygenated sp^2 tertiary carbons [δ$_C$ 146.8 (C-3), 150.0 (C-4)], and four carbonyl groups [δ$_C$ 167.5 (C-9), 173.2 (C-4′), 170.2 (C-5′), 172.1 (C-6′)]. The scaffold of compound 4.**1** was established by a HMBC experiment showing long-range correlations from H-7 to C-1, C-2, C-6, C-8, and C-9, indicating that the aromatic ring and the carbonyl group C-9 were linked to C-7 in the form of a caffeic acid moiety. In addition, COSY correlations of H-1′/H-2′, H-2′/H-1′/H-3′a/H-3′b, H-3′a/H-2′ and H-3b/H-2′ together with HMBC correlations of the three methoxy groups to their respective carbonyls (C-4′, C-5′, and C-6′) and HMBC correlation of H-1′ and

89

C-2′, C-3′, C-5′, C-6′; and of H-2′ and C-1′, C-3′, C-4′, C-5′, and C-6′ suggested the presence of an isocitrate core. The C-1′ hydroxyl of the isocitrate unit is attached to the caffeic acid moiety at C-9 indicated by the long-range correlation from H-1′ (δH 5.46) to C-9 (δC 167.5) (Figure 4.2). The methylated isocitrate moiety of **4.1** is similar to those found in cryptoporic acids isolated from *Cryptoporus sinensis* [16] and *Cryptoporus volvatus* [17,18], which are also conjugates of isocitrate. Since compound **4.1** was also detected in an ethanolic crude extract (Figure S9), the methylation is not a processing artefact. The absolute configuration C-1′ and C-2′ of the isocitrate group was suggested to be (1′*S*,2′*R*) by comparison of its optical rotation sign (negative optical rotation value) with published compounds having (1′*R*,2′*S*) absolute configuration and opposite-in-sign specific rotation (positive optical rotation value) [16,19]. Thus, the methylated isocitrate moiety is in accordance with a L-threo-isocitric acid core ((1*S*,2*R*)-1-hydroxypropane-1,2,3-tricarboxylic acid). Based on the above-mentioned evidence, the structure of **4.1** was elucidated as trimethyl (1*S*,2*R*)-1-(((E)-3-(3,4-dihydroxyphenyl)acryloyl)oxy)propane-1,2,3-tricarboxylate, given the trivial name peperomic ester.

Table 4.2. ^{1}H- and ^{13}C-NMR data of **4.1** (in CD_3OD; δ in ppm, *J* in Hz).

Pos.	δ_H[a], Mult. *J* (Hz)	δ_C[b]	HMBC
1	-	127.4	
2	7.06 d 2.1	115.2	
3	-	146.8	
4	-	150.0	
5	6.79 d 8.2	116.5	
6	6.97 dd 8.2, 2.1	123.3	
7	7.59 d 15.8	148.6	C1, C2, C6, C8, C9
8	6.29 d 15.8	113.4	C1, C7, C9
9	-	167.5	
1′	5.46 d 3.9	72.6	C2′, C3′, C5′, C6′, C9′
2′	3.62 ddd 9.0, 5.5, 3.9	44.2	C1′, C3′, C4′, C5′, C6′
3′a	2.85 d 17.2, 9.0	32.8	C2′, C1′, C4′, C6′
3′b	2.66 d 17.2, 5.5	32.8	C2′, C1′, C4′, C6
4′	-	173.2	
5′	-	170.2	
6′	-	172.1	
OMe	3.73	52.9	C6′
OMe	3.77	53.1	C5′
OMe	3.68	53.4	C4′

[a] Recorded at 400 MHz. [b] Recorded at 100 MHz.

1
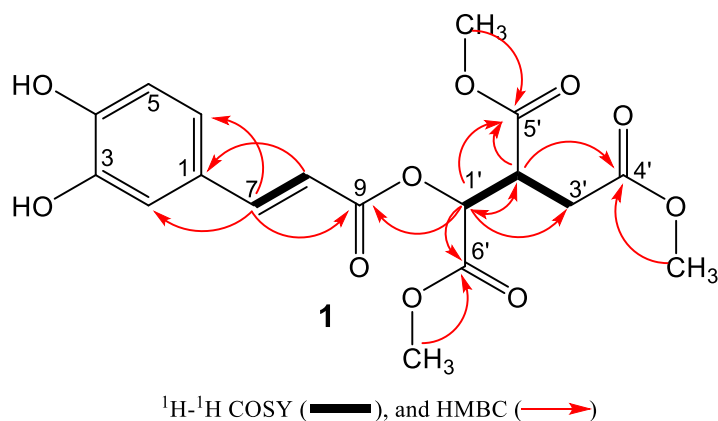
^{1}H-^{1}H COSY (▬▬▬), and HMBC (⟶)

Figure 4.2: Key ^{1}H-^{1}H COSY, and HMBC correlation of **4.1**.

Compound **4.2** (Figure 4.3) was obtained as a white amorphous powder from the ethyl acetate fraction. The HR-ESI-MS measurements of the deprotonated molecular ion at *m/z* 450.1379 [M-H]$^-$ indicated the molecular formula $C_{21}H_{25}NO_{10}$. The IR spectrum displayed absorption for hydroxyl (3250 cm^{-1}) and carbonyl groups (1607 cm^{-1}). The NMR data of compound **4.2** (Table 4.3, Figure 4.3) show the presence of a *N*-[2-(3,4-dihydroxyphenyl) ethyl]-3,4-dihydroxybenzamide moiety [20]. The structure of the aglycon part is the same as in compound **4.3**.

In addition, NMR data indicated the presence of an anomeric carbon [(δ_H 4.79 (1H, d, *J* = 7.5 Hz); δ_C 105.1] together with four methine carbon signals between 71.3 and 78.5 ppm typical for glucose. The coupling constant value of the sugar anomeric proton (*J* = 7.5 Hz) revealed the *β*-configuration of the glucosyl moiety. The linkage of C-1″ from the sugar moiety to 4′OH of the 3,4-dihydroxybenzoate moiety was established based on the HMBC long-range correlation from H-1″ (δ_H 4.79) to C-4′ (δ_C 150.1) (Figure 4.3). This conclusion is supported by the ROESY correlation of H-1″ (δ_H 4.79) with H-5′ (δ_H 7.24). From the above spectroscopic data, the structure of compound **4.2** was established as *N*-[2-(3,4-dihydroxyphenyl)ethyl]-3,4-dihydroxybenzamide 4′-*O*-*β*-D-glucoside, given the trivial name peperoside.

Table 4.3. ^{1}H- and ^{13}C-NMR data of **4.2** (in CD$_3$OD; δ in ppm, *J* in Hz).

Pos.	$\delta_H{}^a$, Mult. *J* (Hz)	$\delta_C{}^b$	HMBC
1	-	132.2	
2	6.70 d 2.1	117.0	C1, C3, C4, C6, C7
3	-	144.7	
4	-	146.2	
5	6.69 d 8.0	116.5	C1, C3, C4, C6, C7
6	6.59 dd 8.0, 2.1	121.1	C2, C3, C7
7	2.75 t 7.6	35.9	C1, C2, C6, C8
8a	3.57 dt 13.2, 7.6	42.8	C1, C7, C7′
8b	3.50 dt 13.2, 7.6	42.8	C1, C7, C7′
1′	-	126.3	
2′	7.25 d 3.1	120.7	C1′, C3′, C4′, C5′, C6′, C7′
3′	-	154,3	
4′	-	150.1	
5′	7.24 d 8.8	117.3	C1′, C3′, C4′, C6′
6′	6.86 dd 8.8, 3.1	120.3	C1′, C3′, C4′, C5′
7′	-	167.8	
1″	4.79 d 7.5	105.1	C4′, C3″, C5″
2″	3.38 m	74.9	
3″	3.41 m	78.1	
4″	3.38 m	78.5	
5″	3.39 m	71.3	
6a″	3.70 dd 12.0, 5.0	62.5	
6b″	3.89 d 12.0	62.5	

[a] Recorded at 400 MHz. [b] Recorded at 100 MHz.

^{1}H-^{1}H COSY (▬), HMBC (⟶), and ROESY (⟷)
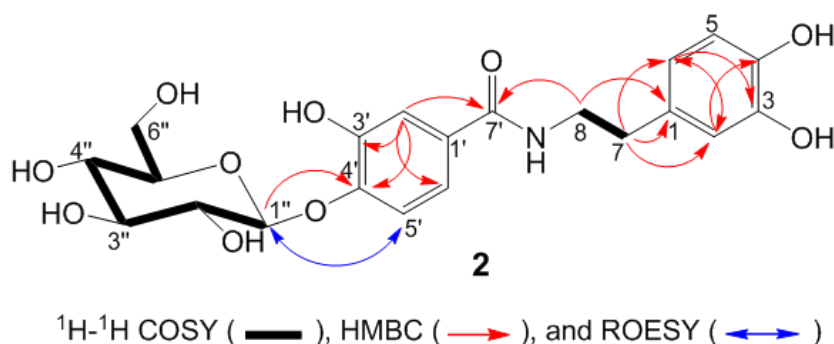
Figure 4.3: Key ^{1}H-^{1}H COSY, HMBC and ROESY correlation of **4.2.**

The phytochemical investigation of the *P. obtusifolia* (L.) A.Dietr. leaves allowed the isolation of five other known compounds, *N*-[2-(3,4-dihydroxyphenyl)ethyl]-3,4-dihydroxybenzamide (**4.3**) [20], becatamide (also known as houttuynamide A, **4.4**) [21], peperobtusin A (**4.5**) [10], peperomin B (**4.6**) [22] and arabinothalictoside (**4.7**) [23]. These compounds were identified by comparing their MS and NMR spectral data with published data, which agree with the data reported for the respective compounds. Among the known constituents, compound 4.**5** was already reported from *P. obtusifolia* while compounds **4.3**, 4.**4**, **4.6**, were isolated from other *Peperomia* species such as *P. duclouxii* [7], *P. tetraphylla* [24]

and *P. japonica* [22], respectively. Compound **4.7** is an unusual nitro natural product which was isolated for the first time from the Japanese plant *Sagittaria trifolia* [25], and later reported in *Aristolochia fordiana* [26] which belong to Piperales and *Annona squamosa* [23].

Peperomia species constituents have previously been reported to exhibit a variety of biological activities, either as extracts or pure compounds [2,27-29]. Thus, the compounds isolated from this species were evaluated for their anthelmintic, antifungal, antibacterial, and anticancer properties. These biological examinations were conducted by using established non-pathogenic model organisms and human cancer cell lines (all BSL-1) in fast-screening assays (Table 4.3, Table 4.5).

The anthelmintic activity was evaluated against *Caenorhabditis elegans*, however, the compounds did not significantly kill the nematodes even when applying a high concentration of 200 µM. Moreover, most of the compounds tested for antifungal effects against the phytopathogens *B. cinerea, S. tritici* and *P. infestans* were considered as inactive since the inhibition of fungal growth at a concentration of 125 µM was less than 50%. An exception was *N*-[2-(3,4-dihydroxyphenyl)ethyl]-3,4-dihydroxybenzamide (**4.3**) which displayed an interesting anti-oomycotic activity against *P. infestans* with an inhibition value of 56% at the same concentration. For the antibacterial assays, the compounds were tested in concentrations of 1 and 100 µM. None of the compounds inhibited the Gram-negative bacterium *A. fischeri* even at the highest test concentration of 100 µM. However, against the Gram-positive *B. subtilis*, peperobtusin A (**4.5**) induced 90% inhibition of bacterial growth when treating at a concentration of 100 µM, suggesting further investigations against human pathogens. Prenylated benzopyrans seem to be the active principle of *Peperomia* against Gram-positive bacteria including resistant *Staphylococcus aureus* and *Enterococcus faecalis* strains [14]. Since all other isolated compounds induced less than 50% inhibition of bacterial growth when applying a concentration of 100 µM (Table 4.3), their half-maximal inhibitory concentration (IC_{50}) values must be estimated to be greater than 100 µM.

Furthermore, the compounds **4.1**-**4.7** were screened for their potential antiproliferative or cytotoxic activity against two human cancer lines, namely prostate adenocarcinoma cells (PC-3) and colorectal adenocarcinoma cells (HT-29). The compounds' effect on the metabolic cancer cell viability was determined by conducting a MTT assay, general cytotoxic effects were determined by using a CV assay, both after 48 h cancer cell treatment with the compounds under investigation. A very potent permeabilizer of cell membranes, digitonin (125 µM), was used as positive control compromising the cells to the point of 0% of cell viability after 48 h. The compounds were tested at two different concentrations, namely 10 nM and 10 µM.

As shown in Table 4.5, most of the compounds exhibited no significant antiproliferative and cytotoxic effect on PC-3 and HT-29 cancer cells, with the exception of peperobtusin A (**4.5**), which strongly inhibited the viability and growth of PC-3 cells in a MTT and CV fast-screening assay after treating the cells with 10 µM of the compound for 48 hours. Under the same fast-screening assay conditions, also a moderate activity of compound **4.5** against the HT-29 colorectal cancer cell line was observed.

Table 4.4. Anthelmintic (*Caenorhabditis elegans*), antifungal (*Botrytis cinerea, Septoria tritici* and *Phytophthora infestans*), and antibacterial (*Bacillus subtilis, Aliivibrio fisheri)* activities of isolated compounds (**4.1-4.7**) from *P. obtusifolia.*

	Anthelmintic assay	Antifungal assays			Antibacterial assays	
	Mortality [%]	Growth inhibition [%][a]			Growth inhibition [%][a]	
	C. elegans	*B. cinerea*	*S. tritici*	*P. infestans*	*B. subtilis*	*A. fischeri*
Comp.	**200 µM**	**125 µM**	**125 µM**	**125 µM**	**100 µM**[b]	**100 µM**[b]
4.1	1.9 ± 0.8	-13.6 ± 17.3	-12.5 ± 17.9	10.1 ± 2.3	8.0 ± 19.0	-5.6 ± 2.60
4.2	0.0 ± 0.0	-27.6 ± 7.6	21.8 ± 8.9	-51.5 ± 16.0	7.0 ± 15.0	-3.1 ± 1.80
4.3	0.0 ± 0.0	-18.5 ± 3.1	-40.0 ± 35.2	56.2 ± 10.3	7.0 ± 2.8	-211.6 ± 27.6
4.4	2.9 ± 1.4	-32.3 ± 28.7	-9.8 ± 8.3	-66.4 ± 30.4	-21.0 ± 28.0	-35.9 ± 19.4
4.5	4.8 ± 1.4	27.0 ± 25.8	46.9 ± 8.3	-6.0 ± 64.4	90.0 ± 2.0	-32.7 ± 12.7
4.6	2.0 ± 1.7	51.4 ± 22.3	-12.9 ± 2.3	-9.4 ± 27.4	-5.0 ± 51.0	30.4 ± 8.4
4.7	1.7 ± 2.4	2.8 ± 19.5	-7.2 ± 1.9	17.1 ± 12.1	5.0 ± 17.0	1.6 ± 3.0
Pos. control	10 µg/ml	125 µM		125µM	100 µM	
	ivermectin	epoxiconazole		terbinafine	chloramphenicol	
	98.7 ± 1.9	92.0 ± 1.4		96.8 ± 1.2	99.0 ± 0	100.0 ± 0

[a] Negative values indicate an increase of fungal or bacterial growth in comparison to the negative control (0% inhibition).
[b] Growth inhibition rates below 50% indicate IC_{50} values > 100 µM.

Table 4.5. Antiproliferative and cytotoxic activities of isolated compounds (**4.1**-**4.7**) from *P. obtusifolia* against human prostate (PC-3) and colorectal (HT-29) cancer cell lines.

	Metabolic cell viability (MTT) / Cytotoxicity (CV) assays			
	Cell viability / Survivals [%]			
	PC-3 (MTT assay)	PC-3 (CV assay)	HT-29 (MTT assay)	HT-29 (CV assay)
Comp.	**10 µM**	**10 µM**	**10 µM**	**10 µM**
4.1	101.4 ± 5.8	97.5 ± 4.1	100.3 ± 4.4	91.0 ± 5.1
4.2	84.1 ± 4.9	84.0 ± 6.9	74.9 ± 6.5	78.2 ± 4.4
4.3	90.6 ± 3.3	98.3 ± 1.3	82.6 ± 4.8	100.3 ± 3.7
4.4	114.4 ± 1.2	92.9 ± 5.0	111.9 ± 1.8	89.0 ± 3.0
4.5	2.4 ± 6.3	-3.4 ± 24.7	59.7 ± 20.5	82.5 ± 4.3
4.6	120.9 ± 4.3	93.7 ± 2.6	117.1 ± 3.0	88.2 ± 3.9
4.7	113.7 ± 4.0	112.2 ± 4.7	115.3 ± 3.9	107.5 ± 2.9

Digitonin (125 µM) was used as positive control compromising the cells to the point of 0% of cell viability / cancer cell survival after 48 h.

Based on its antiproliferative and cytotoxic effects as determined with 10 µM concentration in the initial fast-screening assay, compound **4.5** was subjected to further evaluations of its IC_{50} values in both cancer cell lines. The cells were treated with increasing concentrations up to 100 µM of compound **4.5** for 48 hours, followed by MTT and CV assay read-out, data analyses and calculation of IC_{50} values. The IC_{50} values of compound **4.5** determined by MTT assay, indicating the metabolic viability of the cancer cells, were 25.6 ± 2.8 µM and 45.5 ± 8.8 µM in PC-3 and HT-29 cells, respectively (see Figure 4.4A). The CV assay, reflecting general cytotoxic and anti-proliferative impacts, showed similar IC_{50} values of 36.0 ± 4.1 µM and 58.1 ± 11.2 µM for PC-3 and HT-29 cells, respectively (Figure 4.4B). However, given the result of the preliminary fast-screening (fixed concentration 10 µM) of compound **4.5**, which estimated an IC_{50} value of less than 10 µM, the lower efficacy at the above actual calculated IC_{50} values based on the dose-response curves was unexpected, especially in the case of PC-3 cells. However, the IC_{50} values were reproduced in three different assay formats each with 2-3 biological replicates, namely MTT, CV and resazurin assays (data not shown), and revealed an IC_{50} range of 25 - 45 µM. This implies that fast-screening with a single concentration and a single biological replicate, although with technical quadruplicates, is only a very rough, initial estimation of the compounds' activity.
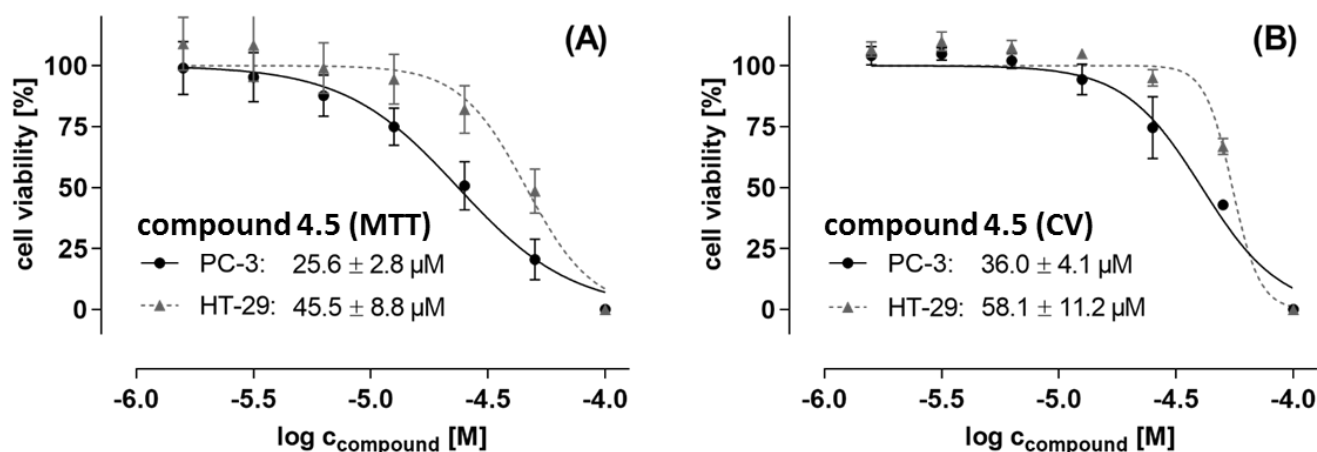
Figure 4.4: Effect of peperobtusin A (**4.5**) on (A) the metabolic cell viability of prostate PC-3 cancer cells and colon HT-29 cancer cells as determined by MTT assay after 48 hours cell treatment. (B) General cytotoxic and antiproliferative effect of **4.5** on both cancer cell lines under comparable treatment conditions as determined by using crystal violet (CV) assay. Data represent biological duplicates, each comprising technical quadruplicates. IC_{50} curves were analyzed and drawn by using SigmaPlot and GraphPad Prism software, respectively. IC_{50} values are given as mean ± SD.

Peperobtusin A (**4.5**) is a prenylated benzopyran with a chiral center at C-2. It was obtained with an optical activity of $[\alpha]_D^{20}$ 0 (*c* 0.28, CHCl$_3$), implying a racemic mixture of the molecule. This result corroborated previously published data [11,30]. The compound was

isolated before from the same species [10,11,14] and other *Peperomia* species, such as *P. tetraphylla* [31], and *P. clusiifolia* [32]. Although there exist a few studies addressing the biological activities of peperobtusin A (**4.5**), this study is the first report in association with the antiproliferative and cytotoxic effect against PC-3 (prostate) and HT-29 (colon) cancer cell lines. Previous investigations indicated the anti-trypanosomal and anti-tumor potential of peperobtusin A. Regarding the anti-trypanosomal activity, the compound with an IC_{50} value of 3.1 µM was almost three times more active than the positive control benzidazole [11]. Furthermore, Da Silva Mota and collaborators also evaluated its cytotoxicity in mammalian cells (murine peritoneal macrophages) and found the compound to be not toxic at the concentration level of its trypanocidal activity [11]. A recent study by Shi et al [31] revealed that peperobtusin A (4.**5**) had anti-proliferation effects against the human lymphoma cell line U937 with an IC_{50} value of 63.26 µM at 24 h, however, exerted only minor effects on other human cancer cell lines as human melanoma (A375), human bladder carcinoma (T24) and human breast epithelial cells (HBL-100). According to Shi et al. [31], the intracellular ROS formation, activation of caspases and P38 MAPK played significant roles in the apoptosis induced by peperobtusin A. Therefore, in future investigations the mode of action of peperobtusin A (**4.5**) in PC3 and HT29 cell lines should be addressed in detail and expanded toxicological investigations should be performed to validate the safety of this compound before developing it as trypanocide.

4.3   Materials and methods

4.3.1   General methods

The following instruments were used for obtaining physical and spectroscopic data: Column chromatography was performed on silica gel (400 - 630 mesh, Merck, Germany), Sephadex LH-20 (Fluka, Steinheim, Germany) and Diaion HP20 (Supelco, Bellefonte, PA, USA). Fractions and substances were monitored by TLC. TLC was conducted on precoated Kieselgel 60 F 254 plates (Merck, Darmstadt, Germany) and the spots were detected either by examining the plates under an UV lamp at 254 and 366 nm or by treating the plates with vanillin or natural product reagents. UV spectra were recorded on a Jasco V-770 UV-Vis/NIR spectrophotometer (Jasco, Pfungstadt, Germany), meanwhile specific rotation was measured with a Jasco P-2000 digital polarimeter (Jasco, Pfungstadt, Germany). The IR (ATR) spectra were carried out in MeOH using a Thermo Nicolet 5700 FT-IR spectrometer (Thermo Nicolet Analytical Instruments, Madison, WI, USA).

NMR spectra were obtained with an Agilent DD2 400 system at +25 °C (Varian, Palo Alto, CA, USA) using a 5-mm inverse detection cryoprobe. The compounds were dissolved in

CD_3OD (99.8% D) or $CDCl_3$ (99.8% D), and the spectra were recorded at 399.915 MHz (^1H) and 100.569 MHz (^{13}C). 1D (^1H and ^{13}C) and 2D ($^1H,^{13}C$ HSQC, $^1H,^{13}C$ HMBC, ^1H-^1H COSY, and $^1H,^1H$ ROESY) spectra were measured using standard CHEMPACK 8.1 pulse sequences implemented in the Varian VNMRJ 4.2 spectrometer software (Varian, Palo Alto, CA, USA). ^1H chemical shifts are referenced to internal TMS (^1H δ = 0 ppm), while ^{13}C chemical shifts are referenced to CD_3OD (^{13}C δ = 49 ppm) or $CDCl_3$ (^{13}C δ = 77.0 ppm).

The semi-preparative HPLC was performed on a Shimadzu prominence system (Kyoto, Japan) equipped with LabSolutions software, LC-20AT pump, SPD-M20A diode array detector, SIL-20A auto sampler and FRC-10A fraction collector unit. Chromatographic separation was carried out using a YMC Pack C18 column (5 µm, 120 Å, 150 mm x 10 mm I.D, YMC, USA) using H_2O (A) and CH_3CN (B) as eluents at a flow rate of 2.2 mL min^{-1}.

The high-resolution mass spectra in both positive and negative ion modes were acquired using either an Orbitrap Elite Mass spectrometer or API 3200 Triple Quadrupole System. The Orbitrap Elite Mass spectrometer (Thermofisher Scientific, Bremen, Germany) equipped with a HESI electrospray ion source (spray voltage 4.0 kV, capillary temperature 275 °C, source heater temperature 80 °C, FTMS resolution 100.000), whereas API 3200 Triple Quadrupole System (Sciex, Framingham, MA, USA) equipped with a turbo ion spray source, which performs ionization with an ion spray voltage on 70 eV. During the measurement, the mass/charge range from 50 to 2000 was scanned.

4.3.2 Plant material

The aerial part of *P. obtusifolia* (L.) A.Dietr. was collected in April 2018 at the Leibniz Institute of Plant Biochemistry (IPB), Halle (Saale), Germany from an ornamental plant grown since 20 years on an east oriented window sill. A voucher specimen (ISW010) was deposited in the IPB collection.

4.3.3 Extraction and isolation

The fresh leaves (267.3 g) of *P. obtusifolia* were dried using a freeze drier and ground to powder form (29.7 g). The powdered material was extracted five times (1.0 L/each) with 80% aqueous methanol at room temperature and yielded 6.4 g of residue after evaporating the solvent *in vacuo*. The residue was suspended in H_2O (250 ml) and then successively partitioned with *n*-hexane and ethyl acetate resulting in the two respective fractions (1.4 g *n*-hexane, 0.8 g EtOAc), as well as an aqueous fraction (3.6 g) (See Figure S20 for isolation scheme).

Part of the EtOAc fraction (0.74 g) was chromatographed on a silica gel column and eluted with a stepwise gradient of CH_2Cl_2: MeOH (1:0 to 0:1) to give seven fractions (E1-E7).

Fraction E1 (32.5 mg) underwent column chromatographic separation over a Sephadex LH-20 column (CH_2Cl_2/MeOH 1:1) affording four sub-fractions (A-D). Further separation of sub-fraction C (4.3 mg) over silica gel (CH_2Cl_2:MeOH 95:5 – 90:10) yielded becatamide (**4.4**, 1.4 mg, R_f = 0.25 in 5% MeOH in CH_2Cl_2) [21]. Fraction E2 (190.5 mg) was chromatographed over a Sephadex-LH20 column (100% MeOH) to afford an amorphous powder that was identified as *N*-[2-(3,4-dihydroxyphenyl)ethyl]-3,4-dihydroxybenzamide (**4.3**, 142.5 mg, R_f = 0.37 in 10% MeOH in CH_2Cl_2) [20]. Fraction E4 (106.3 mg) was purified over semi-preparative HPLC in a gradient system [H_2O (A), CH_3CN (B); 0 min – 5% B > 0-17 min 85.5% B > 17-20 min 100% B, UV at 330 nm, 9.8 min] affording compound **4.2** (14.5 mg).

The *n*-hexane fraction (1.4 g) was chromatographed over a silica gel column and eluted with a stepwise gradient of *n*-hexane, ethyl acetate and methanol to give six fractions (H1-H6). Fraction H1 (197.4 mg) was further chromatographed over a Sephadex-LH 20 column (100% CH_2Cl_2) to afford four sub-fractions (A-D). Purification of sub-fraction C (29.1 mg) by silica gel CC (*n*-hex: CH_2Cl_2 7:3) yielded peperobtusin A (**4.5**, 8.1 mg, R_f = 0.76 in 5% CH_3OH in CH_2Cl_2) [10]. Fraction H2 (279.6 mg) was chromatographed over a Sephadex LH-20 column (CH_2Cl_2/ MeOH 1:1) to give five sub-fractions (A-E). Sub-fraction C (14.7 mg) was purified by silica gel CC (*n*-hex:CH_2Cl_2 3:7-0:1) to afford peperomin B (**4.6**, 3.1 mg, R_f = 0.04 in CH_2Cl_2) [22].

The aqueous fraction (2.3 g) was fractionated over a Diaion-HP20 column eluted with an increasing solvent ratio of water and methanol to give five fractions (A1-A5). Fraction A3 (404.7 mg) was chromatographed over a Sepahdex-LH20 column (100% MeOH) to afford seven sub-fractions (A-G). Sub-fraction B (55.2 mg) was further separated by silica gel CC (CH_2Cl_2:MeOH 7:3) to afford arabinothalictoside (**4.7**, 14.6 mg, R_f = 0.57 in 30% MeOH in CH_2Cl_2) [23]. Sub-fraction D (69.4 mg) was further chromatographed over a silica gel column (CH_2Cl_2: MeOH 8:2 – 0:1) yielding compound **4.1** (7.4 mg, R_f = 0.88 in 30% MeOH in CH_2Cl_2).

Peperomic ester (trimethyl (1*S*,2*R*)-1-(((*E*)-3-(3,4-dihydroxyphenyl)acryloyl)oxy) propane-1,2,3-tricarboxylate, **4.1**). Brownish liquid; IR (ATR) v_{max}: 3402, 1715 cm^{-1}. UV λ_{max} (MeOH) (log e) 218 (4.15), 333 nm (4.21): ^{1}H-NMR (400 MHz, CD_3OD): Table 4.2; ^{13}C-NMR (100 MHz, CD_3OD): Table 4.2; negative-ion HR-ESI-MS *m/z* 395.0975 [M - H]$^-$, (calcd. for $C_{18}H_{19}O_{10}$: 395.0984).

Peperoside (*N*-[2-(3,4-dihydroxyphenyl)ethyl]-3,4-dihydroxybenzamide 4'-*O*-*β*-D-glucoside, **4.2**). White amorphous powder, IR (ATR) v_{max}: 3250, 2931, 2360, and 1607 cm^{-1}. UV λ_{max} (log e) (MeOH) 290 (3.14), 317 nm (3.32). ^{1}H-NMR (400 MHz, CD_3OD): Table 4.3; ^{13}C-NMR (100 MHz, CD_3OD): Table 4.3; negative-ion HR-ESI-MS *m/z* 450.1379 [M - H]$^-$, (calcd. for $C_{21}H_{24}NO_{10}$: 450.1406).

4.3.4 Biological activities

4.3.4.1. Anthelmintic activity

The anthelmintic bioassay was conducted applying the method developed by Thomsen et al. using the model organism *C. elegans*, which was previously demonstrated to correlate with anthelmintic activity against parasitic trematodes [33]. The *C. elegans* Bristol N2 wild-type strain was obtained from the Caenorhabditis Genetic Center (CGC), Minnesota University, Minneapolis, USA. The nematodes were grown on petri plates of NGM (Nematode Growth Media) using uracil auxotroph *E. coli* strain OP50 as food source. The solvent DMSO (2%) and the anthelmintic drug ivermectin (10 μg/ml, nearly 100% dead worms after 30 min incubation) were used as negative and positive controls in all assays, respectively. All assays were carried out in triplicate.

4.3.4.2. Antifungal activity

The antifungal activity was examined against the phytopathogenic ascomycetes *B. cinerea* Pars, and *S. triciti* Desm., and the oomycete *P. infestans* (Mont.) de Bary in 96-well microtiter plate assays according to protocols from the Fungicide Resistance Action Committee (FRAC) with minor modification as described by Otto et al. [34]. Briefly, the isolated compounds were tested at a highest concentration of 125 μM, while the solvent DMSO was used as negative control (max. concentration 2.5%). The commercially used fungicides epoxiconazole and terbinafine (Sigma-Aldrich, Darmstadt, Germany) served as reference compounds. The pathogen growth was evaluated seven days after inoculation by measurement of the optical density (OD) at ƛ 405 nm with a TecanGENios Pro microplate reader (five measurements per well using multiple reads in 3 x 3 square). Each experiment was carried out in triplicates.

4.3.4.3. Antibacterial activity

The isolated compounds (1 and 100 μM) were evaluated against the Gram-negative *A. fischerii* (DSM507) and the Gram-positive *B. subtilis* 168 (DSM 10) as described by dos Santos et al. [35]. The tests were conducted in 96 well plates and are based on bioluminescence (*A. fisheri*) or absorption (*B. subtilis*) read-out. Chloramphenicol (100 μM) was used as a positive control to induce complete inhibition of bacterial growth. The results (mean ± standard deviation value, n = 6) are given in relation to the negative control (bacterial growth, 1% DMSO without test compound) as relative values (percent inhibition). Negative values indicate an increase of bacterial growth.

4.3.4.4. Cytotoxic activity

The cytotoxicity and impact on the metabolic cell viability of isolated compounds at 10 nM and 10 μM was evaluated against PC-3 (human prostate adenocarcinoma) and HT-29 (human colorectal adenocarcinoma) cancer cell lines. Both cell lines were purchased from ATCC (Manassas, VA, USA). The cell culture medium RPMI 1640, the supplements FCS and L-glutamine, as well as PBS and tryp-sin/EDTA were purchased from Capricorn Scientific GmbH (Ebsdorfergrund, Germany). Culture flasks, multi-well plates and further cell culture plastics were from Greiner Bio-One GmbH (Frickenhausen, Germany) and TPP (Trasadingen, Switzerland), respectively. Resazurin used for the cell viability assays was purchased from Sigma-Aldrich GmbH (Taufkirchen, Germany). PC-3 and HT-29 cells were cultured in RPMI 1640 medium supplemented with 10% heat-inactivated FCS, 2 mM L-glutamine and 1% penicillin/streptomycin, and in a humidified atmosphere with 5% CO_2 at 37°C. Routinely, cells were cultured in T-75 flasks until reaching subconfluency (~ 80%), subsequently cells were harvested by washing with PBS and detaching by using trypsin/EDTA (0.05% in PBS) prior to cell passaging and seeding for sub-culturing and assays in 96-well plates, respectively [36].

The cell handling and assay techniques were in accordance with the method described by Khan et al. [36]. In brief, anti-proliferative and cytotoxic effects of the compounds were investigated by performing colorimetric MTT (3-(4,5-dimethylthiazol-2-yl)-2,5-diphenyltetrazolium bromide) and CV (crystal violet)-based cell viability assays (Sigma-Aldrich, Taufkirchen, Germany), respectively. For this purpose, cells were seeded in low densities in 96-well plates using the aforementioned cell culture medium. The cells were allowed to adhere for 24 h, followed by the 48 h compound treatment. Based on 20 mM DMSO stock solutions, the compounds were serially diluted in standard growth media to reach final concentrations of 100, 50, 25, 12.5, 6.25, 3.125, and 1.56 μM for cell treatment. For control measures, cells were treated in parallel with 125 μM digitonin (positive control, for data normalization set to 0% cell viability). Each data point was determined in technical quadruplicates and two independent biological replicates. As soon as the 48 h incubation was finished, cell viability was measured.

For the MTT assay, cells were washed once with PBS, followed by incubation with MTT working solution (0.5 mg/mL MTT in culture medium) for 1 h under standard growth conditions. After discarding the MTT solution, DMSO was added in order to dissolve the formed formazan, followed by measuring formazan absorbance at 570 nm, and additionally at the reference/background wavelength of 670 nm, by using a SpectraMax M5 multi-well plate reader (Molecular Devices, San Jose, CA, USA).

For the CV assay, cells were washed once with PBS and fixed with 4% paraformaldehyde (PFA) for 20 min at room temperature (RT). After discarding the PFA solution, the cells were left to dry for 10 min and then stained with 1% crystal violet solution for 15 min at RT. The cells were washed with water and were dried overnight at RT. Afterwards, acetic acid (33% in ultrapure water) was added to the stained cells and absorbance was measured at 570 nm and 670 nm (reference wavelength) using a SpectraMax M5 multi-well plate reader (Molecular Devices, San Jose, CA, USA). For data analyses, GraphPad Prism version 8.0.2, SigmaPlot 14.0 and Microsoft Excel 2013 were used.The results are shown as a percentage of the control values obtained from untreated cultures, i.e. cell viability in percent.

4.4 Conclusions

The present investigation of a methanol extract from the leaves of *P. obtusifolia* led to the isolation of two new compounds, named peperomic ester (**4.1**) and peperoside (**4.2**) along with five known compounds. The isolated compounds were evaluated for their anthelmintic, antifungal, antibacterial and anticancer activities. Peperoside (**4.2**) and its related compounds (**4.3**, **4.4**) have the advantage of low activity against all organisms/cells tested. Since similar phenethylamides show taste and neuroactive properties [37,38] – which were not part of this study – there use in such tests which usually include human panels or animals appears acceptable.

The known peperobtusin A (**5**) was the most active compound against *B. subtilis* and showed an antiproliferative and cytotoxic effect in the lower micromolar concentration range towards human PC-3 (prostate) and HT-29 (colon) cancer cell lines. The observed antibacterial activity supports the traditional use of *P. obtusifolia* as a skin cleanser. These findings suggest that *P. obtusifolia* might have some general toxicity and thus should be used with care in applications where cytotoxicity is not desired. However, prenylated benzopyran derivatives structurally related to **5** were shown to exhibit selective activity against breast cancer cells but did not influence normal breast cells [39]. The impact of this compound class on the mitochondrial respiratory chain [39,40] and their function as PPAR agonists may play a role in compound selectivity [41]. Thus, more extensive and detailed studies on the anticancer activity of natural prenylated benzopyrans should be undertaken in order to provide an understanding of structural requirements (SAR) for such cytotoxic (or other) activity.

4.5 References

1. Felippe, L.G.; Baldoqui, D.C.; Kato, M.J.; Bolzani, V.d.S.; Guimarães, E.F.; Cicarelli, R.M.B.; Furlan, M., Trypanocidal tetrahydrofuran lignans from *Peperomia blanda*. *Phytochemistry* **2008**, *69*, 445-450.

2. Al-Madhagi, W.M.; Mohd Hashim, N.; Awad Ali, N.A.; Alhadi, A.A.; Abdul Halim, S.N.; Othman, R., Chemical profiling and biological activity of *Peperomia blanda* (Jacq.) Kunth. *PeerJ* **2018**, *6*, e4839.

3. Malquichagua Salazar, K.J.; Delgado Paredes, G.E.; Lluncor, L.R.; Young, M.C.M.; Kato, M.J., Chromenes of polyketide origin from *Peperomia villipetiola*. *Phytochemistry* **2005**, *66*, 573-579.

4. Seeram, N.P.; Lewis, A.W.; Jacobs, H.; Nair, M.G.; McLean, S.; Reynolds, W.F., Proctoriones A−C: 2-Acylcyclohexane-1,3-dione derivatives from *Peperomia proctorii*. *J. Nat. Prod.* **2000**, *63*, 399-402.

5. Wu, J.-l.; Li, N.; Hasegawa, T.; Sakai, J.-i.; Kakuta, S.; Tang, W.; Oka, S.; Kiuchi, M.; Ogura, H.; Kataoka, T., *et* al., Bioactive tetrahydrofuran lignans from *Peperomia dindygulensis*. *J. Nat. Prod.* **2005**, *68*, 1656-1660.

6. Xu, S.; Li, N.; Ning, M.-M.; Zhou, C.-H.; Yang, Q.-R.; Wang, M.-W., Bioactive compounds from *Peperomia pellucida*. *J. Nat. Prod.* **2006**, *69*, 247-250.

7. Li, N.; Wu, J.-l.; Hasegawa, T.; Sakai, J.-i.; Bai, L.-m.; Wang, L.-y.; Kakuta, S.; Furuya, Y.; Ogura, H.; Kataoka, T., *et* al., Bioactive polyketides from *Peperomia duclouxii*. *J. Nat. Prod.* **2007**, *70*, 998-1001.

8. Wang, X.Z.; Cheng, Y.; Wu, H.; Li, N.; Liu, R.; Yang, X.L.; Qiu, Y.-Y.; Wen, H.M.; Liang, J.Y., The natural secolignan peperomin E induces apoptosis of human gastric carcinoma cells via the mitochondrial and PI3K/Akt signaling pathways in vitro and in vivo. *Phytomedicine* **2016**, *23*, 818-827.

9. Batista, A.N.L.; Santos-Pinto, J.; Batista, J.M., Jr.; Souza-Moreira, T.M.; Santoni, M.M.; Zanelli, C.F.; Kato, M.J.; López, S.N.; Palma, M.S.; Furlan, M., The combined use of proteomics and transcriptomics reveals a complex secondary metabolite network in *Peperomia obtusifolia*. *J. Nat. Prod.* **2017**, *80*, 1275-1286.

10. Tanaka, T.; Asai, F.; Iinuma, M. Phenolic compounds from *Peperomia obtusifolia*. *Phytochemistry* **1998**, *49*, 229-232.

11. da Silva Mota, J.; Leite, A.C.; Batista Junior, J.M.; Noelí López, S.; Luz Ambrósio, D.; Duó Passerini, G.; Kato, M.J.; da Silva Bolzani, V.; Barretto Cicarelli, R.M.; Furlan, M., In vitro trypanocidal activity of phenolic derivatives from *Peperomia obtusifolia*. *Planta Med.* **2009**, *75*, 620-623.

12. Mota, J.d.S.; Leite, A.C.; Kato, M.J.; Young, M.C.M.; Bolzani, V.d.S.; Furlan, M., Isoswertisin flavones and other constituents from *Peperomia obtusifolia*. *Nat. Prod. Res.* **2011**, *25*, 1-7.

13. Batista, J.M.; Batista, A.N.L.; Kato, M.J.; Bolzani, V.S.; López, S.N.; Nafie, L.A.; Furlan, M., Further monoterpene chromane esters from *Peperomia obtusifolia*: VCD determination of the absolute configuration of a new diastereomeric mixture. *Tetrahedron Lett.* **2012**, *53*, 6051-6054.

14. Ruiz Mostacero, N.; Castelli, M.V.; Cutró, A.C.; Hollmann, A.; Batista, J.M., Jr.; Furlan, M.; Valles, J.; Fulgueira, C.L.; López, S.N., Antibacterial activity of prenylated benzopyrans from *Peperomia obtusifolia* (Piperaceae). *Nat. Prod. Res.* **2019**, 1-5.

15. Tamayose, C.I.; Romoff, P.; Toyama, D.O.; Gaeta, H.H.; Costa, C.R.C.; Belchor, M.N.; Ortolan, B.D.; Velozo, L.S.M.; Kaplan, M.A.C.; Ferreira, M.J.P., *et* al., Non-clinical studies for evaluation of 8-c-rhamnosyl apigenin purified from *Peperomia obtusifolia* against acute edema. *Int. J. Mol. Sci.* **2017**, *18*, 1972.

16. Wu, W.; Zhao, F.; Ding, R.; Bao, L.; Gao, H.; Lu, J.C.; Yao, X.S.; Zhang, X.-Q.; Liu, H.W., Four new cryptoporic acid derivatives from the fruiting bodies of *Cryptoporus sinensis*, and their inhibitory effects on nitric oxide production. *Chem. Biodivers.* **2011**, *8*, 1529-1538.

17. Zhou, L.Y.; Yu, X.-H.; Lu, B.; Hua, Y., Bioassay-guided isolation of cytotoxic isocryptoporic acids from *Cryptoporus volvatus*. *Molecules* **2016**, *21*, 1692.

18. Pham, H.T.; Lee, K.H.; Jeong, E.; Woo, S.; Yu, J.; Kim, W.Y.; Lim, Y.W.; Kim, K.H.; Kang, K.B., Species prioritization based on spectral dissimilarity: A case study of polyporoid fungal species. *J. Nat. Prod.* **2021**, *84*, 298-309.

19. Chepkirui, C.; Yuyama, K.T.; Wanga, L.A.; Decock, C.; Matasyoh, J.C.; Abraham, W.R.; Stadler, M., Microporenic acids A–G, biofilm inhibitors, and antimicrobial agents from the Basidiomycete *Microporus* species. *J. Nat. Prod.* **2018**, *81*, 778-784.

20. Liao, Y.; Ye, Y.; Li, S.; Zhuang, Y.; Chen, L.; Chen, J.; Cui, Z.; Huo, L.; Liu, S.; Song, G., Synthesis and SARs of dopamine derivatives as potential inhibitors of influenza virus PAN endonuclease. *Eur. J. Med. Chem.* **2020**, *189*, 112048.

21. Park, J.B., Protective effects of veskamide, enferamide, becatamide, and oretamide on H2O2-induced apoptosis of PC-12 cells. *Phytomedicine* **2011**, *18*, 843-847.

22. Chen, C.M.; Jan, F.Y.; Chen, M.T.; Lee, T.J., Peperomins A, B, and C, novel secolignans from *Peperomia japonica*. *Heterocycles* **1989**, *29*, 411-414.

23. Li, H.X.; Yang, S.Y.; Kim, Y.S.; Jang, H.D.; Kim, Y.H.; Li, W., Nitro derivatives and other compounds from sugar apple (*Annona squamosa* L.) leaves exhibit soluble epoxide hydrolase inhibitory activity. *Med. Chem. Res.* **2019**, *28*, 1939-1944.

24. Li, Y.Z.; Tong, A.P.; Huang, J., Two new norlignans and a new lignanamide from *Peperomia tetraphylla*. *Chem. Biodivers.* **2012**, *9*, 769-776.

25. Yoshikawa, M.; Yamaguchi, S.; Murakami, T.; Matsuda, H.; Yamahara, J.; Murakami, N., Absolute stereostructures of trifoliones A, B, C, and D, new biologically active diterpenes from the tuber of *Sagittaria trifolia* L. *Chem. Pharm. Bull.* **1993**, *41*, 1677-1679.

26. Zhou, Z.; Luo, J.; Pan, K.; Kong, L., A new alkaloid glycoside from the rhizomes of *Aristolochia fordiana*. *Nat. Prod. Res.* **2014**, *28*, 1065-1069.

27. Alves, N.S.F.; Setzer, W.N.; da Silva, J.K.R., The chemistry and biological activities of *Peperomia pellucida* (Piperaceae): A critical review. *J. Ethnopharmacol.* **2019**, *232*, 90-102.

28. Ng, Z.X.; Than, M.J.Y.; Yong, P.H. *Peperomia pellucida* (L.) Kunth herbal tea: Effect of fermentation and drying methods on the consumer acceptance, antioxidant and anti-inflammatory activities. *Food Chem.* **2021**, *344*.

29. Gutierrez, Y.V.; Yamaguchi, L.F.; de Moraes, M.M.; Jeffrey, C.S.; Kato, M.J., Natural products from *Peperomia*: Occurrence, biogenesis and bioactivity. *Phytochem Rev* **2016**, *15*, 1009-1033.

30. Batista, J.M., Jr.; Lopez, S.N.; Mota Jda, S.; Vanzolini, K.L.; Cass, Q.B.; Rinaldo, D.; Vilegas, W.; Bolzani Vda, S.; Kato, M.J.; Furlan, M., Resolution and absolute configuration assignment of a natural racemic chromane from *Peperomia obtusifolia* (Piperaceae). *Chirality* **2009**, *21*, 799-801.

31. Shi, L.; Qin, H.; Jin, X.; Yang, X.; Lu, X.; Wang, H.; Wang, R.; Yu, D.; Feng, B., The natural phenolic peperobtusin A induces apoptosis of lymphoma U937 cells via the Caspase dependent and p38 MAPK signaling pathways. *Biomed. Pharmacother.* **2018**, *102*, 772-781.

32. Seeram, N.P.; Jacobs, H.; McLean, S.; Reynolds, W.F., A prenylated benzopyran derivative from *Peperomia clusiifolia*. *Phytochemistry* **1998**, *49*, 1389-1391.

33. Thomsen, H.; Reider, K.; Franke, K.; Wessjohann, L.A.; Keiser, J.; Dagne, E.; Arnold, N., Characterization of constituents and anthelmintic properties of *Hagenia abyssinica*. *Sci. Pharm.* **2012**, *80*, 433-446.

34. Otto, A.; Porzel, A.; Schmidt, J.; Brandt, W.; Wessjohann, L.; Arnold, N., Structure and absolute configuration of pseudohygrophorones A^{12} and B^{12}, alkyl cyclohexenone derivatives from *Hygrophorus abieticola* (Basidiomycetes). *J. Nat. Prod.* **2016**, *79*, 74-80.

35. dos Santos, C.H.C.; de Carvalho, M.G.; Franke, K.; Wessjohann, L., Dammarane-type triterpenoids from the stem of *Ziziphus glaziovii* Warm. (Rhamnaceae). *Phytochemistry* **2019**, *162*, 250-259.

36. Khan, M.F.; Nasr, F.A.; Noman, O.M.; Alyhya, N.A.; Ali, I.; Saoud, M.; Rennert, R.; Dube, M.; Hussain, W.; Green, I.R*., et* al., Cichorins D-F: Three new compounds from *Cichorium intybus* and their biological effects. *Molecules* **2020**, *25*.

37. Krammer, G.; Ley, J.P.; Geißler, K.; Geißler, T.; Gomoll, F.; Welters, P.; Jach, G.; Wessjohann, L., Method for biotechnological production of methylized cinnamic acids and cinnamic acid esters, methylized phenethylamines and the coupling products thereof, particularly of cinnamic acid amides. US-Patent: US10227620B2 (12.03.**2019**)

38. Greger, H. (2016)., Alkamides: a critical reconsideration of a multifunctional class of unsaturated fatty acid amides. *Phytochem. Rev.* **2016**, *15* 729-770.

39. Taha, H.; Looi, C.Y.; Arya, A.; Wong, W.F.; Yap, L.F.; Hasanpourghadi, M.; Mohd, M.A.; Paterson, I.C.; Ali, H.A., (6E,10E) Isopolycerasoidol and (6E,10E) isopolycerasoidol methyl

ester, prenylated benzopyran derivatives from *Pseuduvaria monticola* induce mitochondrial-mediated apoptosis in human breast adenocarcinoma cells. *PLoS One* **2015**, *10*, e0126126.

40. Zafra-Polo, M.C.; González, M.C.; Tormo, J.R.; Estornell, E.; Cortes, D., Polyalthidin: New prenylated benzopyran inhibitor of the mammalian mitochondrial respiratory chain. *J. Nat. Prod.* **1996**, *10*, 913–916.

41. Corés Martinez, D.M.; Sanz Ferrando, M.J.; Bermejo del Castillo, A.; Piqueras Ruiz, L.; Collado Sánchez, A.; Gomes Marques, P.; Vila Dasí, L., Prenylated Benzopyranes as PPAR Agonists. Patent: WO2019129909 (4 July **2019**).

4.6   Supporting information

Supplementary data associated with this article can be found at: https://www.mdpi.com/article/10.3390/molecules27144363/s1.

5. General discussion and perspective of ongoing and future research

Natural products derived from plants, animals, and microorganisms have been studied and used in nutrition and to treat diseases since the beginning of human history. Specifically, plants are of the greatest interest to the pharmaceutical and agrochemical industry due to their diverse and potentially bioactive and agriculturally producible natural products which also have high consumer acceptance [1,2]. Similar to other plant families, the Piperaceae are well-known for their traditional medicinal and culinary uses. The most common commercial product of the Piperaceae is pepper, produced from the fruit of *Piper nigrum* L. This species is grown as a major cash crop in more than 30 tropical nations, including Vietnam, India, Malaysia, Indonesia, China, and Brazil [3,4].

Despite the widespread popularity of *P. nigrum*, many Piperaceae species remain chemically and biologically under - and unexplored. Therefore, the focus of this dissertation was to explore some Piperaceae plants, including one species grown in Malaysia, by characterizing and isolating phytoconstituents and assessing their biological activities. In this regard, two Piperaceae species collected in Malaysia and Germany, namely *Piper sarmentosum* and *Peperomia obtusifolia*, were chemically analyzed, and their biological activity was evaluated (Chapters 2 and 4). Further, LC-MS based metabolomic profiling of *P. sarmentosum* organs (i.e., leaf, stem, root, and fruits) was also performed in this research to have deep insight into this plant's compound distribution (Chapter 3).

The *Piper* genus is characterized by high phytochemical diversity, producing compounds in various classes of specialized metabolites. This chemistry is characteristic for many *Piper* species [5-8], but little metabolite information is available for *P. sarmentosum* [8]. In light of that knowledge, chemical isolation was performed on *P. sarmentosum* leaves (Chapter 2). This plant which is typical of *Piper* grown in South East Asian countries, was collected in Malaysia in 2019. As a result of our isolation process, many of the isolated compounds with structural differences were discovered for the first time in this plant or this genus, and three were described for the first time as new natural products, namely 4''-(3-hydroxy-3-methylglutaroyl)-2''-*β*-D-glucopyranosyl vitexin (**2.1**), kadukoside (**2.2**), and 6-*O*-*trans*-*p*-coumaroyl-D-glucono-1,4-lactone (**2.3**), along with 31 known compounds.

Interestingly, 21 known compounds were isolated for the first time from *P. sarmentosum*. This discovery confirmed that the *Piper* genus contains a broad range of compounds with diverse skeletons, such as alkaloids, lignans, flavonoids, etc [9]. Besides the diverse structures of secondary metabolites, this plant species is known to have bioactivity against human pathogenic bacteria, based on their traditional use. Therefore, the bioactivity

assay was performed against several microorganisms to point out the main metabolites responsible for their bioactivity. However, due to the limitation of the access to humanic pathogen bacteria, the antibacterial assay in this study was performed only against model organisms available at the Leibniz Institute for Plant Biochemistry (IPB), namely *Bacillus subtilis* (Gram-positive bacteria) and *Aliivibrio fischerii* (Gram-negative bacteria). In addition, bioassays against a model organism for parasitic infections plant-pathogens were also performed. The model organism *Caenorhabditis elegans* was used for assaying anthelmintic activity and species *Botrytis cinerea*, *Septoria tritici* and *Phytophthora infestans* were used for antifungal and anti-oomycete activity. Interestingly, many isolated compounds are active against those organisms, especially the new compound kadukoside (**2.2**) shows significant activity against *S. tritici* and *P. infestans*. Therefore, a further study including the possibility of synthesizing this compound and derivatives, is necessary for further use in agriculture. In addition to the bioactivity against several organisms, some isolated compounds from this *Piper* species i.e., isoasarone (**2.12**), *trans*-asarone (**2.15**) and aristolactam BII (**2.22**) have a neuroprotective potential which is noteworthy for further development.

In general, the biological activities of *P. sarmentosum* reported in this study are moderate or weak. On the cytotoxic point of view, the results indicated that the plant itself is generally safe to consume, as the plant is traditionally used as food by many people in Malaysia and neighbouring countries. On the other hand, it is possible that the isolated compounds target specific human pathogenic bacteria but this can only be confirmed with more antibacterial assays against pathogenic bacteria. Furthermore, there are some possibilities for synergistic effects among the compounds or extract to increase activity. *In vivo* assays would give an indication of possible synergistic effect as sometime compounds can be pro-drugs which are converted to an active form in the body. The active forms can then work together giving a synergistic effect.

A number of metabolite classes previously reported from the same *Piper* genus, such as piperamides, and lignanamides, could not be isolated in this study from *P. sarmentosum*. This could be mainly due to the fact that leaves were used as starting material, which have only a low content of these constituents. Furthermore, there is the possibility that the distribution of secondary metabolites can be influenced by factors such as geographical, climatic and experimental conditions [10]. However, our primary goal is not to assess these factors, but to allow to discriminate the organs themselves and to provide thus a basis for selected applications. Therefore, the investigation of the wide-ranging metabolite presence in this species and the comparative evaluation of metabolites among organs (leaves, stems, roots, and fruits) were

performed to address this question (Chapter 3). In our search for high-throughput and comprehensive techniques, we postulated that methods that can rapidly cluster plant organs based on metabolite profile similarity would be helpful. Extensive analytical approaches such as untargeted LC-MS with a combination of multivariate data analysis are renowned techniques that can be easily applied to such experimental models due to the fact that samples can be quickly prepared and analyzed. Therefore, LC-MS-based metabolomic approaches were used in this experiment to achieve useful information for bioactive compounds discovery and their preferential formation in specific organs. This method (metabolite profiling) is a complementary method to the isolation work because it gives more information regarding the metabolites which are not able to be isolated. In addition, metabolite profiling is also beneficial in guiding the isolation process. This approach can improve the efficiency of natural product prioritization and accelerate the targeted isolation of key natural products [11].

According to the result in Chapter 2, most isolated compounds have been detected by the RP-UHPLC-QqTOF-MS. Therefore, this instrument was used for the metabolites profiling study (Chapter 3) due to the specificity of the analysis. In total, 20 samples from four organs were extracted for this study. The key point of the metabolite profiling study is that all samples are treated in the same manner from the weight, extraction process, until the concentration to minimize the error. In addition, the concentration used for the LC-MS measurement is one of the critical points for the measurement. Therefore, the serial dilution of the extracts was necessary, and this resulted in a concentration of 4.0 mg/ml (concentration for MS measurement) which is the suitable concentration for this experiment.

Herein, a detailed MS/MS fragmentation pattern analysis revealed the presence of 154 metabolites that were tentatively identified and classified, mostly alkaloids and flavonoids. The correlations between the organs and the relative abundance of these compounds were presented using multivariate analysis (i.e., principal component analysis and hierarchical clustering algorithm). As a result, the distribution of metabolites in the investigated organs is very different. For instance, stems of *P. sarmentosum* contained the most significant amount of aporphine alkaloids in comparison to other organs. Moreover, leaves contain relatively more flavonoids, and fruits and roots have a vast number of piperamides types A-E. Additionally, several compounds were successfully identified, screened and quantified as unique metabolites for the discrimination of different *P. sarmentosum* organs, for instance, the neolignane andamanicin (**P122**), flavonoids (**P30**, **P36**) and *trans*-asarone (**P95**) are the significant metabolites in the leaves. Furthermore, the benzylisoquinolines group includes aporphine-type compounds like magnoflorines (**P12, P21**), piperolactam B (**P75**) and peperolactam A (**P70**) as

the unique metabolites found in stems. Compounds pellitorine (**P116**), brachyamide B (**P114**) and guineensine (**P136**) had a powerful discriminating effect on fruits and roots.

Furthermore, along the annotation process in LC-MS-based metabolomics, one metabolite is often represented by multiple peaks or features in LC-MS data with distinct *m/z* values and abundance levels but at similar retention times due to the presence of isotopes, adducts and neutral loss fragments. Of note, the abundance level among adducts peaks as well as the amount of formed adducts will vary from one metabolite to another, as well as for the same metabolite depending on experimental conditions [12,13]. This can make MS1 spectral information in LC/MS poorly reproducible for annotation purposes [14]. However, some adducts and neutral losses are more frequent than others. An example of this was andamanicin (**P122**), which was represented by two different features of relatively different intensities, namely the protonated molecular ion $[M+H]^+$ and the corresponding ammonium adduct $[M+NH_4]^+$ (Chapter 3, Figure 3.11B). Thus, data evaluation based on the retention time will facilitate the annotation process.

On the other point, the abundant LC-MS peaks observed in the leaves named/labeled as vitexin-2"-*O*-galactoside (**P30**), flavonoid conjugate (**P36**), *trans*-asarone (**P95**) and andamanicin (**P122**) have been successfully identified. These compounds were isolated as the major compounds in this study. This indicates that, in addition to the ionization condition of the LC-MS, the abundance of the peak was also affected by the compound content of the samples tested.

In this study also, it was found that several annotated compounds exist as isomers, the majority of which are piperamide-type, such as piperettine and piperettyline-like isomers. The structural features of these compounds suggest the occurrence of cis/trans double-bond isomerization. One of the factors that generate isomerization is exposure to sunlight. However, the isomers may be formed predominantly biosynthetically within the plant or depending on external processes during plant development. The impact of sunlight on the compound stability also possible occur during experimental work [15]. Therefore, to avoid the formation of artifacts, the operational steps associated with sample treatment, sample preparation and analysis under strict light exclusion should be prioritized. Due to the rare chemicals not commercially available at the time of this research, we were unable to purely identified the isomeric compounds.

Overall, this study in Chapter 3 provides extensive data on the metabolic profiles of *P. sarmentosum*, supplying useful information for bioactive compounds discovery and their preferential formation in specific organs. This can be used to optimize production and

harvesting as well as to maximize the plant's economic value as herbal medicine or in food applications. Another point that would be interesting related to this study is the possibility of using the MS-Imaging approach to observe the distribution of metabolites within the organ. However, due to the limited access to fresh material, this procedure was not performed in this study. More research is needed to determine how secondary metabolite production and accumulation from specific organs relate to the biosynthesis pathway of respective metabolites. Furthermore, identification of the various secondary metabolite transporters involved and their mechanisms is also interesting to be discussed in the future.Therefore, this approach is highly recommended for future research.

As mentioned above, one Piperaceae species (*P. obtusifolia*), which has been grown at IPB Halle for many years, was also studied in this research (Chapter 4). In the same procedure as the other species, the isolation process was performed on this species. As the output, two compounds, named peperomic ester (**4.1)** and peperoside (**4.2**) along with five known compounds, were isolated from the leaves of *P. obtusifolia*. Nevertheless, the unusual natural product, peperomic ester (**4.1**) provoked the question of whether the compound, that contains an isocitrate moiety, was isolated as a truly natural product or rather an artefact formed during isolation. In order to prove that the isocitrate-containing compound is not an artificial constituent, an ethanol crude extract of this plant was prepared with the additional process to avoid the presence of methyl groups in the solvent, followed by HRESI-MS. As a result, the previously isolated methylated isocitrate present in the extract was detected, proving that this isolated compound is an authentic natural product. Compound **4.2** and its derivatives (**4.3** and **4.4**) also showed low activity against all organisms/cells tested, making those compounds more potential for further development for medicinal purposes. The antibacterial activity against Gram-positive *Bacillus subtilis* was observed from peperobtusin A (**4.5**) which induced 90% inhibition of bacterial growth at a concentration of 100 µM. It also exhibited high activity against the prostate cancer cell line with IC_{50} values of 25.6 µM and 36.0 µM in MTT and CV assays, respectively. These findings suggest that *P. obtusifolia* might have some general toxicity and thus should be used with care in applications where cytotoxicity is not desired. However, it also suggests that more extensive and detailed studies on the anticancer activity of natural prenylated benzopyrans should be undertaken to understand structural requirements (SAR) for such cytotoxic (or other) activity.

In conclusion, this work demonstrated the role of natural products in bioactive compound discovery, in particular members of the Piperaceae family as a potential source of new bioactive compounds. Further research should be continually encouraged to successfully

achieve such aims, so we can take maximum advantage of what nature can offer in a sustainable way that is beneficial in and of itself.

5.1 References

1. Atanasov, A. G.; Zotchev, S. B.; Dirsch, V. M.; Orhan, I. E.; Banach, M.; Rollinger, J. M.; Barreca, D.; the International Natural Product Sciences, T.; Supuran, C. T.; Natural products in drug discovery: Advances and opportunities. *Nat. Rev. Drug Discov.* **2021,** 20, 200-216.
2. Newman, D. J.; Cragg, G. M., Natural products as sources of new drugs over the nearly four decades from 01/1981 to 09/2019. *J. Nat. Prod.* **2020,** 83, 770-803.
3. Ahmad, N.; Fazal, H.; Abbasi, B. H.; Rashid, M.; Mahmood, T.; Fatima, N., Efficient regeneration and antioxidant potential in regenerated tissues of *Piper nigrum* L. *Plant Cell Tiss. Org.* **2010,** 102, 129-134.
4. Hao, C. Y.; Xia, Z. Q.; Fan, R.; Tan, L. H.; Hu, L. S.; Wu, B. D.; Wu, H. S., De novo transcriptome sequencing of black pepper (*Piper nigrum* L.) and an analysis of genes involved in phenylpropanoid metabolism in response to Phytophthora capsici. *BMC Genomics* **2016,** 17.
5. Gutierrez, R. M. P.; Gonzalez, A. M. N.; Hoyo-Vadillo, C., Alkaloids from Piper: A review of its phytochemistry and pharmacology. *Mini-Rev. Med. Chem.* **2013,** 13, 163-193.
6. Salazar, D.; Jaramillo, M. A.; Marquis, R. J., Chemical similarity and local community assembly in the species rich tropical genus *Piper. Ecology* **2016,** 97, 3176-3183.
7. Gomez-Calvario, V.; Rios, M. Y., ^{1}H and ^{13}C NMR data, occurrence, biosynthesis, and biological activity of *Piper* amides. *Magn. Reson. Chem.* **2019,** 57, 994-1070.
8. Sun, X.; Chen, W.; Dai, W.; Xin, H.; Rahmand, K.; Wang, Y.; Zhang, J.; Zhang, S.; Xu, L.; Han, T., *Piper sarmentosum* Roxb.: A review on its botany, traditional uses, phytochemistry, and pharmacological activities. *J. Ethnopharmacol.* **2020,** 263, 112897.
9. Salehi, B.; Zakaria, Z. A.; Gyawali, R.; Ibrahim, S. A.; Rajkovic, J.; Shinwari, Z. K.; Khan, T.; Sharifi-Rad, J.; Ozleyen, A.; Turkdonmez, E.; Valussi, M.; Tumer, T. B.; Monzote Fidalgo, L.; Martorell, M.; Setzer, W. N., *Piper* species: A comprehensive review on their phytochemistry, biological activities and applications. *Molecules* **2019,** 24, 1364.
10. Gad, H. A.; Mukhammadiev, E. A.; Zengen, G.; Musayeib, N. M. A.; Hussain, H.; Bin Ware, I.; Ashour, M. L.; Mamadalieva, N. Z., Chemometric analysis based on GC-MS chemical profiles of three *Stachys* species from Uzbekistan and their biological activity. *Plants* **2022,** 11, 1215.
11. Wolfender, J. L.; Litaudon, M.; Touboul, D.; Queiroz, E. F., Innovative omics-based approaches for prioritisation and targeted isolation of natural products - new strategies for drug discovery. *Nat. Prod. Rep.* **2019,** 36, 855-868.
12. Vinaixa, M.; Schymanski, E. L.; Neumann, S.; Navarro, M.; Salek, R. M.; Yanes, O., Mass spectral databases for LC/MS- and GC/MS-based metabolomics: State of the field and future prospects. *Trac-Trend Anal. Chem.* **2016,** 78, 23-35.
13. Stricker, T.; Bonner, R.; Lisacek, F.; Hopfgartner, G., Adduct annotation in liquid chromatography/high-resolution mass spectrometry to enhance compound identification. *Anal. Bioanal. Chem.* **2021,** 413, 503-517.
14. Domingo-Almenara, X.; Montenegro-Burke, J. R.; Benton, H. P.; Siuzdak, G., Annotation: A computational solution for streamlining metabolomics analysis. *Anal. Chem.* **2018,** 90, 480-489.
15. Parviainen, R. Synthesis, isomer separation and quantification of minor alkaloids in pepper fruits using high performance liquid chromatography. Master thesis's University of Helsinki, 2022.

Appendix

Authors contribution

Chapter 2. Ismail Ware, Katrin Franke, Mthandazo Dube, Hesham El-Enshasy, Ludger A. Wessjohann. Characterization and bioactive potential of secondary metabolites isolated from *Piper sarmentosum Roxb.* Manuscript in preparation.

In this project Ismail Ware performed the isolation and structural assignment of the constituents. Katrin Franke supported the structural elucidation, while Mthandazo Dube performed anthelmintic assay. Hesham El-Enshasy provided the plant material. Ismail Ware wrote the first draft of the manuscript. This project was designed, supervised, and edited by Ludger Wessjohann, and Katrin Franke.

Chapter 3. Ismail Ware, Ismail Ware, Katrin Franke, Andrej Frolov, Kseniia Bureiko, Elana Kysil, Maizatulakmal Yahayu, Hesham El-Enshasy, Ludger A. Wessjohann. Organ-specific metabolite variations in *Piper sarmentosum* Roxb. approached by LC-MS-based metabolic profiling. Manuscript in preparation.

In this project, all practical work, including data analysis and interpretation was performed by Ismail Ware. Katrin Franke and Andrej Frolov provided help with data analysis and interpretation. Hesham El-Enshasy and Maizatulakmal Yahayu provided the plant material while Kseniia Bureiko and Elana Kysil helped for MS measurements and statistical analysis. Ismail Ware wrote the manuscript first draft. This project was planned, supervised, and edited by Ludger Wessjohann and Katrin Franke.

Chapter 4. Ismail Ware, Katrin Franke, Hidayat Hussain, Ibrahim Morgan, Robert Rennert, Ludger A. Wessjohann. Bioactive phenolic compounds from *Peperomia obtusifolia.* This chapter was published in *Molecules* journal.

In this project Ismail Ware performed the isolation and structural assignment of the constituents. Katrin Franke and Hidayat Hussain helped in the structural elucidation, while Robert Rennert and Ibrahim Morgan performed biological studies. Ismail Ware wrote the first draft of the manuscript. This project was designed, supervised, and edited by Ludger Wessjohann, and Katrin Franke.

Chapter 2 - Characterization and bioactive potential of secondary metabolites isolated from *Piper sarmentosum* Roxb.

TABLE OF CONTENTS   **PAGE**

4"-(3-Hydroxy-3-methylglutaroyl)-2"-*β*-D-glucopyranosyl vitexin.

Figure S2.1: ^{1}H NMR spectrum of compound **2.1** (400 MHz, MeOH-*d*4)

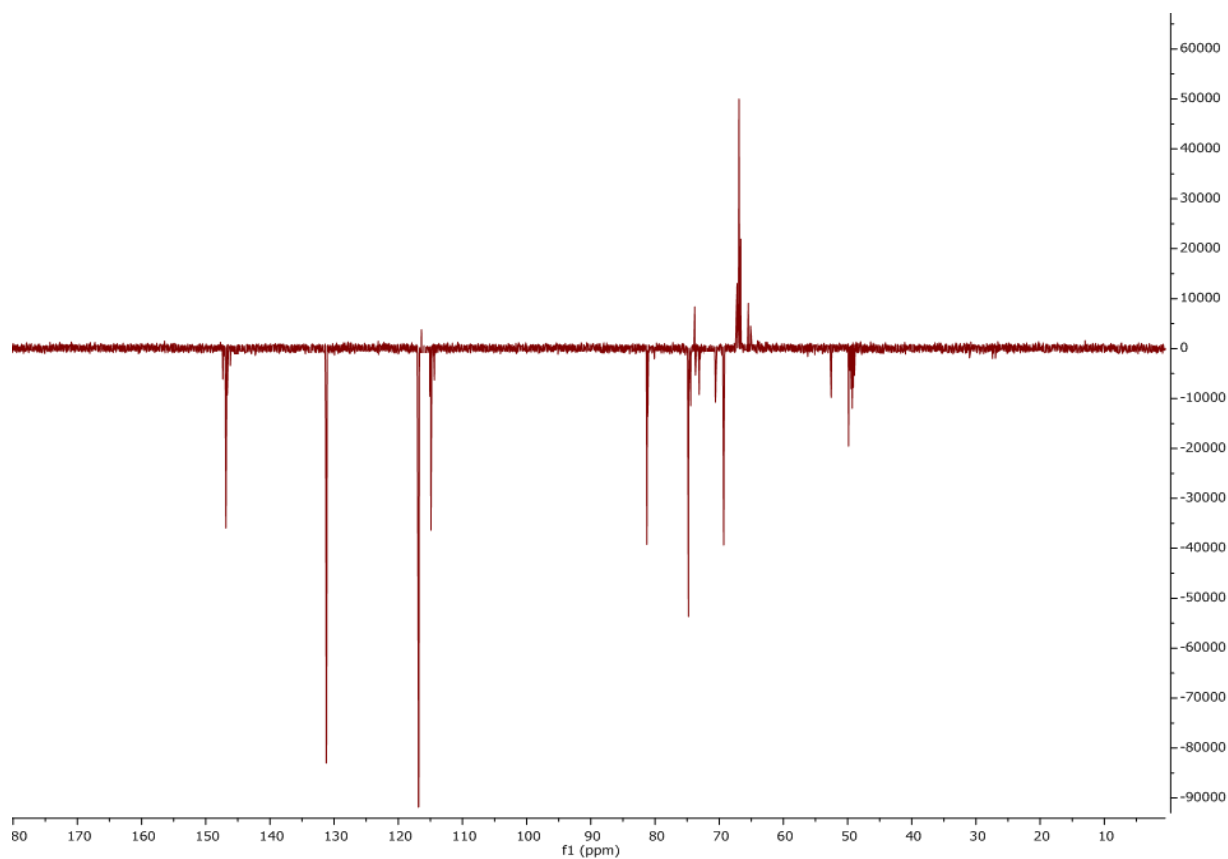**Figure S2.2**: ^{13}C NMR spectrum of compound **2.1** (100 MHz, MeOH-*d*4)
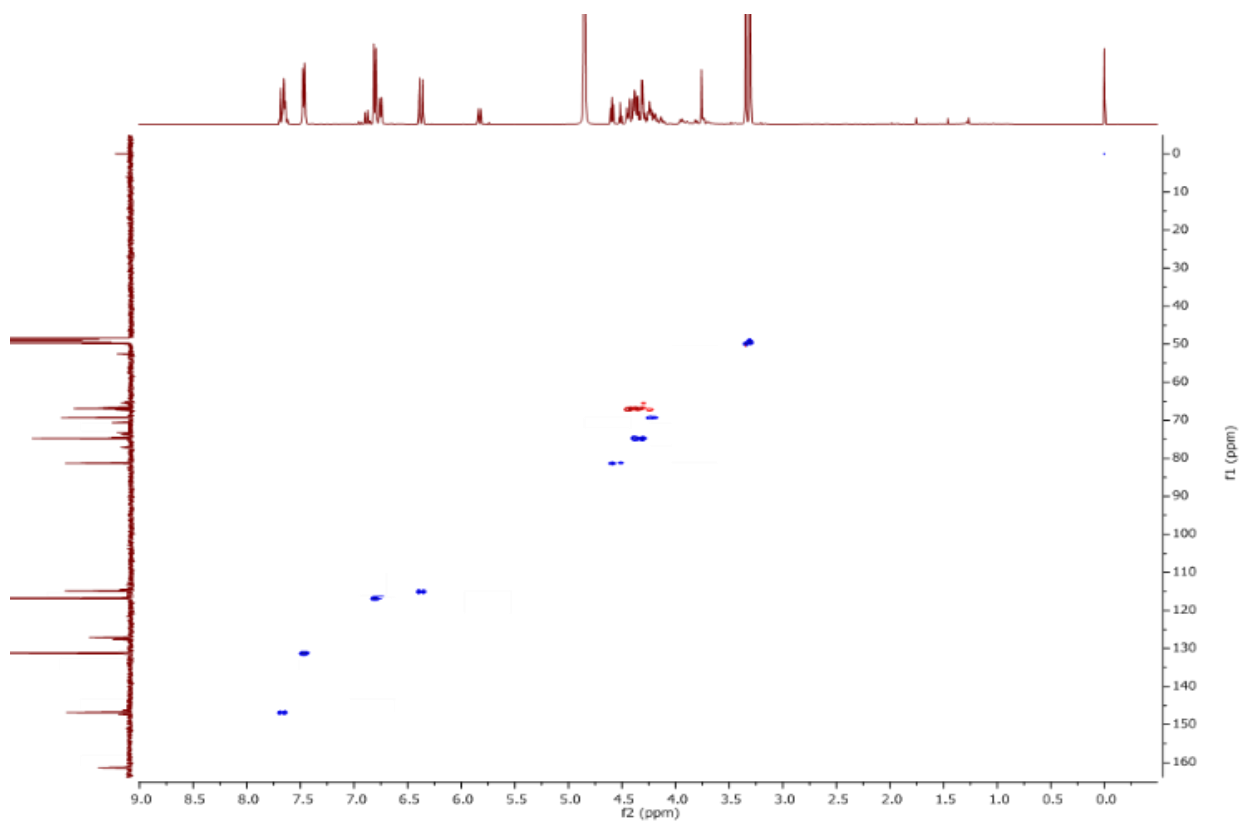
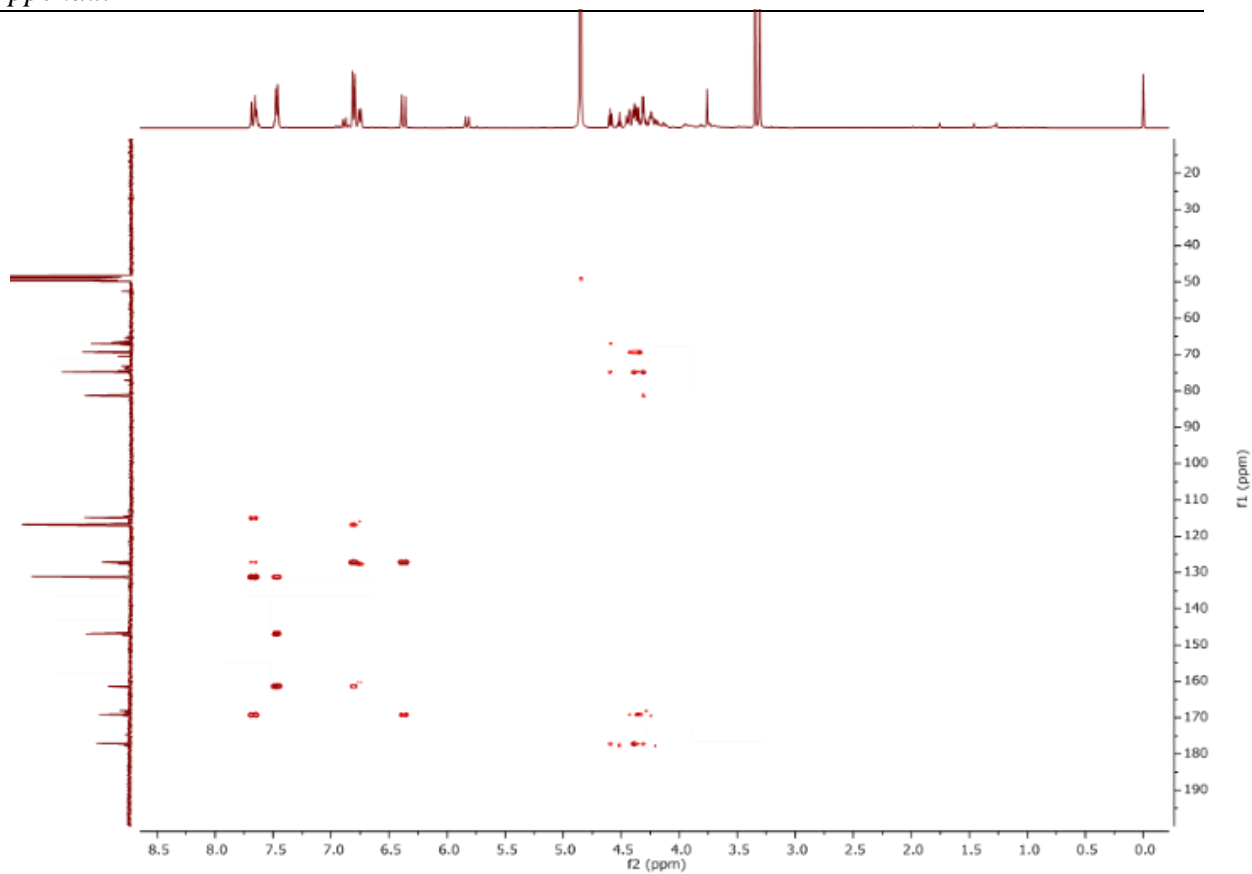**Figure S2.3**: HSQC spectrum of compound **2.1** (400 MHz, MeOH-*d*4)
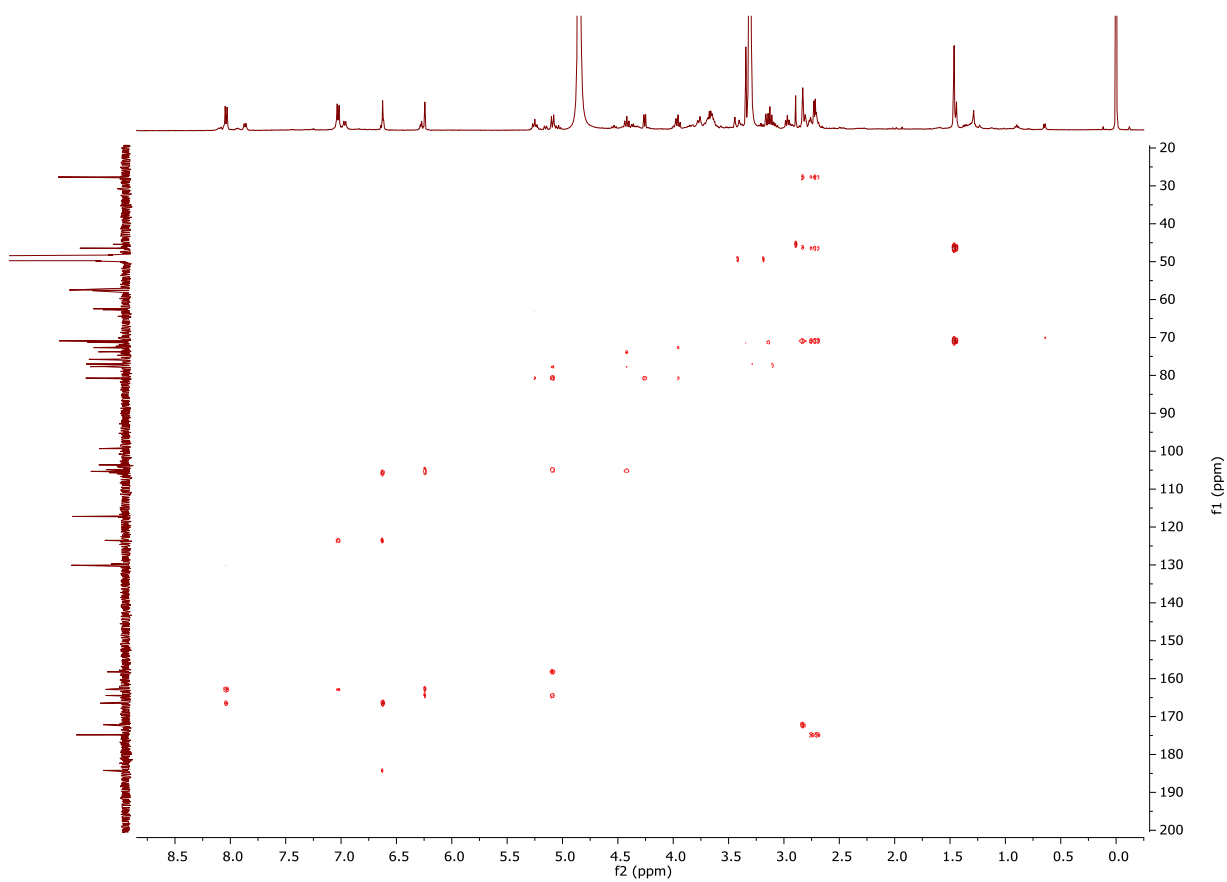
Figure S2.4: HMBC spectrum of compound **2.1** (400 MHz, MeOH-*d*4)
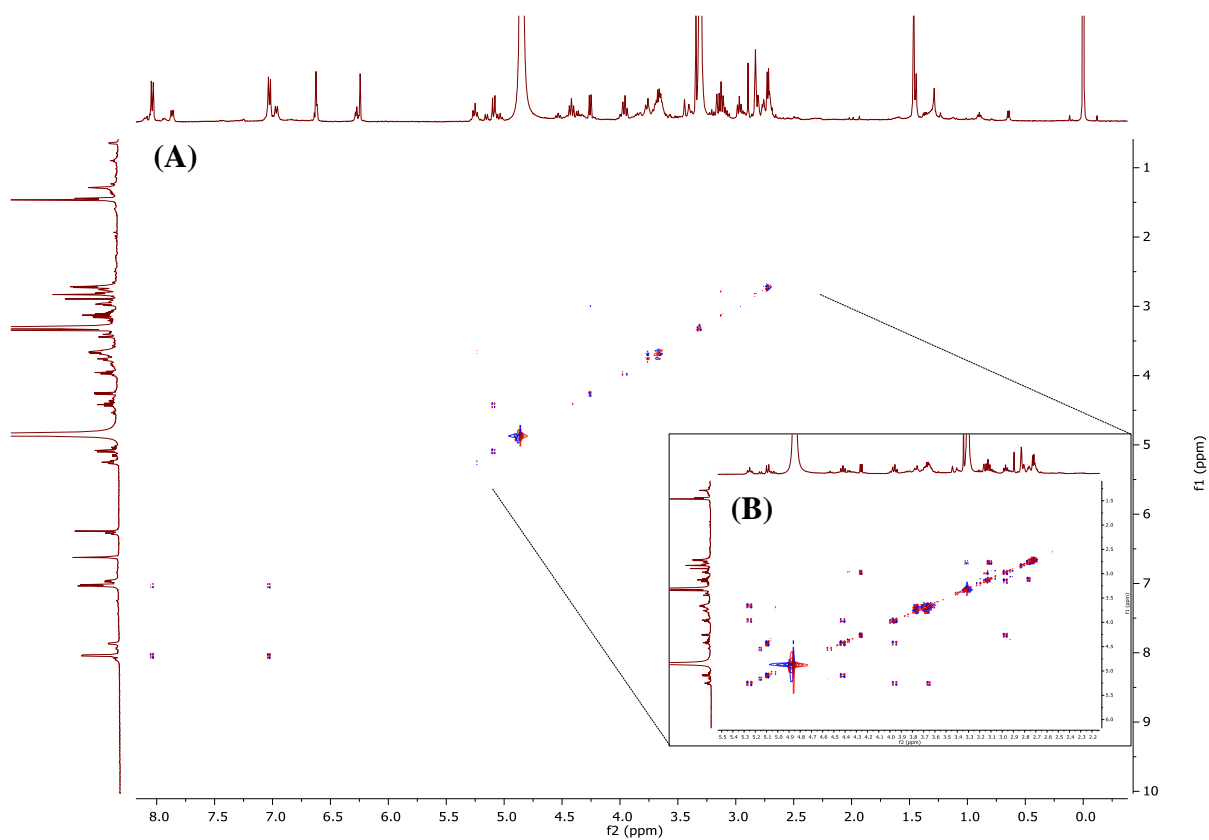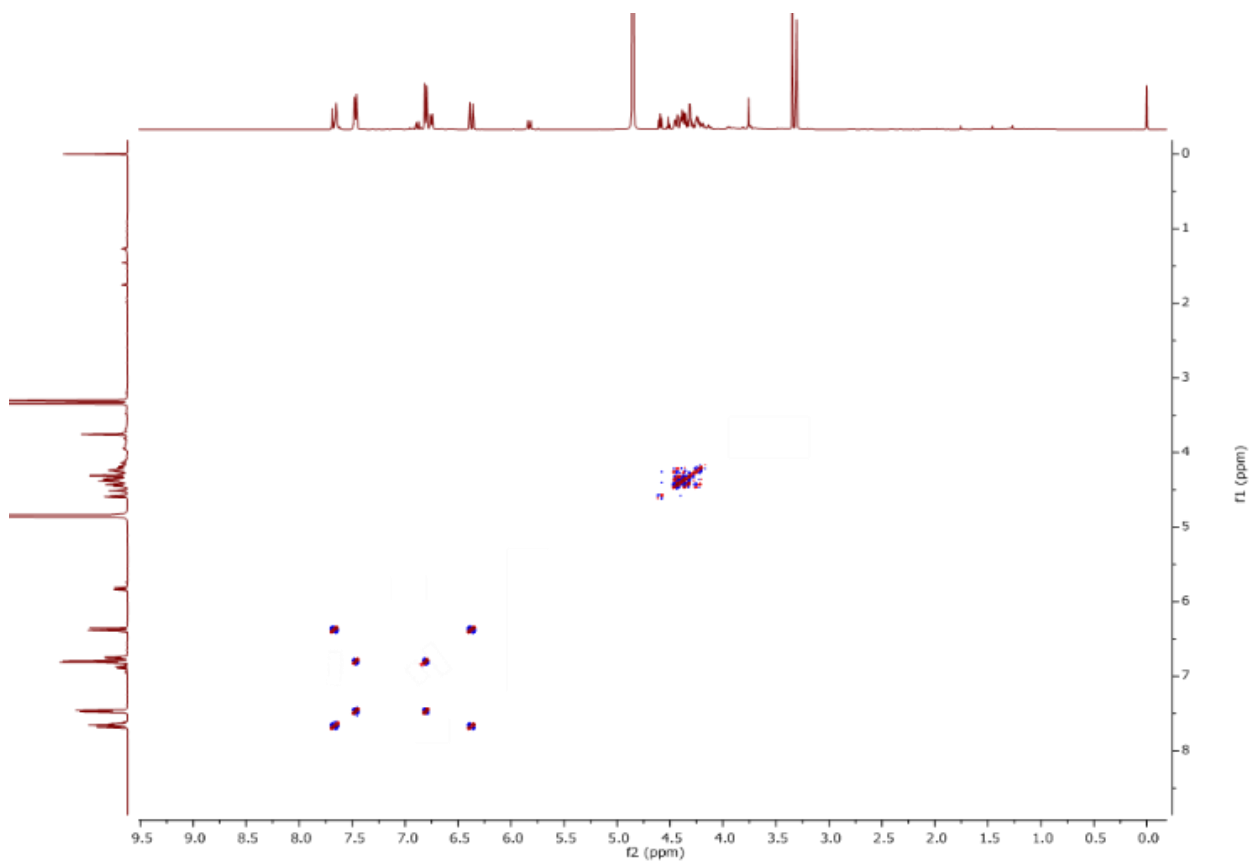
Figure S2.5: ^{1}H-^{1}H COSY spectrum of compound **2.1**; A) full spectrum, B) glycoside region (400 MHz, MeOH-*d*4)
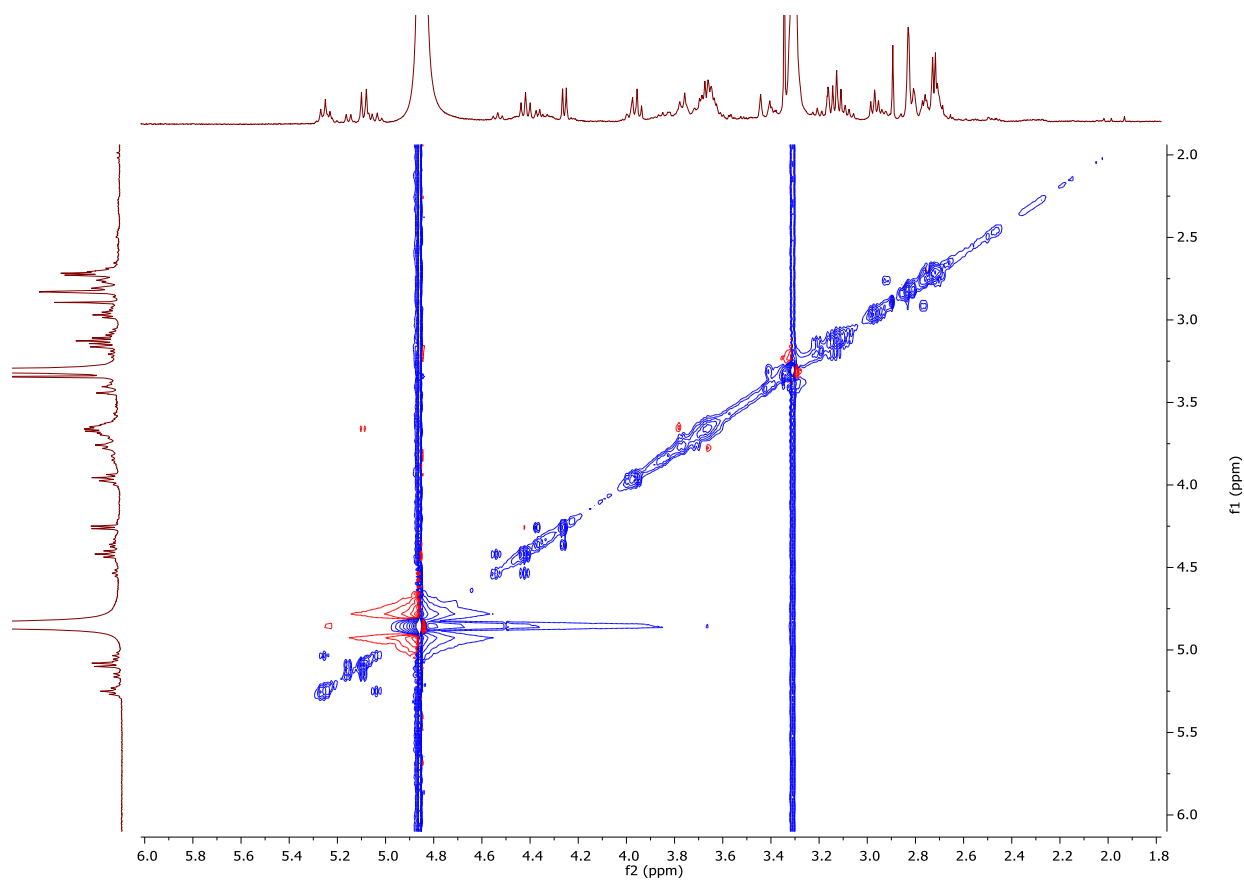
Figure S2.6: 2D-ROESY spectrum at glycoside region of compound **2.1** (400 MHz, MeOH-*d*4)
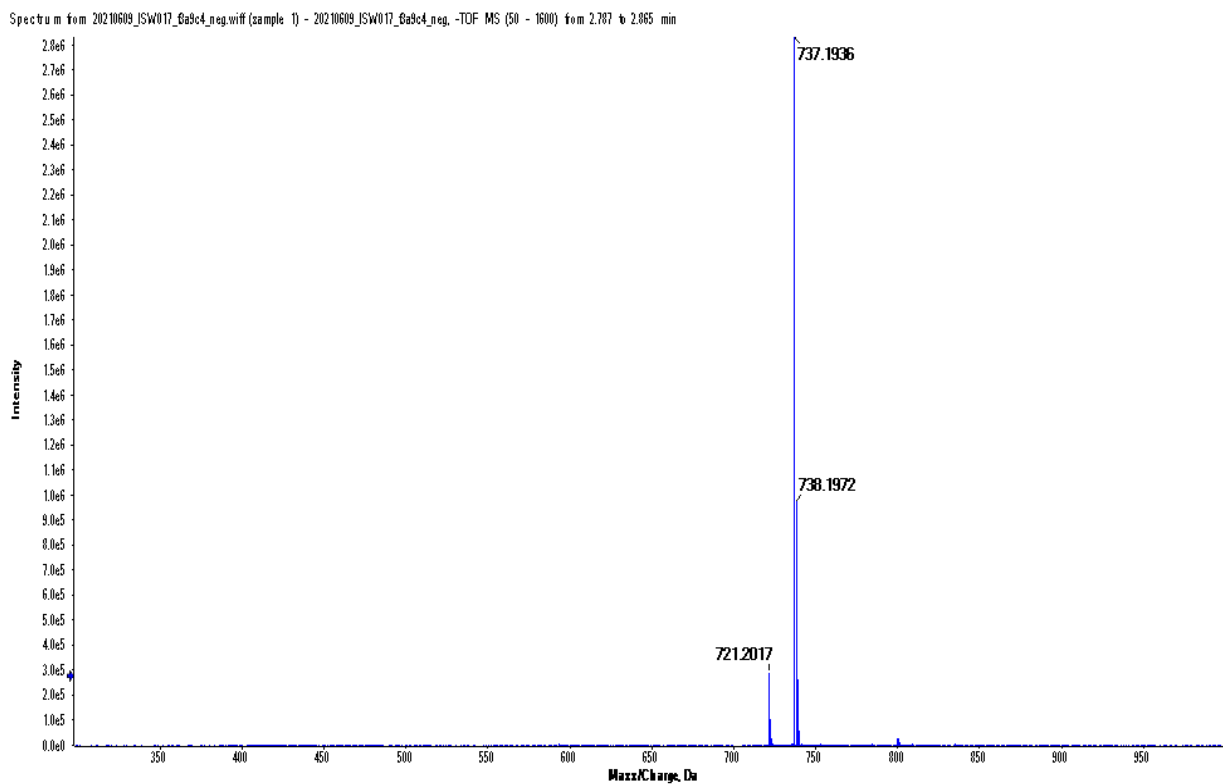
Figure S2.7: ESI-HRMS spectrum of compound **2.1** in negative ion mode
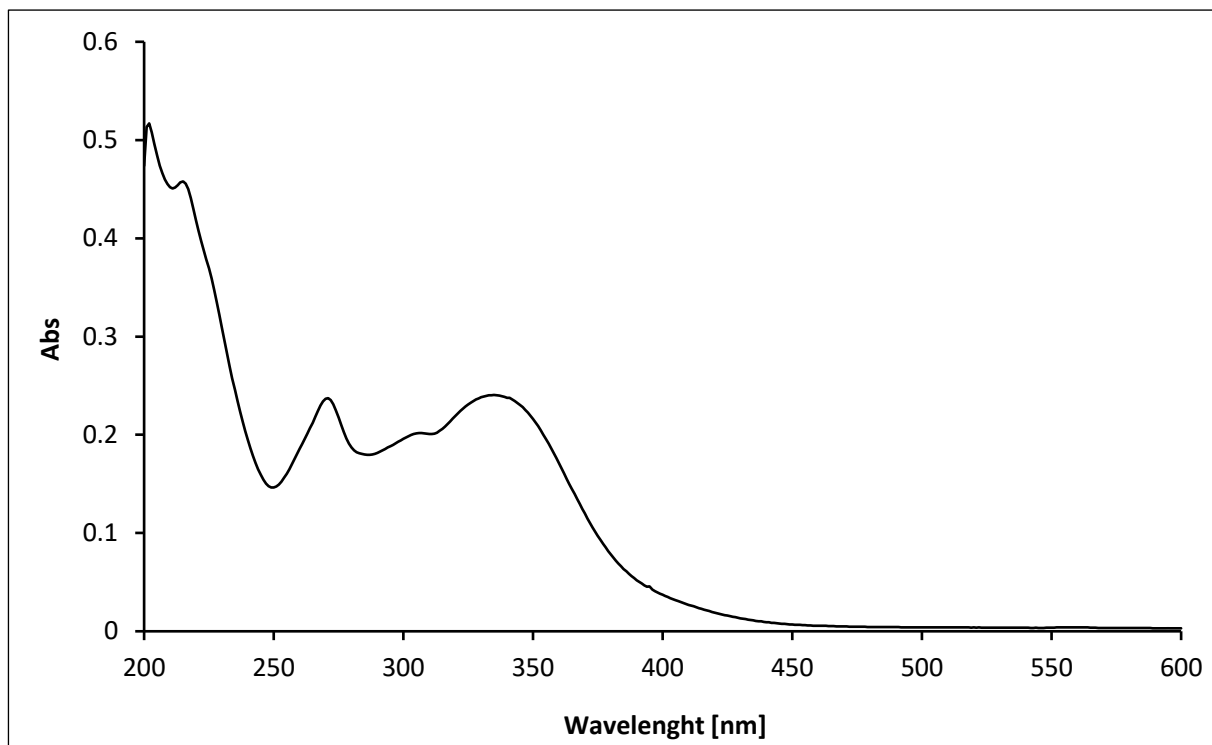
Figure S2.8: UV spectrum of compound **2.1** in MeOH

Table S2.1: Polarimeter data of compound **2.1**.

Light Source	WI
Wavelength	589 nm
Sample Aperture	Ø 3.0
Light Aperture	Ø 1.0
D.I.T.	5 sec
Cycle Times	20
Cycle Interval	5 sec
Path Length	50 mm
Concentration	0.153 W/V%
Factor	1.0000
Temp. Correct	0
Sample	**ISW017_f3a9c4**
Comment	1.53 mg / 1 ml Methanol
Optical Rotation	
Average	-0.0084 deg
S.D.	0.0003 deg
R.S.D.	4.1097 %
Specific O.R.	
Average	-10.9346
S.D.	0.4494
Temperatur	23.5° C

4-Allyl-5-methoxy-2-(β-D-glucopyranosyloxy-3-(4-methoxyphenyl) propanoate (Kadukoside)
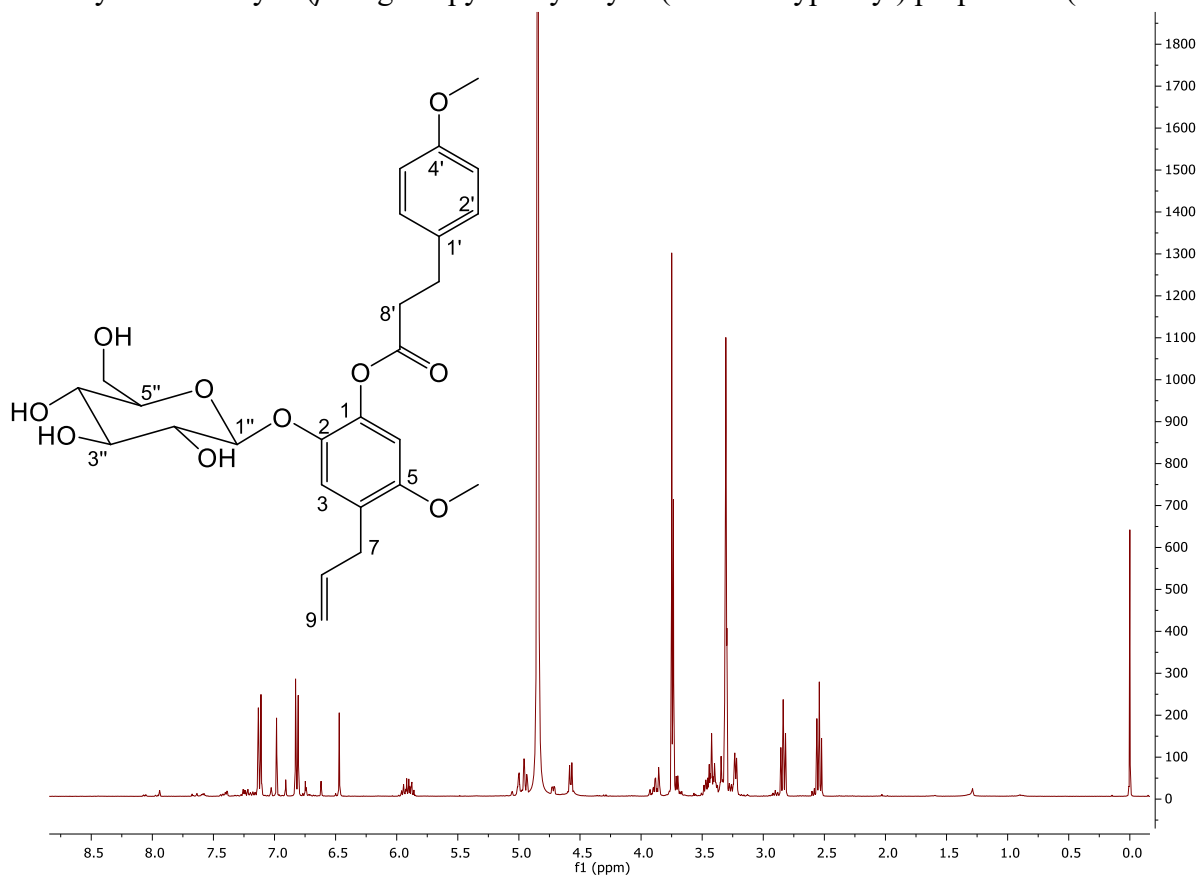
Figure S2.9: ¹H NMR spectrum of compound **2.2** (400 MHz, MeOH-*d*4)
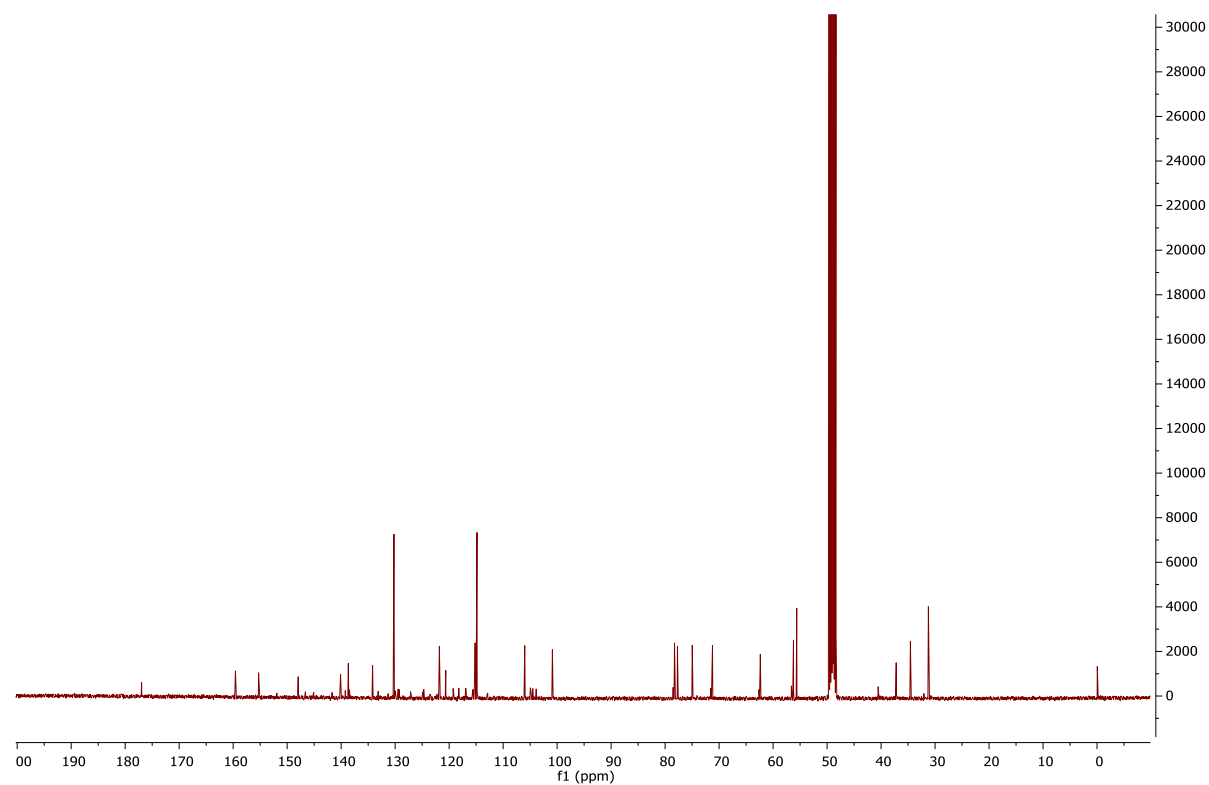
Figure S2.10 : ¹³C NMR spectrum of compound **2.2** (400 MHz, MeOH-*d*4)
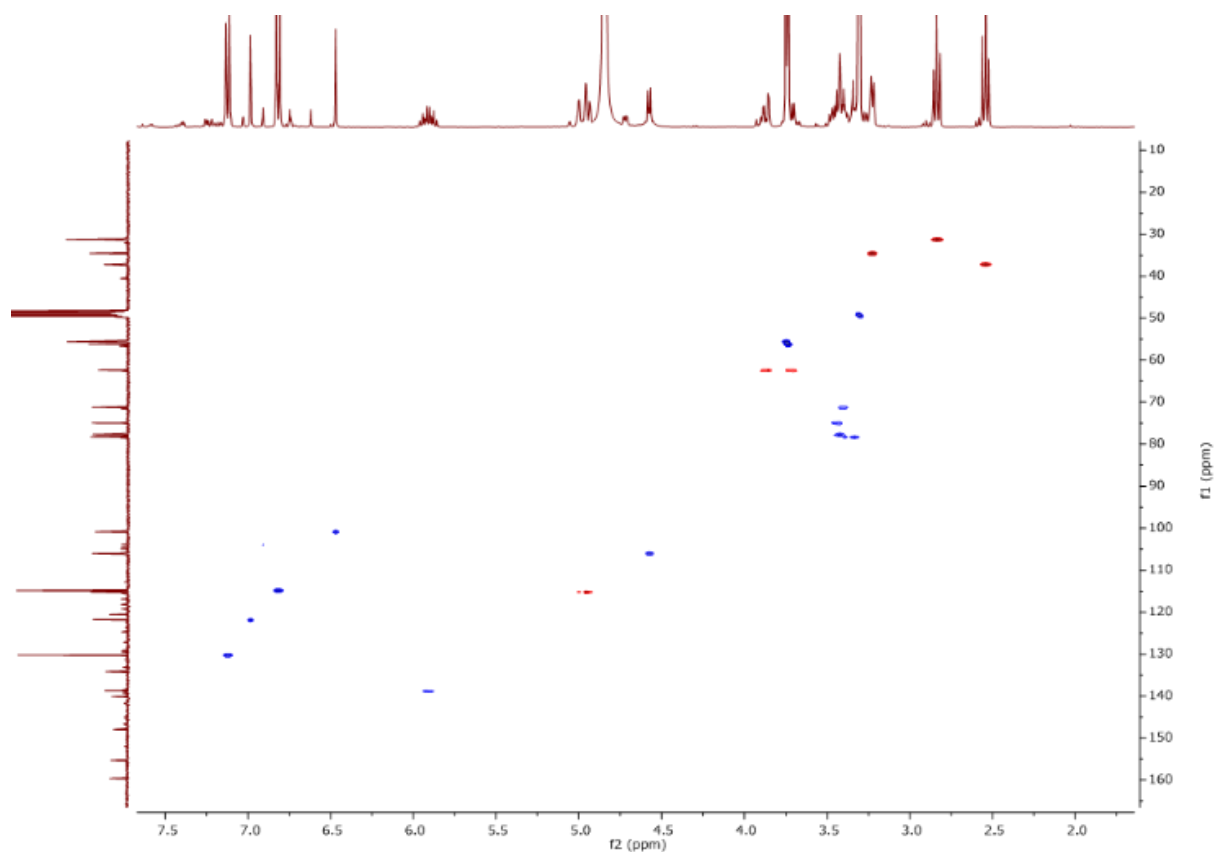
Figure S2.11: HSQC spectrum of compound **2.2** (400 MHz, MeOH-*d*4)
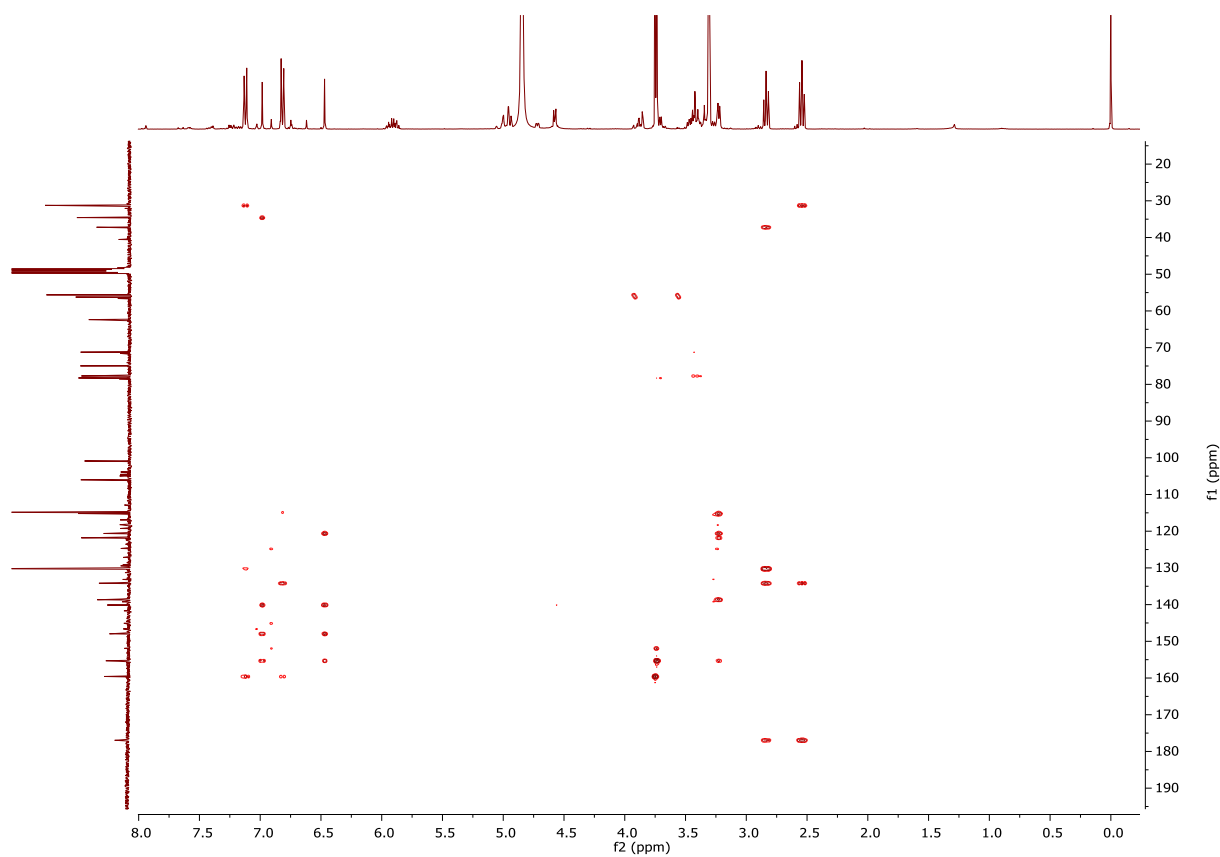
Figure S2.12: HMBC spectrum of compound **2.2** (400 MHz, MeOH-*d*4)
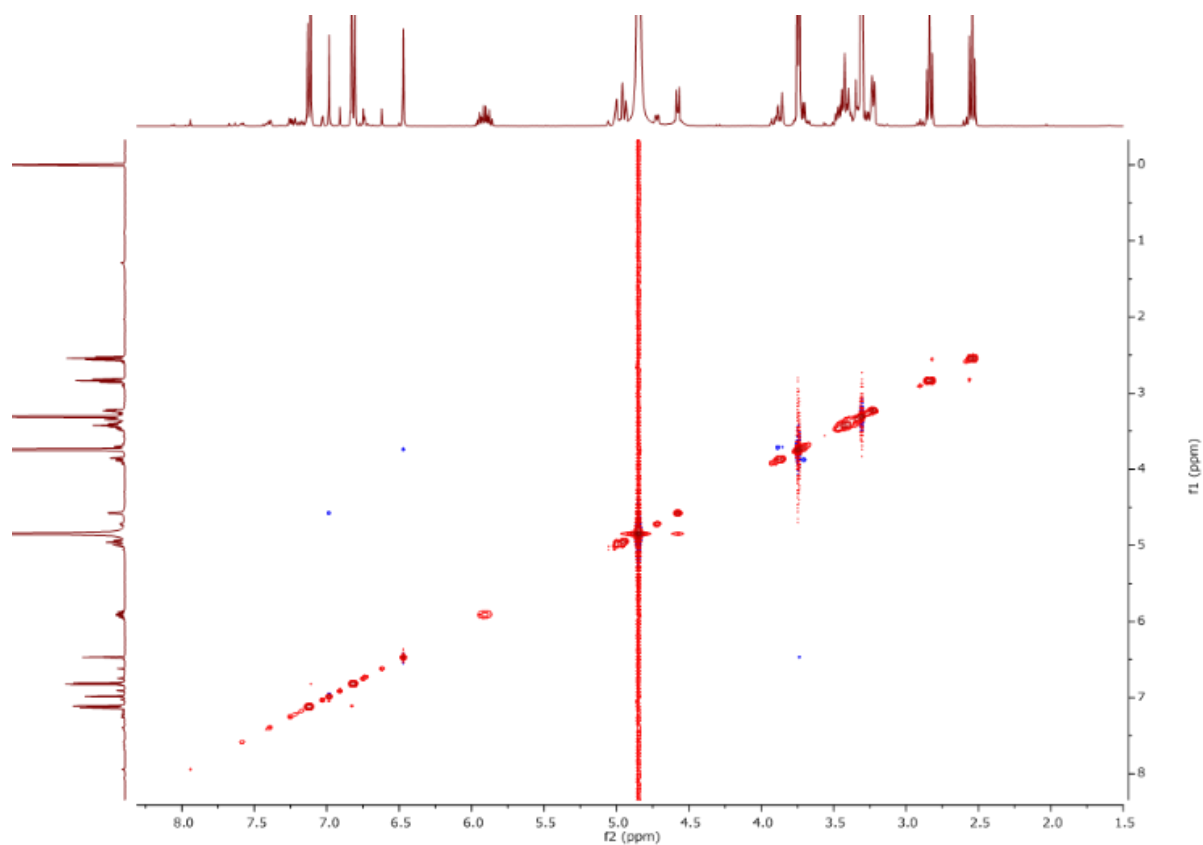
Figure S2.13: 2D-NOESY spectrum of compound **2.2** (400 MHz, MeOH-*d*4)
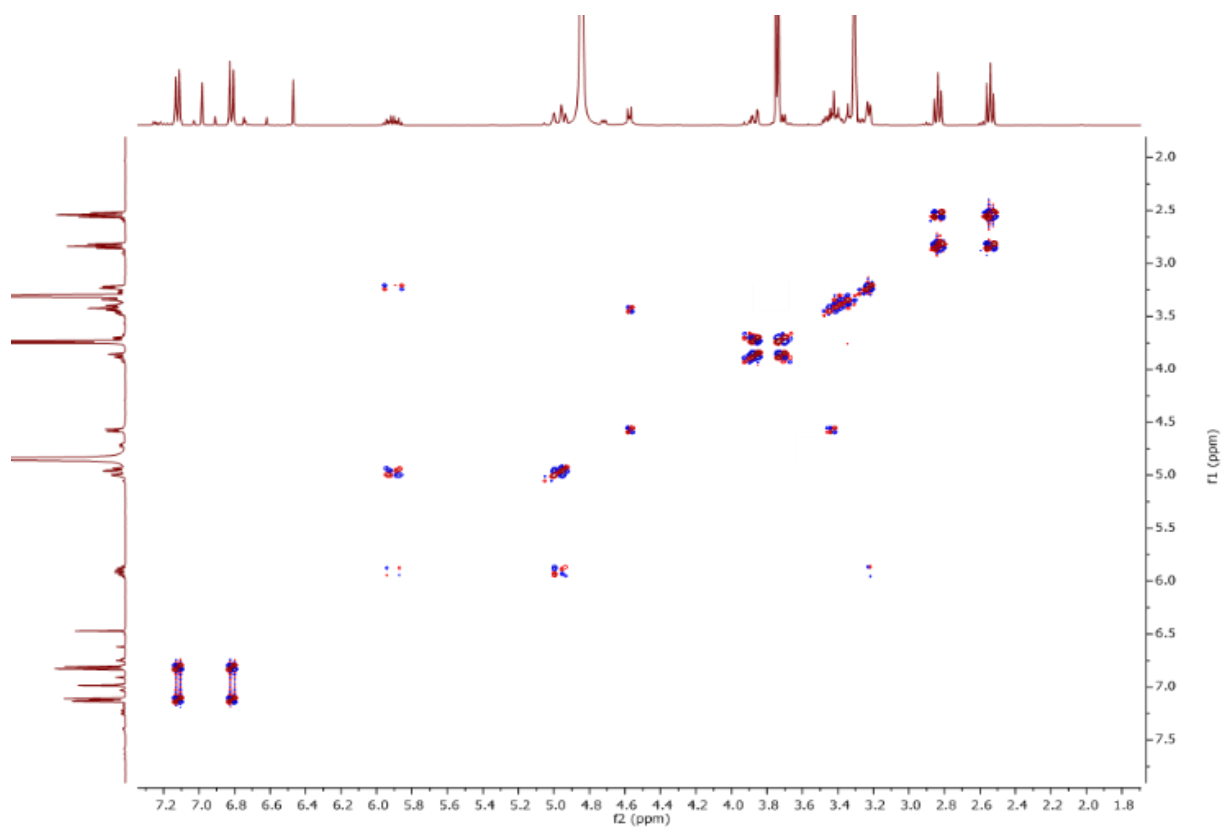
Figure S2.14: ¹H-¹H COSY spectrum of compound **2.2** (400 MHz, MeOH-*d*4)
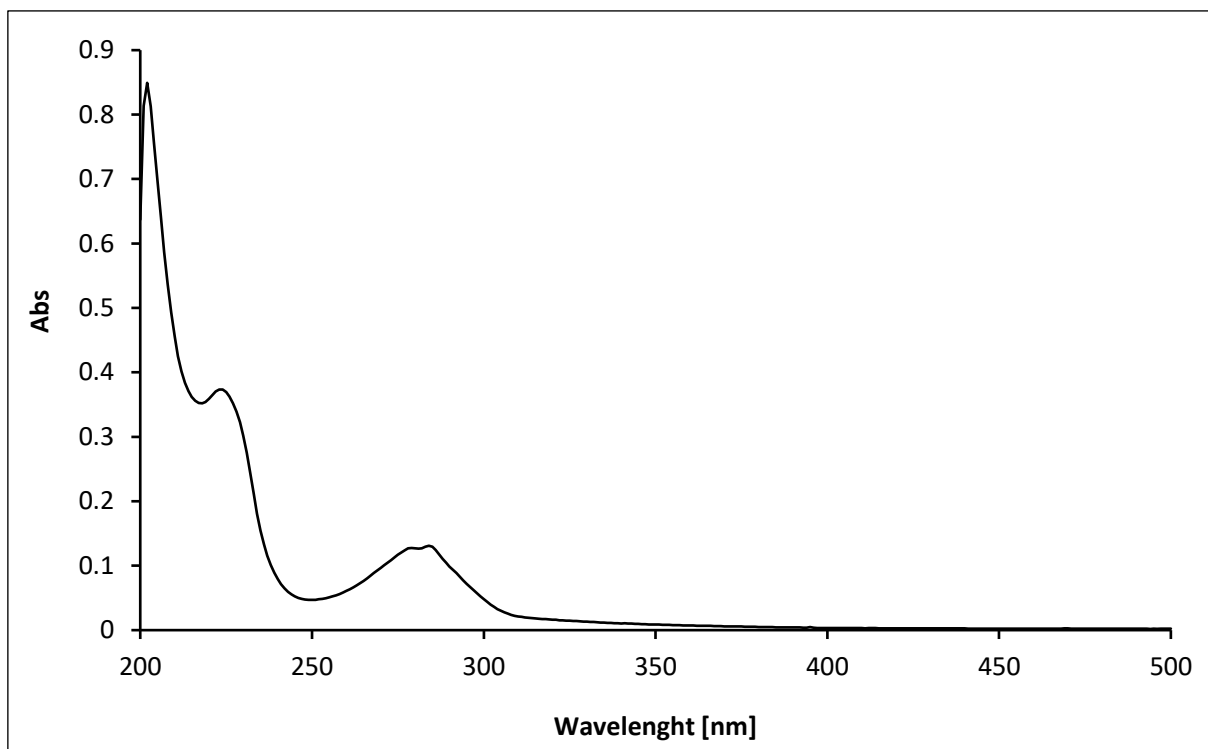
Figure S2.15: UV spectrum of compound **2.2** in MeOH

Spectrum from ISW016_f6de_8a_pos.wiff (sample 1) - ISW016_f6de_8a_pos, +TOF MS (100 - 2500) from 0.433 min, thresholded

505.2036

506.2033
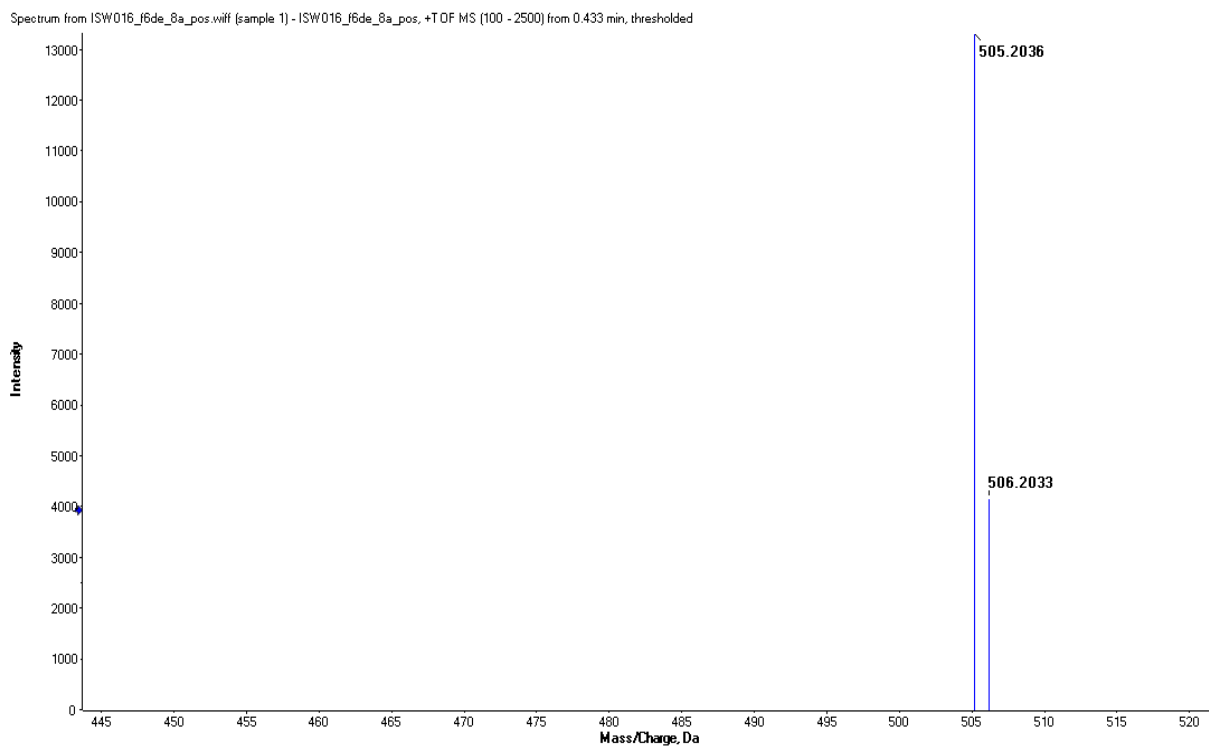
Figure S2.16: ESI-HRMS spectrum of compound **2.2** in positive ion mode

6-O-*trans*-*p*-Coumaroyl-D-glucono-1,4-lactone
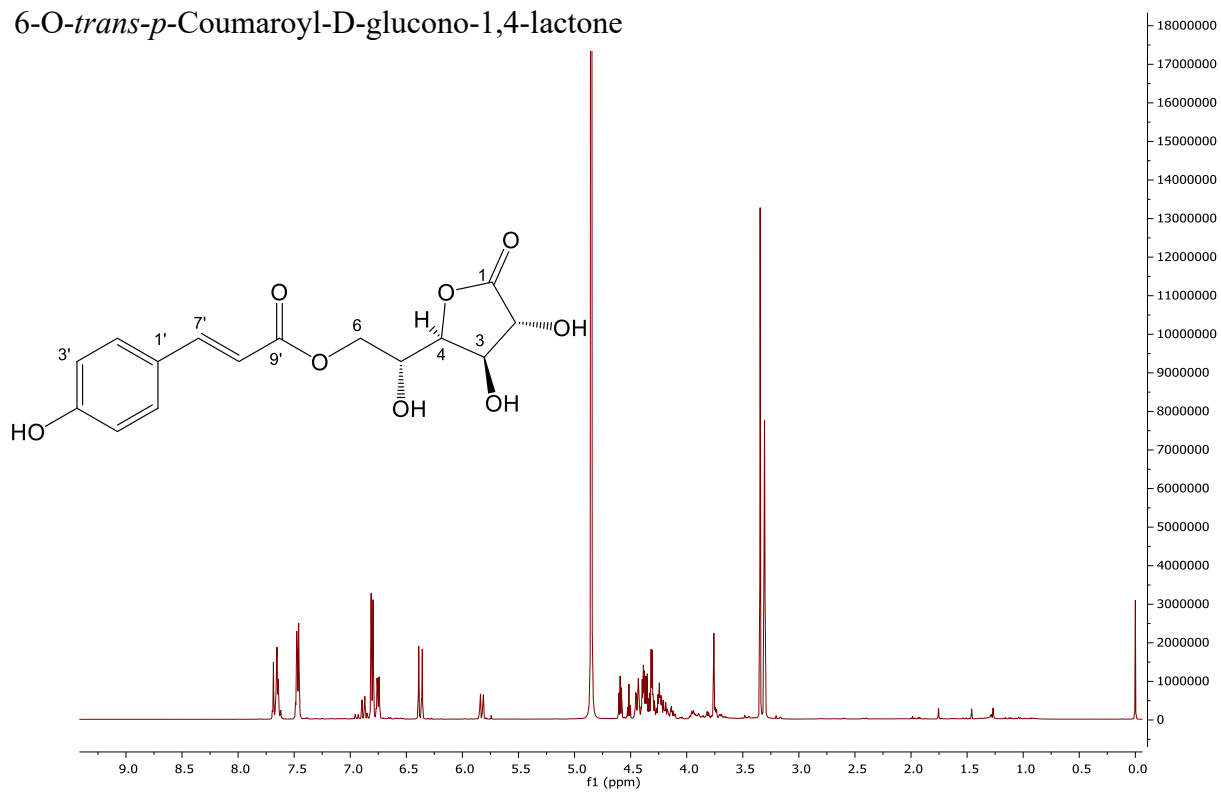
Figure S2.17: ^{1}H NMR spectrum of compound **2.3** (400 MHz, MeOH-*d*4)
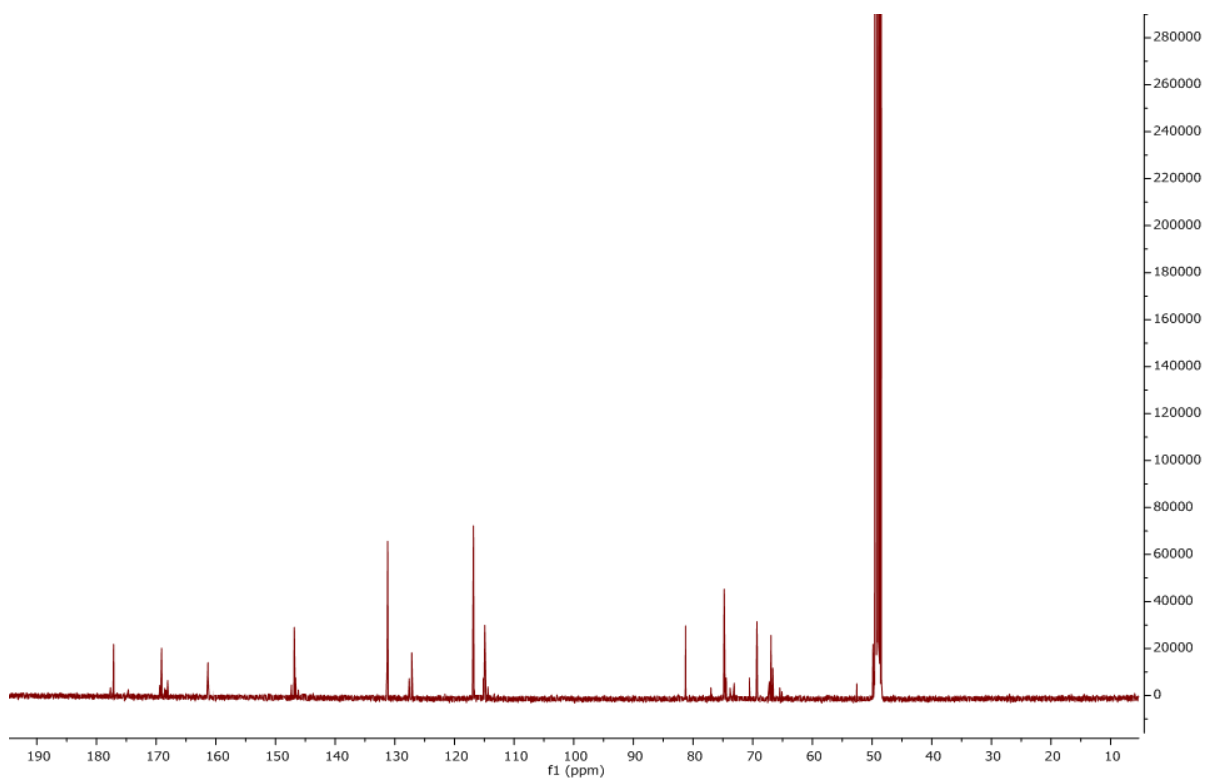
Figure S2.18: ^{13}C NMR spectrum of compound **2.3** (100 MHz, MeOH-*d*4)

Figure S2.19: DEPT135 spectrum of compound **2.3** (100 MHz, MeOH-*d*4)

Figure S2.20: HSQC spectrum of compound **2.3** (400 MHz, MeOH-*d*4)

Figure S2.21: HMBC spectrum of compound **2.3** (400 MHz, MeOH-*d*4)

Figure S2.22: ¹H-¹H COSY spectrum of compound **2.3** (400 MHz, MeOH-*d*4)
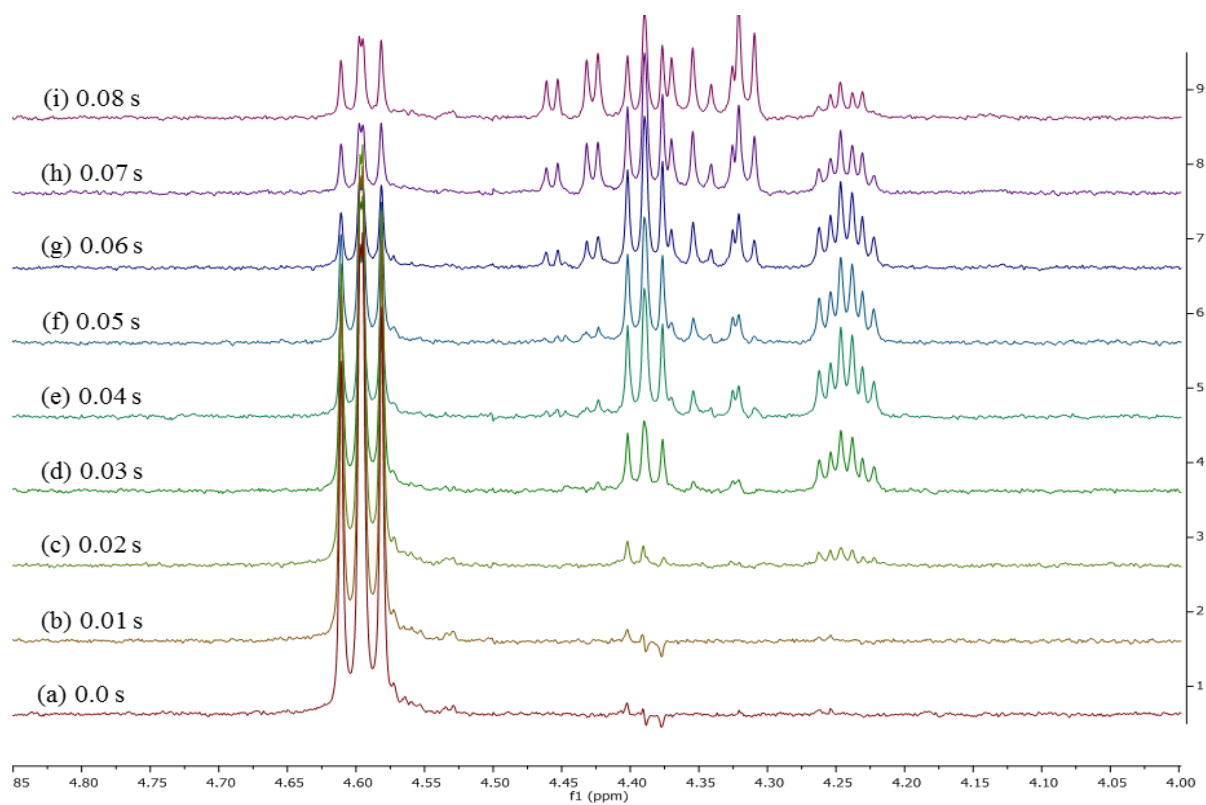
Figure S2.23: 1D-TOCSY spectrum of compound **2.3** with selective excitation of H-4 (δ_H 4.59) and mixing times (400 MHz, MeOH-*d*4)
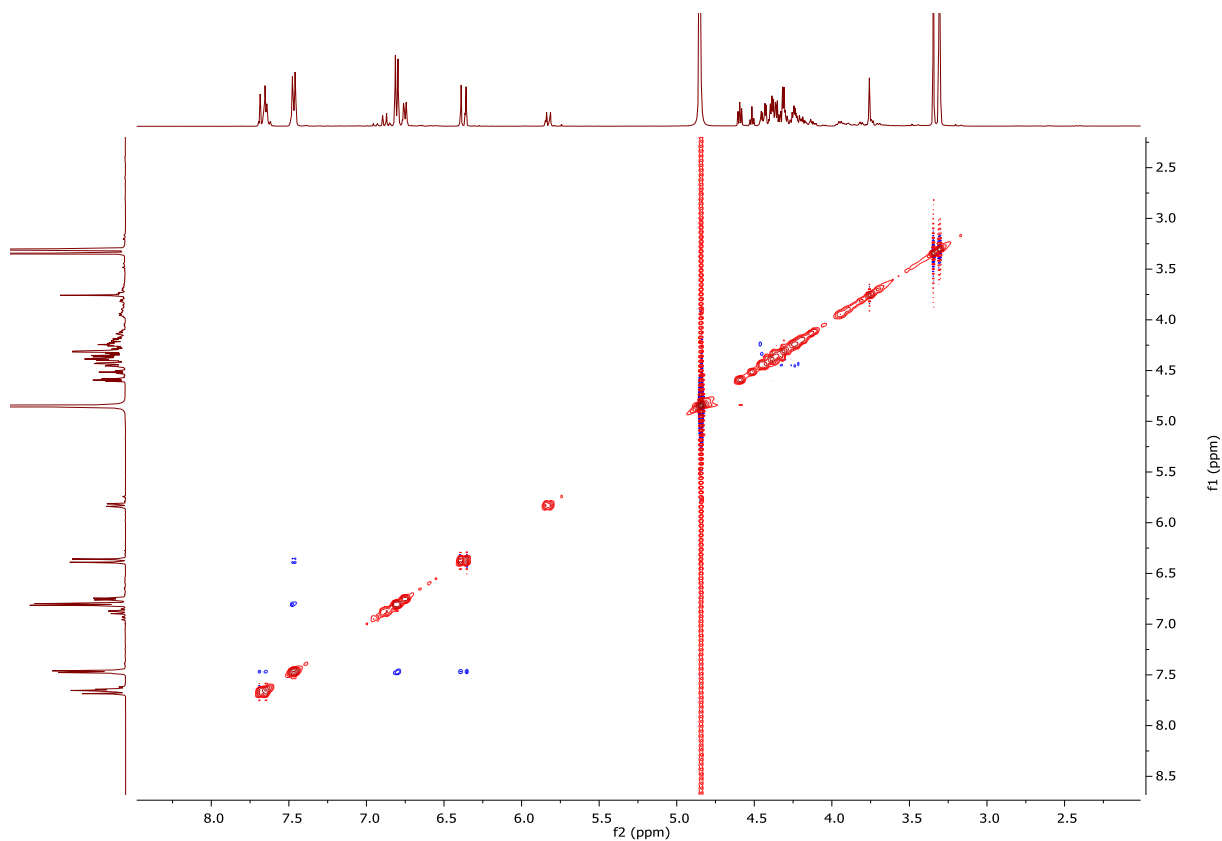
Figure S2.24: 2D-NOESY spectrum of compound **2.3** (400 MHz, MeOH-*d*4)

Spectrum from ISW017_f3b2g_neg.wiff (sample 1) - ISW017_f3b2g, -TOF MS (50 - 1600) from 4.468 to 4.518 min
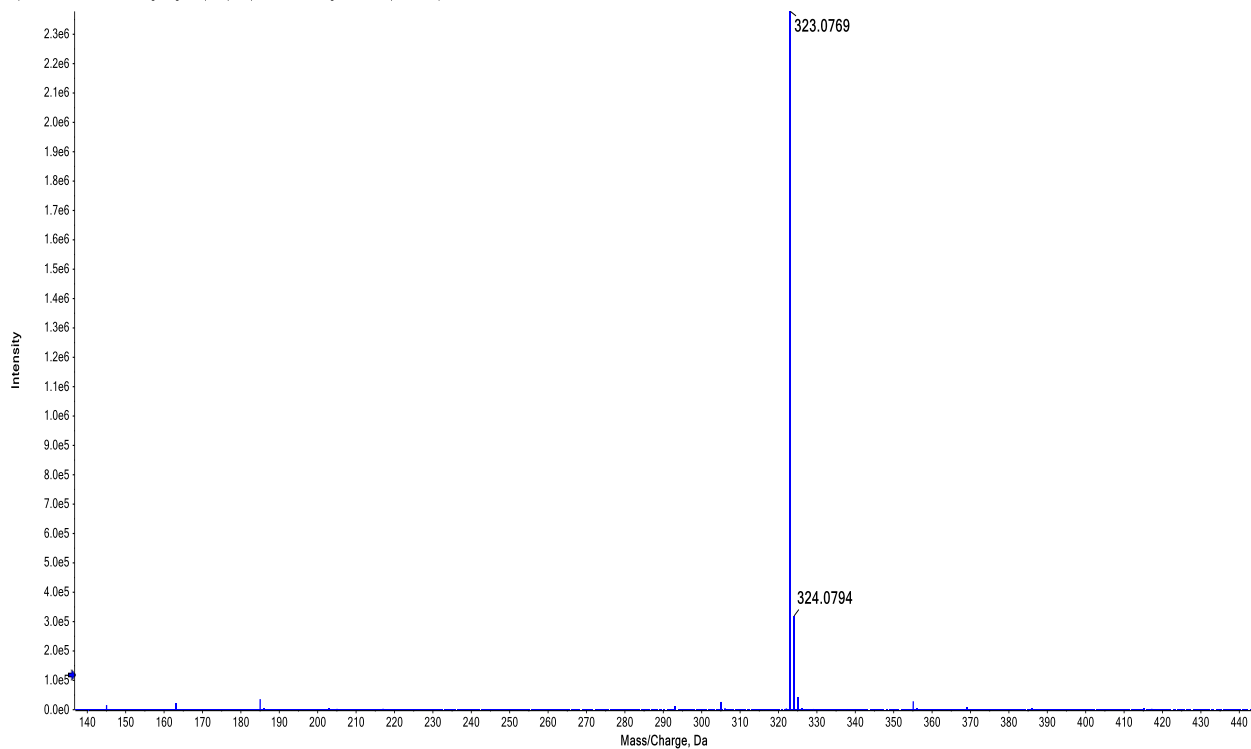
Figure S2.25: ESI-HRMS spectrum of compound **2.3** in negative ion mode
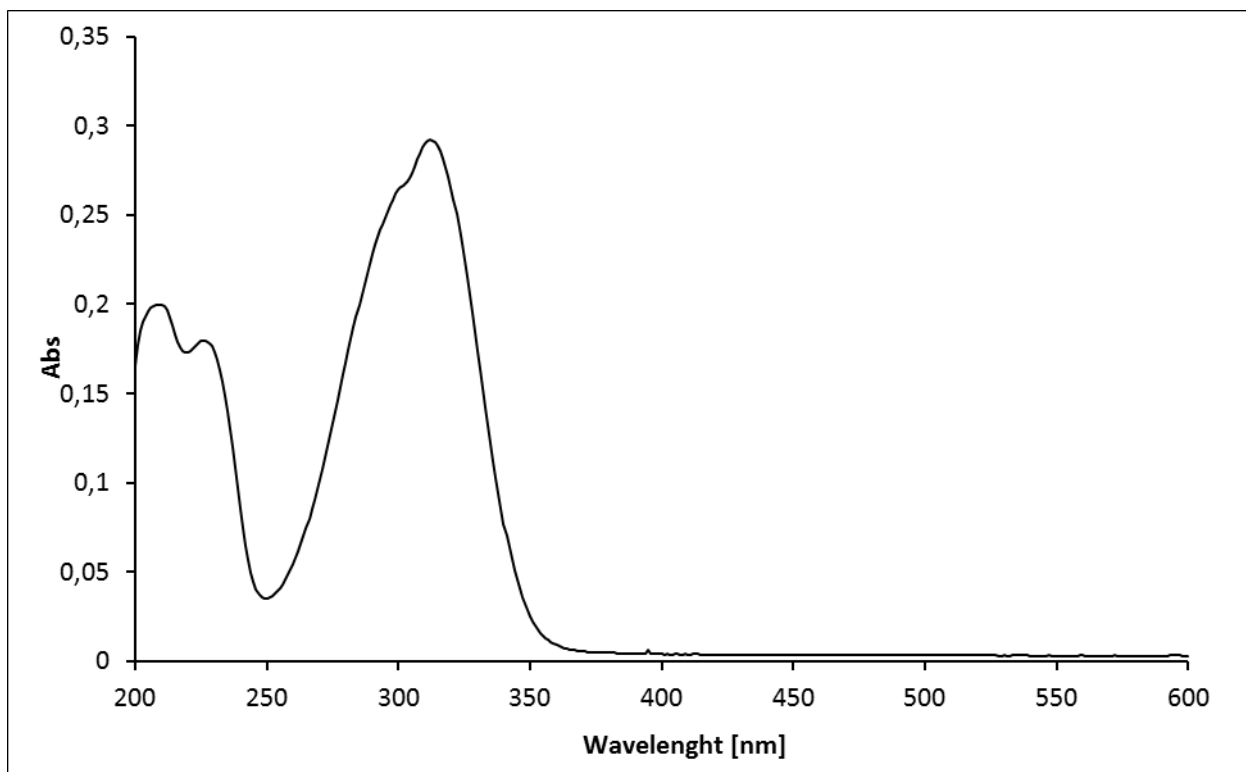
Figure S2.26: UV spectrum of compound **2.3** in MeOH

Table S2.2: Polarimeter data of compound **2.3**.

Light Source	WI
Wavelength	589 nm
Sample Aperture	Ø 3.0
Light Aperture	Ø 1.0
D.I.T.	5 sec
Cycle Times	20
Cycle Interval	5 sec
Path Length	50 mm
Concentration	0.247 W/V%
Factor	1.0000
Temp. Correct	0
Sample	**ISW017_f3b2g**
Comment	2.47 mg / 1 ml Methanol
Optical Rotation	
Average	0.0050 deg
S.D.	0.0002 deg
R.S.D.	4.2827 %
Specific O.R.	
Average	4.0445
S.D.	0.1732
Temperatur	23.2° C
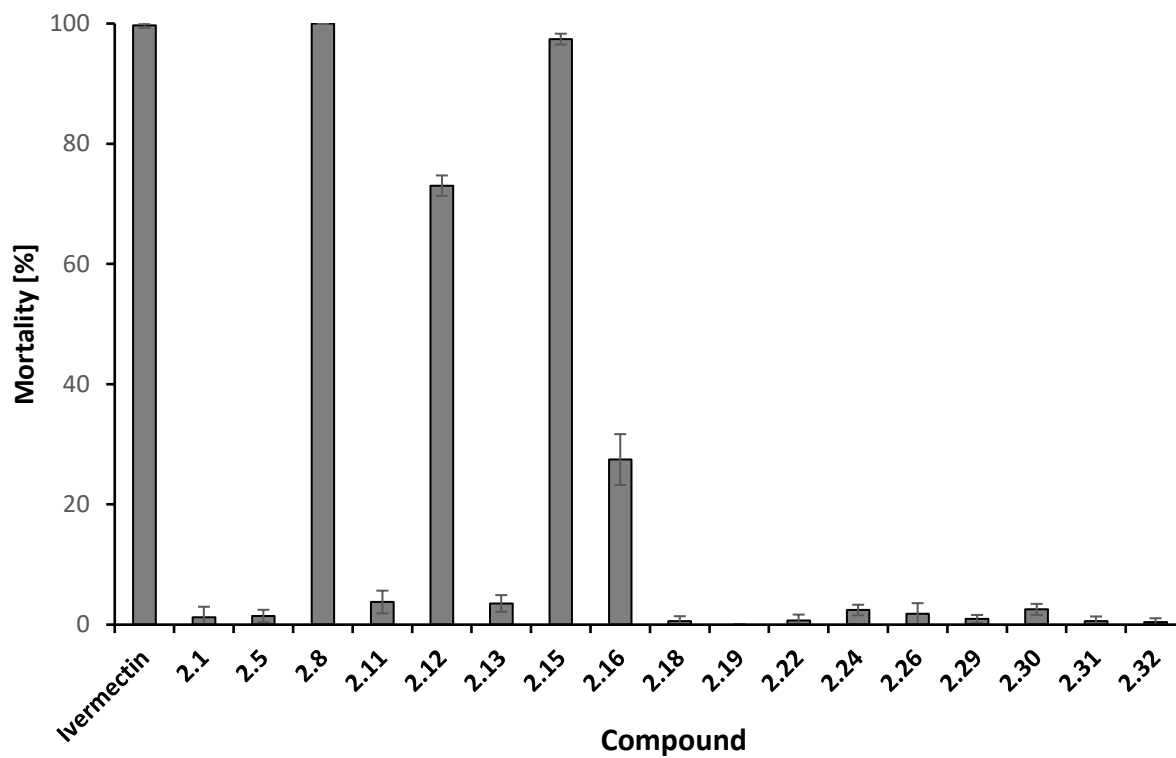
Figure S2.27: Screening of anthelmintic activity against *C. elegans* of isolated compounds at 500 ppm. Positive control ivermectin 10 μg/mL killed 100% of the nematodes. Mortality % based on three replicates.

Table S2.3: Antifungal (*Botrytis cinerea, Septoria tritici*), antioomycotic (*Phytophthora infestans*), and antibacterial (*Aliivibrio fisheri*) activities of isolated compounds from *P. sarmentosum*.

	Antifungal assays			Antibacterial assays
	Growth inhibition [%][a]			Growth inhibition [%][a]
	B. cinerea	*S. tritici*	*P. infestans*	*A. fischeri*
Compound	**125 μM**	**125 μM**	**125 μM**	**100 μM**[b]
2.1	-18.6 ± 13.4	14.6 ± 15.5	-10.7 ± 3.0	-13.9 ± 11.4
2.2	6.8 ± 20.5	84.9 ± 3.4	94.4 ± 0.7	-33.2 ± 19.3
2.3	15.6 ± 6.7	12.1 ± 9.9	4.2 ± 2.4	8.2 ± 12.1
2.4	7.7 ± 11.1	48.3 ± 4.2	-39.6 ± 8.5	2.1 ± 9.7
2.5	-49.9 ± 9.4	22.3 ± 6.6	-12.4 ± 9.5	-7.1 ± 13.6
2.6	20.8 ± 6.3	-33.9 ± 16.4	-9.2 ± 9.4	-41.4 ± 19.8
2.7	29.9 ± 10.3	-11.7 ± 14.5	1.1 ± 2.0	-34.67 ± 26.3
2.8	48.4 ± 10.9	44.9 ± 8.3	-31.0 ± 13.0	-3.3 ± 9.2
2.9	21.6 ± 5.1	-7.7 ± 8.1	-12.6 ± 9.3	-43.5 ± 12.9
2.10	1.9 ± 6.9	13.2 ± 7.3	3.1 ± 2.8	-4.7 ± 11.7
2.11	20.1 ± 4.7	42.3 ± 1.9	0.4 ± 10.0	-15.4 ± 10.3
2.12	39.2 ± 14.3	44.1 ± 1.9	28.5 ± 1.8	-73.9 ± 27.4
2.13	-	-	-	-
2.14	-	-	-	-
2.15	96.9 ± 1.6	-0.1 ± 5.2	20.0 ± 2.5	-49.4 ± 6.4
2.16	8.3 ± 6.1	6.7 ± 5.6	-5.4 ± 9.1	6.2 ± 7.6
2.17	-	-	-	-
2.18	5.2 ± 1.6	0.8 ± 6.8	-18.1 ± 17.9	40.7 ± 4.8
2.19	2.6 ± 6.2	-7.5 ± 6.9	-10.3 ± 5.5	85.4 ± 0.2
2.20	-	-	-	-
2.21	33.9 ± 9.0	6.3 ± 23.8	0.8 ± 1.6	100. ± 0.1
2.22	-36.3 ± 24.5	-7.1 ± 16.3	-31.5 ± 16.7	-53.3 ± 15.6
2.23	81.9 ± 1.7	44.5 ± 3.9	2.4 ± 6.8	99.6 ± 0.3
2.24	87.8 ± 7.5	36.8 ± 4.5	7.5 ± 4.3	41.1 ± 3.9
2.25	28.4 ± 5.5	-1.8 ± 7.5	27.2 ± 13.9	-16.2 ± 8.6
2.26	32.9 ± 12.5	-13.5 ± 10.7	-7.8 ± 6.6	-91.7 ± 16.1
2.27	-	-	-	-
2.28	30.4 ± 3.8	12.1 ± 17.4	3.1 ± 3.5	-55.5 ± 19.1
2.29	0.4 ± 4.8	34.5 ± 6.4	-35.7 ± 0.6	-5.3 ± 16.6
2.30	32.8 ± 5.8	-1.9 ± 13.7	-22.9 ± 4.6	14.1 ± 13.0
2.31	37.7 ± 3.1	-25.1 ± 20.2	-19.5 ± 10.7	8.4 ± 4.1
2.32	34.8 ± 6.6	-31.1 ± 29.3	-18.6 ± 7.1	-14.5 ± 6.8
2.33	-	-	-	-
2.34	-	-	-	-
Pos. control	125 μM epoxiconazole		125 μM terbinafine	100 μM chloramphenicol
	92.0 ± 1.4		96.8 ± 1.2	99.0 ± 0

[a] Negative values indicate an increase of fungal or bacterial growth in comparison to the negative control (0% inhibition).
[b] Growth inhibition rates below 50% indicate IC_{50} values > 100 μM.
– indicates not tested.

Chapter 3 - Organ-specific metabolite variations in *Piper sarmentosum* Roxb. approached by LC-MS-based metabolic profiling

Metabolite annotation: Detailed classification of selected piperamide groups
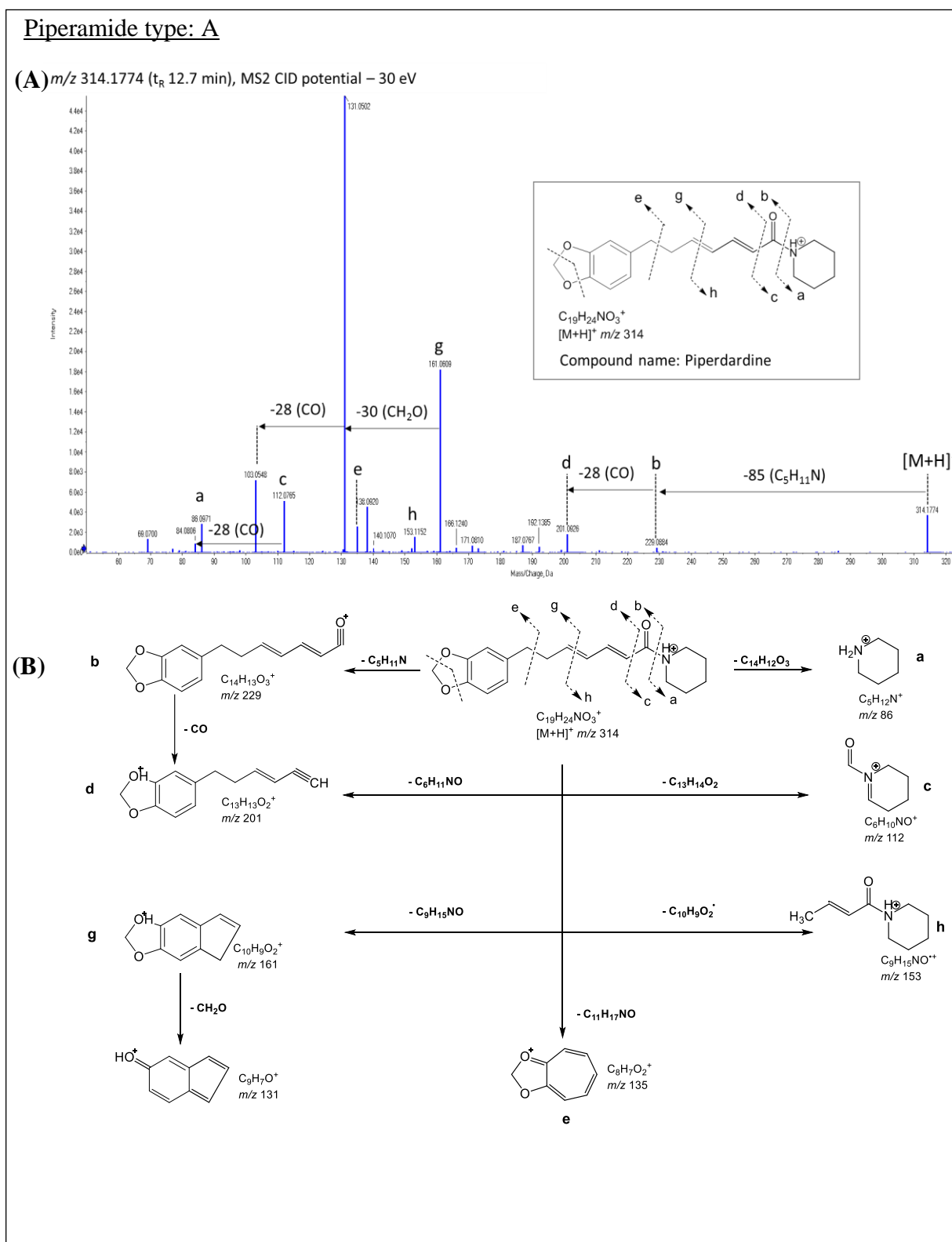

Figure S3.1: Metabolite annotation of selected piperamide type A compound (**P108**): **(A)** MS/MS spectra, **(B)** proposed fragmentation pathway of key ions.
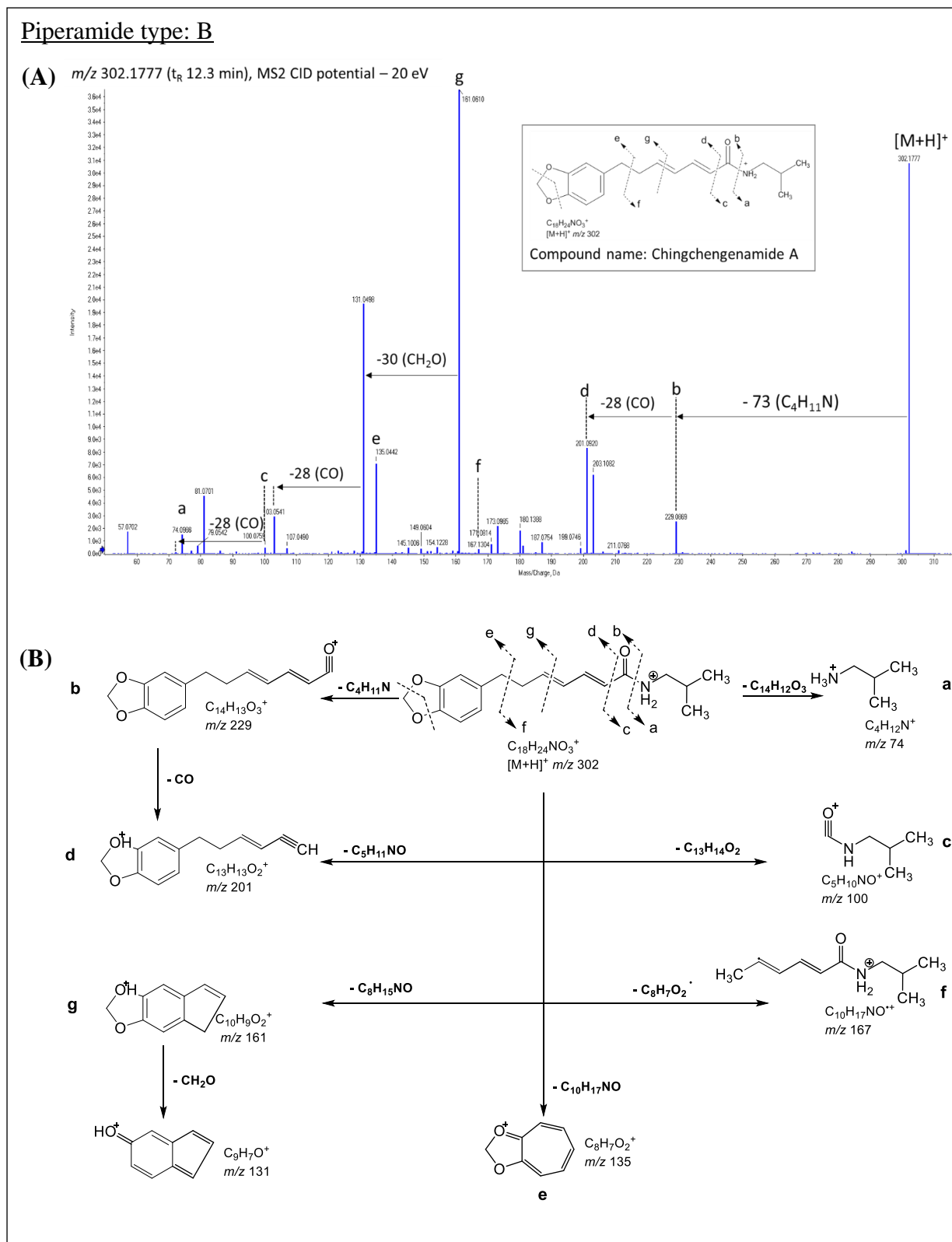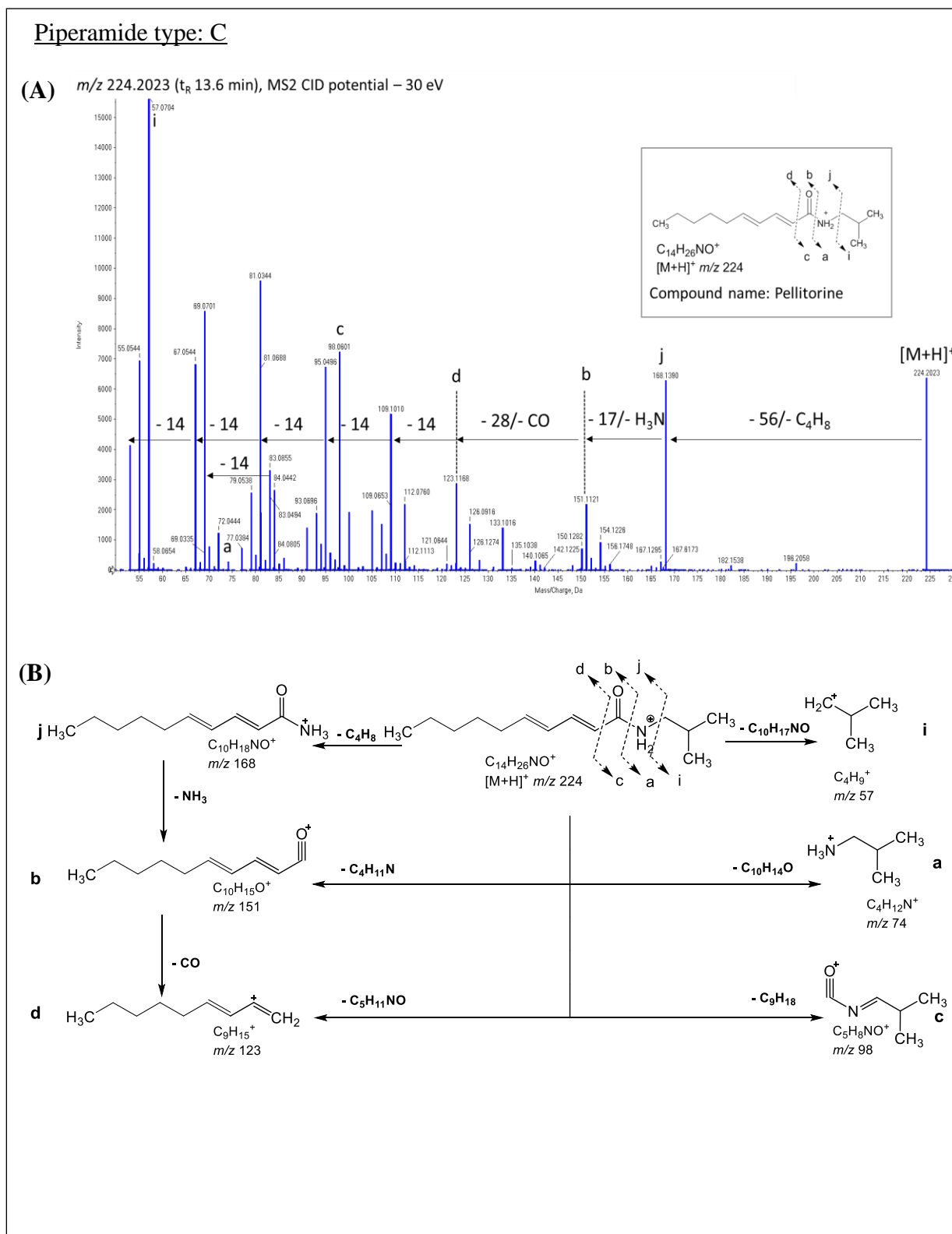
Piperamide type: B

(A) *m/z* 302.1777 (t$_R$ 12.3 min), MS2 CID potential – 20 eV

(B)

Figure S3.2: Metabolite annotation of a selected piperamide type B compound (**P105**): **(A)** MS/MS spectra, **(B)** proposed fragmentation pathway of key ions.

Figure S3.3: Metabolite annotation of selected piperamide type C compound (**P116**): **(A)** MS/MS spectra, **(B)** proposed fragmentation pathway of key ions.
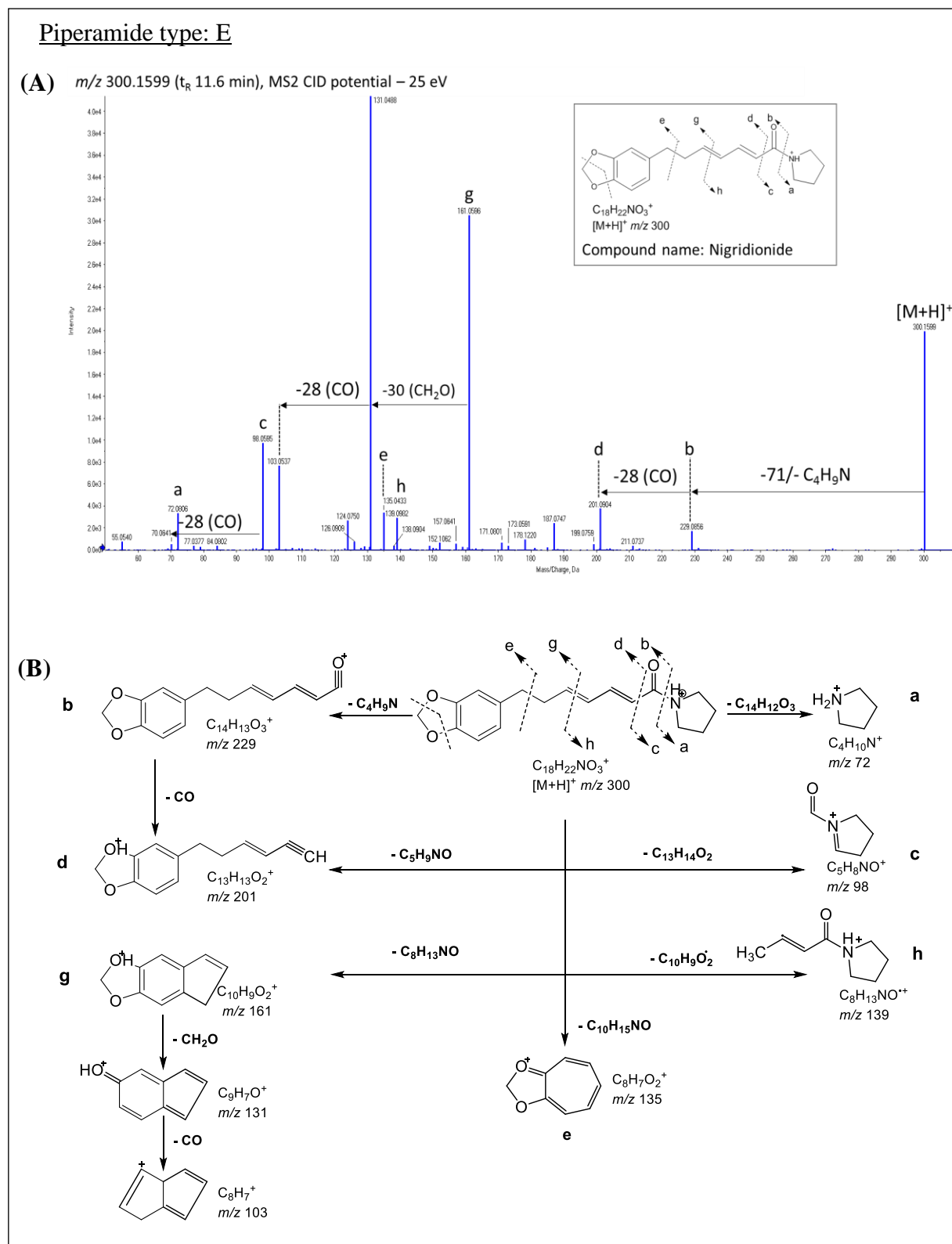
Piperamide type: E

(A) *m/z* 300.1599 (t$_R$ 11.6 min), MS2 CID potential – 25 eV

(B)

Figure S3.4: Metabolite annotation of selected piperamide type E compound (**P93**): **(A)** MS/MS spectra, **(B)** proposed fragmentation pathway of key ions.
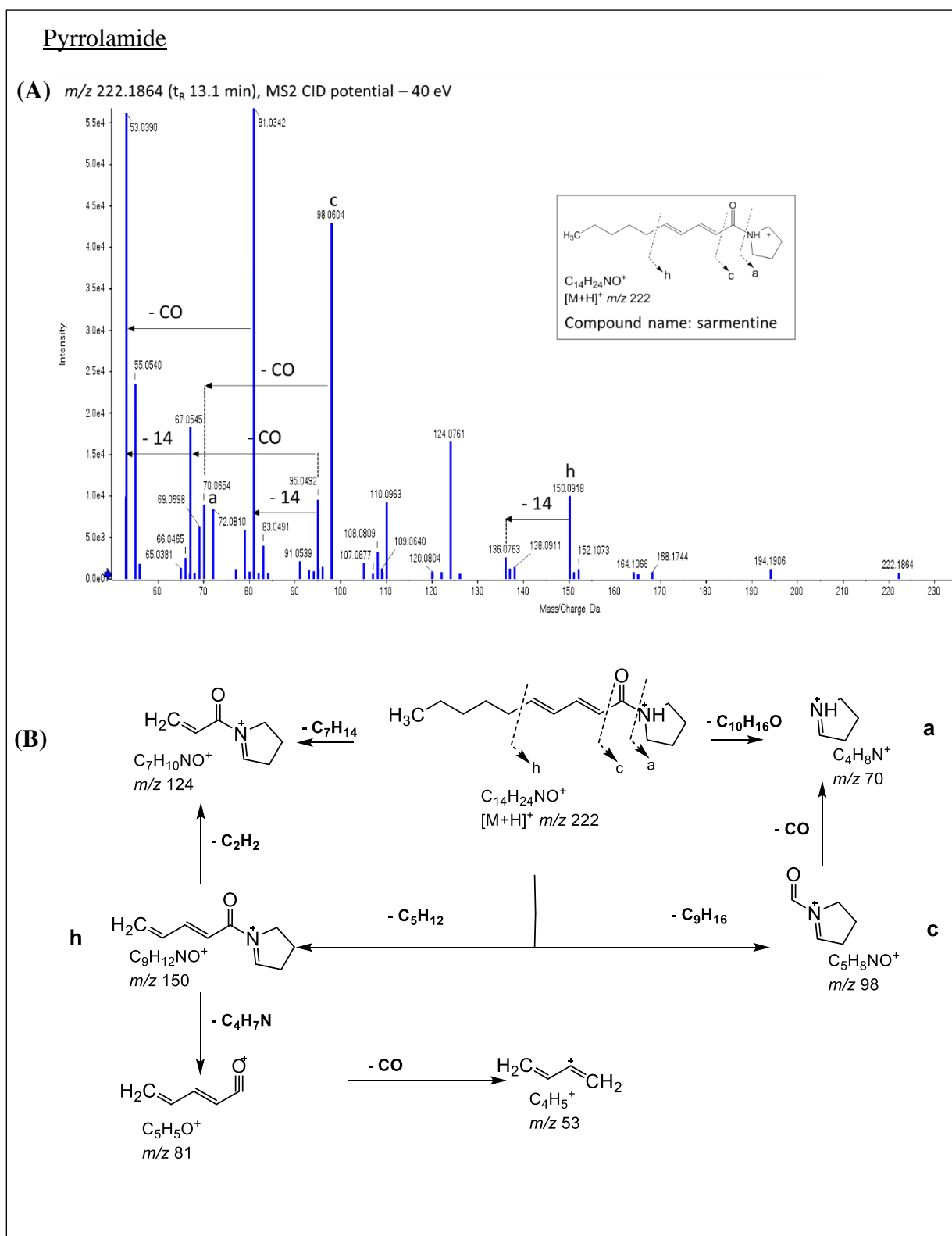
Pyrrolamide

(A) *m/z* 222.1864 (t$_R$ 13.1 min), MS2 CID potential – 40 eV

(B)

Figure S3.5: Metabolite annotation of selected pyrrolamide compound (**P112**): **(A)** MS/MS spectra, **(B)** proposed fragmentation pathway of key ions.
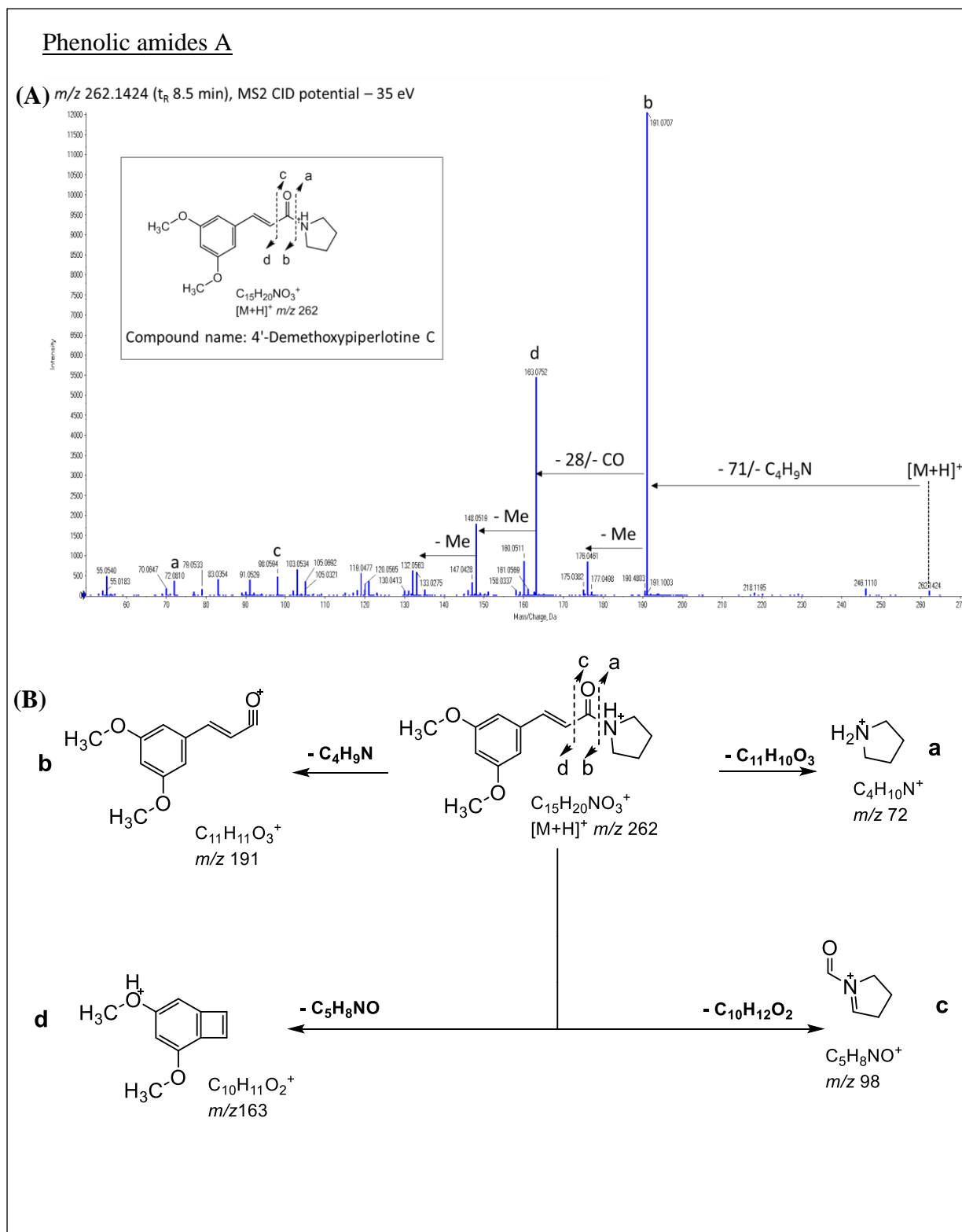
Phenolic amides A

Figure S3.6: Metabolite annotation of selected phenolic amide A compound (**P62**): **(A)** MS/MS spectra, **(B)** proposed fragmentation pathway of key ions.
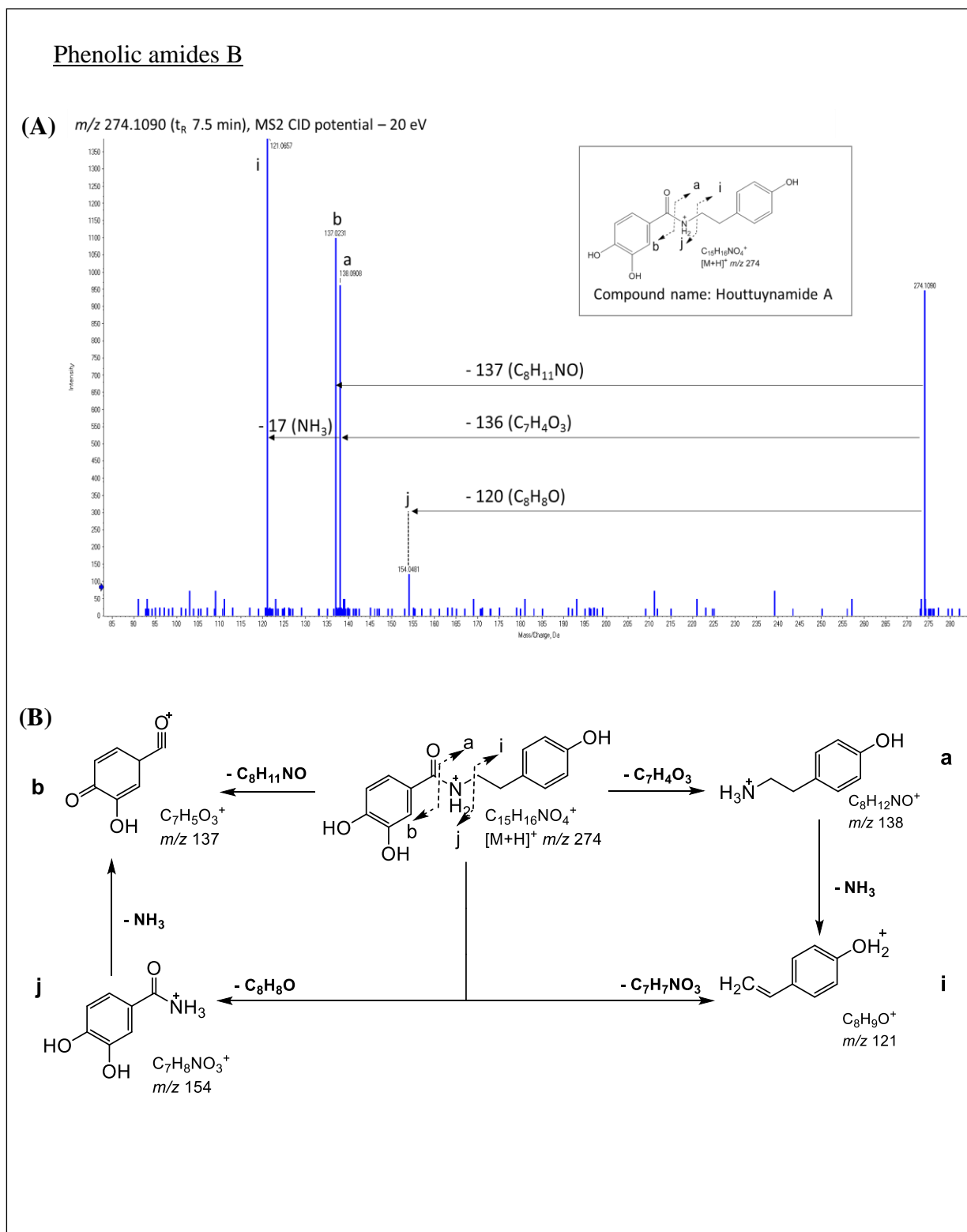
Figure S3.7: Metabolite annotation of selected phenolic amide B compound (**P52**): **(A)** MS/MS spectra, **(B)** proposed fragmentation pathway of key ions.
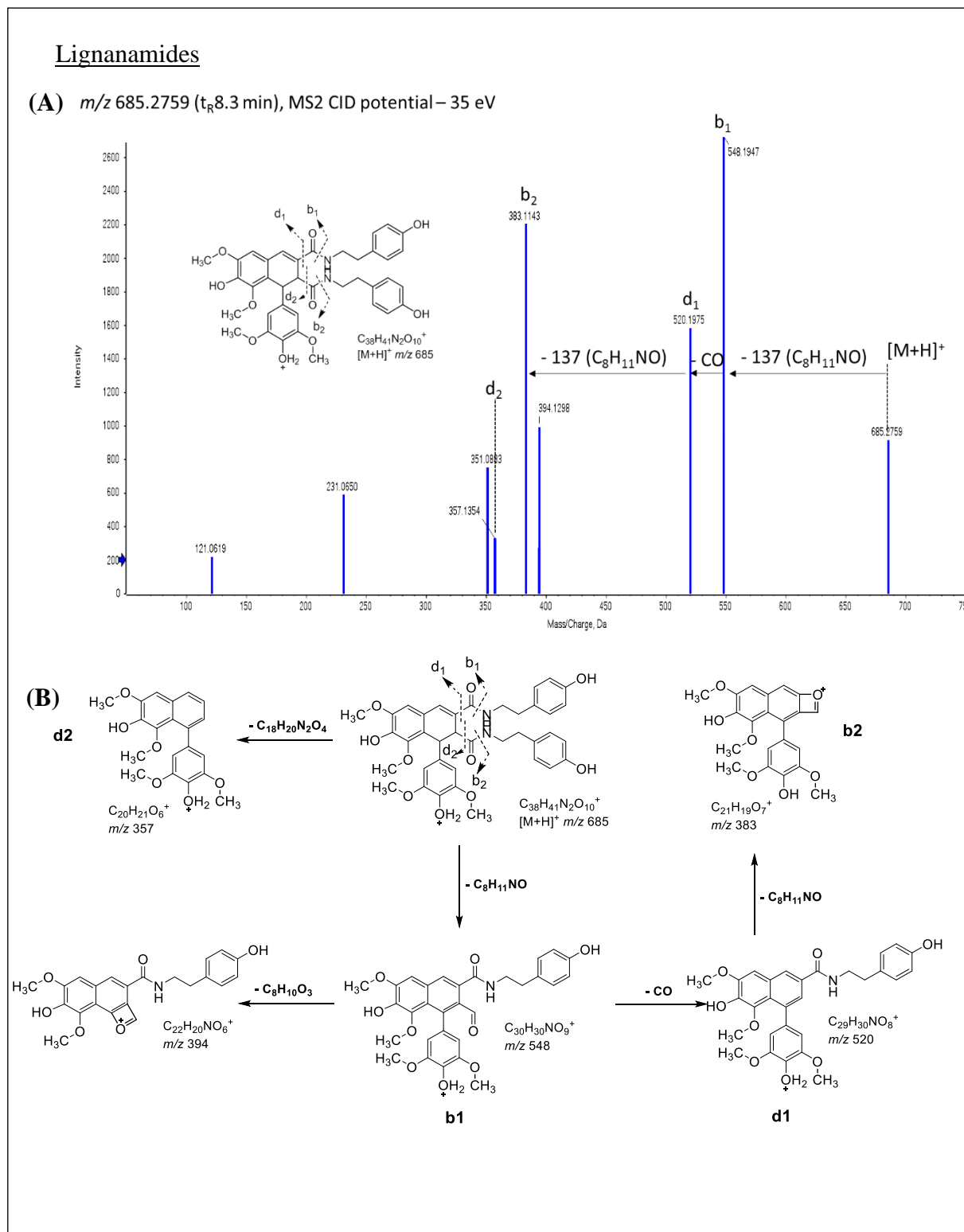
Figure S3.8: Metabolite annotation of selected lignanamide compound (**P58**): **(A)** MS/MS spectra, **(B)** proposed fragmentation pathway of key ions.

Curriculum vitae

Personal details

Name: Ismail Bin Ware

Date/place of birth: 01st January 1983 in Sabah, Malaysia

Nationality: Malaysian

Education

10. 2017 – 2023	PhD Candidate (Dr. rer. nat.) – Leibniz Institute of Plant Biochemistry, Department of Bioorganic Chemistry, IPB, Halle (Saale), Germany
	Research topic: Bioactive metabolites from Piperaceae *Supervisor:* Prof. Dr. Ludger A. Wessjohann
2014	Master of Bioprocess Engineering, Universiti Teknologi Malaysia
	Topic: Inhibition of melanogenesis through the deactivation of tyrosinase activity in melanoma cells by *Labisia pumila* fractions *Supervisor:* Prof. Dr. Mohamad Roji Sarmidi
2007	BSc. (Hons.) in Applied Chemistry – Universiti Teknologi Mara, Malaysia
2004	Diploma in Science, Universiti Teknologi Mara, Malaysia

Work/research experience

10.2017 – Present	Researcher (Natural Products and Metabolomics Group) Department of Bioorganic Chemistry, Leibniz Institute of Plant Biochemistry, IPB, Halle (Saale), Germany
12.2008 – Present	Research Officer – Institute of Bioproduct Development, Universiti Teknologi Malaysia.
06.2008 – 11.2008	Chemist – CCM Duopharma Berhad.

Publications

Ware, I.; Franke, K.; Hussain, H.; Morgan, I.; Rennert, R.; Wessjohann, L.A. Bioactive phenolic compounds from *Peperomia obtusifolia*. *Molecules* **2022**, *27*, 4363. https://doi.org/10.3390/molecules27144363.

Gad, H.A.; Mukhammadiev, E.A.; Zengen, G.; Musayeib, N.M.A.; Hussain, H.; **Bin Ware, I**.; Ashour, M.L.; Mamadalieva, N.Z. Chemometric analysis based on GC-MS chemical profiles of three *Stachys* species from Uzbekistan and their biological activity. *Plants* **2022**, *11*, 1215. https://doi.org/10.3390/plants11091215

Poster (PhD research work)

May 2022	Comparative metabolite analysis of *Piper sarmentosum* organs approached by LC-MS-based metabolic profiling. I. Ware, K. Franke, A. Frolov, K. Bureiko, H. El-Enshasy, L. A. Wessjohann. Trends in Natural Products Research: A Young Scientists' Meeting, Crete, Greece.
June 2022	Comparative metabolite analysis of *Piper sarmentosum* organs approached by LC-MS-based metabolic profiling. I. Ware, K. Franke, A. Frolov, K. Bureiko, H. El-Enshasy, L. A. Wessjohann. Plant Science Student Conference 2022, Online conference.
May 2019	Secondary metabolite isolation of *Peperomia obtusifolia* (L.) A.Dietr. I. Ware, K. Franke, L. A. Wessjohann. Plant Science Student Conference 2019, IPB Halle (Saale).

Declaration

I declare that I have completed this dissertation without unauthorized help of a second party and only with the assistance acknowledged therein. I have appropriately acknowledged and referenced all text passages that are derived literally from or based on the content of published or unpublished work of other authors. The thesis is submitted to the Faculty of Natural Sciences II of the Martin-Luther University Halle-Wittenberg and has not been presented elsewhere for the purpose of gaining a doctoral degree.

Erklärung

Hiermit erkläre ich an Eides Statt, dass ich die vorliegende Arbeit selbständig und nur unter Verwendung der angegebenen Literatur und Hilfsmittel angefertigt habe. Die Dissertation wurde ausschließlich der Naturwissenschaftlichen Fakultät II der Martin-Luther-Universität Halle-Wittenberg vorgelegt und bisher an keiner anderen Hochschule oder Universität zur Erlangung des Doktorgrades eingereicht.

Datum	Ismail Bin Ware